MODELS AND APPLICATIONS FOR WEATHER STATISTICS RELATED TO BUILDING HEATING AND COOLING LOADS

BY

DARYL GREGORY ERBS

A thesis submitted in partial fulfillment of the
requirements for the degree of

DOCTOR OF PHILOSOPHY
(Mechanical Engineering)

at the

UNIVERSITY OF WISCONSIN-MADISON

1984

MODELS AND APPLICATIONS FOR WEATHER STATISTICS
RELATED TO BUILDING HEATING AND COOLING LOADS

Daryl Gregory Erbs
Under the supervision of Associate Professor Sanford A. Klein

ABSTRACT

A model is developed for the monthly distribution of hourly ambient temperature using long-term measurements for 9 U.S. locations, and a degree-day model is derived from the temperature distribution model. Additional relationships are provided which allow the degree-day and distribution models to be used with only monthly-average daily ambient temperature as input. If the monthly-average daily solar radiation is available, the models can be used to estimate bin data or degree-days for individual hours of the day, and the monthly-average ambient temperature for an hour or a portion of the day can be estimated. The models are tested by comparing measured and estimated bin data and degree-days for 17 locations.

A model is presented for the bivariate distribution of sol-air temperature and ambient temperature. Two dimensional sol-air temperature/ambient temperature bin data estimated with the model are compared with bin data compiled from the long-term hourly measurements for 9 locations. The sol-air degree-day concept is introduced, and models are developed for the estimation of heating and cooling sol-air degree-days. The only input required to use the

sol-air temperature models are the monthly-average daily values of ambient temperature and solar radiation.

Distribution models are also developed for relative humidity and wet-bulb temperature. The estimation of two-dimensional dry-bulb temperature/humidity ratio bin data is described for a bivariate distribution function based on the distribution models for either dry-bulb (ambient) temperature and relative humidity or wet-bulb temperature and relative humidity. Bin data estimated with each of these bivariate distribution methods are compared to bin data compiled from hourly data, and applications are presented. Additional relationships are developed which allow these distribution functions to be used with monthly-average daily ambient temperature and solar radiation as input.

A correction for the effect of building thermal capacitance on the heating and cooling loads for a building is derived from an analytic solution for the temperature response of a lumped capacitance building. The correction procedure is a function of distribution models for solar radiation and ambient temperature. The sol-air degree-day models and the capacitance correction models are combined and the loads estimated with this combination are compared to loads obtained with detailed simulation methods.

APPROVED:

Sanford A. Klein, Advisor S. A. Klein

 Date 1/13/84

ACKNOWLEDGMENTS

The research described in this thesis is the result of an evolutionary process. Each new topic represents a step in a progression whose direction was highly dependent on the results of the previous steps. Consequently, I was often unsure of what I would be researching a few months down the road. My academic advisors, Professors Sanford A. Klein and William A. Beckman, were a continual source of encouragement and direction, and much of what was accomplished is a result of their perseverence. More than once they convinced me to do something I knew could not be done; occasionally I was right. I am particularly indebted to Professor Klein for all of his time, effort and helpful suggestions.

Although he was not one of my official advisors, Professor John W. Mitchell was a constant source of ideas and enthusiasm. His interest in my work was a strong motivating factor, and I would like to thank him for all he has done. I would like to thank Professor John A. Duffie for his encouragement and for all of the help he has given me over the past few years, and I would also like to thank Shirley Quamme for all of her hard work.

My fellow graduate students have been a much appreciated source of ideas, encouragement and amusement. Thanks to Jim and Mark for their thoughts, their friendship and for helping me maintain a proper perspective. I would also like to thank my former office mate Mike

for making life as a graduate student more interesting.

To Jackie, who was probably aware of my destiny as a graduate student before I was, I give my love and appreciation for all of her help and for all she has endured. Her encouragement and her help have been important factors in making my career as a student a productive one. I would also like to thank my parents for getting me started on the right track so long ago.

Finally, I would like to express my appreciation to all of the people who were responsible for financing this research. I would like to thank the taxpayers, who were ultimately responsible for a grant from the Department of Energy. I would also like to thank the General Motors Corporation for support through their fellowship program and the American Society of Heating, Refrigerating and Air Conditioning Engineers for a grant-in-aid in support of my research.

TABLE OF CONTENTS

TABLE OF CONTENTS (continued) Page

TABLE OF CONTENTS (continued) Page

TABLE OF CONTENTS (continued) Page

TABLE OF CONTENTS (continued)

LIST OF FIGURES

LIST OF FIGURES (continued)

LIST OF FIGURES (continued)

LIST OF FIGURES (continued)

LIST OF FIGURES (continued)

LIST OF TABLES

NOMENCLATURE

Additional nomenclature is defined locally as needed.

a	Ground reflectance for solar radiation
A	Peak-to-peak amplitude of the diurnal variation of monthly-average hourly ambient temperature [°C]
	Peak-to-peak amplitude of the diurnal variation of monthly-average hourly relative humidity
A_c	Solar collector area [m^2]
A_g	Glazing area [m^2]
A_{wb}	Peak-to-peak amplitude of the diurnal variation of monthly-average hourly wet-bulb temperature [°C]
COP	Coefficient of performance
DA	The summation of all positive differences between the observed value and a base (constant) value for a variable
DB	The summation of all positive differences between a base value and the observed values for a variable
D_C	Cooling degree-days for a month [°C-days]
D_{CV}	Ventilation cooling degree-days for a month [°C-days]
D'_H	Heating degree-days for a single day [°C-days]
D_H	Heating degree-days for a month [°C-days]
D_{SC}	Monthly sol-air cooling degree-days [°C-days]
D_{SCV}	Monthly sol-air ventilation cooling degree-days [°C-days]
D_{SH}	Monthly sol-air heating degree-days [°C-days]
E_{cool}	Change in internal energy for a building during a period of excess losses [MJ]

NOMENCLATURE (continued)

$\dot{E}_{del}$	Energy delivery rate of a heat pump [KW]
$\dot{E}_{eg}$	Rate of excess gains for a building [KW]
E_{eg}	Total excess gains for daytime period [MJ]
E_{gain}	Additional daytime building gains due to a decrease in the interior temperature during the nighttime period [MJ]
$\dot{E}_{int}$	Rate of internal heat generation [KW]
E_{loss}	Additional nighttime building losses due to an increase in interior temperature during the daytime period [MJ]
$\dot{E}_{s}$	Rate of solar gains for a building [KW]
E_{stor}	Energy storage by a building during a period of excess gains [MJ]
$\dot{E}_{w}$	Work input rate to a heat pump [KW]
FBW	Fraction of heat pump energy delivery which is work input to the heat pump
FNP	Fraction of heat pump energy delivery which is non-purchased (extracted from ambient sources)
F_R	Solar collector heat removal factor
GVF	View factor from a surface to the ground
h	Nondimensional temperature scale variable defined by Equation (3-3)
h^*	Nondimensional temperature scale variable defined by Equation (3-19)
h_o	Outside surface combined radiative and convective heat transfer coefficient [W/m^2-°C]
H	Daily total (beam + diffuse) solar radiation on a horizontal plane [MJ/m^2-day]

NOMENCLATURE (continued)

H_T	Daily total solar radiation on an inclined surface [MJ/m^2-day]
I	Hourly total solar radiation on a horizontal plane [KJ/m^2-hour]
I_c	Critical solar radiation level for an hour [KJ/m^2-hour]
I_d	Hourly diffuse solar radiation [KJ/m^2-hour]
I_o	Hourly extraterrestrial solar radiation [KJ/m^2-hour]
I_T	Solar radiation incident on a tilted surface over the period of an hour [KJ/m^2-hour]
k_T	The ratio of the hourly total solar radiation to the hourly extraterrestrial solar radiation for a horizontal surface
K_T	The ratio of the daily total solar radiation to the daily extraterrestrial solar radiation for a horizontal surface
ℓ	Nondimensional degree-day variable defined in Equation (3-2)
$\dot{m}_a$	Mass flow rate of air [kg/s]
$\dot{m}C_p$	Mass flow rate-specific heat product (capacitance rate) [W/°C]
MC	"Effective" building thermal capacitance [MJ/°C]
n	Number of data values or bins
N	Number of days in a month
PLF	Ratio of the instantaneous load for a building to the steady-state capacity of the conditioning equipment (part load fraction)
P(Y)	Probability density function (PDF) for the variable Y
Q_{wall}	Heat flux at the outside surface of a wall [W/m^2]

NOMENCLATURE (continued)

$Q(Y)$	Cumulative distribution function (CDF) for the variable Y
R_b	Ratio of the beam radiation intensity on an inclined surface to that on a horizontal surface
RH	Relative humidity
SVF	View factor from a surface to the sky
t	Time [hours]
t^*	Periodic time of day defined by Equation (3-10) [radians]
T	Temperature [°C]
T_a	Daily average dry-bulb (ambient) temperature [°C]
$T_{a,h}$	Ambient temperature for an individual hour of the day [°C]
$\hat{T}_{a,d}$	Average ambient temperature for the daytime period [°C]
$\hat{T}_{a,n}$	Average ambient temperature for the nighttime period [°C]
$\overline{T}_{a,t1-t2}$	Monthly-average ambient temperature for the hours of the day between t_1 and t_2 [°C]
$\overline{T}_{a,T1-T2}$	Average value of the ambient temperatures between T_1 and T_2 for the period of a month [°C]
T_b	Base temperature [°C]
T_{eq}	Equilibrium temperature for a building [°C]
T_r	Thermostat setting (heating or cooling) [°C]
T_{rh}	Heating thermostat setpoing [°C]
T_{rc}	Cooling thermostat setpoint [°C]
T_{sa}	Sol-air temperature for a surface [°C]

NOMENCLATURE (continued)

T_{wall}	Outside wall surface temperature [°C]
T_{wb}	Wet-bulb temperature [°C]
UA or (UA)	Building conductance between inside and outside air temperatures [W/°C]
U_L	Solar collector heat loss coefficient [W/m^2-°C]
W	Humidity-hours for a month[Kg water-hours/Kg dry air]
α	Solar absorptance
β	Tilt of a surface from horizontal [degrees]
γ	Hour angle of the sun [radians]
γ_s	Sunset hour angle [radians]
Δt_{chg}	Charging time interval for a building [hours]
Δt_d	Length of daytime period [hours]
Δt_{dchg}	Discharging time interval for a building [hours]
Δt_n	Length of nighttime period [hours]
ΔT_a	Difference between the average ambient temperature for the daytime and nighttime periods [°C]
ΔT_{eq}	Difference between the equilibrium temperature for a building and the thermostat setting [°C]
ΔT_f	Change in the interior temperature of a building during a period when the interior temperature is allowed to float [°C]
ΔT_{set}	Difference between the cooling and heating thermostat setpoints [°C]
$\rho_x(j)$	Autocorrelation coefficient for deviations of the variable x from its average value for a lag of j hours
ρ_{xy}	Cross-correlation coefficient between deviations of the variables x and y from their average values

NOMENCLATURE (continued)

σ	Standard deviation of a variable Standard deviation of hourly ambient temperatures for a month [°C]
σ_m	Standard deviation of the monthly-average ambient temperatures for a particular month of the year [°C]
σ_{wb}	Standard deviation of hourly wet-bulb temperatures for a month [°C]
σ_{yr}	Standard deviation of the 12 long-term values of monthly-average ambient temperature for a year [°C]
τ	Thermal time constant for a building [hours]
$(\tau\alpha)$	Transmittance-absorptance product for glazing-room system
$(\tau\alpha)_c$	Transmittance-absorptance product for a solar collector
ϕ	Hourly utilizability for solar radiation
$\overline{\phi}$	Daily utilizability for solar radiation
ω	Humidity ratio [Kg water/Kg dry air]
ω_s	Saturation humidity ratio [Kg water/Kg dry air]

Subscripts

d	Daytime
f	Floating
h	Hourly
i and j	Individual surfaces or data values
max	Maximum value of occurrence
min	Minimum value of occurrence
n	Nighttime

NOMENCLATURE (continued)

o	Overall

An overbar indicates a monthly-average value for a variable.

A hat indicates either 1. An average over several hours for an indiviudal day or 2. The estimated value of a variable.

CHAPTER 1

1. INTRODUCTION

1.1 Objectives

One of the primary functions of a building is to shield the occupants from the surrounding environment. The shell of the building protects against unwanted solar radiation, precipitation and winds, and it allows the temperature and humidity of the air contained inside the building to be controlled within the bounds required for human comfort. Heat and mass transfer occur across the surfaces which make up the shell, and energy must be supplied to maintain a difference between the desired conditions inside the building and the ambient conditions.

The amount of energy which is required to heat and cool a building depends on the climate, the size and design of the building, the interior conditions which are maintained and type of equipment used. The climate, which refers to the weather patterns which are normally observed at a location, represents a set of variables influencing the heating and cooling loads for a building that cannot be directly controlled. However, the climatic variables of interest, such as dry-bulb temperature, solar radiation, air moisture content and wind speed, can be measured and recorded. The relationship between the load for a building and the ambient conditions is based on physical laws governing the transport of mass and energy, making

it possible to simulate the building load for a given set of weather data.

Historically, the most common use of building load models has been for the estimation of design loads. The design load for a building is the load which in theory is only exceeded a small percentage of the time (usually 2.5 or 5%) over the lifetime of the building. The capacities of the heating and cooling equipment are based on the heating and cooling design loads, although a margin of safety is usually added to guarantee that the load can always be met. ASHRAE (1981) has developed an extensive procedure for the estimation of heating and cooling design loads, and design load weather data are provided for a large number of locations in the United States. Design heating and cooling loads have traditionally been calculated by hand.

More recently, there has been extensive research [ASHRAE (1981)] into methods for the estimation of heating and cooling loads for the entire heating and cooling seasons. The increasing cost of the energy required to heat and cool buildings and the decreasing cost of computers are largely responsible for this trend. The calculation of the building load over an extended period of time is more computationally intensive than the estimation of a design load. It also is no longer appropriate to multiply the calculated load by a safety factor, since the primary interest in estimating seasonal loads is the determination of optimum levels of insulation, comparing alternate building designs, and other purposes which depend on

accurate load estimates.

Building load models for the estimation of seasonal (or shorter time periods) loads can be categorized into simulation methods and design methods. Simulation methods, of which DOE-2 [DOE-2 (1980)], BLAST (BLAST (1979)] and TRNSYS [Klein (1981)], are examples, model the time variation of the heat flows and temperatures associated with the building and conditioning equipment. The weather variables which affect the load or equipment performance must be known for each time step in the simulation, which is generally an hour or less in size. Simulation methods allow great flexibility in modeling, and they have the potential for providing an extremely detailed representation of the building and equipment. Because of this level of detail, it is possible to simulate the loads for complex systems with high accuracy.

The drawbacks to the use of simulation methods are directly related to the complexity of the methods. A large number of equations are usually solved for each time step in the simulation, resulting in computer programs which are large in size and which require a relatively fast computer in order to be practical. The inputs used to describe the building and the equipment are usually large in number and there is often a need for training (or extensive practicing) before a user can successfully model a building. The need for hourly weather data which are representative of long-term average conditions also creates a problem, since single year data sets designed to represent the long-term distributions of the variables involved

are only available for a small number of locations.

The alternative to simulation methods is what are referred to as design methods. Design methods vary widely in complexity, but they all share the trait that the time variations in the temperatures and heat flows are not modeled on a short time basis. Most design methods provide load estimates on a month-by-month basis. The weather data used in the estimation of loads and equipment performance range from multi-dimensional bin data to single measure statistics like degree-days. Design methods generally require much less computational effort than simulation methods, allowing their use on small computers, programmable calculators and even by hand (including graphical representations) in some instances. Design methods also require less effort on the part of the user, since there are fewer inputs to supply and less output to sort through. The weather data input for most design methods range from monthly-averages for the variables of interest to bin data. These inputs are available for a large number of locations, allowing design methods to be used for more locations than simulation methods.

The drawbacks commonly associated with design methods are limitations on the types of buildings and conditioning equipment which can be considered and the reduced accuracy which may result when the method does not properly account for all of the weather variables or building factors affecting the load. The underlying basis for design methods, and therefore the source of the limitations, are the weather statistics used in the calculations. The manner in which the build-

ing loads are modeled on a simplified basis defines the weather statistic required. If historical measurements or estimation procedures are not available for the weather statistic needed for a design procedure, the design procedure is of little value. Therefore, any improvements in the flexibility and accuracy of design methods for the estimation of building loads are dependent on the development of more comprehensive weather statistics along with accurate models for the estimation of these statistics.

The objectives of the research described in the chapters that follow have been concerned with improving the weather statistics available for the estimation of building heating and cooling loads and the performance of the equipment used to condition buildings. Simplified models are developed for the estimation of weather statistics commonly used in the estimation of building loads. These simplified models are based on characterizations of the distribution functions for the variables involved in each of the statistics, and the only meteorological inputs required to use the models are monthly-average values of weather variables which are readily available. Additional models are developed for combined weather and building property statistics. The dependence of building loads on the time sequence of the weather and on the interaction between different weather variables is also investigated, and models are developed to correct for the effects of these factors.

1.2 Organization

The modeling of weather statistics for different meteorological variables is similar in many respects for each of the variables. Chapter 2 discusses the weather variables which affect the heating and cooling load for a building and describes the physical mechanisms involved. An understanding of the relationship of building loads to the weather is essential in deciding which variables to consider and what type of statistical functions are required. A description of the statistical models which are used in the chapters that follow is provided along with definitions for the measures of accuracy used to test the models developed. Assumptions which are common to the weather statistics for all variables and a description of the modeling process are also included in Chapter 2.

Chapter 3 presents the distribution model developed for dry-bulb (ambient) temperature and the degree-day models derived from the temperature distribution model. Additional relationships are provided for the estimation of the standard deviation of the monthly-average temperature and the diurnal variation of the monthly-average temperature. The distribution and degree-day models are tested by comparing estimated bin data and degree-days to values compiled from long-term hourly data for 9 U.S. locations.

Chapter 4 develops a model for the two-dimensional distribution of sol-air temperature and ambient temperature and a model for sol-air degree-days. The sol-air temperature concept allows the effects

of ambient temperature and solar radiation on building loads to be combined into a single building-weather statistic. The distribution and degree-day models are based on the ambient temperature distribution model developed in Chapter 3 and existing distribution models for solar radiation. Estimated sol-air temperature/ambient temperature bin data and sol-air degree-days are compared to values compiled from long-term hourly data.

Distribution models for relative humidity and wet-bulb temperature are presented in Chapter 5. Relationships are developed for the estimation of the diurnal variation of monthly-average relative humidity and wet-bulb temperature, the standard deviation of wet-bulb temperature and the monthly-average values of relative humidity and wet-bulb temperature. The estimation of two-dimensional humidity ratio/dry-bulb temperature bin data using the distribution function for relative humidity and either the distribution function for dry-bulb temperature or the distribution function for wet-bulb temperature is described. Two-dimensional bin data estimated with these two procedures and with two simplified procedures are compared to bin data compiled from hourly data.

Chapter 6 is a derivation of correction factors to account for the effect of building thermal capacitance on heating and cooling loads. The building mass is modeled as a lumped capacitance, and an energy balance is used to determine the effect of energy storage by the building on the building loads. The relationships developed for the correction factors are based on existing functions for the dis-

tributions of solar radiation and ambient temperature.

Chapter 7 contains a number of applications for the weather statistics modeled in the previous chapters. The performance of an air-to-air heat pump is calculated using ambient temperature bin data, and the performance of a solar-source heat pump is calculated using sol-air temperature/ambient temperature bin data. The sol-air degree-day models of Chapter 4 and the capacitance correction models of Chapter 6 are combined to estimate the heating and cooling loads for several different buildings, which are then compared to the loads obtained using the simulation program TRNSYS. Finally, humidity ratio/ambient (dry-bulb) temperature bin data are used to calculate the sensible and latent loads on the evaporator for a residential air conditioner. In all of the applications involving bin data, results are presented for both estimated and measured bin data.

Chapter 8 is a summary of what has been accomplished in the research which is described in Chapters 3 through 7. The usefulness and the limitations of the models presented are discussed, and recommended directions for further study in the field of building load related weather statistics are given.

CHAPTER 2

2. BUILDING HEATING AND COOLING LOADS

2.1 Weather Variables Influencing Heat Losses and Gains

2.1.1 Ambient Temperature

Differences between the ambient temperature,[1] T_a, and the air temperature inside a building result in heat conduction through the shell of the building. Although the steady-state rate of heat loss or gain through the building shell by conduction is a simple function of the magnitude of the temperature difference and the thermal resistance of the shell, the ambient temperature is rarely constant for any appreciable length of time. The heat transfer rate is variable and steady state conditions are never reached. A change in ambient temperature results in an immediate change in heat flux at the outer surface of a wall, but there is a time lag before the heat flux at the inner surface responds to the temperature change.

The difference in heat transfer rates at the inner and outer surfaces of a structural member at a particular instant in time depends on the thermal diffusivity of the material, the thickness of the member, and the temperature history at both surfaces. A sheet

---

[1] The term ambient temperature is used to refer to the dry-bulb temperature, and the two will be used interchangeably. Dry-bulb temperature is the preferred term when humidity variables are being discussed.

of window glass responds almost instantly to variations in ambient temperature, while a thick masonry wall may have a time lag as large as 12 hours [ASHRAE (1981)]. If the heat flux at the outer surface of a wall fluctuates between positive and negative values within a time period which is comparable in size (or smaller) to the time lag for the wall, there will be some cancellation of heat flow within the wall. The net heat transfer at each surface will be the same over a long interval of time (a month, for example), but the magnitude of the flux at the inner surface will be smaller on the average than the magnitude at the outer surface and possibly only in one direction. When the heat flux at the outer surface is always in the same direction, the effect of a thermal time delay is to smooth fluctuations in the heat transfer rate at the inner surface.

Infiltration is the flow of ambient air into a building through openings in the shell. These openings include gaps where building materials are joined together, imperfect seals on doors and windows, and chimneys and other exhaust ducts. The inflow of ambient air must be accompanied by the outflow of air at the inside air temperature, resulting in the convective transport of energy. The infiltration rate is a function of the tightness of the structure and the inside-outside pressure difference. Higher infiltration rates generally occur in the heating season due to higher wind speeds and the use of inside air for combustion in the furnace (or fireplace). Convective heat losses due to infiltration are often comparable in size to conduction losses. Although there may be some heat transfer as

air flows through gaps in building materials, the time lag for infiltration is generally negligible.

Ambient temperature also affects the rate of infrared radiative heat loss or gain at the outer surfaces. The surface temperatures of the ground, plants and surrounding buildings are strongly influenced by the ambient air temperature. Radiative exchange also occurs with water vapor and carbon dioxide in the atmosphere. Although air temperature is a function of height, effective sky temperatures for long-wave radiation can be expressed as a function of surface air temperature [Duffie and Beckman (1980)]. The effective sky temperature is the equivalent blackbody temperature for the sky, resulting in the same radiative heat transfer to the sky for a sky emittance of 1 as that which actually occurs.

The performance of certain types of equipment used in the heating and cooling of buildings is a function of ambient temperature. For example, the capacity and coefficient of performance for a vapor compression heat pump with an outside air coil decrease with increasing ambient temperature when used for cooling and decrease with decreasing ambient temperature when used for heating.

2.1.2 Solar Radiation

Solar radiation transmitted by windows and absorbed by surfaces inside a structure represents a form of internal gains. The temperature of the absorbing surface is elevated above the inside air temperature, resulting in energy transfer to the room air and storage

of energy in the building mass. The room air temperature and the inside surface temperatures of the shell increase as a result of the incoming solar energy, and the rate of conduction heat loss due to inside-outside temperature differences is increased from what it would be if there was no incident solar radiation. Solar radiation can only result in a net flow of energy into the building. Solar gains are more variable on both a diurnal and day-to-day basis than gains or losses due to ambient temperature effects. The transmission of solar energy into a building can be controlled through the use of curtains and other shading devices.

Solar radiation is also absorbed on the outer surfaces of the walls and roof. The absorbed solar energy reduces conduction losses (or increases conduction gains) from the values due to ambient temperature effects only. Not all of the solar radiation absorbed at the outer surface represents a gain for the structure. If the conductance between the outer surface and the surroundings is high, the effect on the surface temperature will be small. A thermal circuit for an outer surface is shown in Figure 2.1. An energy balance can be written as

$$h_o(T_a - T_{wall}) + \alpha I_T = Q_{wall} \qquad (2\text{-}1)$$

where h_o is the outer surface combined radiative and convective heat transfer coefficient based on T_a, T_{wall} is the surface temperature, I_T is the incident solar radiation, α is the solar absorptivity of the wall, and Q_{wall} is the surface heat flux. Equation (2-1) can be

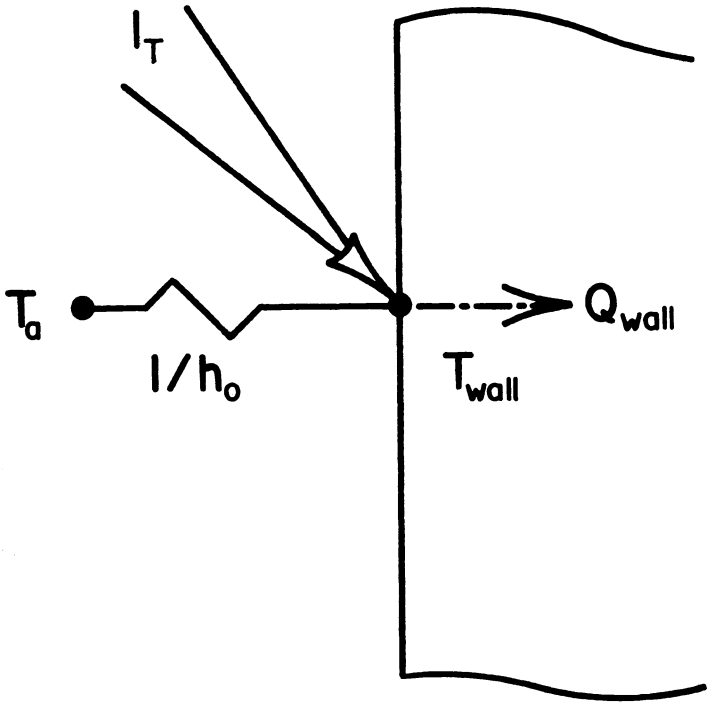

$$Q_{wall} = h_o(T_a - T_{wall}) + \alpha I_T$$

Figure 2.1 Energy Balance for Outer Surface of a Wall

rewritten as

$$h_o(T_{sa} - T_{wall}) = Q_{wall} \qquad (2\text{-}2)$$

where T_{sa}, the sol-air temperature, is defined by

$$T_{sa} \equiv T_a + \alpha I_T/h_o \qquad (2\text{-}3)$$

The sol-air temperature is the ambient temperature which would result in the same heat transfer rate without solar radiation as that which occurs with solar radiation and the true ambient temperature. The difference between the sol-air and ambient temperatures indicates the importance of solar radiation absorption by outside surfaces. Small values of h_o and high values of α can result in a substantial modification of the heat losses or gains for a building. Solar radiation also indirectly affects the sol-air temperatures for a building by warming the ground and other surfaces to which the building radiates. A large percentage (typically 50%) of the infrared heat exchange for the walls of a building occurs with the surroundings.

Solar energy can be collected and used to help satisfy the heating and cooling requirements of a building. The performance of solar collectors and equipment which is operated using the collected solar energy is dependent on the availability of solar radiation. Conditioning equipment (e.g., the condensing coil for a vapor compression air conditioner) may also be affected by solar radiation if the equipment is exposed to the sun and its performance is a func-

tion of temperature.

2.1.3 Air Moisture Content

The effects of air moisture content on the energy required to heat or cool a building are primarily connected with maintaining a comfortable humidity level. Our perception of comfort is a function of the water vapor content of the air. The humidity within a building is often maintained within a range to avoid discomfort. Humidity is also controlled to prevent damage to materials and to provide consistency in manufacturing processes. Water vapor is removed from air in the process of cooling the air to provide temperature control. Infiltration is the only significant mechanism for transporting ambient water vapor into a structure. Although the mass flow rate of water vapor which infiltrates is generally small, the high latent heat of vaporization of water can cause the energy required for humidity control to become a significant fraction of the total cooling load in humid climates.

The long-wave radiative exchange of energy between a building and the sky is affected by the presence of water vapor in the atmosphere. Water has a strong absorption band in the infrared wavelength region, and the emissivity and absorptivity of the sky for long-wave radiation are a function of the amount of water vapor present. When the air is dry, the effective sky temperature is substantially less than the ambient temperature, and heat losses to the sky can be significant even when surface temperatures are

close to the ambient temperature.

The performance of certain types of equipment used in the air conditioning of buildings is a function of ambient humidity. Cooling towers, which are commonly used to cool water for the condensers of large chillers, reject the heat of condensation from the chillers to the ambient air by evaporating water. The final temperature of the water leaving the cooling tower, which influences the performance of the chiller, is closely tied to the wet-bulb temperature of the ambient air. Wet-bulb temperature also has a strong effect on the performance of evaporative and desiccant cooling systems.

2.1.4 Wind Speed

The effects that ambient temperature, solar radiation and ambient humidity have on the heating and cooling loads of a building are influenced by wind speed. The windward wall of a building impedes the flow of air, reducing the wind speed and increasing the pressure of the air. At the same time, flow separation occurs on the leeward wall, lowering the pressure. These pressure differences across the walls result in air infiltration, with the infiltration rate a direct function of wind speed. Changes in infiltration rates lead to changes in the sensible and latent loads due to ambient temperature and humidity.

Wind speed also affects the convective heat transfer coefficient on surfaces exposed to the wind. The thermal conductance of the building shell varies with the outside convection coefficient,

although for a well-insulated building surface, the change in the overall resistance (conduction only) is small even for large variations in h_o. Windows represent the only common structural member in a well-insulated building where variations in the outer surface convective heat transfer coefficient have a significant effect.

A much more important effect is the dependence of the sol-air temperature for a building surface on the convection coefficient. The sol-air temperature for a given incident radiation level varies with the inverse of h_o. Low values of h_o, corresponding to low values of wind speed, can significantly increase the energy gains due to solar radiation absorption by outer surfaces. Variations in h_o also affect the performance of certain types of equipment, such as solar collectors and cooling towers.

Wind speed is more time and spatially variable than ambient temperature, solar radiation or ambient humidity. The wind speed near a building is strongly influenced by the building itself and by surrounding structures; wind speed patterns in a group of buildings are highly variable and not easily modeled. Measurements of temperature, solar radiation or ambient humidity taken at an airport may be reasonably representative of conditions inside a city or in a rural area. (Deviations due to heat island effects, pollutants and other localized aerosols, and local moisture sources tend to be small and constant over a fairly large area.) In contrast, wind speed measurements made at an airport are only representative of

uniform, level ground. The wind speeds near the surfaces of a building may be very different from those far removed from the influence of the building.

2.2 Weather Statistics for the Estimation of Heating and Cooling Loads

The weather variables which affect the heating and cooling loads for buildings were described in the preceeding section. In the chapters that follow, models will be developed for the estimation of three basic types of statistics. A description of each is provided here to avoid repeated explanation.

2.2.1 Basic Types of Statistics

The probability density function (PDF) for a variable describes the range over which a variable is distributed and how the variable is distributed over its range of values. A unit area probability density function must satisfy the conditions

$$\int_{Y_{min}}^{Y_{max}} P(Y)dY = 1 \qquad (2\text{-}4)$$

$$\int_{Y_{min}}^{Y_{max}} YP(Y)dY = \overline{Y} \qquad (2\text{-}5)$$

where P(Y) is the probability density function for the variable Y, Y_{min} is the minimum value of Y which occurs, Y_{max} is the maximum value of Y and $\overline{Y}$ is the average value of Y represented by the PDF. Equation (2-4) is a definition of the term "unit area." All PDF's used in the chapters that follow are unit area functions. Equation (2-5) constrains the distribution to have the correct mean. These two conditions are useful in the selection of mathematical functions suitable for representing a PDF and in the fitting of a function to data, but they do not uniquely determine the shape of the PDF curve.

Figure 2.2 is an example of a probability density function for ambient temperature. The probability of observing a particular value of temperature is equal to zero; finite probabilities exist only for an interval of temperature. This point is reflected in the units of the ordinate. If the PDF shown is representative of ambient temperatures for a month, the number of hours the ambient temperature is within a temperature interval is given by the product of the number of hours in the month and the integral of the PDF over the range of temperature defined by the interval.

The probability density function for a variable is generally developed from a set of measured data, and it is often represented by a mathematical function. In the case of weather variables, PDF's which are representative of long-term average conditions are the most useful, and the measured data should be for a period of several years (ten years or more appears to be good rule of thumb). Since the measurements are recorded at finite intervals of time, the

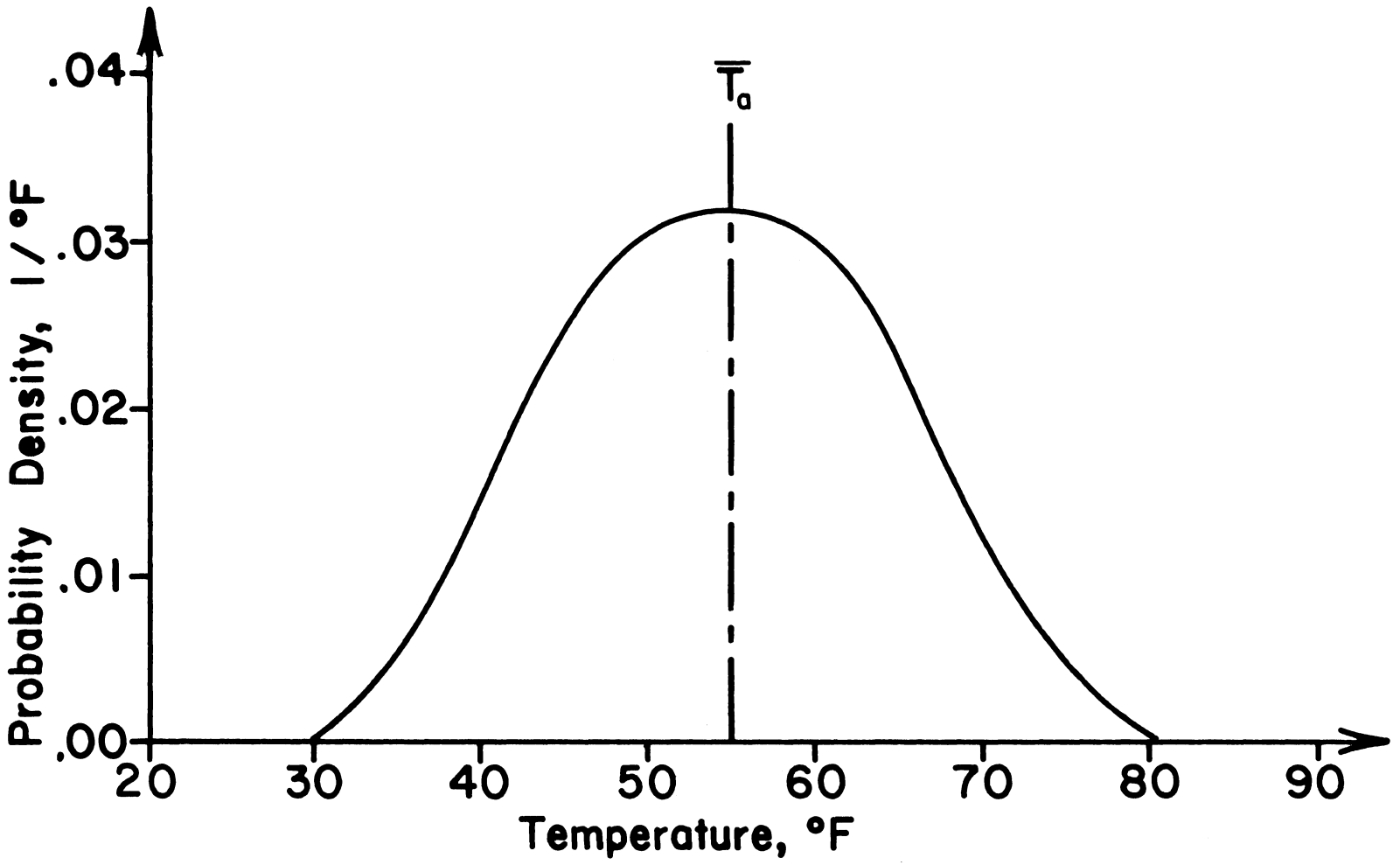

Figure 2.2 Typical Probability Density Function for Ambient Temperature

measured data are discrete in nature. The PDF, which is continuous, represents the actual distribution of the variable, which is also continuous. The measured data are a sample of the population represented by the PDF.

The development of a PDF from measured data is complicated by the fact that the measurements are of limited resolution. The precision of the instrument and the number of digits recorded define a confidence interval for each measured value. When using measured data, the range for the variable is normally divided into a set of intervals known as bins, and the fraction of the total time the variable is within each bin is determined. The proper bin size to use in developing the PDF from measured data is determined by the resolution of the data. If too small a bin size is chosen, some bins will contain no observations and the discrete PDF will be discontinuous; if too large a bin size is chosen, some of the details in the measured data will be smoothed and lost. The fractional frequency of occurrence for each bin is divided by the bin width, resulting in a value of probability density for each bin. The discrete values of probability density are associated with the midpoint value of the independent variable for each bin, and a continuous function or curve is fit to these points.

The integral of the probability density function over a range of the variable it describes gives the fraction of the total time the variable was within that range. If the lower limit of integration is the minimum value of occurrence for the variable and the

upper limit is the variable itself, and not a definite value, the resulting indefinite integral is the cumulative distribution function (CDF) for the variable. Formally,

$$Q(Y) \equiv \int_{Y_{min}}^{Y} P(Y')dY' \qquad (2\text{-}6)$$

where Q(Y) is the cumulative distribution function for Y. The cumulative distribution function gives the fractional time the variable is less than or equal to a particular value. Figure 2.3 shows the cumulative distribution function which corresponds to the probability density function shown in Figure 2.2. The fraction of the total time that the variable is within a particular range is given by the difference in the values of the CDF for the endpoints of the range.

The probability density function and the cumulative distribution function as described above are for the distribution over the range associated with a single variable. Distribution functions which involve only a single independent variable are referred to as one-dimensional or univariate. Measurements are often available for a number of meteorological variables at the same time. Although univariate distribution functions can be developed for each variable, multivariate probability density or cumulative distribution functions can also be used to represent simultaneous data for more than one variable. A multivariate PDF is a function of each of the variables

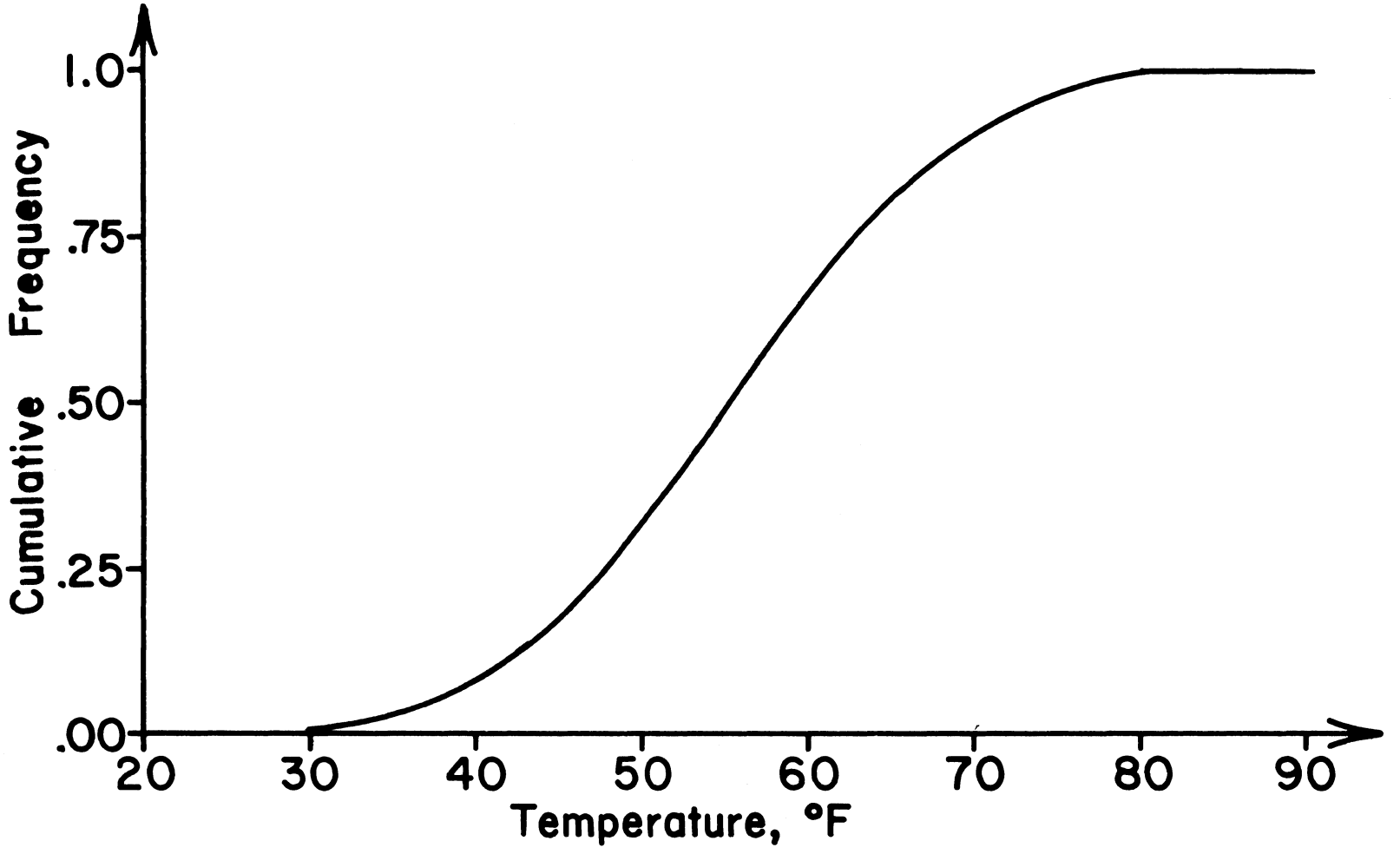

Figure 2.3 Typical Cumulative Distribution for Ambient Temperature

it represents. As a result, a graphical form of the PDF requires more than a single dimension for the independent variables. For example, in a Cartesian coordinate system the x and y axes are used to represent each of the independent variables and the z axis is used to represent the probability density for a bivariate (two-dimensional) PDF. If more than two weather variables are described by a PDF, it becomes difficult to visualize the PDF, as more than three dimensions are required.

Multivariate distribution functions provide information about the coincidence of the variables represented which is not contained in the set of univariate distributions for the same variables. A multivariate PDF gives the probability associated with each possible combination of values for the independent variables. A univariate PDF for one of the variables can only give the average probability for that variable over the entire range of each of the remaining variables. Any one of the univariate PDF's can be obtained from the multivariate PDF by integrating over all values of the remaining independent variables.

Bin data do not represent a distinct type of weather statistic, as they are a discrete form of the PDF. Since bin data are easily compiled from measured data, they are more commonly available than continuous representations of the PDF for a variable. Bin data are often reported as the number of hours a variable was in each bin; as such, they are not discrete probability densities but integrated probabilities for intervals of the variable. Two-dimensional bin data

are easily described in tabular form, with rows representing bins of one variable and columns representing bins of the other independent variable. The value given at each location in the table is the number of hours (or fraction of time). Describing two-dimensional distributions with mathematical functions or even by graphical methods is generally more difficult.

A third statistic is the accumulation of one-sided differences between a base value of a variable and the set of values which occur for the variable. Degree-days is one example of this type of statistic. Heating-degree days is the sum of all positive differences between the base temperature, T_b, and the observed values of ambient temperature. If measured data are available, the differences can be found and summed (with negative differences set equal to zero) by processing the values one at a time. If, however, a probability density function is available for a variable, the accumulated positive differences for values below the base value can be found from

$$DB = \int_{Y_{min}}^{Y_b} N(Y_b - Y)P(Y)dY \qquad (2\text{-}7)$$

where DB is the accumulation of positive differences between the base value and the variable, Y is the variable of interest, Y_b is the base value, Y_{min} is the lower bound on the range for Y and N is the time period represented by P(Y).

A corresponding accumulation function exists for differences when the variable is greater than the base value; cooling degree-days is an example of the accumulation of positive differences between the variable and the base value.

$$DA = \int_{Y_b}^{Y_{max}} N(Y - Y_b)P(Y)dY \qquad (2\text{-}8)$$

DA is the accumulation of positive differences between the variable and the base value and Y_{max} is the upper bound for the range of Y. A useful property when values of both DA and DB are required for the same base value is

$$DA = DB - N(Y_b - \overline{Y}) \qquad (2\text{-}9)$$

where $\overline{Y}$ is the average value of Y.

The cumulative distribution function can also be used to derive models for DB and DA. Integration of Equations (2-7) and (2-8) by parts leads to

$$DB = \int_{Y_{min}}^{Y_b} NQ(Y)dY \qquad (2\text{-}10)$$

and

$$DA = N(Y_{max} - Y_b) - \int_{Y_b}^{Y_{max}} NQ(Y)dY \qquad (2\text{-}11)$$

The results obtained using Equations (2-7) and (2-8) or Equations (2-10) and (2-11) will be equivalent.

2.2.2 Simplifications In the Use of Weather Statistics

The distribution functions for a variable provide a convenient means of representing the values contained in the original set of measurements. The time sequence in which the observations occurred, however, is not information obtainable from the distribution function. Bin data and accumulated differences, which are determined from the distribution function, also provide no information on the time series of the data. The estimation of building heating and cooling loads with weather statistics generally relies on the assumption that the load for the building is not a strong function of the time sequence of the weather. The load can be estimated for a month, but the load for any particular day can only be represented by the average for all days.

The time sequence of the weather is important if the current building load or the conditioning equipment performance has a memory (i.e., is a function of previous weather conditions). Building thermal capacitance represents the most common form of memory affecting heating and cooling loads for buildings.

If the instantaneous rate of energy gains for a building exceeds the instantaneous rate of energy losses, the internal energy of the building will increase unless cooling is supplied. Similarly, if the rate of losses exceeds the rate of gains, the internal energy will decrease unless heating is supplied. Changes in internal energy for a building are accompanied by changes in the internal air temperature.

There is usually a range of interior temperature, referred to as the deadband, where no corrective action (heating or cooling) is taken. While the interior temperature is floating in the deadband, there are net heat losses or gains for the building, but there is no heating or cooling load. These short-term fluctuations in the internal energy of a building permit excess gains for one period of time to offset excess losses for a later time period, and vice versa.

For locations where the annual heating or cooling loads are large, the internal temperature only floats when the net rate of excess gains or losses is relatively small compared to the maximum rates which occur. When this is the case, the effect of building thermal capacitance on the load represents a small fraction of the annual load, although there are exceptions to this rule. One exception is a passive solar house with large glazing areas and a large amount of thermal capacitance.

It is still possible to use weather statistics for the estimation of loads when memory is important, but corrections must be applied to account for the effect of memory. The correction is a

function of both the memory of the building and the climate of the location.

The physical characteristics of the building and the conditioning equipment should also be constant for all days in the month. If weather statistics are available for each hour of the day, the building and equipment descriptions can vary for each hour of the day provided the same diurnal variation occurs for all days in the month. An example of a characteristic which often has the same diurnal variation for all days in a month is the thermostat setting.

The heating or cooling load for a building is a function of several meteorological variables. The weather statistics which are described and modeled in the present study are based on distribution functions for a single variable. It has not been necessary to model the coincidence of occurrence for the different variables beyond that contained in the monthly-average values used as input. The approach taken was to assume that the deviations of the variables from their average values are uncorrelated among the different variables. If two variables are uncorrelated, the probability density for a particular value of one of the variables is the same for any value of the other variable. If the variables are cross-correlated, the distribution function for one of the variables is also a function of the other variable. The distribution function for each of the variables when considered separately is not influenced by dependence on the other variables. The assumption of no cross-correlation is only required when the distributions of several variables

are used simultaneously and the distribution models for each variable are only a function of that variable.

The lack of correlation among weather variables is not a required assumption for the use of weather statistics in general. It is, however, a very common assumption. Multi-dimensional bin data developed from weather measurements represent any coincidence of the variables which exists in the observations, but such data are not widely available. Bin data are available which provide some indication of the coincidence of dry-bulb and wet-bulb temperatures [Air Force (1978)], and work is underway to develop more comprehensive two-dimensional bin data for these variables [Seaton and Wright (1983)]. Only single-variable bin data are available for the remaining combinations of more than one variable. In addition, accumulated difference statistics, which are available for solar radiation and ambient temperature, do not represent the coincidence between the variable they are based on and other weather variables.

2.2.3 Practical Considerations

One of the advantages to using weather statistics in place of simulation methods is the potential for greatly simplifying the computational effort. A primary concern in the development of estimation procedures for existing types of weather statistics and in the definition, use and estimation of new weather statistics is simplicity. Improvements in the accuracy of load estimation procedures must be weighed against the increased complexity associated

with the improvements. Certain load estimation problems may be too complex or the accuracy requirements too severe to use statistical representations of the weather. In these situations, the use of simulation tools with serial weather data is warranted.

Weather statistics which describe the variation of one or two variables at a time can usually be modeled in a simple manner. Problems involving more than two weather variables can often be broken down into several simpler problems, each of which only involves one or two of the variables. The successful use of weather statistics for the estimation of building loads is often a matter of choosing the right perspective from which to analyze the problem.

Distribution function models permit the estimation of weather statistics for locations where values have not been compiled from long-term measurements, expanding the number of locations where weather statistics can be used for load estimation. Input data required by the distribution models are generally monthly-average values of the variable(s) being modeled, information about the range or variance of the variable(s), and possibly measures of coincidence or skewness. The usefulness of a model is directly related to the availability of the required input. The accuracy of a distribution model is of limited value when the model is only valid for a particular climate or geographical region or when obtaining the input data requires a great deal of effort. Monthly-average values of ambient temperature, global solar radiation, relative humidity and wind speed are published for several hundred locations in the U.S. alone.

Distribution function models which only require monthly-average values of one or more of these variables and which are independent of location provide the degree of flexibility necessary for widespread usage.

2.3 Measures of Error and Correlation

2.3.1 Errors and Uncertainties

The accuracy of the distribution models and relationships developed are generally tested by comparison with measured data. Graphical comparisons are used whenever possible, as this type of comparison can provide detailed information in a concise and readily understandable manner. However, the large amount of information contained in a graphical comparison can make it difficult to quickly judge the accuracy of a method, and it may be desirable to represent the error associated with a relationship by a single number. Two standard measures of error will be used in addition to graphs to compare models with measured or reference data.

The bias error is the average difference between the estimated and the measured values for a variable. As its name implies, it represents an offset for the estimation procedure, and it is usually indicative of a systematic problem with the model. The bias error is given by

$$\text{Bias Error} = \sum_{i=1}^{n} (\hat{Y}_i - Y_i)/n \qquad (2\text{-}12)$$

where Y_i is the measured value and $\hat{Y}_i$ is the estimated value for each of the n observations.

The root mean square (RMS) error is a measure of the size of the differences between the model and the measured data. The RMS error is given by

$$\text{RMS error} = \sqrt{\sum_{i=1}^{n} (\hat{Y}_i - Y_i)^2/n} \qquad (2\text{-}13)$$

The RMS error is not the average magnitude of the errors, and it does not indicate whether there is a bias present in the model. It is, however, a useful measure of the accuracy of an estimation method. Large errors are usually of more concern than are small errors when a method is considered; the RMS error places more weight on larger errors by summing the squares of the errors. A model which has a bias error of zero may still have a large RMS error, indicating that although the model is correct on the average, there is still uncertainty in any single estimate.

The standard deviation is similar in form to the RMS error, but it measures the variability of a set of data.

$$\sigma = \sqrt{\sum_{i=1}^{n} (Y_i - \bar{Y})^2/(n - 1)} \qquad (2\text{-}14)$$

where σ is the standard deviation of Y. One use of the standard deviation is to scale the independent variable for a distribution func-

tion. The normal distribution is completely defined by the mean and standard deviation of a variable. The standard deviation can also be used to measure the range of dependent variable values which occur for a particular value of an independent variable. When used in this manner, the standard deviation is a lower bound on the RMS error for a relationship between the dependent and independent variables.

2.3.2 Correlation of Variables

A convenient measure of the correlation between two variables is the cross-correlation coefficient, ρ_{xy}, defined by

$$\rho_{xy} \equiv \frac{\sum_{i=1}^{n} (X_i - \bar{X})(Y_i - \bar{Y})}{\sqrt{\sum_{i=1}^{n} (X_i - \bar{X})^2 \sum_{i=1}^{n} (Y_i - \bar{Y})^2}} \qquad (2\text{-}15)$$

where X and Y are the variables of interest. The range for ρ_{xy} is from -1 to 1. Negative values of ρ_{xy} are the result of greater than average values of X occurring at the same time as less than average values of Y and less than average values of X occurring with greater than average values of Y. Positive values of ρ_{xy} indicate positive and negative deviations from the average for the two variables tend to occur at the same time. If ρ_{xy} is close to zero, the two variables are nearly independent. The cross-correlation coefficients

calculated in the chapters that follow are all based on hourly values of X_i and Y_i for the same value of time. It is also possible to calculate a cross-correlation coefficient between X_i and Y_{i-j}, where j is the number of time intervals separating the value of time when X_i was observed and the value of time when Y_{i-j} was observed.

The autocorrelation coefficient of a variable, $\rho_x(j)$ is a measure of the correlation of a variable with itself for different time lags.

$$\rho_x(j) \equiv \frac{\sum_{i=1+j}^{n} (X_i - \bar{X})(X_{i-j} - \bar{X})}{\sqrt{\sum_{i=1+j}^{n} (X_i - \bar{X})^2 \sum_{i=1+j}^{n} (X_{i-j} - \bar{X})^2}} \qquad (2\text{-}16)$$

where j is the time lag (the units are the time interval associated with the measurements). The autocorrelation of a variable describes its time variability. The range for $\rho_x(j)$ is also -1 to 1, but for meteorological variables $\rho_x(j)$ is generally found to be positive. A value of $\rho_x(j)$ close to 1 indicates the variable changes slowly with respect to time. As j becomes large, $\rho_x(j)$ will approach zero. A value of $\rho_x(j)$ which is close to 0 for small values of j indicates the variable is not influenced significantly by its own time history.

2.4 Model Development and Fitting

2.4.1 Model Development

The distribution function models which are developed in Chapters 3, 4 and 5 are represented by mathematical equations. Relationships are also presented for the estimation of means, standard deviations and diurnal variations of the weather variables modeled. These equations represent curve fits to measured data, and the success in developing the models and relationships presented was highly dependent on the process of finding a suitable equation form and fitting it to the data.

The process of developing a model form is often more of an art than a science. In some instances, it is possible to derive model forms from mass, momentum or energy balances. The capacitance correction relationships presented in Chapter 6 were developed in this manner. When the model form is not determined by a physical description of what is being modeled, or if it is not practical (or possible) to describe the problem in a fundamental manner, empiricism is required in finding a suitable model form. The independent variables for a model may be chosen on the basis of intuition and experience, or it may be possible to determine the independent variables from a differential equation (which cannot be solved) describing the dependent variable. It is generally much easier to choose the independent variables than it is to choose a suitable model form.

The relationships presented in Chapters 3, 4, and 5 are largely empirical in nature. The development of these relationships was generally an iterative process. For each dependent variable that was modeled, a set of prospective independent variables was compiled. The dependent variable was then plotted against the independent variables, both one at a time and in various combinations. Those independent variables which appeared to be correlated with the dependent variable were used in the development of a model, although in some instances an independent variable which was initially believed to be significantly correlated with the dependent variable was eliminated from the model when it was found that inclusion of the variable did not significantly improve the model accuracy.

The model forms were usually based on an inspection of the graphical relationship between the measured values of the dependent and independent variables. Representative curves for standard distribution function forms are given in Hastings (1975) and in many statistical textbooks, and it was possible to use these forms in some instances. Polynomial functions and combinations of exponential functions were often used. A number of different forms were generally fit to each data set, with each new form based on the inadequacies of the previous form.

2.4.2 Model Fitting

The determination of the best parameter values for a given model form and set of measured data was accomplished through the use of

two computer programs. If the model form was linear in the parameters, MINITAB [Ryan (1976)] was used in fitting the model. If the model form was nonlinear in the parameters, the nonlinear regression routine NREG [Ryshpan (1972)] was used. A model is linear in a parameter if the derivative of the model with respect to the parameter is not a function of that parameter. For a model to be linear, it must be linear for all of the parameters.

MINITAB and NREG provide confidence intervals for the parameter estimates, although the confidence intervals provided by NREG are based on a linearization of the model. The programs also indicate the degree of correlation among the model parameters. These indicators of improper model form were used along with systematic patterns in the model residuals (differences between the measured and predicted values of the dependent variable) to help find the correct model form. The sum of squares for the model residuals and the magnitude of the largest residual were used to judge the accuracy of the models.

CHAPTER 3

3. AMBIENT TEMPERATURE DISTRIBUTION MODELS AND STATISTICS

3.1 Literature Review

3.1.1 Ambient Temperature Distribution Models

One possible reason for the lack of distribution models for ambient temperature is the availability of ambient temperature bin data. Ambient temperature bin data are tabulated for each month of the year and for the entire year for 213 locations in the U.S. in Air Force Manual 88-29, Engineering Weather Data [Air Force (1978)]. The bin size for these data is 2.78°C (5°F), and the day has been split into 3 8-hour periods. Since bin data represent a discretization of the probability density function, problems requiring use of the PDF (or CDF) for ambient temperature can be solved numerically using ambient temperature bin data. The Air Force bin data are in printed form, making their use somewhat cumbersome in computer applications.

An ambient temperature distribution model was developed by Anderson et al. (1982) as part of a technique for predicting the performance of air-to-air heat pumps. The probability density function of hourly ambient temperature for a month was assumed to be triangular in shape, and the temperature spread (base width of the triangle) was fixed at 32°C for all months and locations. The only

input required to use his model are values of long-term monthly-average temperature. The choice of such a simple distribution function was based, in part, on the relative insensitivity of heat pump performance calculations to the shape of the ambient temperature distribution. The triangular shape was not supported by comparisons with PDF curves for measured data. The constant temperature spread biases the distribution model towards locations where the actual spread is close to 32°C, although it would be possible to remove this restriction by allowing the base width to vary.

3.1.2 Degree-Day Models

Degree-days, an accumulated difference statistic for ambient temperature, are widely used and reported. Unfortunately, most of the historical degree-day data are for a single base temperature, T_b, of 18.3°C (65°F). A recent study by Fischer et al. (1982) indicates that a base temperature of 18.3°C may be inappropriate for structures being built today. Hourly temperature records are available on magnetic tape (and as written records) [Butson and Hatch (1979)] for hundreds of locations, but the direct calculation of degree-days from long-term hourly measurements is costly and time consuming. The widespread interest in degree-days has led to the development of a number of models for the estimation of degree-days at any value of base temperature.

Thom developed (1954a) a relationship for the estimation of monthly heating degree-days at any value of base temperature which

only requires long-term monthly-average temperature and the standard deviation of the monthly-average temperature as inputs. The monthly-average ambient temperature is tabulated for many locations [Knapp (1980)], and monthly maps providing isolines of the standard deviation of the monthly-average ambient temperature are available for the U.S. [Whiting (1978)].

Thom assumed (1952) that daily average temperatures for a particular day of the year are normally distributed. The normal distribution is convenient in that it can be completely characterized by its mean and standard deviation. Thom used the relationship defined in Equation (2-7) along with properties for a truncated normal distribution to develop a relationship for $E(D'_H)$, the long-term average heating degree-days for a particular day of the year.

$$E(D'_H) = Q(T_b)(T_b - E(T_a) + \sigma P(T_b)/Q(T_b)) \qquad (3\text{-}1)$$

where $E(T_a)$ is the long-term average daily temperature, $P(T_b)$ is the probability density for the ambient temperature normal distribution at a temperature equal to T_b, $Q(T_b)$ is the cumulative probability of the ambient temperature being less than the base temperature, and σ is the standard deviation of the daily ambient temperature.

Thom assumed that the degree-day relationship given by Equation (3-1) can be used to represent a hypothetical "average" day of the month. The average ambient temperature and the standard deviation for this "average" day are such that its degree-day value is equal to

the long-term average daily degree-day value for the month. The long-term average degree-days for the month is the product of the mean value for the "average" day and the number of days in the month, N. $E(T_a)$ is replaced by $\overline{T}_a$, the long-term monthly-average daily temperature, and the value of σ used is for the combined temperature distribution of all days in the month.

Thom did not have access to values of σ, and direct calculation from temperature records was too time consuming without computers. He chose to approximate σ with $\sigma_m\sqrt{N}$, where σ_m is the standard deviation of $\overline{T}_a$ (σ_m measures year-to-year variation of the average ambient temperature for a month). The autocorrelation of ambient temperature causes $\sigma_m\sqrt{N}$ to be substantially larger than σ, and the relationship given in Equation (3-1) can no longer be used directly.

Thom did not know the exact relationship between σ and σ_m. He assumed that σ and σ_m only differ by a constant of proportionality, and he defined a new variable

$$\ell \equiv (E(D'_H) - T_b + \overline{T}_a)/\sigma_m\sqrt{N} \qquad (3\text{-}2)$$

which is a function of the nondimensional temperature scale variable h, where

$$h \equiv (T_b - \overline{T}_a)/\sigma_m\sqrt{N} \qquad (3\text{-}3)$$

The heating degree-days for a month, D_H, are given by

$$D_H = N(T_b - \overline{T}_a + \ell\sigma_m\sqrt{N}\,) \qquad (3\text{-}4)$$

The variable ℓ replaces the ratio of $P(T_b)/Q(T_b)$ for a normal distribution used in Equation (3-1). This substitution corrects for the approximation of σ with $\sigma_m\sqrt{N}$.

Thom developed a relationship between ℓ and h using measured degree-day data for 30 locations. He later (1966) fit the following equations to the ℓ and h data:

For $h > 0$,

$$\ell = 0.34\exp(-4.7h) - 0.15\exp(-7.8h) \qquad (3\text{-}5)$$

and for $h < 0$,

$$\ell = 0.34\exp(4.7h) - 0.15\exp(7.8h) - h$$

The development of the empirical relationship between ℓ and h does not require that the ambient temperatures for a month be normally distributed. Thom never demonstrated that the monthly ambient temperature distribution is normal, and in the next section, evidence is presented which indicates it is not normal for measured data. The empirical relationship between ℓ and h provides a better representation of the long-term distribution of ambient temperature for a month than the normal distribution does. Thom later extended the method (1966) to allow the estimation of cooling degree-days above any base temperature.

The relationship between ℓ and h developed by Thom can be differentiated (via Equation (2-10)) to derive a cumulative distribution function for ambient temperature. Since the form of Equation

(3-5) depends on the sign of h, two expressions must be derived for Q(h).

For $h > 0$,

$$Q(h) = 1 - 1.60\exp(-4.7h) + 1.17\exp(-7.8h) \qquad (3\text{-}6)$$

and for $h < 0$,

$$Q(h) = 1.60\exp(4.7h) - 1.17\exp(7.8h)$$

The expression developed for degree-days by Thom assumes the distribution of ambient temperature is symmetric about the monthly-average ambient temperature. The two expressions given for Q(h) in Equation (3-6) should equal 0.5 when the temperature is equal to the monthly-average value (h is equal to 0). However, this is not the case, as Q(0) is found to be 0.43 for the first expression and 0.57 for the second. This discontinuity prevents Thom's degree-day model from being used for the estimation of ambient temperature bin data.

Thom fit an equation to the degree-day versus base temperature data, for which a "best fit" was one that minimized the sum of the squared differences between the measured and predicted degree-days. The two expressions in Equation (3-5) give exactly the same degree-day value for a base temperature equal to the monthly-average ambient temperature, but the slopes of the two expressions, which represent a cumulative distribution function for ambient temperature, are not equal.

The degree-day estimation procedure developed by Steadman (1978) and the procedure developed by Aceituno (1979) are identical. They were both derived assuming the mean daily temperature is normally distributed for a month, resulting in the same relationship Thom had derived 24 years earlier. As was the case for Thom's work, no evidence is presented to support the use of the normal distribution for the ambient temperature probability density function. The problem of obtaining values of σ is not addressed by Aceituno, while Steadman gives six "rule of thumb" values to represent different climates and seasons. Steadman also demonstrates the relationship between the cumulative distribution and degree-day functions (Equation (2-10)) for the special case of a normal distribution.

Lunde (1982) presents a method for the estimation of heating degree-days which is a function of the difference between the base temperature and the monthly-average ambient temperature and the annual degree-day total at a base temperature of 18.3°C. No discussion is offered as to the assumptions made in the development of the method or the source of the degree-day data (for base temperatures other than 18.3°C) used to develop the curves and equation provided.

Walsh and Miller (1983) also discuss the estimation of degree-days when it is assumed that ambient temperature is normally distributed for a month. It is noted that the distributions of observed temperatures can depart significantly from normality, but the estimation procedure still gives accurate results. They present a method for estimating the standard deviation of ambient temperature which

makes use of monthly-average data readily available in Australia. A means of estimating the year-to-year variation of degree-day values for a day or month is developed by assuming degree-day values are also normally distributed.

Harris et al. (1965) recognized that heating degree-days for a base temperature of 18.3°C were not appropriate for many buildings. A correction factor which is only a function of the seasonal degree-day total was developed. The correction gives the percent change in seasonal degree-days for each degree change in base temperature. The relationship provided was developed from measured degree-day data for a number of base temperatures at 46 locations. The correction factor is not a function of base temperature, implying the number of days (or hours) that the ambient temperature was less than the base temperature is constant. This is not always correct, since once the base temperature value is less than the maximum value of ambient temperature for the season, the number of hours the ambient temperature was less than the base temperature is a function of the base temperature.

Hitchin (1981) presents correction charts for the estimation of degree-days at nonstandard base temperatures. Annual heating degree-day totals for a range of base temperatures at a number of British and Irish locations were used to develop the charts. The charts are designed to correct measured values for a base temperature of 15.6°C to base temperatures ranging between 5 and 20°C. A different chart is required for each of three climate types: inland sites, south and

west coastal sites, and east coastal sites. The correction given by the charts is a function of both the degree-day total and the base temperature. If degree-days for a base of 15.6°C are not available, it is recommended that Thom's method be used to estimate degree-days for a base of 15.6°C and the charts used to correct the estimate to the desired base temperature. The accuracy of the charts is compared with the accuracy of the estimation methods presented by Thom and by Steadman using measured degree-day data for Britain and Ireland.

3.2 A Distribution Function Model for Ambient Temperature

3.2.1 Long-Term Temperature Data

Hourly SOLMET (1979) data for Madison, WI, Washington, DC, Albuquerque, NM, Miami, FL, Fort Worth, TX, Columbia, MO, New York, NY, Phoenix, AZ and Seattle, WA were used to examine the distribution of ambient temperature. An average of 20 years of data were available for each location. The observations were originally recorded in units of degrees Fahrenheit, but the values had been converted to the Centigrade scale by the National Climatic Center. Before the temperature data were used to develop distribution curves, the values were converted back to Fahrenheit and rounded to the nearest degree.

The hourly temperature measurements for each location were separated by hour of the day and month of the year. Bin data were

compiled using a bin width of 2°F for each hour and month, yielding 288 (12 X 24) bin data sets for each location. The number of hours in each bin was divided by the total hours in the data set (for that hour, month and location) and by the bin width (2°F) to convert the bin data to discrete probability density data. The probability density data were used to generate discrete cumulative distribution data sets for each hour, month and location.

Monthly-average temperature, the standard deviation of ambient temperature and the standard deviation of monthly-average ambient temperature were also calculated on an hourly basis from the measured temperatures. The independent variable for the probability density and cumulative distribution bin data was transformed from temperature to h, where h is defined by Equation (3-3), using measured values of monthly-average hourly ambient temperature and the standard deviation of the monthly-average ambient temperature. Probability density and cumulative distribution bin data sets were also generated by transforming the temperature values to values of h', where h' is scaled using σ in place of $\sigma_m\sqrt{N}$. By using h or h' in place of temperature, the distribution curves become centered on the same value of the independent variable (zero), and the range of the independent variable required to encompass the measured data is nearly the same for all of the bin data sets. If the temperatures for a month were normally distributed, the range of h' would be exactly the same for each distribution.

A single cumulative distribution bin data set was developed for each location by averaging the 288 hourly bin data sets. The standard deviation of the hourly CDF curves from the average CDF curve was calculated to provide an indication of the seasonal variability of the distribution curves. The distribution curves based on h were compared with those based on h'. The use of h', which uses the measured standard deviation of daily ambient temperature to non-dimensionalize the temperature scale, did not result in any significant reduction in the seasonal or locational variation of the distribution curves when compared to the curves developed using h. Values of σ_m have been tabulated and published in the form of maps for the U.S. Since values of σ are not readily available for most locations, h was chosen as the independent variable for ambient temperature distribution modeling efforts.

The average cumulative distribution curves for each location are shown in Figure 3.1, along with plus and minus one standard deviation of the hourly curves. The average distributions are similar for all of the locations, but seasonal and locational variations are present. The distribution functions are skewed towards greater than average temperatures for most of the locations. This skewness can be seen in the cumulative distribution curves by comparing the ordinates for h values of -1 and +1. For a symmetric distribution, the fraction of the total hours for an h value of -1 should equal one minus the fraction of the total hours for h equal to +1. The distributions for Miami are noticeably skewed, but for

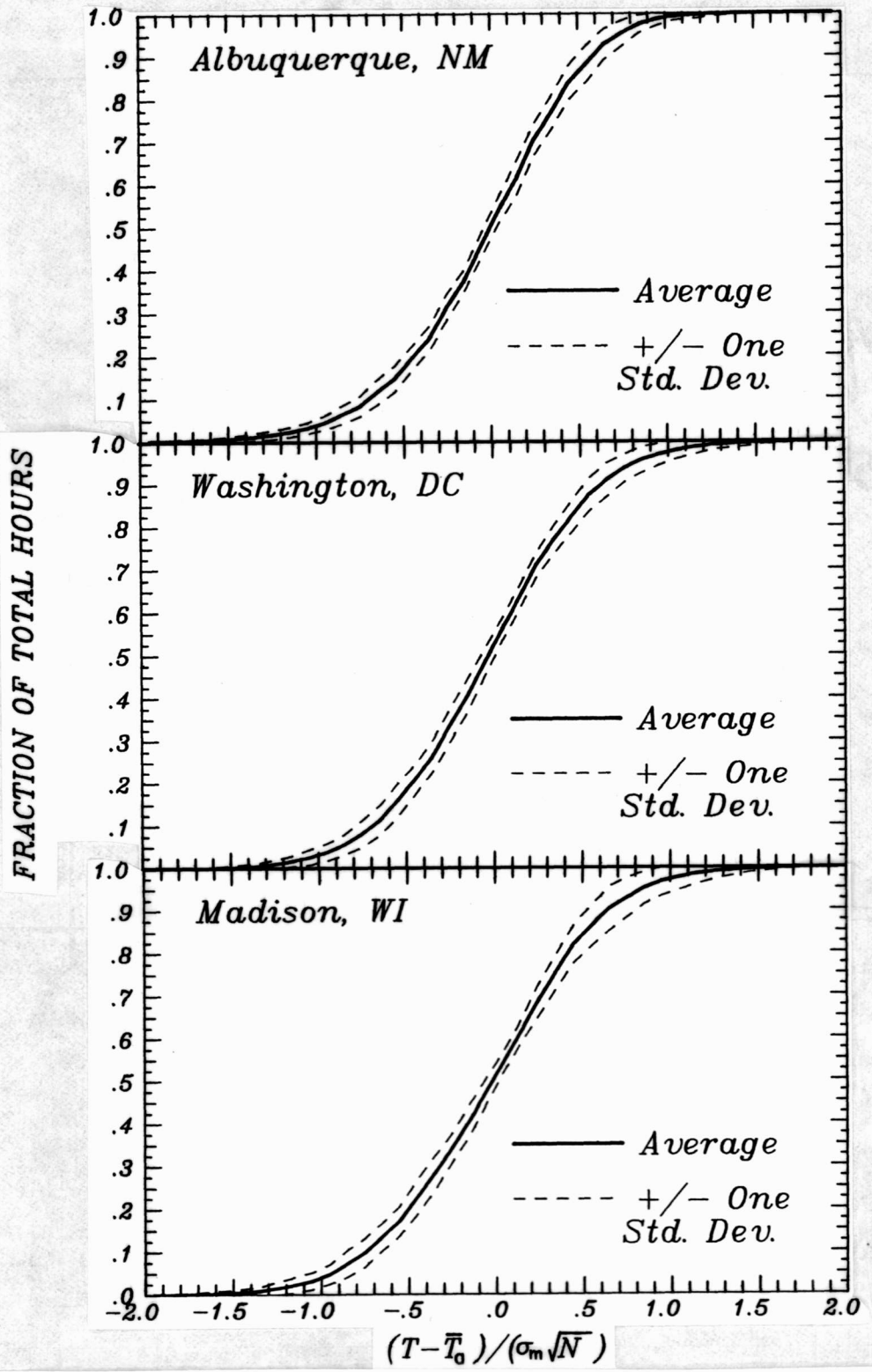

Figure 3.1 Ambient Temperature Cumulative Distributions for 9 U.S. Locations

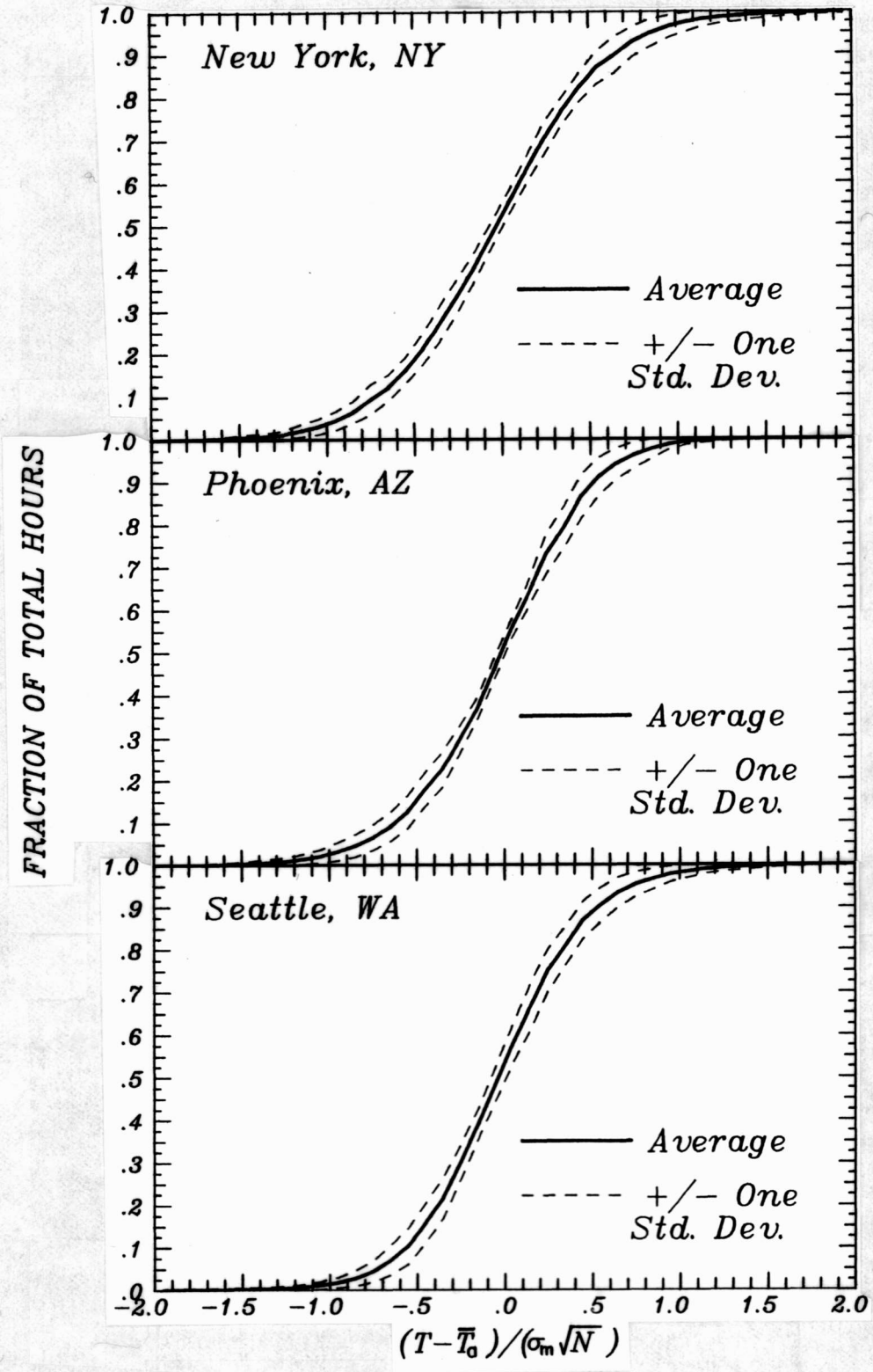

Figure 3.1 (cont.)

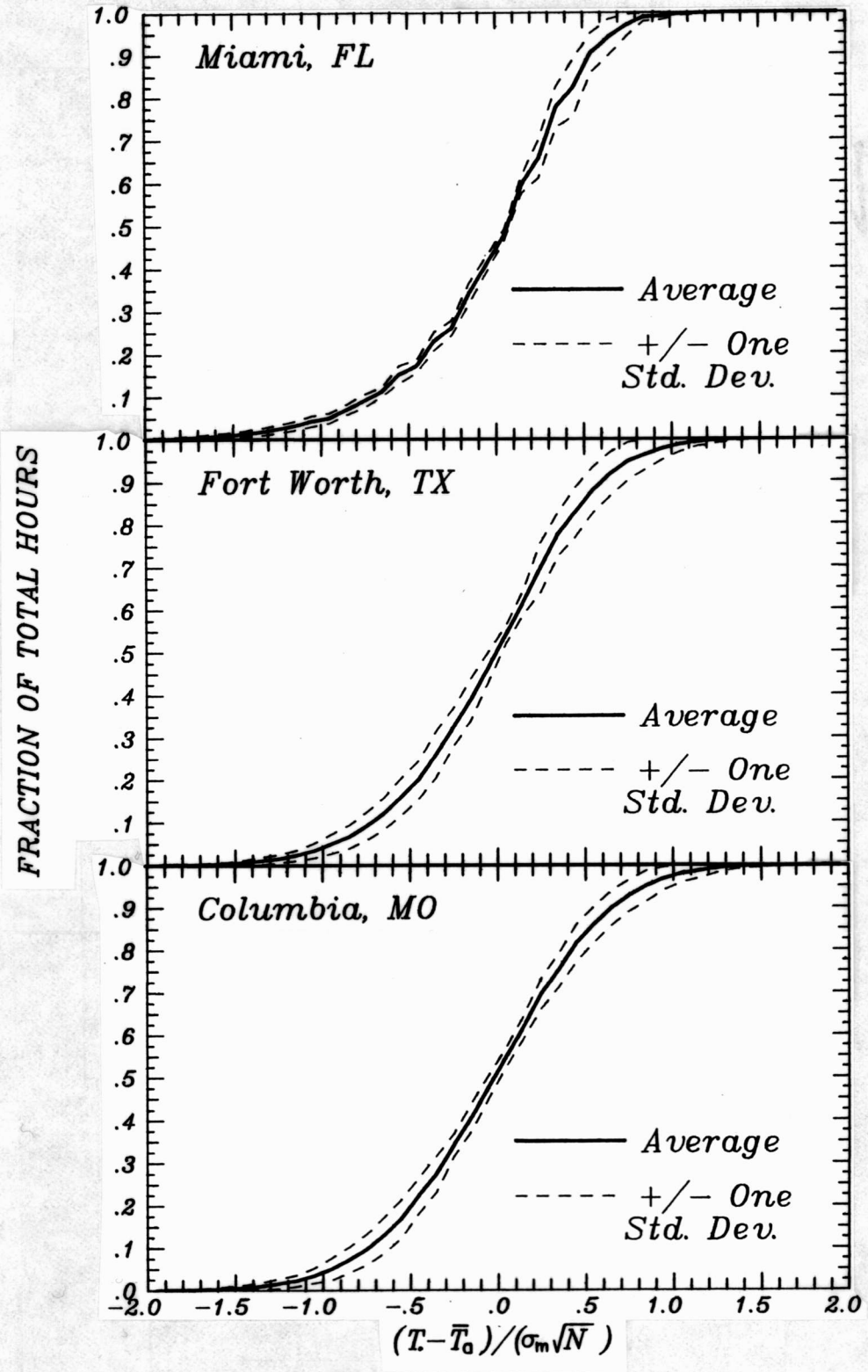

Figure 3.1 (cont.)

many of the locations the degree of skewness is small. The Seattle data exhibit the opposite behavior, indicating the mode is less than the average temperature most of the time at this location.

The probability density bin data were studied on a month-by-month basis for each location. In Miami, the shifting of the mode to higher than average temperatures occurs primarily in the winter months. One possible explanation is a warming effect due to the close proximity to the ocean. Air masses traveling across the ocean would tend to be constant in temperature due to the large thermal mass of the water. The skewness observed in Seattle, another coastal location, is the result of the mode shifting to lower than average temperatures during the summer months. This may be the result of cool oceanic air masses. The monthly distributions in Madison and Columbia were skewed in the direction of 0°C during the late fall, winter and early spring months. The ample supply of moisture in the form of surface water (liquid and solid) and ground water combined with the high heat of fusion for water may be the cause of this trend.

3.2.2 Model Development

In addition to the skewness described in the previous subsection, the shape of the distributions vary in other manners. An example is the peak at the mode of the PDF, which is quite sharp in some locations and broad in others. To be able to model skewness and other forms of shape variations, it is necessary to identify a variable or

variables related to the shapes of the distributions and to quantify the changes in shape which occur. No consistent trends could be found using readily available meteorological data. Since the distributions are skewed both to the left and right of the average temperature at different times of the year, the use of a symmetric monthly distribution model is a simple means of representing a "typical" distribution of ambient temperature. Although this leads to systematic errors for certain locations, it results in a single model which is general for all locations and of acceptable accuracy for bin data and degree-day estimation, as shown below.

The cumulative distribution data for the 9 locations were used to fit the following single parameter relationship for the cumulative distribution of ambient temperature:

$$Q(h) = (1 + \tanh(1.698h))/2. = 1/(1 + \exp(-3.396h)) \qquad (3\text{-}7)$$

The corresponding probability density function is

$$P(h) = 0.849/(\cosh^2(1.698h)) \qquad (3\text{-}8)$$

The mathematical form chosen for the cumulative distribution function has the correct range, 0 to 1, but the domain for h, which extends from negative to positive infinity, is not representative of actual conditions. The effect of the infinitely long distribution tails is negligible, as 99.8% of the area under the PDF represented by Equation (3-8) lies between values of h of -2 and 2. The ambient temperature distribution model has the important advantage of being

a simple function of exponentials, which are represented on most calculators and computers.

3.2.3 Relationships for the Mean and Standard Deviation

Ambient temperature is one of the most widely available weather variables, but generally only daily values are recorded. Ambient temperature follows a cyclic variation over the course of a day, leading to significant differences between monthly-average daytime and nighttime temperatures. It is often necessary to know the monthly-average ambient temperature for a particular hour or portion of the day. Measured monthly-average hourly ambient temperatures for the 9 SOLMET locations were used to develop a curve for the normalized diurnal variation of $\overline{T}_{a,h}$. The diurnal variation curves for each month were standardized by subtracting the monthly-average daily ambient temperature from the monthly-average hourly ambient temperature for each hour of the day and dividing the resulting differences by the peak-to-peak amplitude for that curve. A fourier series was fit to the average curve for the 9 locations.

$$(\overline{T}_{a,h} - \overline{T}_a)/A = 0.4632\cos(t^*-3.805) + 0.0984\cos(2t^*-0.360) + 0.0168\cos(3t^*-0.822) + 0.0138\cos(4t^*-3.513) \quad (3\text{-}9)$$

where A is the amplitude of the diurnal variation (peak-to-peak) and t^* is given by

$$t^* = 2\pi(t-1)/24 \quad (3\text{-}10)$$

where t is in hours with 1 corresponding to 1 AM and 24 corresponding to midnight. The average of the 108 (12 months X 9 locations) standardized curves is represented by the solid curve in Figure 3.2. The long dashes are plus and minus one standard deviation of the individual monthly curves from the average and the short dashes (which are hard to distinguish from the average curve for the measured data) are the curve fit given by Equation (3-9).

The amplitude of the diurnal variation of ambient temperature is a function of the average difference in the radiation balances for the daytime and nighttime hours. The solar radiation received during the daytime for a particular location and time of year is mainly determined by the clearness of the atmosphere. The clearness of the atmosphere is in turn a function of the water vapor content, with clouds the most important form of atmospheric water vapor. Radiative losses at night are also a function of the cloud cover and atmospheric moisture content due to the strong absorption band of water vapor in the infrared wavelength region. As a result, clear days tend to have large diurnal temperature swings and cloudy days tend to have small diurnal swings. The ratio of the total solar radiation incident on a horizontal surface in a month to the monthly extraterrestrial radiation on a horizontal surface, $\overline{K}_T$, is a convenient measure of atmospheric clearness. A relationship was established between A and $\overline{K}_T$ using the SOLMET data. The relationship, compared to the measured data in Figure 3.3, is

$$A = 25.8\overline{K}_T - 5.21 \qquad (3\text{-}11)$$

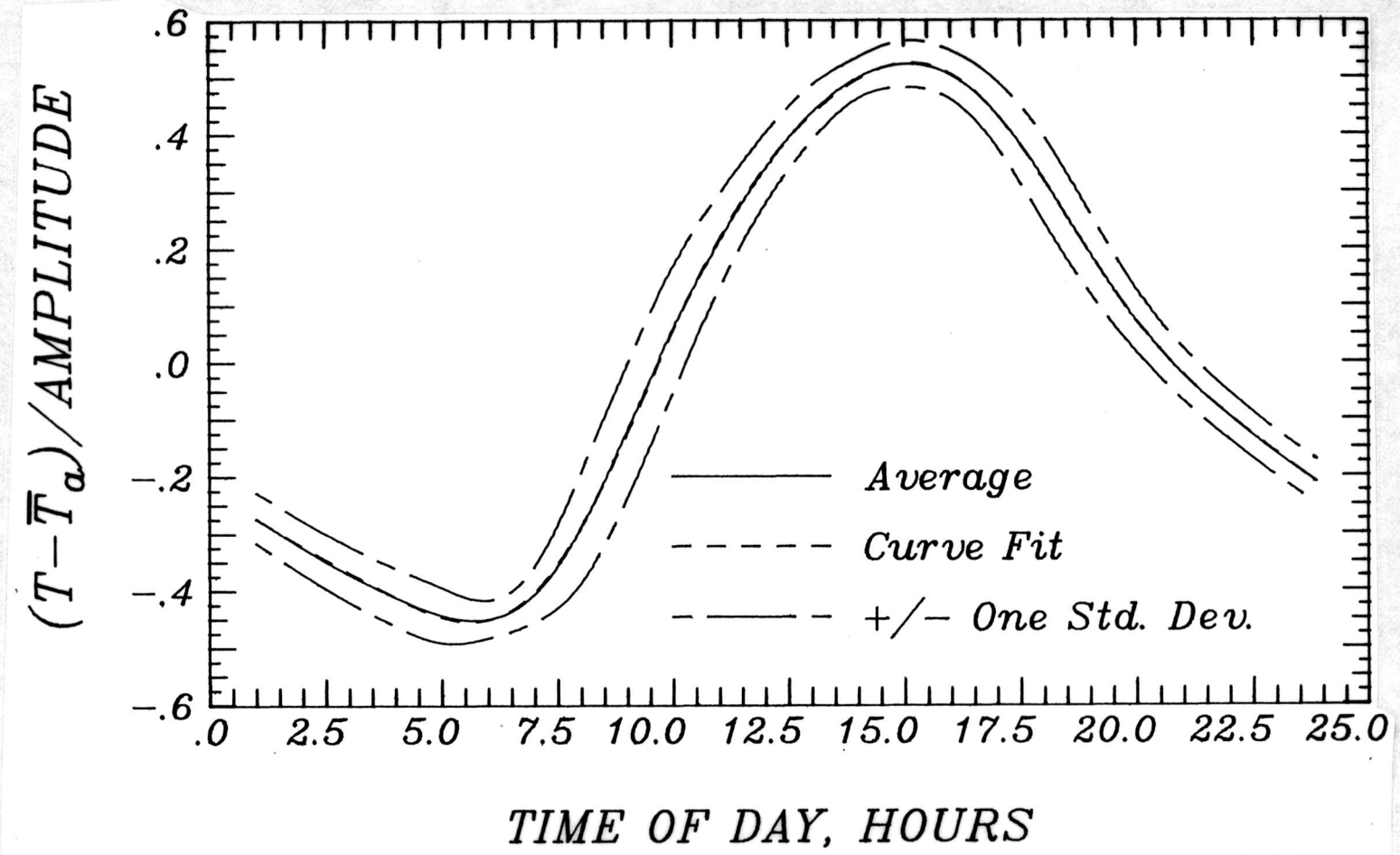

Figure 3.2 Standardized Diurnal Variation of Monthly-Average Ambient Temperature

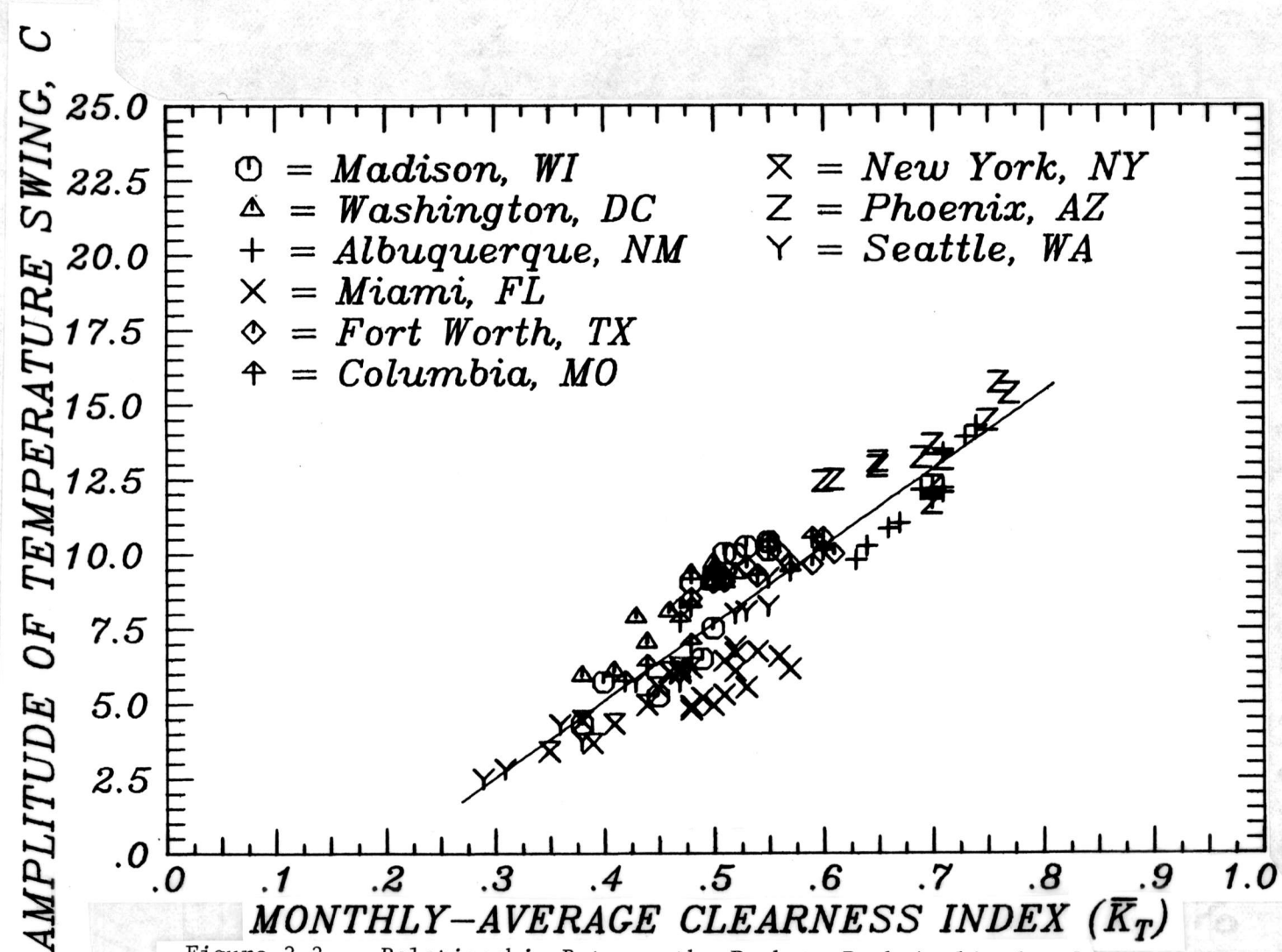

Figure 3.3 Relationship Between the Peak-to-Peak Amplitude of the Diurnal Variation of Monthly-Average Ambient Temperature and Monthly-Average Clearness Index

where A is in degrees Celsius. Although there is scatter in the comparison shown, the relationship for A provides a reasonably accurate means of estimating the monthly-average hourly ambient temperature for locations where only the monthly-average daily temperature is available.

The standard deviation of the monthly-average ambient temperature is required as input to the distribution model for T_a. It was noted above that measured values of σ_m have been published in the form of maps for the U.S. During the colder months of the year, ambient temperature is more variable than during the warmer months. This is true of both daily and monthly-average temperatures (the two being statistically related) for all nine U.S. locations investigated. Thom observed (1954b) the same trend in the temperature data he worked with. There is, however, evidence that this trend is not found consistently on other continents [Walsh (1983)]. The variability of $\overline{T}_a$ for a month from year to year is also related to the variation in $\overline{T}_a$ from month to month over the course of a year. The standard deviation of the monthly-average temperatures from the annual average temperature, σ_{yr}, provides a convenient measure of the annual variation of $\overline{T}_a$. A relationship was developed for the estimation of σ_m using the measured data.

$$\sigma_m = 1.45 - 0.0290\overline{T}_a + 0.0664\sigma_{yr} \qquad (3\text{-}12)$$

where $\overline{T}_a$ and σ_{yr} are in degrees Celsius. The diurnal variation of σ_m is small for the locations investigated, and no consistent patterns

were discernable. It is recommended that Equation (3-12) be used for both individual hours and the entire day. The measured values of σ_m are compared to Equation (3-12) in Figure 3-4. The scatter in the comparison shown is significant, but the estimated values of σ_m are of sufficient accuracy to result in accurate bin data and degree-day estimates, as demonstrated in comparisons with measured data given below.

3.3 Applications for the Ambient Temperature Distribution Function

3.3.1 Estimation Techniques

The estimation of ambient temperature bin data makes use of the cumulative distribution function. The value of Q(T) represents the fraction of the month the ambient temperature has a value less than or equal to T. Thus, the difference between $Q(T_2)$ and $Q(T_1)$ is the fraction of the month the ambient temperature is between T_2 and T_1. Once a temperature range has been chosen and divided into a number of intervals (bins), the fraction of the month that the ambient temperature is in each bin is estimated by the difference between $Q(T_u)$ and $Q(T_\ell)$, where T_u and T_ℓ are the upper and lower temperature values defining each bin. Since T_u for one bin is T_ℓ for the next (warmer) bin, Q(T) must be evaluated n+1 times for n bins. Although traditionally equally sized bins are used, bin data can be estimated for any set of bin sizes desired. The range of ambient temperature which needs to be considered when estimating bin data

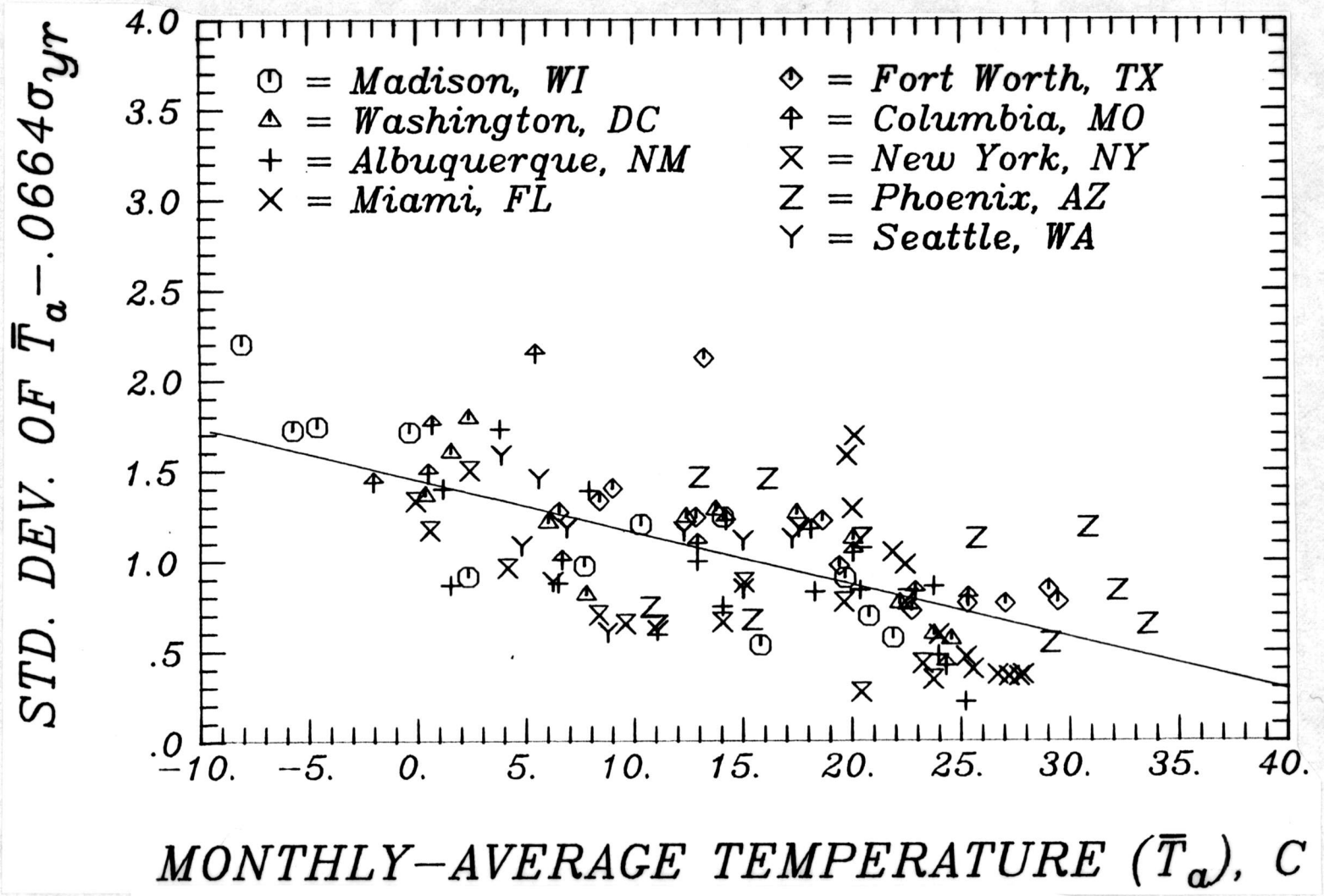

Figure 3.4 Relationship Between the Standard Deviation of Monthly-Average Ambient Temperature and Monthly-Average Ambient Temperature

for a month is given by

$$\bar{T}_a - 2\sigma_m\sqrt{N} < T_a < \bar{T}_a + 2\sigma_m\sqrt{N} \qquad (3\text{-}13)$$

where, as mentioned above, this range contains 99.8% of the hours for the month as represented by the distribution model.

When ambient temperature bin data are used, it is generally assumed that all of the hours within a bin have a temperature equal to the midpoint value for the bin. If the size of the temperature bins is relatively small, this is a good approximation. But if the temperature interval is in excess of 5°C, as a rule of thumb, the midpoint of the interval may not be a good estimate of the average value for ambient temperatures within the interval. The probability density function for ambient temperature can be integrated to obtain a more accurate value.

$$\bar{T}_{a,T1-T2} = \frac{\sigma_m\sqrt{N}[(Bh_2)\tanh(Bh_2)+\ln\cosh(Bh_1)-(Bh_1)\tanh(Bh_1)-\ln\cosh(Bh_2)]}{[B(\tanh(Bh_2) - \tanh(Bh_1))]} + \bar{T}_a \qquad (3\text{-}14)$$

where $\bar{T}_{a,T1-T2}$ is the average ambient temperature for ambient temperatures between T_1 and T_2 ($T_2 > T_1$), h_2 and h_1 are evaluated at T_2 and T_1, respectively, and B is equal to 1.698.

When calculating the average ambient temperature for all temperatures above or below a reference value, the following simplifications apply:

If $h_2 > 3$ (average for temperatures above T_1),

$$\overline{T}_{a,T1-T_{max}} = \frac{\sigma_m\sqrt{N}\,[0.69315 + \ln\cosh(Bh_1) - (Bh_1)\tanh(Bh_1)]}{[B(1 - \tanh(Bh_1))]} + \overline{T}_a \tag{3-15}$$

If $h_1 < -3$ (average for temperatures below T_2),

$$\overline{T}_{a,T_{min}-T2} = \frac{\sigma_m\sqrt{N}\,[(Bh_2)\tanh(Bh_2) - \ln\cosh(Bh_2) - 0.69315]}{[B(\tanh(Bh_2) + 1)]} + \overline{T}_a \tag{3-16}$$

The monthly-average ambient temperature for a segment of the day can be estimated using the integral of Equation (3-9). Integration of the relationship will tend to cancel the contributions of harmonics which have a period close to or less than the period over which the integration is performed. In most cases it is a good approximation to use only the first two terms of the Fourier series, which yields

$$(\overline{T}_{a,t1-t2} - \overline{T}_a) = (12/(\pi(t_2^*-t_1^*)))[0.4632(\sin(t_2^*-3.805) - \sin(t_1^*-3.805)) + 0.0984(\sin(2t_2^*-0.360) - \sin(2t_1^*-0.360))] \tag{3-17}$$

where $\overline{T}_{a,t1-t2}$ is the monthly-average temperature for the hours of the day between t_1 and t_2.

3.3.2 Comparison with Measured Data

The expression for Q(h) given in Equation (3-7) was used to estimate monthly bin data for each location, which were then summed over all 12 months to create 9 sets of estimated annual bin data. The values of $\overline{T}_a$ used were averages from the measured data, while σ_m was both calculated from the measured data and estimated from Equation (3-12). Annual bin data were also developed from the long-term hourly temperature measurements for each location. A bin size of 5°F was chosen to allow comparisons between the SOLMET data and data published by the Air Force. The measured bin data (heavy solid lines), bin data estimated using values of σ_m calculated from the hourly data (solid lines) and bin data estimated using values of σ_m obtained from Equation (3-12) (dashed lines) are compared in Figure 3.5.

The estimated bin data are within 10% of the measured bin data for most bins. The general shape and the range of the measured data are reproduced in the estimated data with a few exceptions. In Madison, the skewing of the temperature distributions towards 32°F in the winter months leads to a peak in the measured bin data which is not present in the estimated bin data due to the symmetric nature of the distribution model. Skewness in the measured data for Albuquerque and Phoenix, with the degree and direction of skewness a function of the time of year, leads to a flatter profile in the measured bin data than is predicted. The bin data estimated using

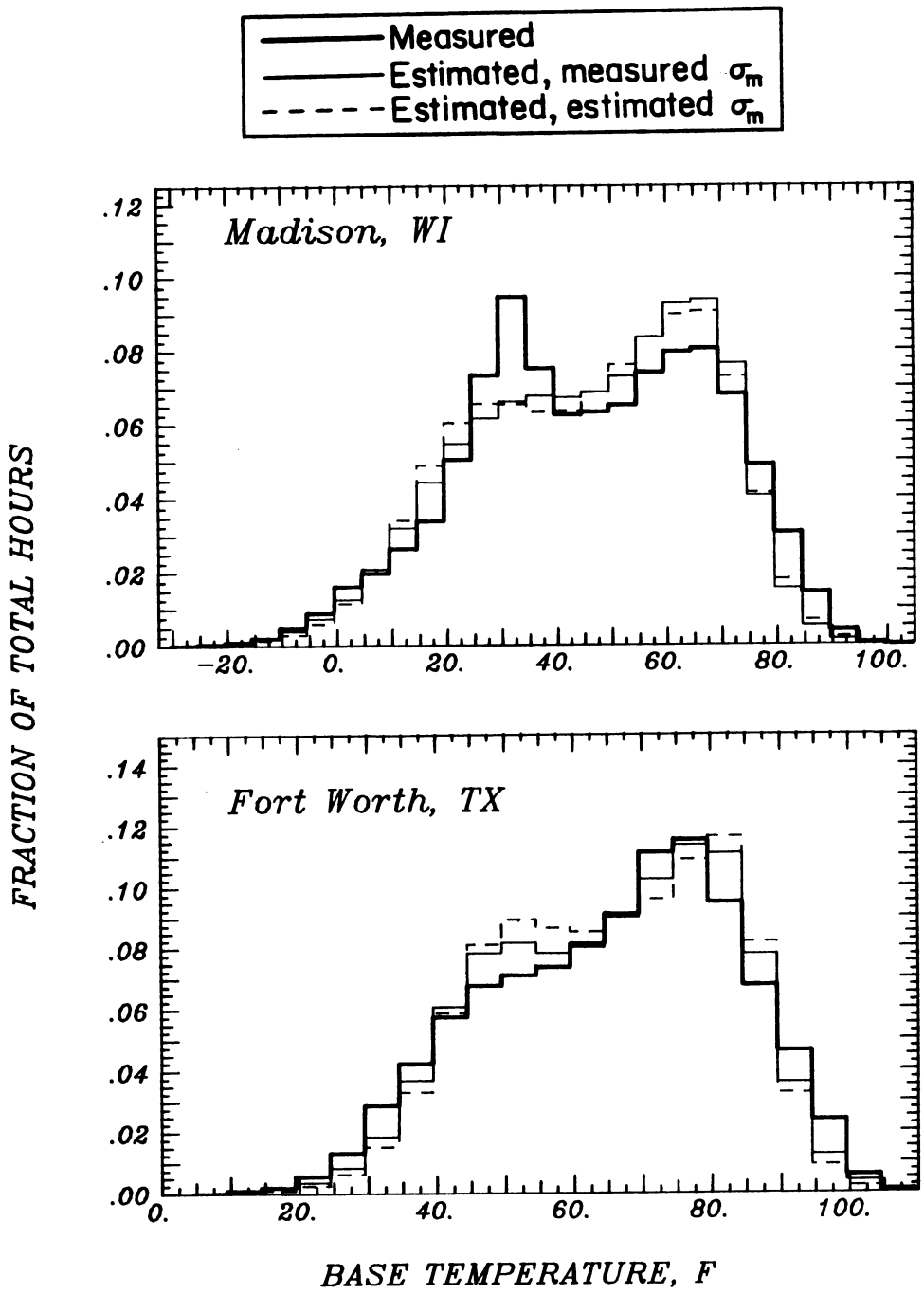

Figure 3.5 Measured and Estimated Ambient Temperature Bin Data for 9 SOLMET Locations

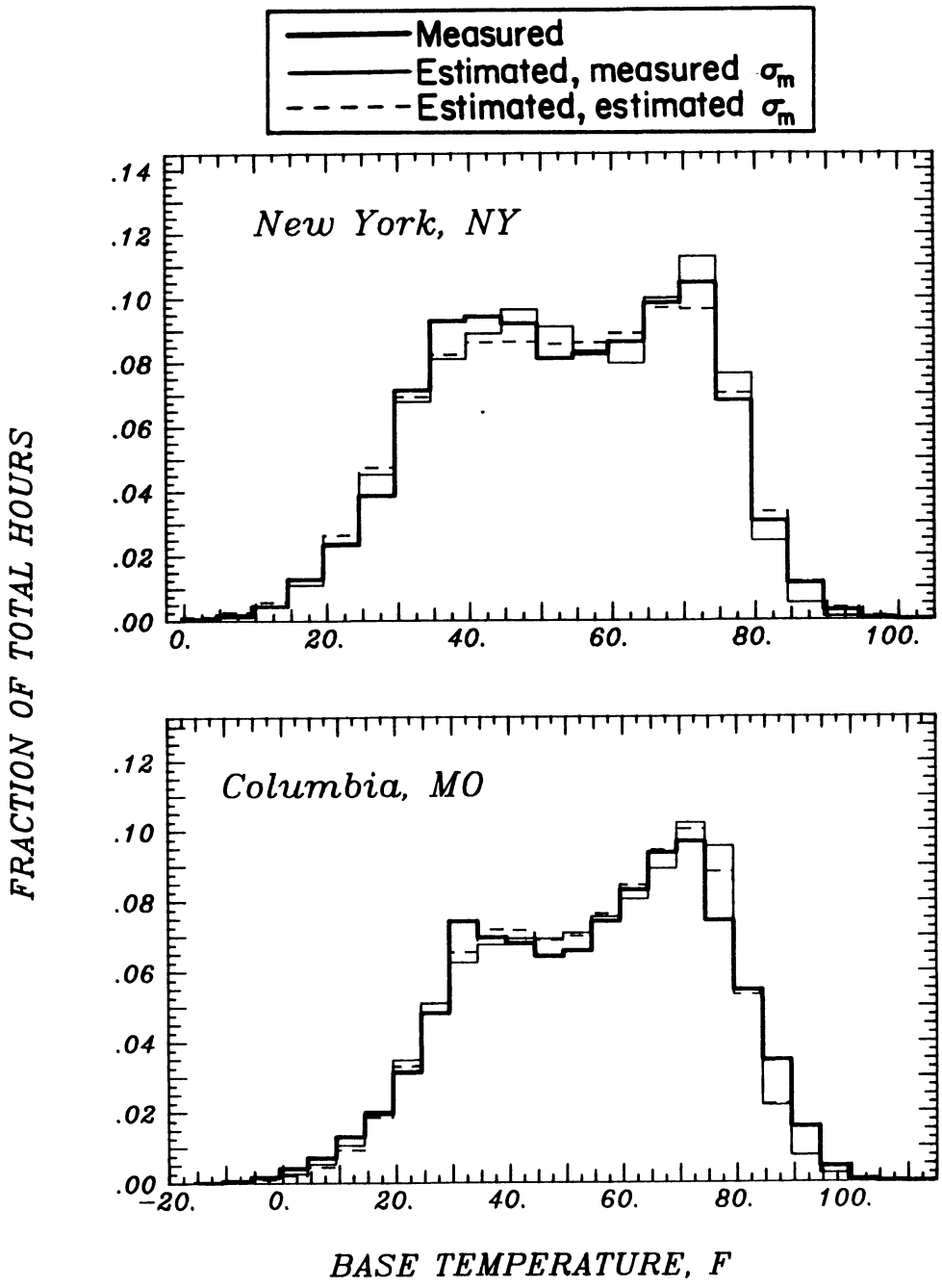

Figure 3.5 (cont.)

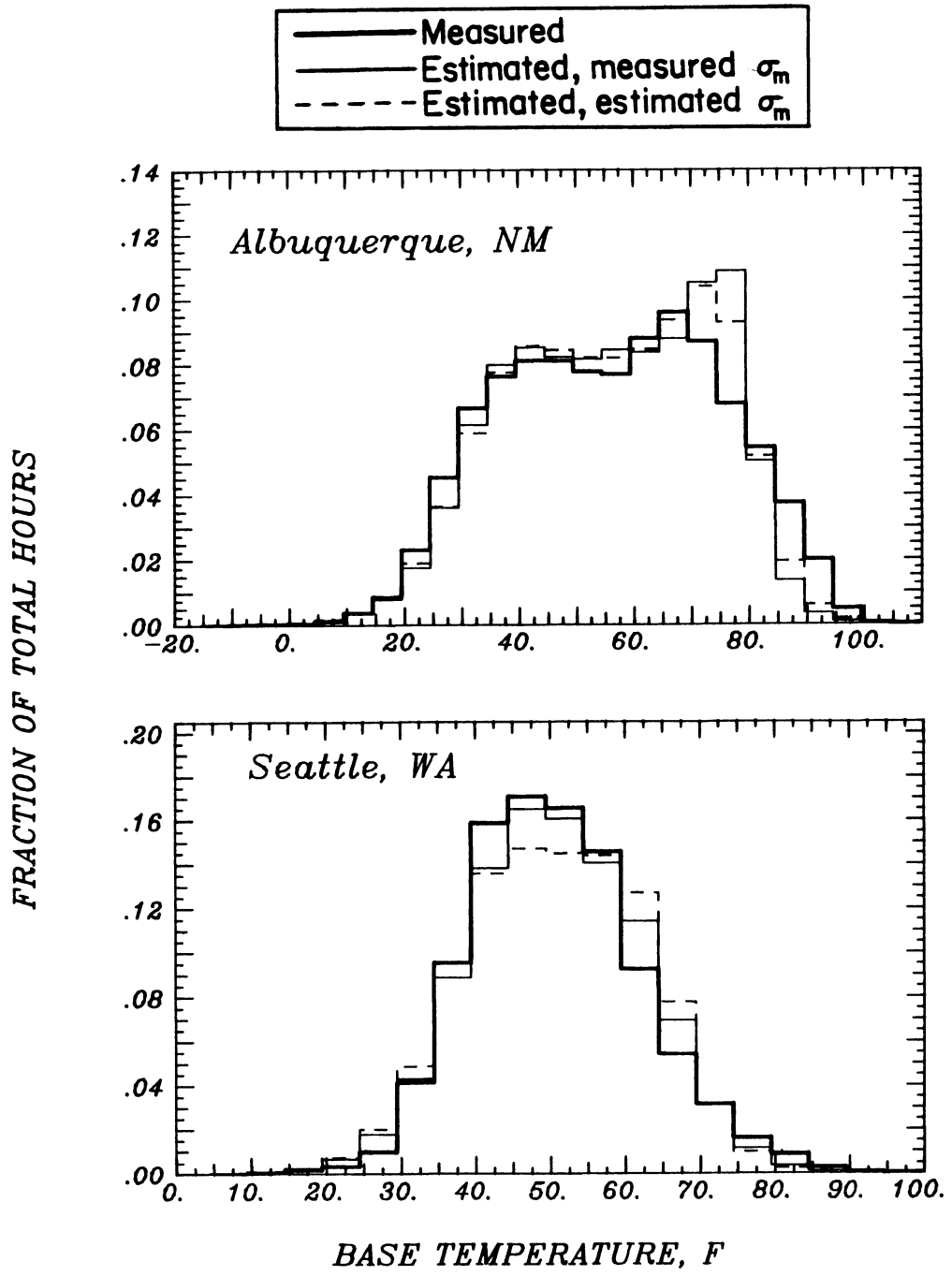

Figure 3.5 (cont.)

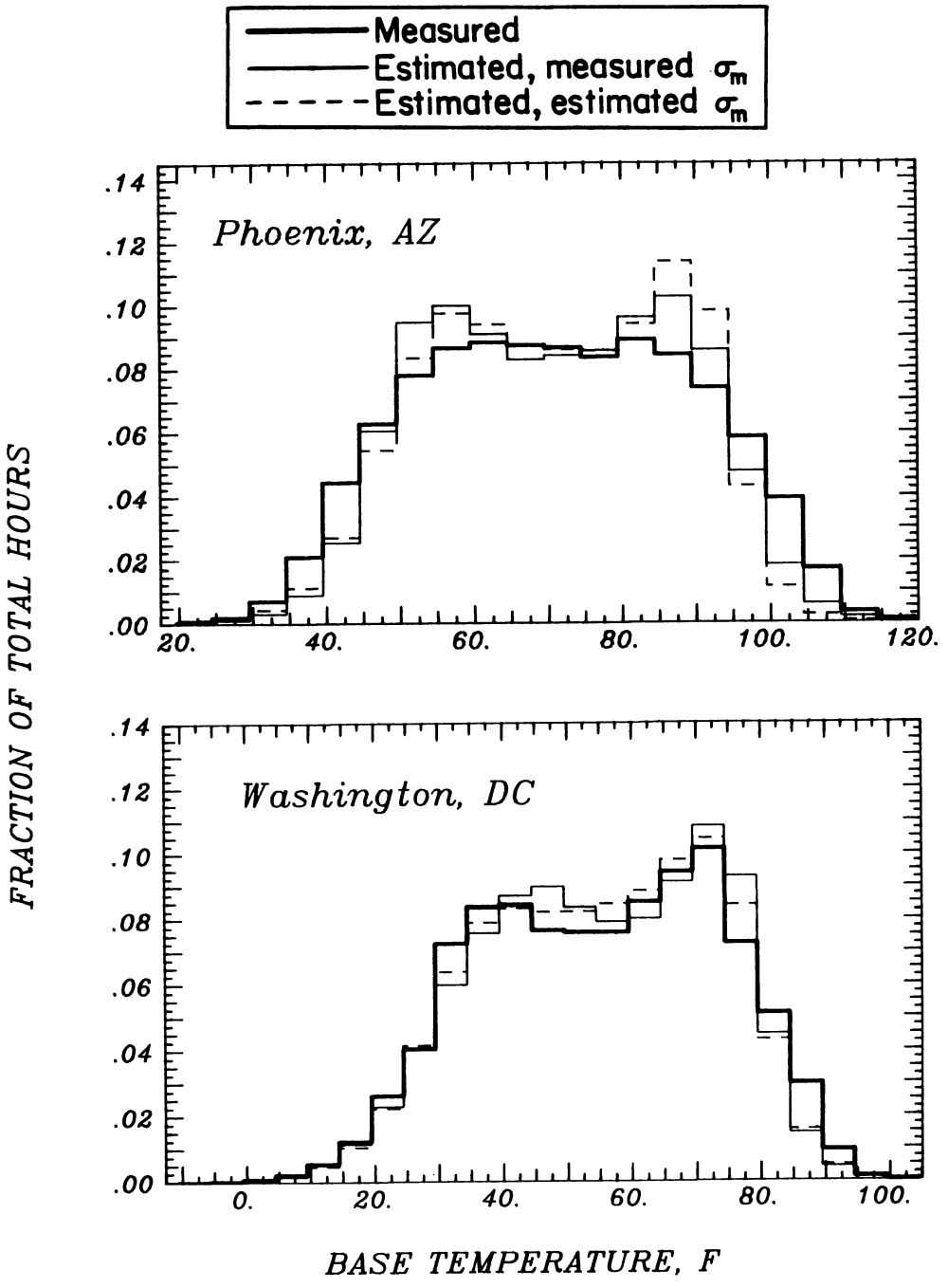

Figure 3.5 (cont.)

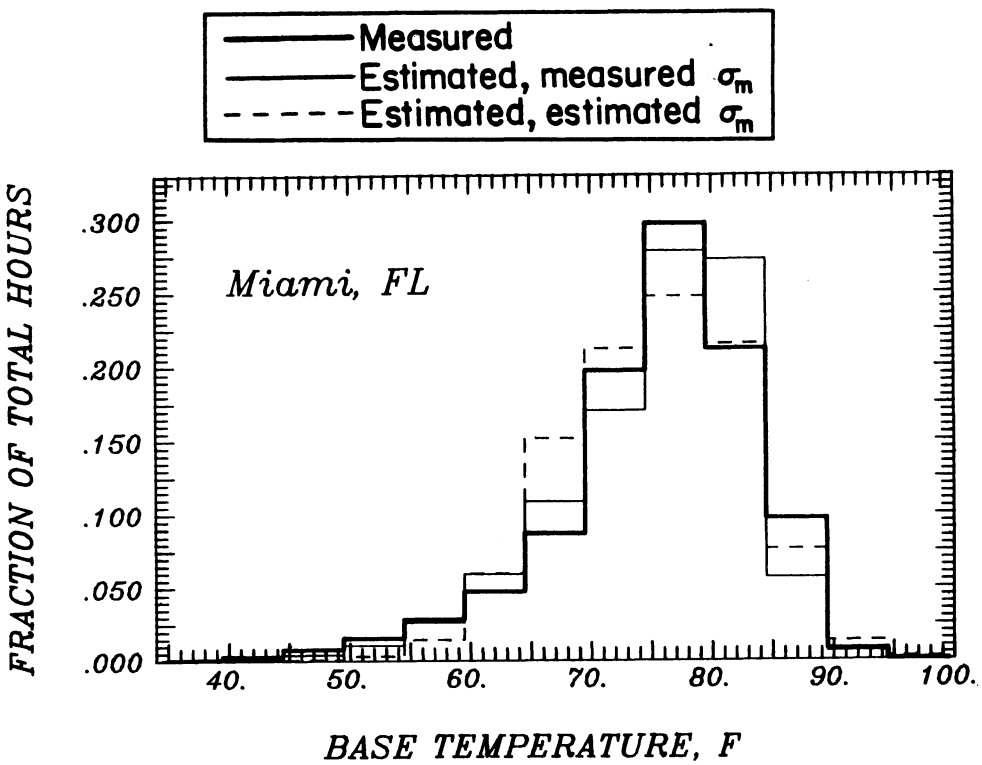

Figure 3.5 (cont.)

estimated values of σ_m are comparable in accuracy to the bin data estimated using measured values of σ_m for the 9 locations.

Annual ambient temperature bin data were also obtained from the Air Force (1978) for 12 locations, 8 of which are locations not included in the SOLMET station network. The Air Force bin data for the 4 locations for which SOLMET data are also available are not significantly different from the SOLMET data, indicating the Air Force bin data are representative of long-term average conditions. The data for the remaining 8 locations provide an independent test of the ambient temperature distribution function. Values of $\overline{T}_a$ were obtained from Knapp (1980) and used as input to Equations (3-7) and (3-12). The measured annual bin data (solid lines) and the estimated annual bin data (dashed lines) are compared in Figure 3.6.

The agreement between the estimated and measured bin data for the Air Force locations is qualitatively similar to the agreement observed for the SOLMET locations. The spike in the Barrow data is at 32°F; similar peaks (although not as severe) are also present in the measured data for Albany, Glascow and Harrisburg. The measured data for Reno are skewed during the warmer months, causing a single peak in the measured data even though the monthly-average temperature is different for each month. Although systematic differences exist between the measured and estimated data for individual locations, the symmetric distribution model represents a good compromise for the wide range of climates investigated.

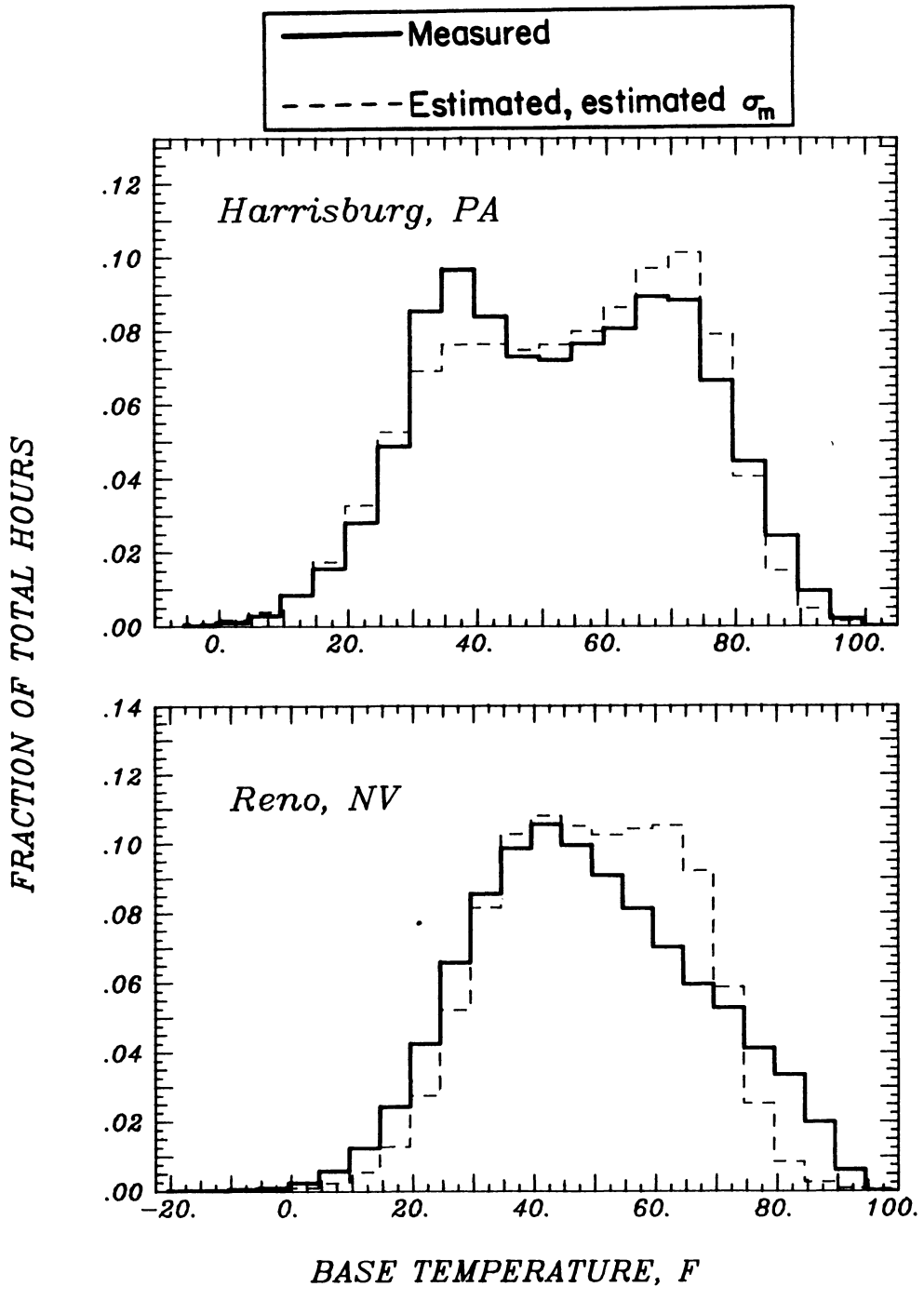

Figure 3.6 Measured and Estimated Ambient Temperature Bin Data for 8 Air Force Locations

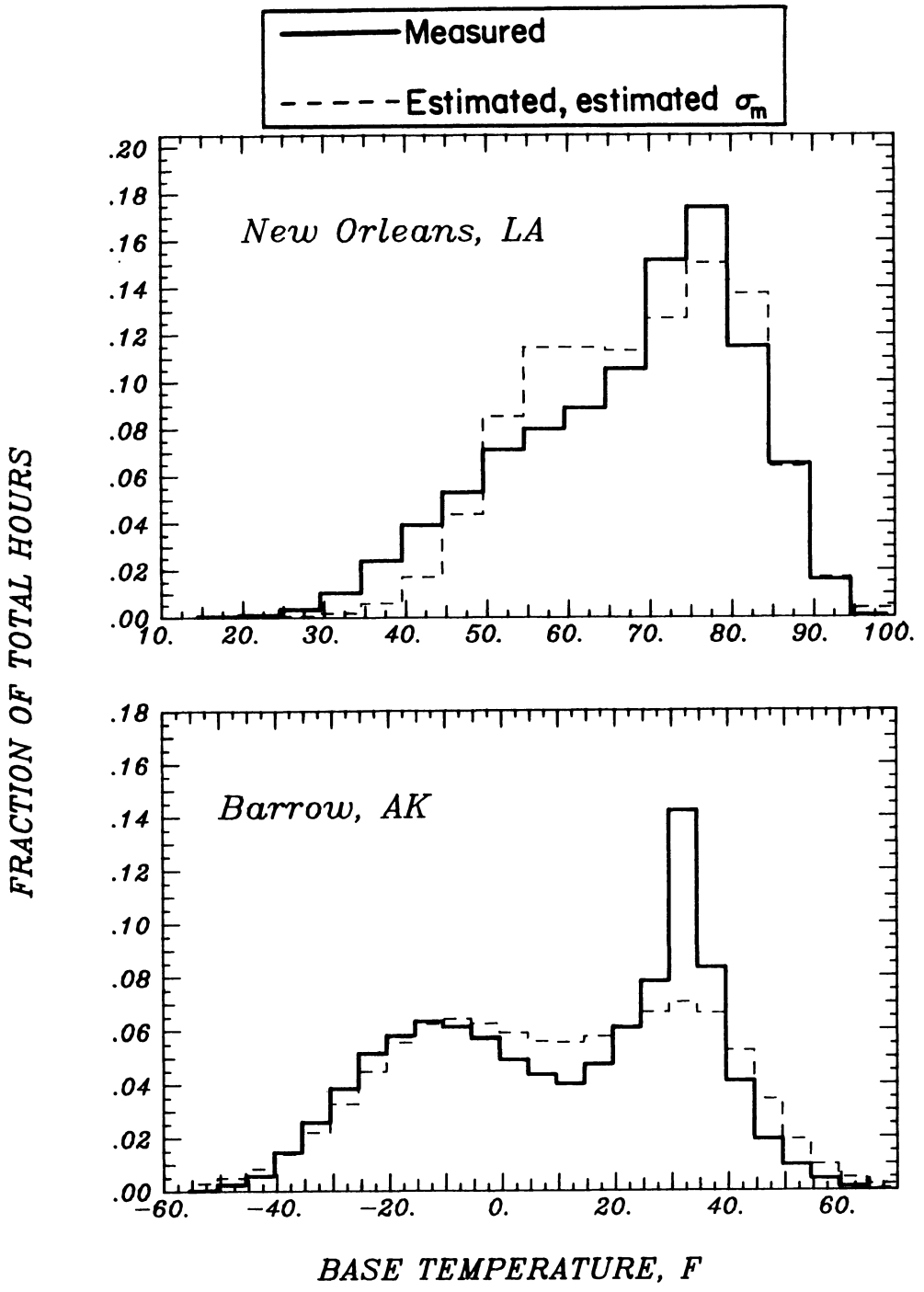

Figure 3.6 (cont.)

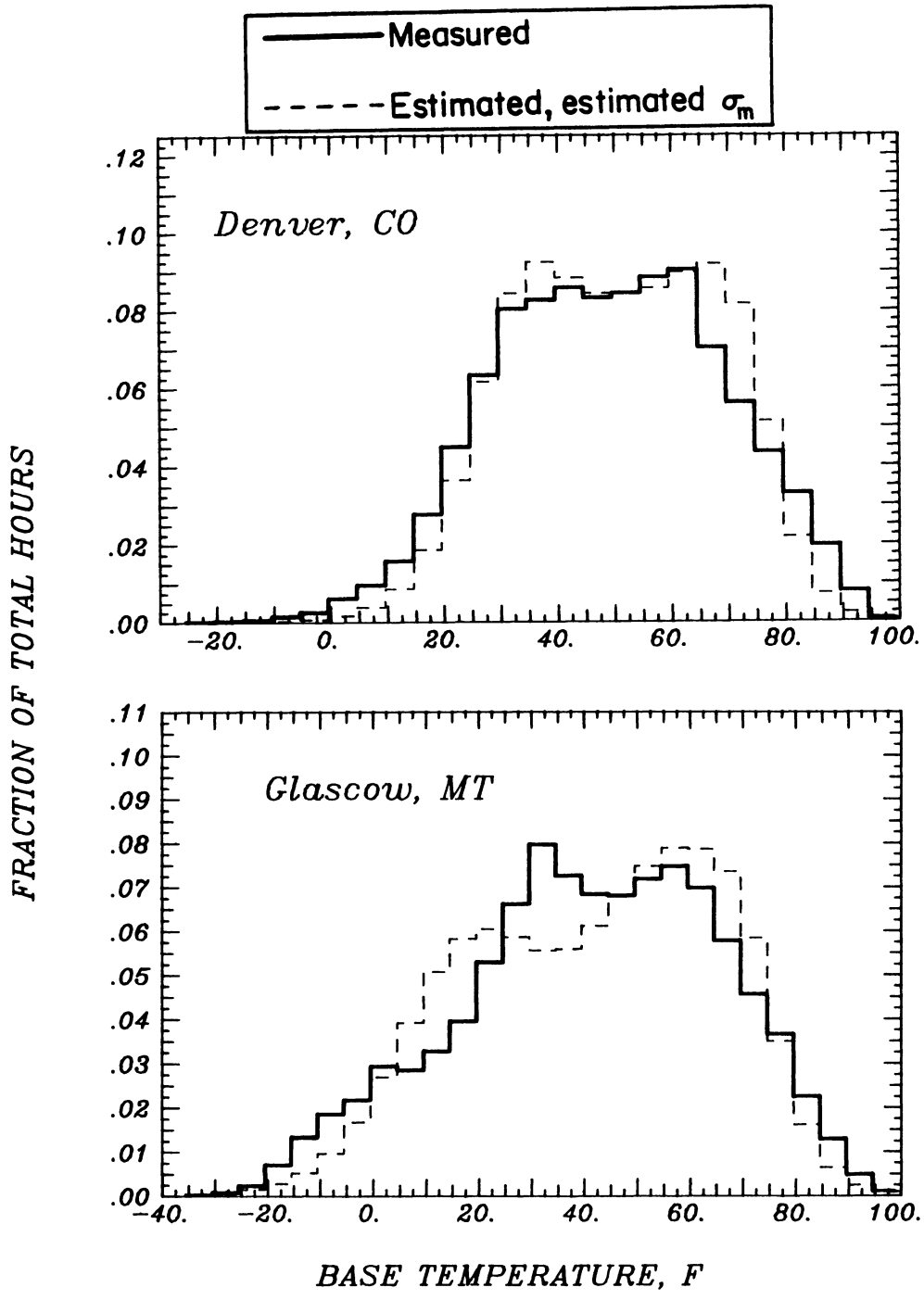

Figure 3.6 (cont.)

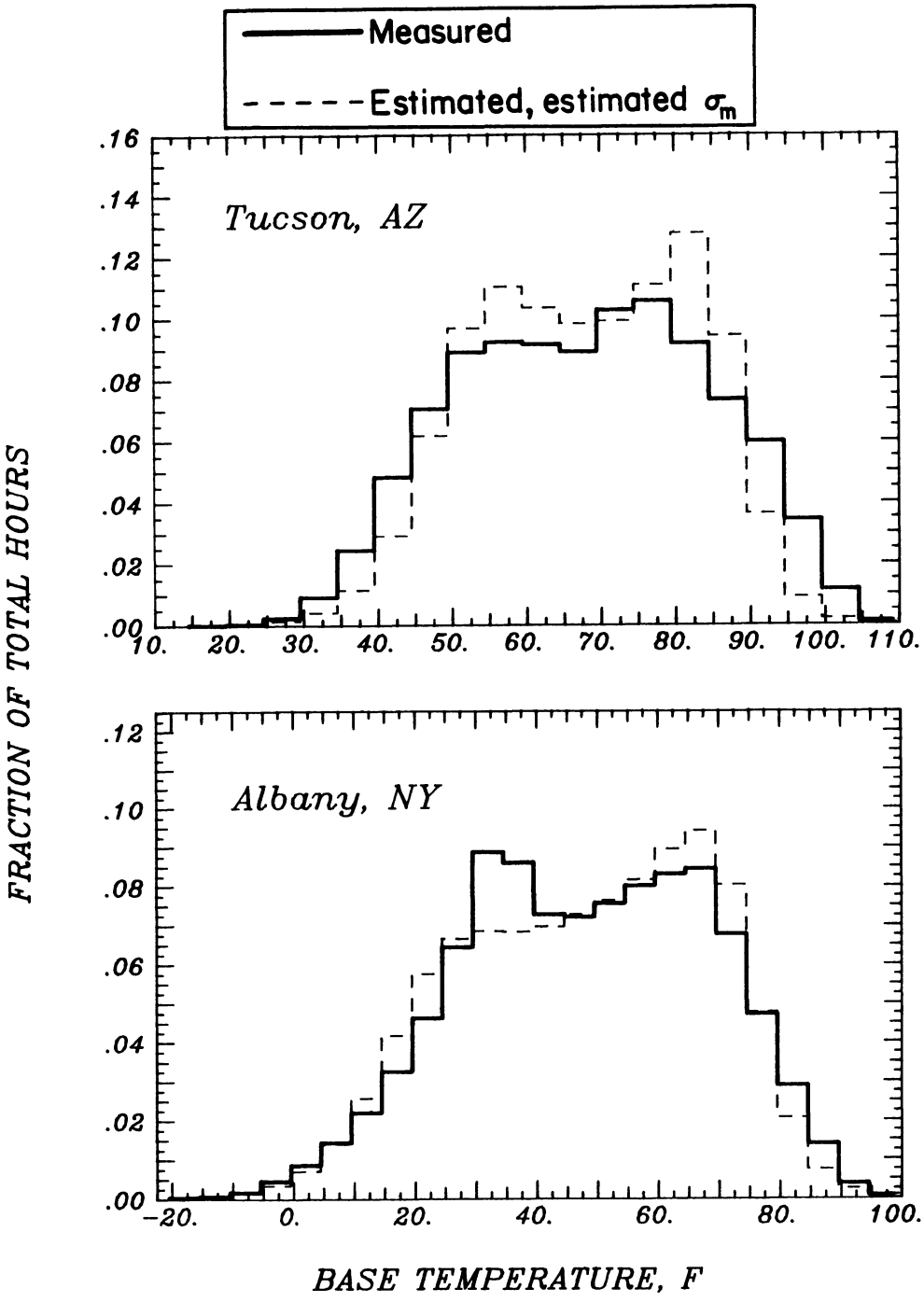

Figure 3.6 (cont.)

3.4 A Distribution Model for Degree-Days

3.4.1 Model Development

A relationship for the estimation of heating degree-days was derived by integration of the cumulative distribution model for ambient temperature. The general form of the integral was given in Equation (2-10). The independent variable was changed from T to h, and the integration performed. The constant of integration was evaluated using the boundary condition that for a base temperature below the minimum ambient temperature, there are no heating degree-days. The result is

$$D_H(T_b) = \sigma_m N^{3/2}[h/2. + \ln \cosh(Bh)/2 + 0.2041] \qquad (3\text{-}18)$$

where N is the number of days in the month and D_H has units of degree-days.

The degree-day relationship can also be used for an hour of the day or part of the day by using the monthly-average temperature for the hours of interest in the evaluation of h and multiplying Equation (3-18) by the fraction of the day included. Since the temperature distribution model is symmetric about the mean, cooling degree-days, D_C, can be estimated from Equation (3-18) by replacing D_H with D_C and h with h^*, where h^* is defined by

$$h^* \equiv (\overline{T}_a - T_b)/(\sigma_m\sqrt{N}) \qquad (3\text{-}19)$$

Cooling degree-days can also be estimated for any part of the day by

replacing $\overline{T}_a$ with the appropriate average and multiplying by the fraction of the day considered. D_C can also be found using Equation (2-9) if the heating and cooling base temperatures are the same.

Solar and other internal gains can lead to values of base temperature well below the thermostat setting, T_r. Cooling loads which occur when the ambient temperature is between the base and thermostat temperatures can be satisfied, at least in part, by ventilating the structure with ambient air. The reduction in the cooling load due to ventilation is not accounted for in the relationship given above for D_C (or in tabulated cooling-degree days). When ambient air is used to supply cooling, ventilation cooling degree-days, D_{CV}, should be used in place of traditional cooling degree-days.

Ventilation cooling degree-days accumulate differently than traditional cooling degree-days during those hours when the ambient temperature is between the base and thermostat setpoint temperatures. The same cooling degree-days accumulate for those hours when the ambient temperature is above T_r whether the structure is ventilated or not.

The cooling degree-days for hours having a temperature greater than T_r, but for a base temperature of T_b is calculated in two parts. First, the cooling degree-days for a base temperature of T_r is estimated. Then, the increase in cooling degree-days for each hour resulting from a lowering of the base temperature from T_r to T_b is added to the cooling degree-days for a base temperature T_r. This

increase is given by the product of the number of hours the ambient temperature is above T_r, $(1 - Q(T_r))$, and the change in temperature elevation above the base temperature, $(T_r - T_b)$, for each of these hours.

The ventilation cooling degree-days for those hours when the ambient temperature is between T_b and T_r are handled by treating the ventilation as an internal cooling source and allowing the base temperature for these hours to be a function of the ambient temperature and the ventilation rate. The cooling rate supplied by ventilation is $\dot{m}C_p(T_r - T_a)$, where $\dot{m}C_p$ is the capacitance rate of the ventilation flow stream. The cooling degree-days are then evaluated by performing the integration indicated in Equation (2-8), but only over the temperature range from T_b to T_r and using T_b' in place of T_b, where

$$T_b' = T_b + \dot{m}C_p(T_r - T)/(UA) \qquad (3\text{-}20)$$

The overall conductance for the building, (UA), excludes the conductance associated with the ventilation air. Equation (3-8) was substituted into Equation (2-8) for the PDF, the independent variable was changed from T to h and the integration performed.

The degree-day expression for ambient temperatures between T_b and T_r is added to the expression representing the ventilation cooling degree-days for ambient temperatures greater than T_r, resulting in the following relationship for D_{CV}:

$$D_{CV} = \left[\frac{\sigma_m N^{3/2}}{2B}\right]\left[\frac{\dot{m}C_p+(UA)}{(UA)}\right]\Big(\ln\cosh(Bh^*_{bv})-\ln\cosh(Bh^*_r) + [(Bh^*_r)-(Bh^*_{bv})]\tanh(Bh^*_r)\Big) + D_C(T_r) + N[1 - Q(T_r)](T_r - T_b) \quad (3\text{-}21)$$

where h^*_{bv} is evaluated at a temperature of T_{bv} and h^*_r at a temperature of T_r, and where T_{bv} is given by

$$T_{bv} = [(UA)T_b + \dot{m}C_pT_r]/[(UA) + \dot{m}C_p] \quad (3\text{-}22)$$

For a ventilation rate of zero, the value of D_{CV} given by Equation (3-21) is equal to the value of D_C given by Equation (3-18). For an infinite ventilation rate, T_{bv} is equal to T_r, and only the last two terms in Equation (3-21), which represent cooling degree-days for values of T_a above T_r, remain.

3.4.2 Comparison of Measured and Estimated Degree-Days

The hourly temperature records for the 9 SOLMET locations were used to calculate annual heating and cooling degree-days. The base temperatures considered were between 1 and 20°C for heating and between 10 and 29°C for cooling. Heating and cooling degree-days were then estimated from Equations (3-18) and (3-19) on a monthly basis, and the monthly values were summed to give annual totals. Values of $\overline{T}_a$ were calculated from the hourly data, while σ_m was both calcu-

lated from the hourly data and estimated from Equation (3-12). The degree-day relationships developed by Thom were also used to estimate annual heating and cooling degree-days from measured values of $\overline{T}_a$ and σ_m. Annual bias errors were determined as a function of base temperature for each estimation procedure.

The annual heating degree-days calculated from the hourly temperature measurements are represented by the heavy solid lines in Figure 3.7. The remaining lines in the figure represent the absolute values of the annual bias errors for the estimation procedures used. The solid lines are for Equation (3-18) and measured σ_m, the short dashes are for Equation (3-18) and estimated σ_m and the alternating long and short dashes are for Thom's method and measured σ_m.

The estimated annual heating degree-days are within 175°C-days of the measured values at all 9 locations for the range of base temperatures considered. Measured values of σ_m result in somewhat more accurate estimates when Equation (3-18) is used. Although Thom's method is more accurate for Seattle, Equation (3-18) has a smaller combined error for the 9 locations. The errors for the 3 estimation procedures are generally within 50°C-days on an annual basis.

The heating degree-day estimates compared in Figure 3.7 do not include the diurnal variation of ambient temperature, as $\overline{T}_a$ was used as input. The estimation of annual heating degree-days with the 3 procedures was repeated, but on an hourly basis. Measured

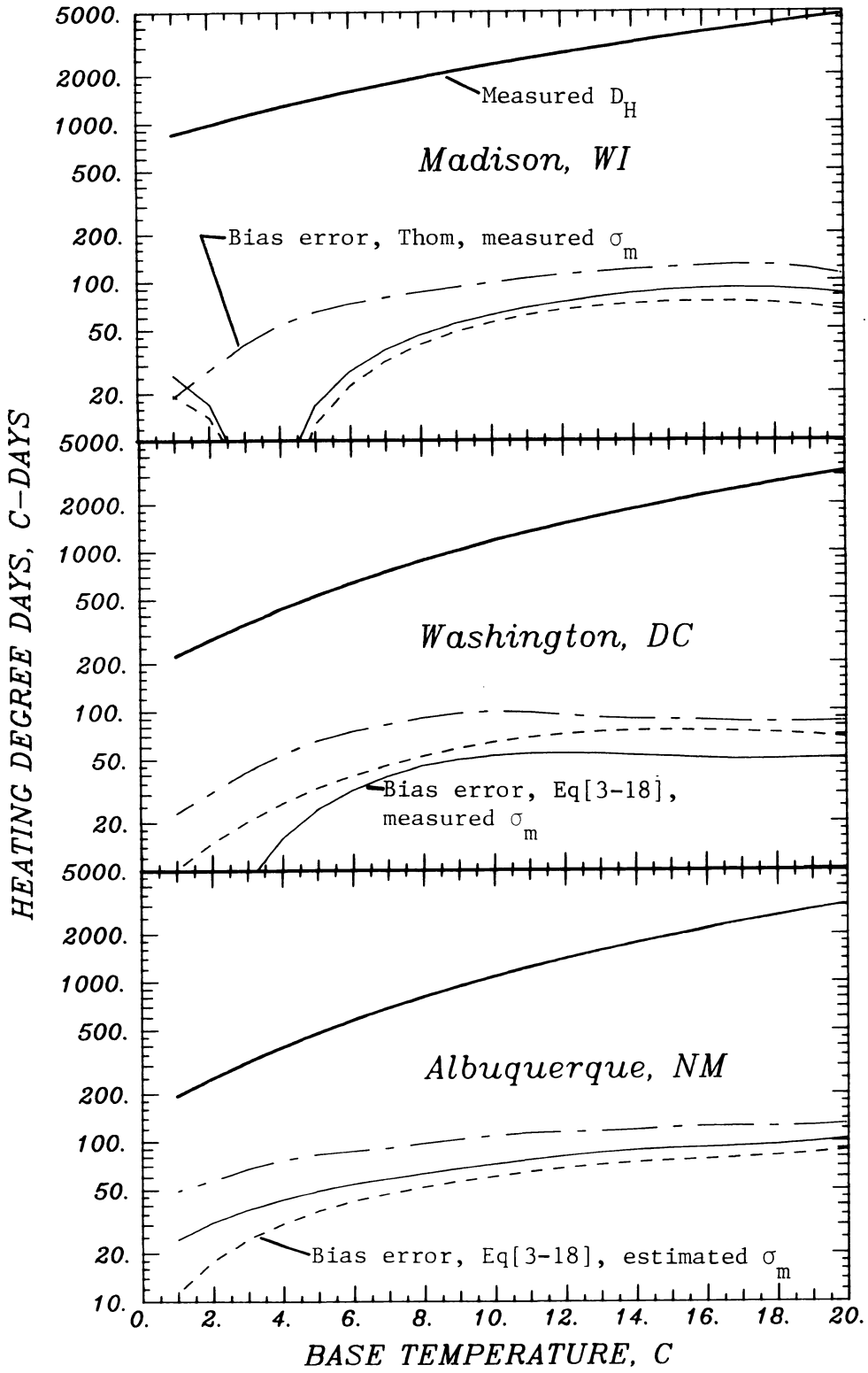

Figure 3.7 Measured Annual Heating Degree-Days and Bias Errors for Degree-Days Estimated on a Daily Basis

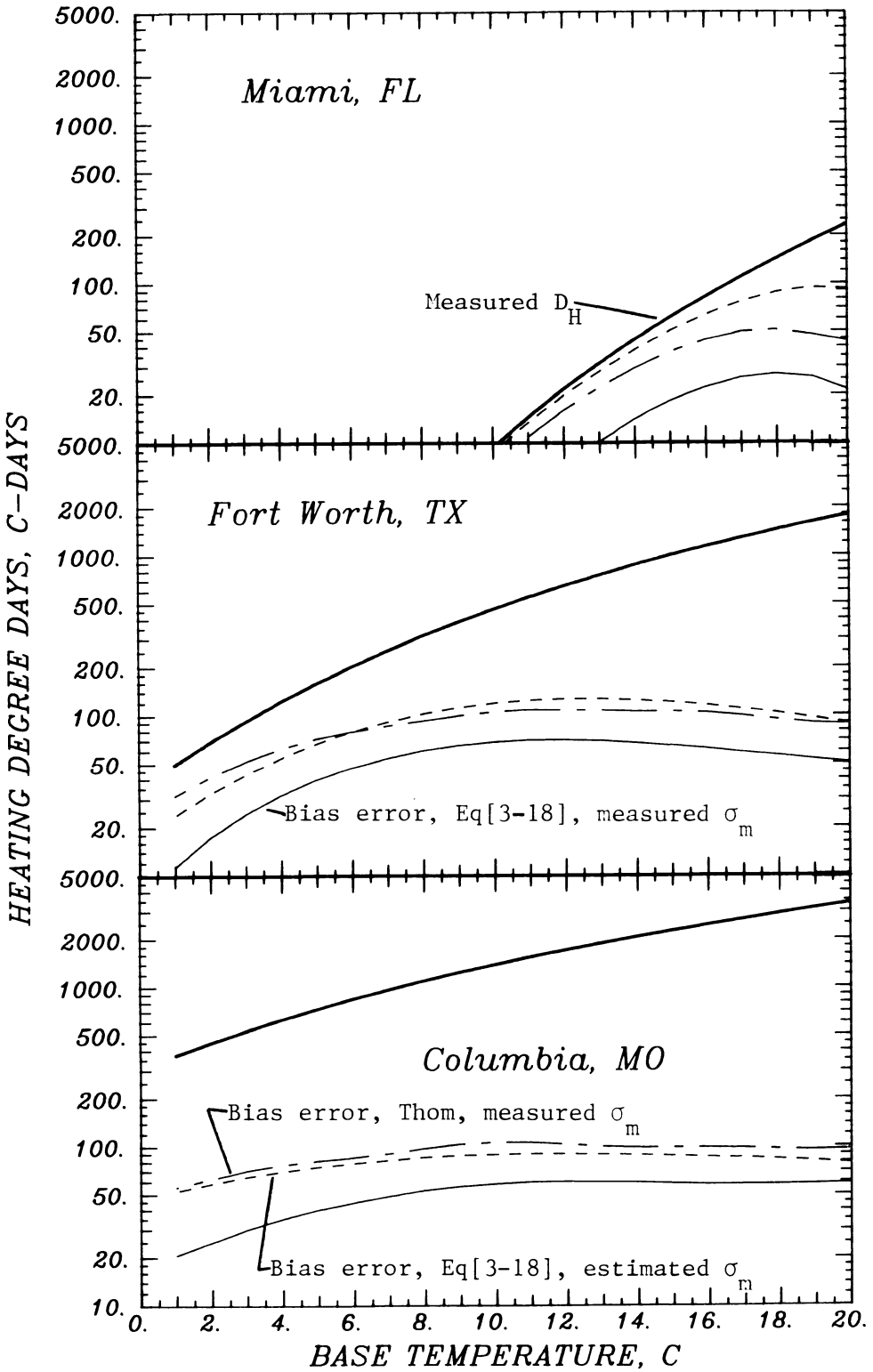

Figure 3.7 (cont.)

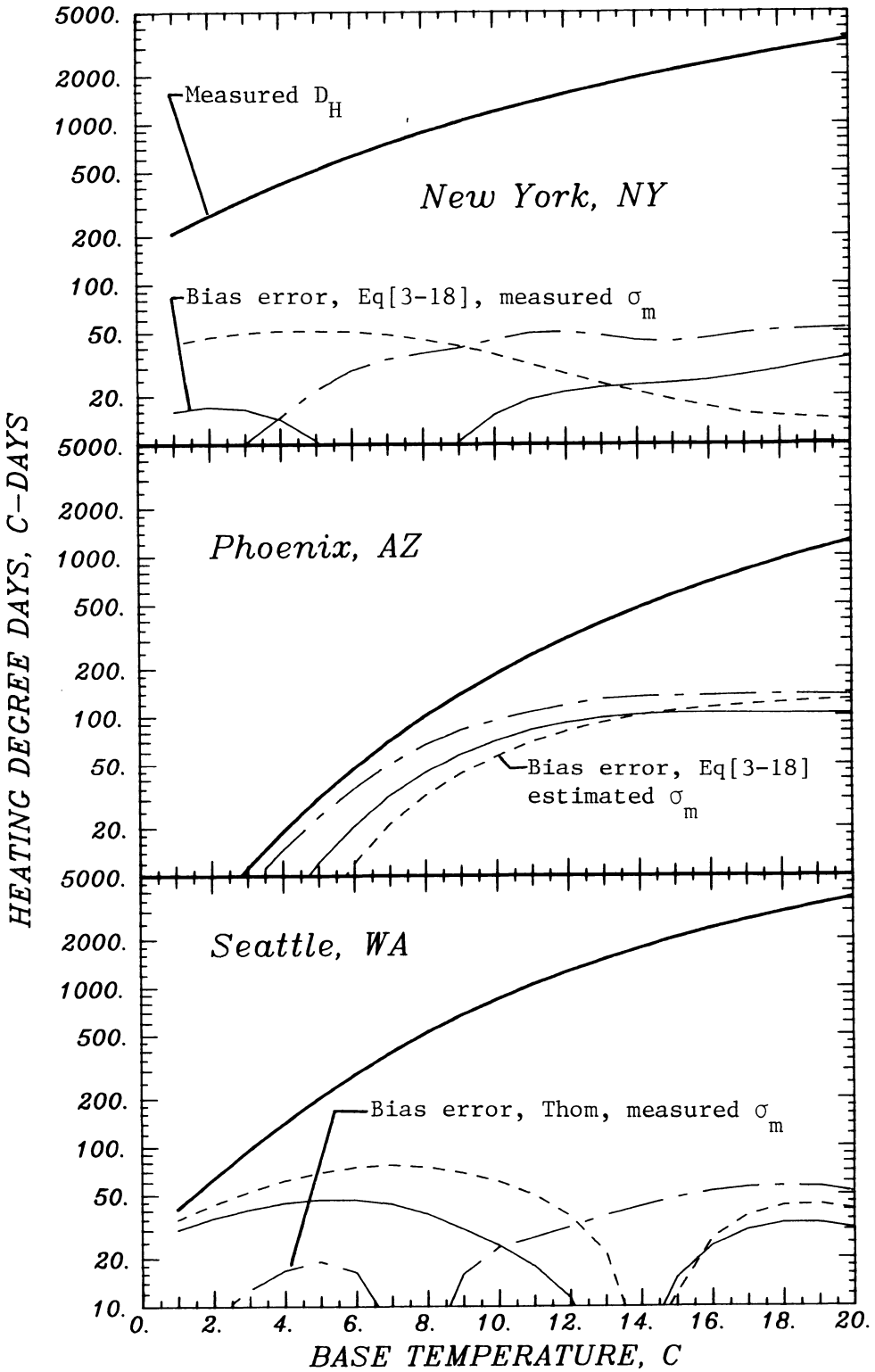

Figure 3.7 (cont.)

values of $\overline{T}_a$ and $\overline{K}_T$ were used as input to Equations (3-9) and (3-11) to estimate values of $\overline{T}_{a,h}$ for each month. The degree-days for each hour of the day were summed to give daily totals for each month, and the monthly totals summed to give annual totals. The daily value of σ_m (measured and estimated) was used for each hour of the day. The annual bias errors for the degree-days estimated on an hourly basis are shown in Figure 3.8. Some improvement in accuracy is obtained by including the diurnal variation of monthly-average ambient temperature, with the largest reduction in errors occurring at the locations having the largest diurnal variation in $\overline{T}_{a,h}$.

Cooling degree-days were also estimated with the 3 procedures described above. The comparisons for estimates obtained using daily calculations and measured values of $\overline{T}_a$ are shown in Figure 3.9. The largest bias error is 150°C-days. Equation (3-18) is more accurate on the average than Thom's relationship, although the difference in accuracy is slight. The use of estimated values of σ_m results in cooling degree-day estimates comparable in accuracy to estimates obtained using measured values of σ_m. The cooling degree-days estimated on an hourly basis are compared to the measured data in Figure 3.10. The improvement in accuracy which results from the inclusion of the diurnal variation of ambient temperature is more pronounced for cooling degree-days than for heating degree-days.

While the degree-days calculated from the data in the present study used hourly values of temperature, the degree-days published

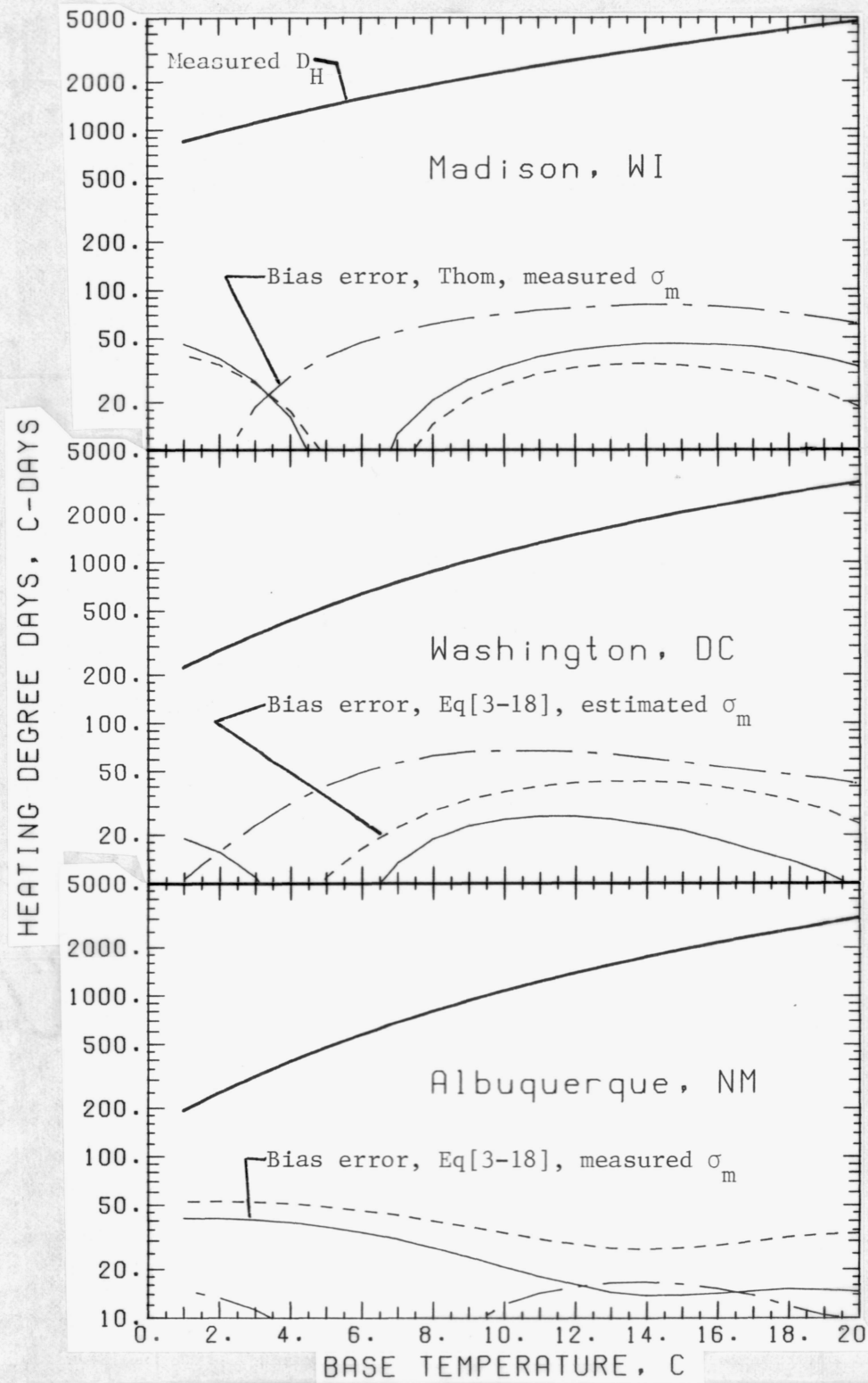

Figure 3.8 Measured Annual Heating Degree-Days and Bias Errors for Degree-Days Estimated on an Hourly Basis

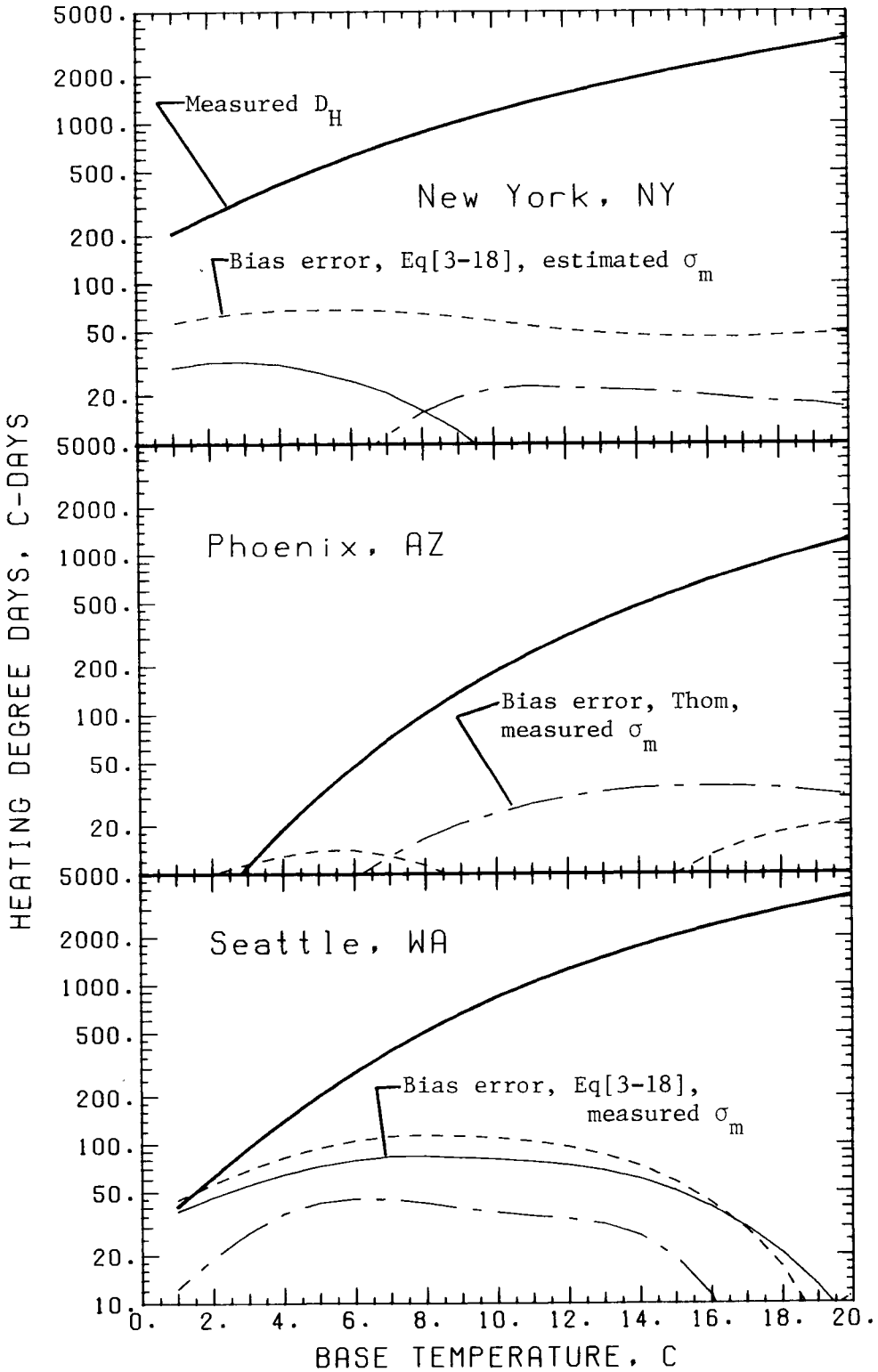

Figure 3.8 (cont.)

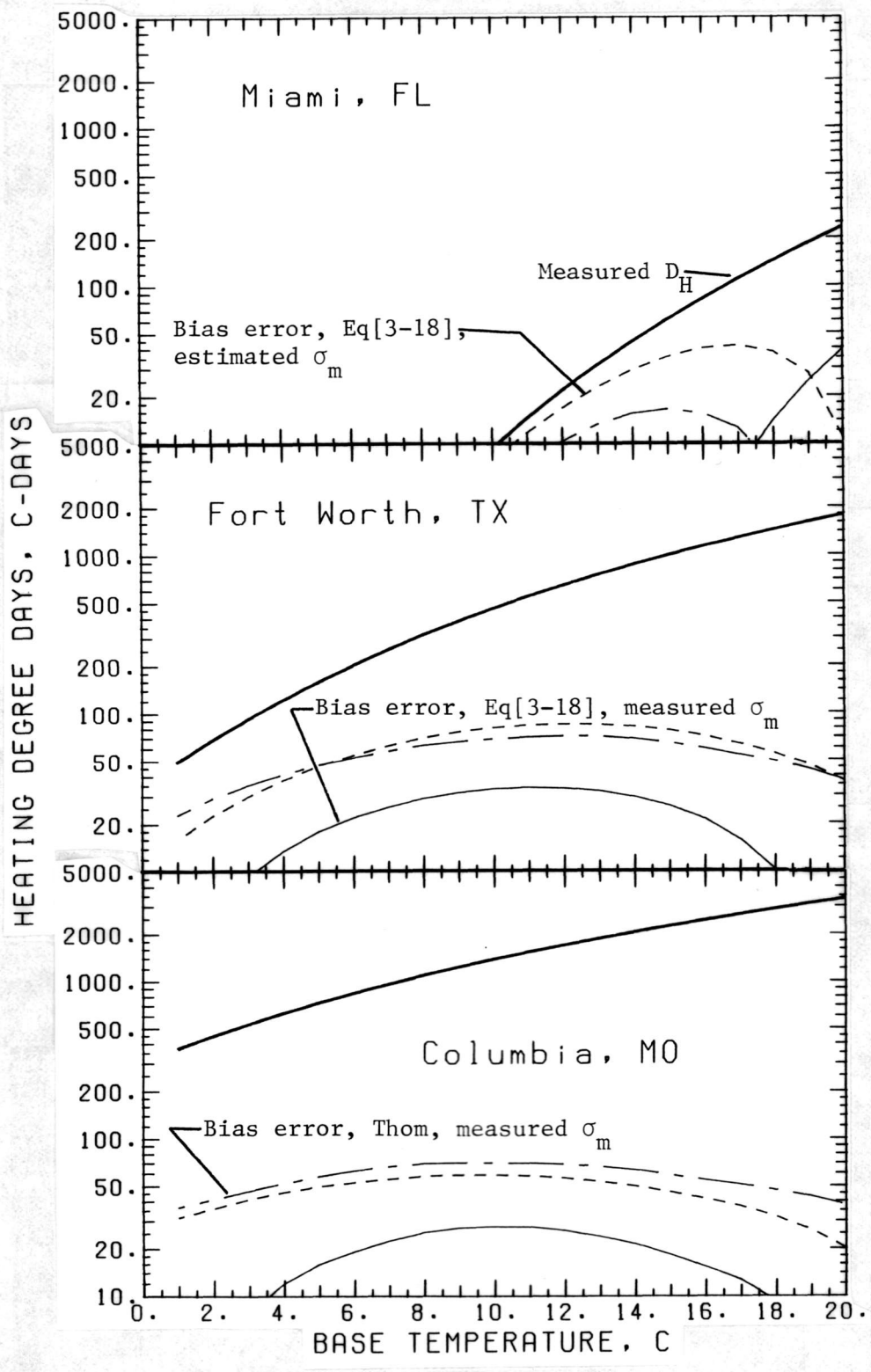

Figure 3.8 (cont.)

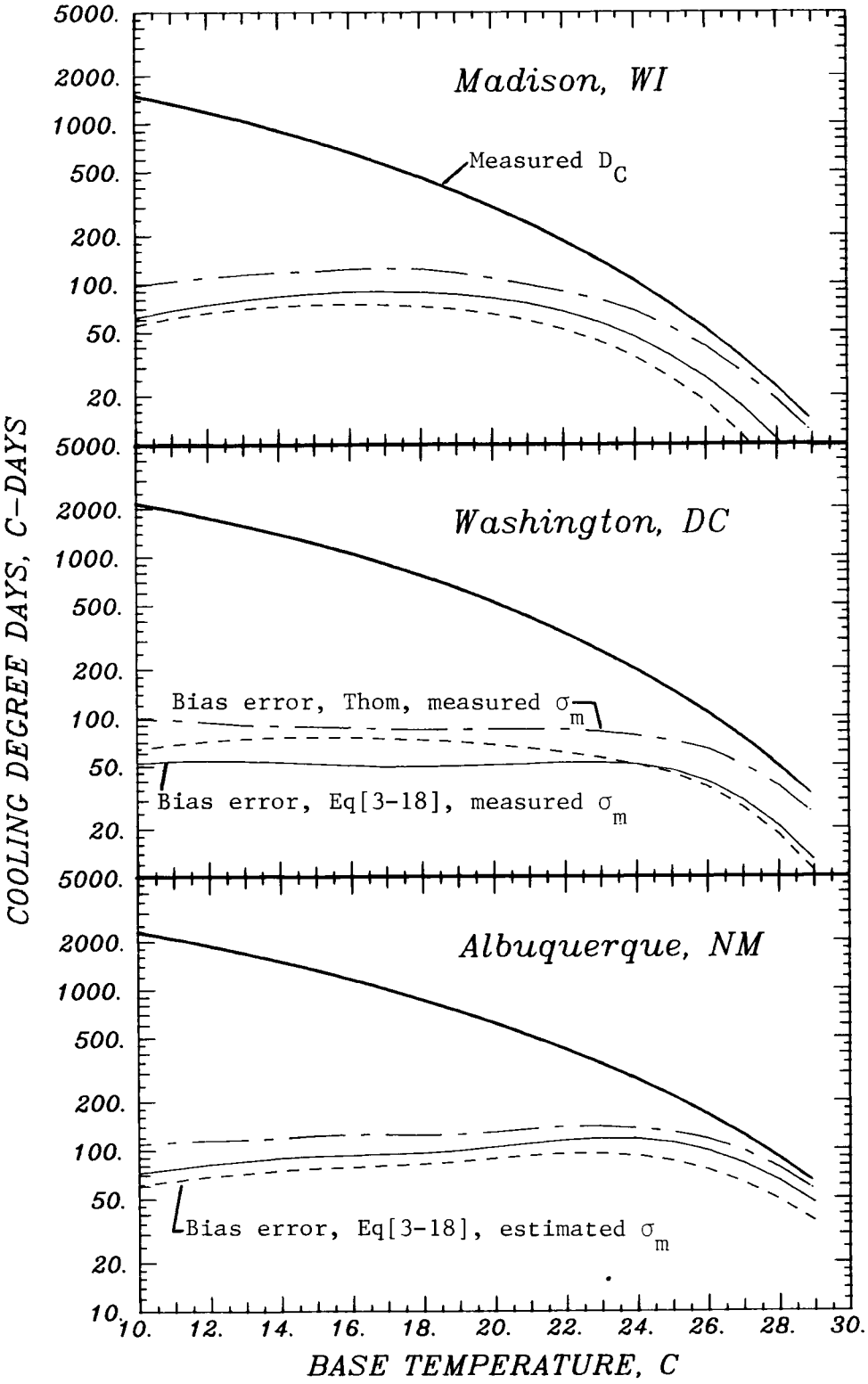

Figure 3.9 Measured Annual Cooling Degree-Days and Bias Errors for Degree-Days Estimated on a Daily Basis

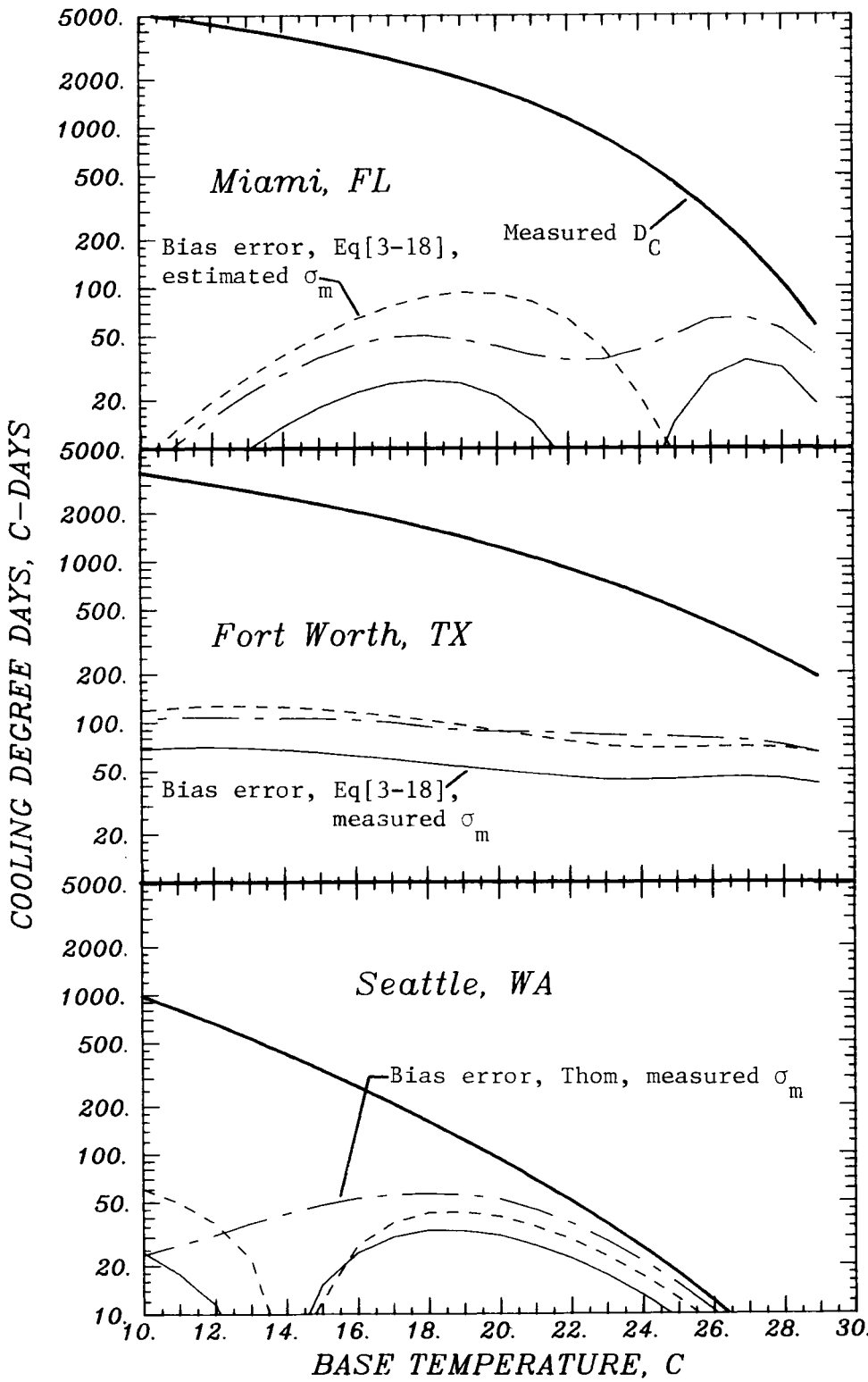

Figure 3.9 (cont.)

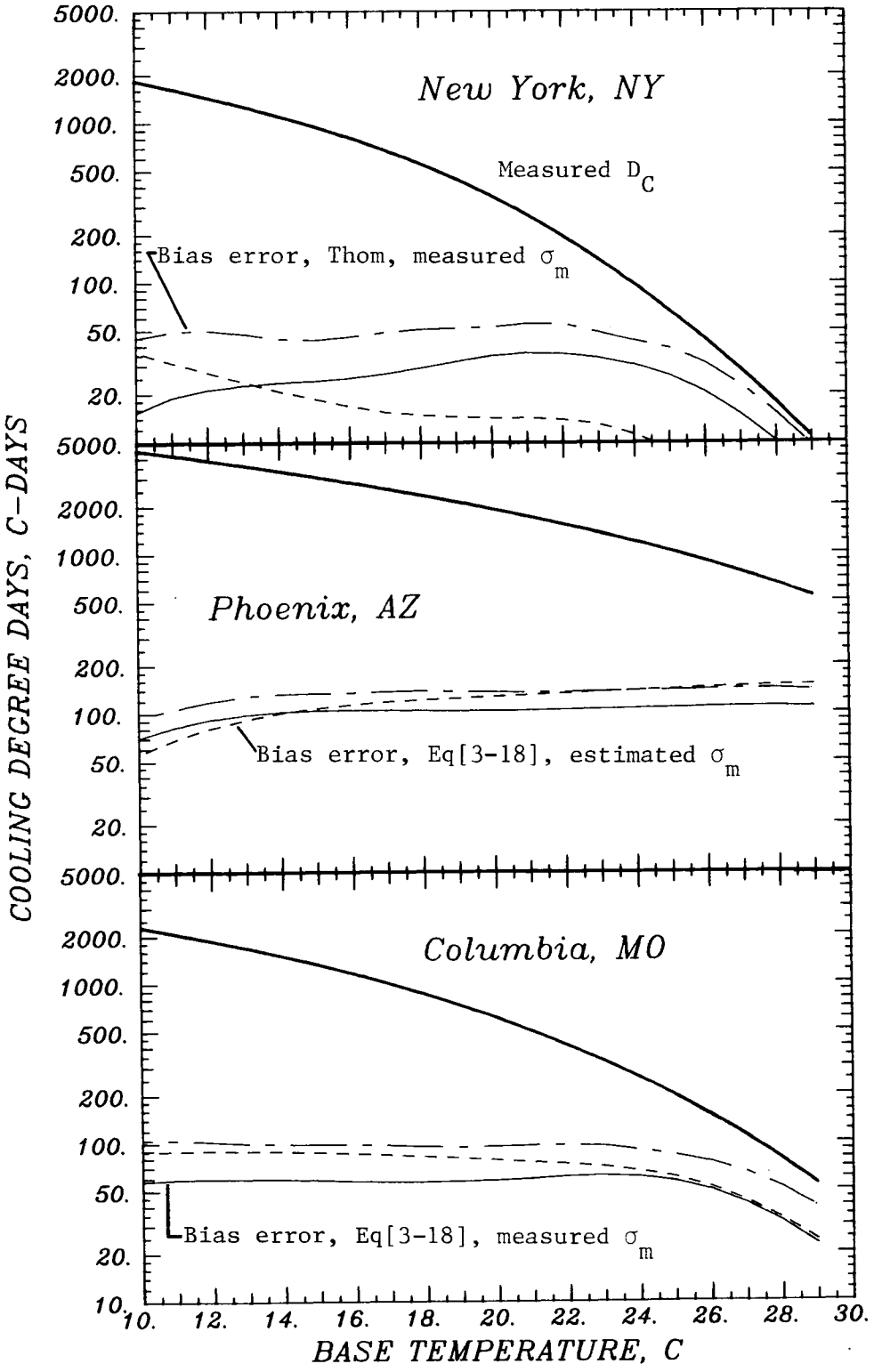

Figure 3.9 (cont.)

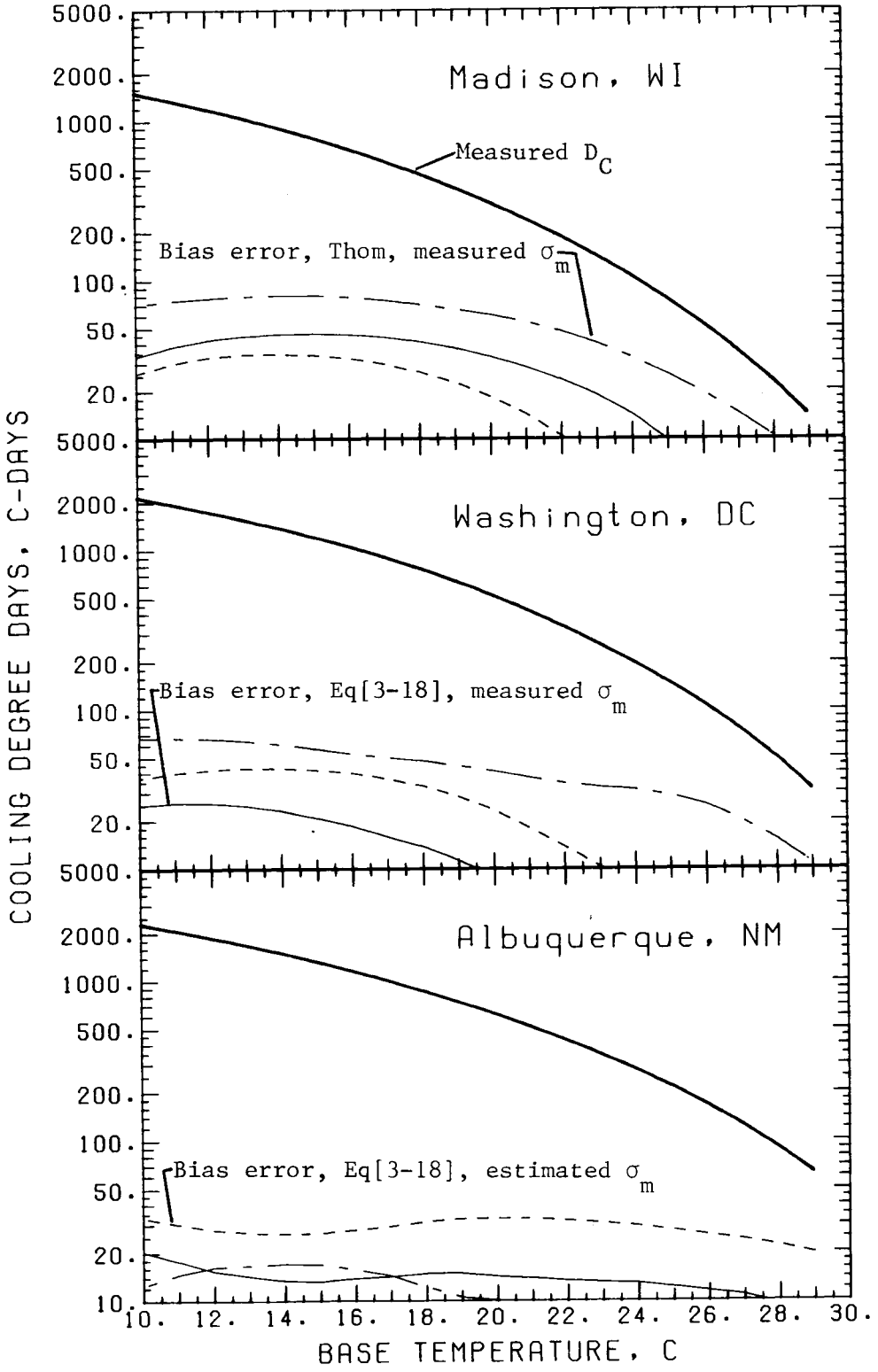

Figure 3.10 Measured Annual Cooling Degree-Days and Bias Errors for Degree-Days Estimated on an Hourly Basis

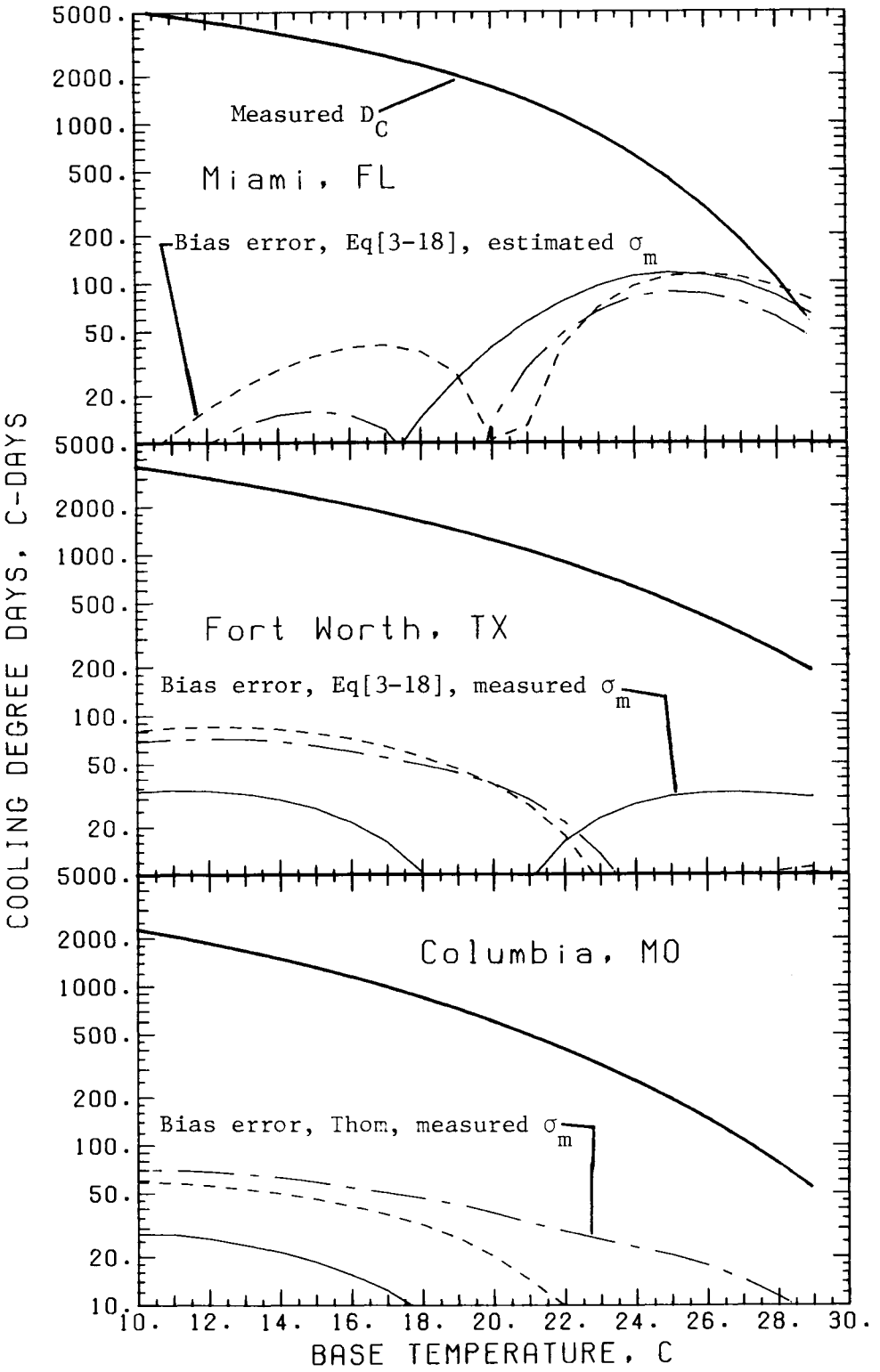

Figure 3.10 (cont.)

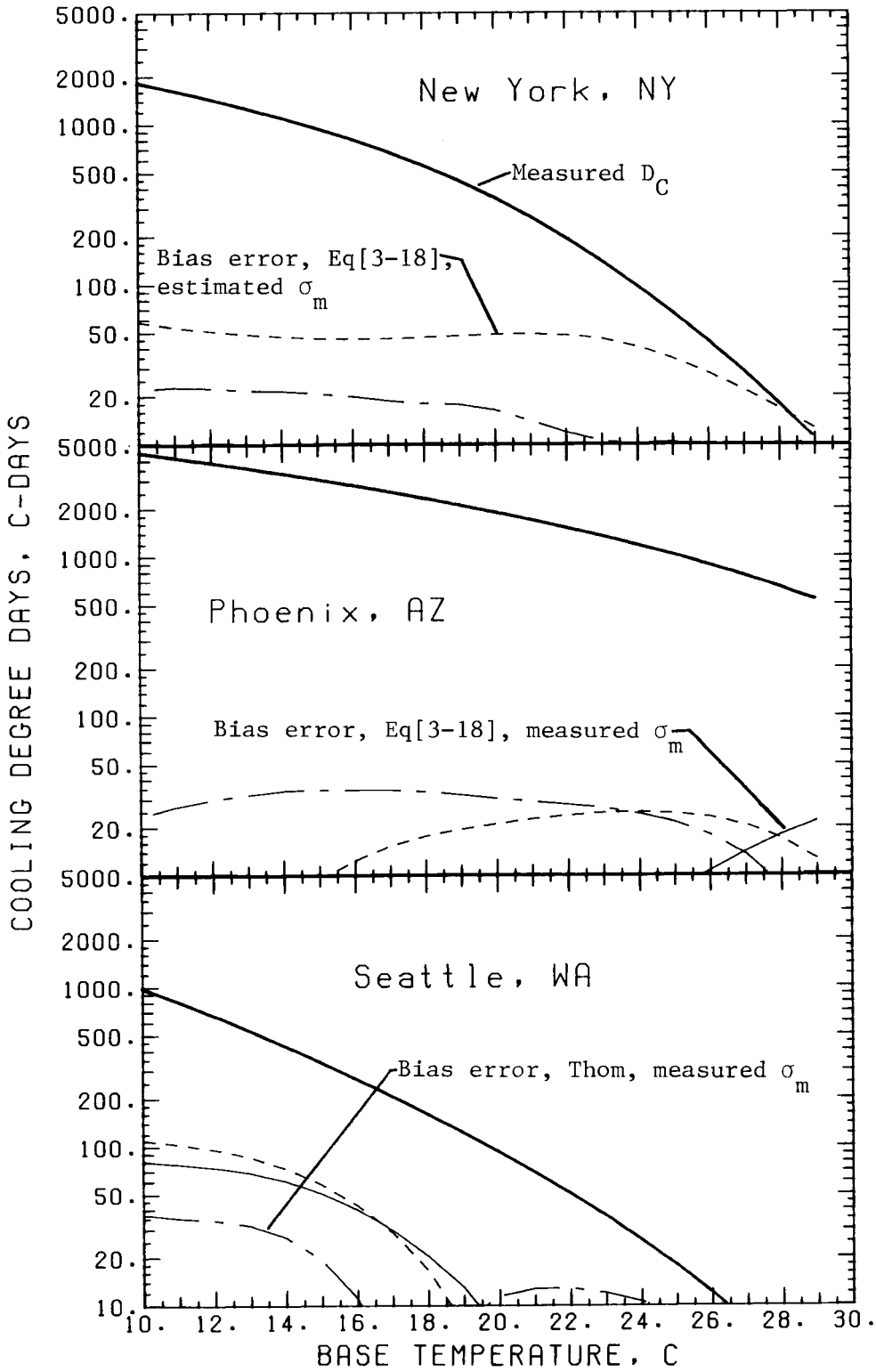

Figure 3.10 (cont.)

by the National Climatic Center for a base temperature of 18.3°C are found using the average of the daily minimum and maximum ambient temperatures. Heating degree-days were also calculated for the 9 SOLMET locations using the average of the maximum and minimum hourly temperatures for each day in the long-term data. For the 9 locations, the differences between degree-days calculated using the hourly values of temperature and degree-days calculated using the average of the maximum and minimum hourly temperatures were from 50 to 200°C-days on an annual basis.

3.5 Summary

The degree-day expression developed by Thom was found to be unsuitable for the estimation of ambient temperature bin data. A symmetric distribution function model for the monthly distribution of ambient temperature was developed from long-term hourly SOLMET data for 9 U.S. locations. A relationship was established between the standard deviation of the monthly-average ambient temperature and the monthly-average ambient temperature. Relationships were also developed for the diurnal variation of the monthly-average hourly ambient temperature. The ambient temperature distribution model was used to derive models for heating and cooling degree-days. A model was also developed for ventilation cooling degree-days to account for the effect of ventilation of buildings with ambient air when the ambient temperature is between the cooling base and thermostat set-point temperatures.

The relationships presented allow the estimation of daily ambient temperature bin data and heating and cooling degree-days from a single input, the monthly-average daily ambient temperature. If the monthly-average clearness index is known, bin data and degree-days can be estimated for any hour of the day. Estimated bin data and degree-days were compared to bin data and degree-days developed from long-term hourly temperature records, and the agreement was found to be within 10% for bin data and within 175°C-days for annual heating and cooling degree-days. The errors for the degree-day estimates are comparable in size to the differences between degree-days calculated using hourly values of temperature and degree-days calculated with the method used by the National Weather Service.

CHAPTER 4

4. SOL-AIR TEMPERATURE STATISTICS

4.1 Literature Review

The sol-air temperature concept, defined in Equation (2-1), was developed to simplify the estimation of design cooling loads [ASHRAE (1981)]. The sol-air temperature allows effects of ambient temperature, solar radiation and wind speed to be combined and treated simultaneously. The peak cooling load for a building may not occur on the day with the highest ambient temperature or the day with the most solar radiation, since it is the combined effect of 3 variables which results in a cooling load. The sol-air temperature concept provides a means for the development of cooling load design data which are more comprehensive than those based on ambient temperature or solar radiation alone. The most widely used procedure for the estimation of cooling design loads [ASHRAE (1981] is based on the conservative assumption that the maximum ambient temperature and solar radiation occur on the same day, although not for the same hour of the day.

Sol-air temperature is also useful in determining the integrated heating and cooling energy consumption of buildings. The increasing popularity of passively heated solar homes has led to design methods which include the effects of both ambient temperature and solar radiation. The Solar Load Ratio (or Solar Savings Fraction) method

[Balcomb et al. (1983)] presents a set of empirical relationships based on simulations of passive solar buildings. Another design method is that developed by Monsen et al. (1981, 1982) for the analysis of direct gain and collector-storage wall systems. While these methods are not formulated in terms of sol-air temperature, they attempt to model the combined effect of ambient temperature and solar radiation on the heating load for a structure. Both methods rely on heating degree-days to account for ambient temperature effects. Solar effects are treated somewhat differently, but the monthly-average solar radiation is input to each method. These methods are intended only for the estimation of heating loads, and they are only designed to consider solar radiation which enters through south facing apertures. The correlation of ambient temperature and solar radiation and the possible interaction of these variables is not addressed directly by either method.

The estimation of the solar contribution to building cooling loads has received recent attention. The modified bin method developed by ASHRAE (1981) and the modified building load and temperature bin calculation method (MBLTBM) [Parken and Kelley (1981)] are based on ambient temperature bin data. The ASHRAE method treats solar radiation as a linear function of ambient temperature. The MBLTBM uses the seasonal-average incident solar radiation for gains due to transmission, while solar radiation absorbed by walls is a linear function of ambient temperature. No evidence is given in the development of either of these methods to support the use of a linear

relationship between solar radiation and ambient temperature.

4.2 A Bivariate Distribution Model for Sol-Air and Ambient Temperatures

A two-dimensional distribution model for sol-air temperature and ambient temperature describes not only the distribution of each temperature, but also the coincidence of sol-air temperature and ambient temperature. The sol-air temperature for a surface is not purely a meteorological variable, as it is a function of the absorptance, emittance and orientation of the surface. The variation of sol-air temperature for a given surface, however, is only a function of meteorological variables. The bivariate distribution function for sol-air and ambient temperatures involves the distributions of solar radiation, ambient temperature and wind speed. The cross-correlation between ambient temperature and sol-air temperature is the result of cross-correlations among these 3 basic variables. Only the cross-correlation of solar radiation and ambient temperature was considered in the development of a bivariate distribution model for sol-air temperature and ambient temperature in order to simplify the model.

4.2.1 Interrelationship of Solar Radiation and Ambient Temperature

The cross-correlation of solar radiation and ambient temperature (defined by Equation (2-15)) was investigated by calculating ρ_{Ta-kT} for each of the 9 SOLMET locations. Hourly values of ambient

temperature and clearness index were used, but only for those hours of the day when the sun was above the horizon. The use of the hourly clearness index (k_T), the ratio of the horizontal hourly solar radiation at the earth's surface to the extraterrestrial solar radiation for the hour, eliminates the seasonal variation in solar radiation resulting from geometrical considerations. The cross-correlation between T_a and k_T was calculated by lumping all daylight hours together. Correlation of the monthly-average hourly ambient temperature and clearness index is not included in the values of ρ_{Ta-kT}, since ρ_{Ta-kT} is based on deviations of the variables from their monthly-average hourly values.

Table 4.1 lists the monthly cross-correlation coefficients between ambient temperature and solar radiation for each of the 9 SOLMET locations. A seasonal pattern exists in the values of ρ_{Ta-kT} for most locations, with Phoenix and Fort Worth the exceptions. The pattern consists of negative or very small cross-correlations during the winter months which become positive during the spring, summer and fall months. The largest correlations are positive values for summer months. The correlation is significant during the summer months in Miami, Seattle and Fort Worth, but for the remaining months and locations ambient temperature and solar radiation variations are not highly correlated.

The monthly-average hourly values of ambient temperature and clearness index are often correlated. During the winter months, when the ambient temperature is less than the annual average, there is an

Table 4.1 Monthly Cross-Correlation Coefficients for Variations of Hourly Ambient Temperature and Hourly Clearness Index From Their Average Values.

	Location								
Month	Madison	Washington	Albuquerque	Miami	Fort Worth	Columbia	New York	Phoenix	Seattle
Jan	-0.38	-0.13	-0.01	-0.02	0.17	-0.13	-0.24	0.05	-0.19
Feb	-0.32	-0.11	0.15	-0.03	0.18	-0.05	-0.16	0.11	-0.06
Mar	-0.09	0.08	0.19	0.04	0.23	0.13	0.03	0.25	0.19
Apr	0.19	0.23	0.23	0.12	0.10	0.23	0.25	0.23	0.33
May	0.28	0.32	0.26	0.34	0.30	0.32	0.33	0.09	0.37
June	0.32	0.35	0.29	0.61	0.43	0.36	0.33	0.02	0.52
July	0.30	0.33	0.40	0.61	0.47	0.31	0.36	0.37	0.52
Aug	0.25	0.27	0.42	0.59	0.49	0.33	0.29	0.32	0.50
Sep	0.16	0.21	0.33	0.62	0.38	0.25	0.14	0.24	0.40
Oct	0.14	-.02	0.27	0.24	0.22	0.14	-0.03	0.31	0.21
Nov	-0.03	-0.06	0.12	0.00	0.12	0.07	-0.13	0.10	-0.12
Dec	-0.34	-0.13	0.08	-0.11	0.14	-0.05	-0.20	0.15	-0.16

increase in cloud cover in many locations, and the clearness index is also less than the annual average. A correlation also results from diurnal variations of temperature and atmospheric clearness. Over the course of the day, the fraction of the extraterrestrial radiation transmitted tends to be a maximum near solar noon due to atmospheric path length effects. (The diurnal variation of the monthly-average hourly clearness index is shown in Figure 4.3.) The diurnal profile for monthly-average ambient temperature presented in Chapter 3 indicates that on the average, the ambient temperature is highest at 3 PM. From sunrise until noon, both the monthly-average ambient temperature and the monthly-average clearness index increase, and from 3 PM until sunset, they both decrease. Between noon and 3 PM, the monthly-average ambient temperature increases while the monthly-average clearness decreases, but the changes are relatively small over this time interval. These seasonal and diurnal effects result in a positive correlation between $\overline{T}_{a,h}$ and $\overline{k}_T$.

4.2.2 A Model for Sol-Air Temperature/Ambient Temperature Bin Data

The bivariate distribution of ambient temperature and sol-air temperature is a function of 3 meteorological variables and the properties of the surface of interest. The development of a model capable of representing the distributions and cross-correlation of sol-air temperature and ambient temperature for an arbitrary surface is complex. A number of simplifying assumptions were made to allow the use of existing distribution models for ambient temperature and

clearness index to represent the bivariate distribution of sol-air temperature and ambient temperature.

As mentioned at the beginning of this section, the cross-correlations of ambient temperature or solar radiation with wind speed were not analyzed. The first simplification made in modeling the two-dimensional distribution of ambient temperature and sol-air temperature was the assumption that the outside surface heat transfer coefficient, h_o, is constant for a month. This assumption allows the distribution of values of h_o to be replaced by the monthly-average value of h_o. As mentioned in Chapter 2, wind speed is very difficult to predict near a building. Since the convective component of h_o varies as a fractional power of wind speed and the radiative component is only indirectly related to wind speed, the variation of h_o relative to the average value is smaller than the variation of wind speed.

The sol-air temperature is only a function of the incident radiation and the ambient temperature for a fixed value of the outside surface heat transfer coefficient and constant surface characteristics. Modeling the bivariate distribution of sol-air temperature and ambient temperature is equivalent to modeling the bivariate distribution of ambient temperature and incident solar radiation for this situation. If the distribution model is further restricted to a particular hour of the day, the geometrical relationship between the sun and a fixed surface is reasonably constant over the period of a month. The incident radiation can be expressed as a

simple function of clearness index [Duffie and Beckman (1980)], and the distribution of sol-air and ambient temperatures can be modeled using the two-dimensional distribution of ambient temperature and clearness index.

The distribution model for ambient temperature described in Chapter 3 and a distribution model for clearness index developed by Hollands and Huget (1983) from the generalized distribution curves of Liu and Jordan (1960) can be combined to yield a bivariate distribution model for hourly ambient temperature and clearness index. Since both of the distribution models are univariate, the variations of hourly ambient temperature and solar radiation from their monthly-average hourly values must be assumed uncorrelated for a particular hour and month. The cross-correlation coefficients given above indicate that the variations of ambient temperature and clearness index are weakly correlated for most months and locations. Although error is introduced by assuming the variations of ambient temperature and clearness index are uncorrelated, it was decided that the complexity required to include the cross-correlation of variations of $T_{a,h}$ and k_T in a bivariate distribution model is not justified by the potential increase in accuracy of bin data or accumulated difference statistics estimated with the bivariate distribution model.

The primary interest in a bivariate distribution model for sol-air temperature and ambient temperature is the estimation of a two-dimensional bin data. A sol-air temperature/ambient temperature bin

is formed by the intersection of a sol-air temperature bin and an ambient temperature bin. A set of ambient temperature bins and a set of sol-air temperature bins results in a two-dimensional grid of sol-air temperature/ambient temperature bins when plotted on Cartesian co-ordinates, as shown in Figure 4.1. For each ambient temperature bin, there is a set of sol-air temperature bins. The hours in an ambient temperature bin are divided among the sol-air temperature bins for that ambient temperature bin according to the distribution of sol-air temperature.

The sol-air temperature as defined by Equation (2-1) cannot be less than the ambient temperature. For each ambient temperature bin, only the sol-air temperature bins which contain sol-air temperature values greater than or equal to the minimum temperature for the ambient temperature bin are of interest. A more compact form for the sol-air temperature/ambient temperature bin data is obtained by replacing the sol-air temperature scale with the difference between the sol-air temperature and the ambient temperature, referred to more simply as the sol-air temperature difference. This form eliminates those bins where there can never be any data. The sol-air temperature interval corresponding to a sol-air temperature difference bin is equal to the sum of the ambient temperature value for the midpoint of the ambient temperature bin and the interval of sol-air temperature for the sol-air temperature difference bin. Sol-air temperature difference/ambient temperature bin data are equivalent to sol-air temperature/ambient temperature bin data, and the

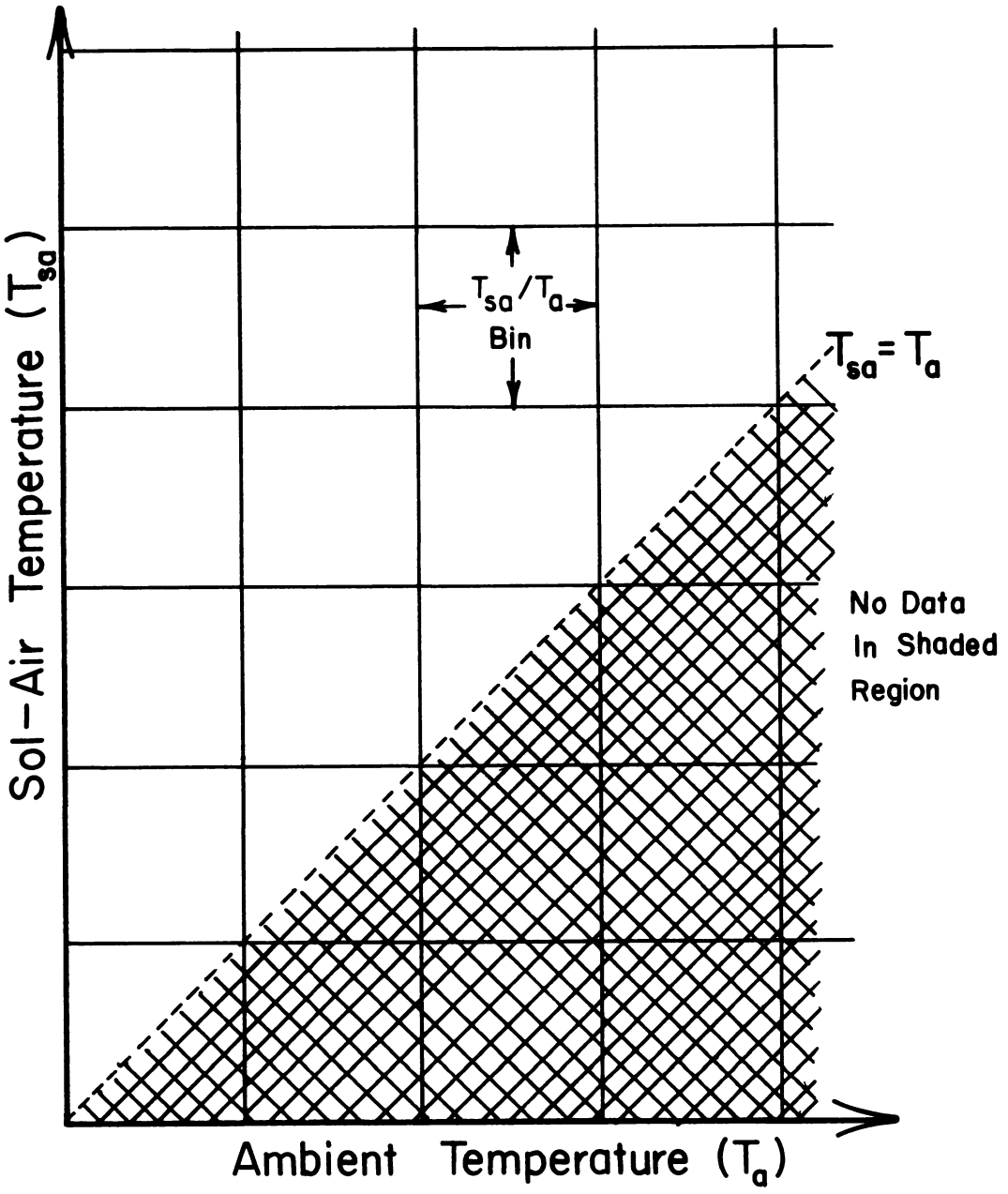

Figure 4.1 Two-Dimensional Grid for Sol-Air Temperature/ Ambient Temperature Bin Data

two terms will be used interchangeably.

It is only necessary to estimate sol-air temperature/ambient temperature bin data for the hours of the day when the sun is above the horizon. During the nighttime hours, the sol-air temperature is assumed to equal the ambient temperature, and one-dimensional ambient temperature bin data are all that are required. During the daytime hours, it is necessary to estimate the sol-air temperature/ambient temperature bin data separately for each hour of the day. This restriction allows a bivariate distribution model for hourly clearness index and ambient temperature to be used to model the bivariate distribution of sol-air temperature and ambient temperature. The bin data are then summed for each daytime hour to obtain the bin data for the entire day.

In the first step of the estimation procedure, the total number of hours in the month for an hour of the day is distributed among the set of ambient temperature bins. The number of bins and the size of each bin define the range of ambient temperature considered. The estimation of ambient temperature bin data is described in Chapter 3. The hours in each ambient temperature bin are then distributed among the sol-air temperature difference bins for each ambient temperature bin.

Since the solar radiation distribution is assumed to be independent of the ambient temperature distribution, the fraction of the total hours in each of the sol-air temperature difference bins is the same for all ambient temperature bins. This allows a single set

of fractions (which sum to one) to be estimated for the set of sol-air temperature difference bins. This set of fractions can then be used repeatedly to distribute the hours in each ambient temperature bin among the corresponding sol-air temperature difference bins.

The fraction of the time the difference between the sol-air and ambient temperatures is in each of the sol-air temperature difference bins is determined using the distribution function for the clearness index. The definition of the average sol-air temperature for an hour can be rearranged to find the incident radiation level for a particular value of the sol-air temperature difference.

$$I_T = h_o(T_{sa,h} - T_{a,h})/\alpha \qquad (4\text{-}1)$$

The incident radiation can be estimated from

$$I_T = \bar{I}_o k_T[R_b + aGVF + (I_d/I)(SVF - R_b)] \qquad (4\text{-}2)$$

where $\bar{I}_o$ is the hourly extraterrestrial radiation for the average day of the month, I_d/I is the fraction of the hourly radiation which is diffuse, R_b is the ratio of beam radiation intensity for the tilted surface to that for a horizontal surface, a is the ground reflectance and GVF and SVF are the view factors from the surface to the ground and sky, respectively. Geometrical relationships for R_b are given in Duffie and Beckman (1980). Equation (4-2) is based on the assumption that sky and ground-reflected diffuse radiation is isotropic. GVF and SVF are given by

$$GVF = (1 - \cos\beta)/2 \qquad (4\text{-}3)$$

$$SVF = (1 + \cos\beta)/2 \qquad (4\text{-}4)$$

where β is the slope of the surface from horizontal.

The only terms in the right hand side of Equation (4-2) which cannot be treated as constants for the period of a month are the clearness index and the diffuse radiation fraction. The diffuse radiation fraction can be expressed as a function of the clearness index. By substituting one of the available relationships between I_d/I and k_T into Equation (4-2), a relationship between the incident radiation level for a surface and the clearness index is obtained. This relationship between I_T and k_T is combined with Equation (4-1), allowing the transformation of sol-air temperature difference bins to bins of clearness index. The fraction of the time the sol-air temperature difference is in a sol-air temperature difference bin is equal to the fraction of the time the clearness index is in the corresponding clearness index bin.

The Orgill and Hollands diffuse fraction relationship (1977) was used in defining the relationship between the clearness index and the sol-air temperature difference because of its simple form. This relationship was developed from measured data for Canada, but it was shown to also be representative of measured data for the U.S. and Australia [Erbs et al. (1982)]. The Orgill and Hollands relationship consists of three equations, each for a different range of clearness index. When the three diffuse fraction equations are com-

bined with Equations (4-1) and (4-2), the following relationships result:

For k_T less than 0.35,

$$h_o(T_{sa,h} - T_{a,h})/\alpha\bar{I}_o = (SVF + aGVF)k_T - 0.249(SVF - R_b)k_T^2 \quad (4\text{-}5)$$

For k_T between 0.35 and 0.75,

$$h_o(T_{sa,h} - T_{a,h})/\alpha\bar{I}_o = (1.557SVF + aGVF - 0.557R_b)k_T - 1.84(SVF - R_b)k_T^2 \quad (4\text{-}6)$$

and for k_T greater than 0.75,

$$h_o(T_{sa,h} - T_{a,h})/\alpha\bar{I}_o = (0.823R_b + 0.177SVF + aGVF)k_T \quad (4\text{-}7)$$

The relationship between the sol-air temperature difference, $T_{sa,h} - T_{a,h}$, and the clearness index represented in the above set of equations can be of two general forms, both of which are illustrated in Figure 4.2. Also shown in the figure are horizontal lines representing 4 values of the sol-air temperature difference. The numbered points represent valid solutions for the clearness index for each of the sol-air temperature differences.

When the sol-air temperature is a monotonically increasing function of the clearness index (Curve A), there can only be one value of clearness index for each value of the sol-air temperature

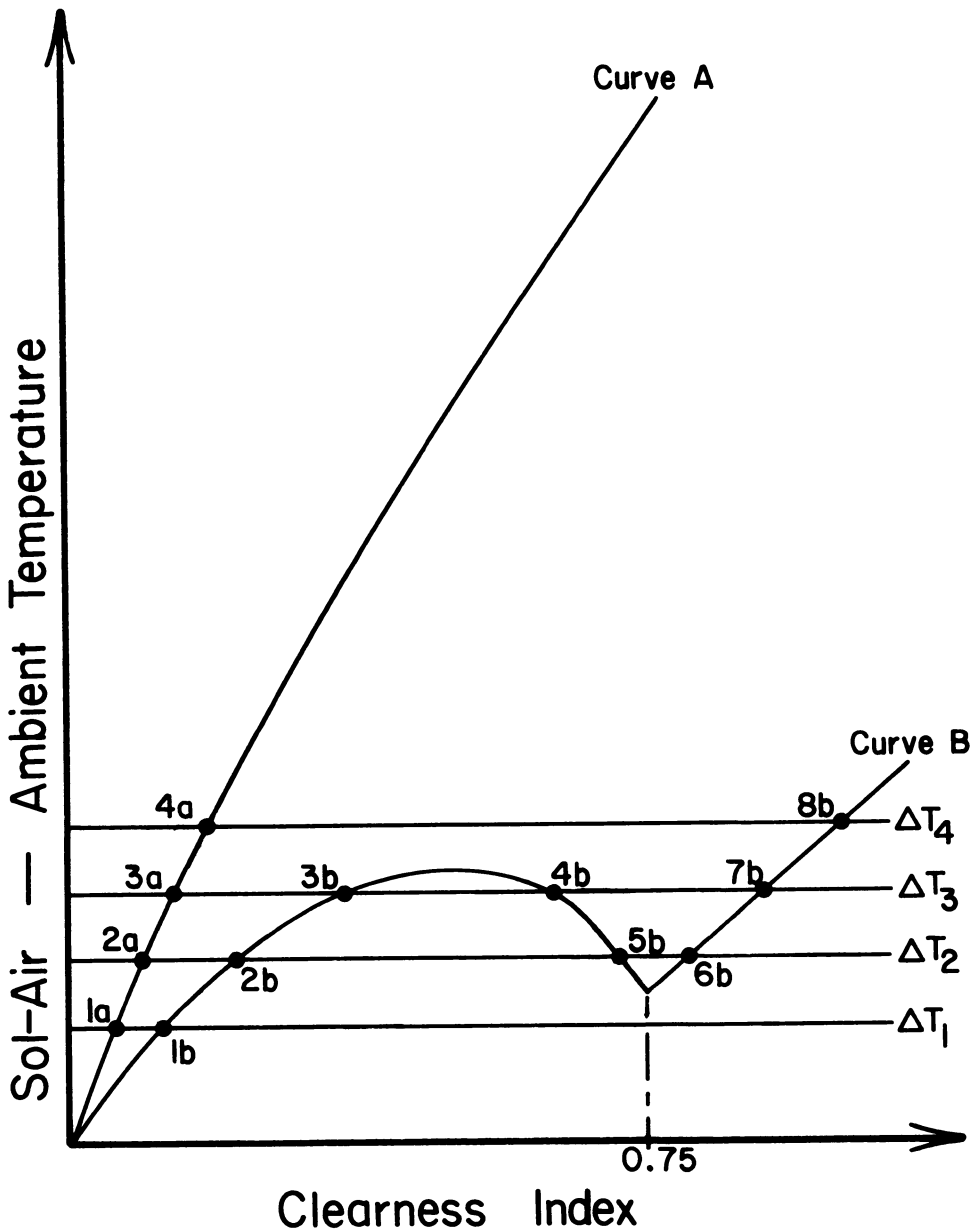

Figure 4.2 Relationship Between the Sol-Air Temperature Difference and the Hourly Clearness Index

difference. It is, however, possible for the sol-air temperature difference to decrease with increasing clearness index over a limited range of clearness index (Curve B). When this occurs, there are values of $T_{sa,h} - T_{a,h}$ for which three valid solutions for k_T exist. The range of clearness index where more than one valid solution can exist is from 0.35 to 0.75. This range is determined by the diffuse fraction relationship used, and a different diffuse relationship would result in a different range over which more than one solution is possible. For a solution to be valid, it must lie within the limits of clearness index for the equation which was solved.

The procedure for estimating the fraction of the time the sol-air temperature difference is in a sol-air temperature difference bin depends on the number of valid solutions for clearness index for the two values of sol-air temperature difference which define the bin. The possible solutions, which are demonstrated in Figure 4.2, are:

1. If there is only one value of k_T for each of the values of $T_{sa,h} - T_{a,h}$ defining a bin, the fraction for the bin is the difference between $Q(k_T)$ for the two values. Points 2a and 1a in Figure 4.2 are an example of this situation.

2. If there is one value of k_T for the lower value of sol-air temperature difference and three values for the upper sol-air temperature difference, as in the intersections of the lines for

ΔT_1 and ΔT_2 with Curve B, the fraction for the bin is the sum of the difference in $Q(k_T)$ for the lower (1b) and the smallest of the upper values of k_T (2b) and the difference in $Q(k_T)$ for the remaining two upper values (5b and 6b).

3. If there are three values of k_T for each value of the sol-air temperature difference defining a bin, as in the intersections of ΔT_2 and ΔT_3 with Curve B, the fraction for the bin is the sum of the differences in $Q(k_T)$ for each of the three pairs of values of k_T (2b and 3b, 4b and 5b, and 6b and 7b).

4. If there are three values of k_T for the lower value of sol-air temperature difference and one for the upper sol-air temperature difference, the fraction for the bin is the sum of the difference in $Q(k_T)$ for the two smallest values of k_T (3b and 4b) and the difference in $Q(k_T)$ for the remaining two values of k_T (7b and 8b).

The maximum value of k_T represented by the clearness index distribution model developed by Hollands and Huget is 0.864. If the solution for k_T for a value of sol-air temperature difference is greater than 0.864, the value of k_T should be set equal to 0.864. Differences in $Q(k_T)$ for pairs of k_T values defining a sol-air temperature bin must always be positive, and it should be noted that in case 3, the largest value of clearness index for the second pair of values (5b) is for the smaller value of sol-air temperature difference (ΔT_2).

The procedure described above is used to estimate the fractional probability of occurrence for a set of sol-air temperature difference bins. The number of hours in a sol-air temperature difference/ambient temperature bin is equal to the product of the number of hours in the ambient temperature bin and the probability for the sol-air temperature difference bin. The hours in each of the ambient temperature bins are distributed into the set of sol-air temperature difference bins for each ambient temperature bin with this set of fractions.

The number of bins and the bin sizes must be chosen for the sol-air temperature difference scale. Since the bin data for each hour of the day are normally summed over all daylight hours, it is desirable to use the same bin size for all hours. The number of bins required is determined by the bin size and the maximum difference between the sol-air temperature and the ambient temperature for the month. The distribution function for clearness index is based on a maximum value of clearness index of 0.864. This value of clearness index can be used to calculate an upper limit for the sol-air temperature difference for all daylight hours.

The estimation of sol-air temperature/ambient temperature bin data for an hour of the day requires monthly-average hourly values of clearness index and ambient temperature as input. Tabulated values of the monthly-average daily clearness index and ambient temperature are available for many locations in the U.S. and Canada, but monthly-average hourly values are generally not provided. The

monthly-average hourly ambient temperature can be estimated from the daily value and relationships given in Chapter 3. The diurnal variation of the monthly-average hourly clearness index is based on a relationship first proposed by Liu and Jordan (1960) and later curve fit by Collares-Pereira and Rabl (1979).

$$\overline{I}/\overline{H} = (a + b\cos\gamma)(\overline{I}_o/\overline{H}_o) \tag{4-11}$$

where

$$a = 0.409 + 0.5016\sin(\gamma_s - 1.047) \tag{4-12}$$

$$b = 0.6609 - 0.4767\sin(\gamma_s - 1.047) \tag{4-13}$$

and where $\overline{I}$ is the monthly-average hourly horizontal radiation, $\overline{H}$ is the monthly-average daily horizontal radiation, $\overline{I}_o$ and $\overline{H}_o$ are the monthly-average hourly and daily extraterrestrial radiation, γ is the angular position of the earth relative to solar noon (morning is negative) in radians, and γ_s is the angular rotation of the earth from solar noon to sunset in radians.

Equation (4-11) can be rearranged to provide the desired relationship,

$$\overline{k}_T = (a + b\cos\gamma)\overline{K}_T \tag{4-14}$$

The hourly data for the 9 SOLMET locations are compared to Equation (4-14) in Figure 4.3. The symbols represent averages of the hourly

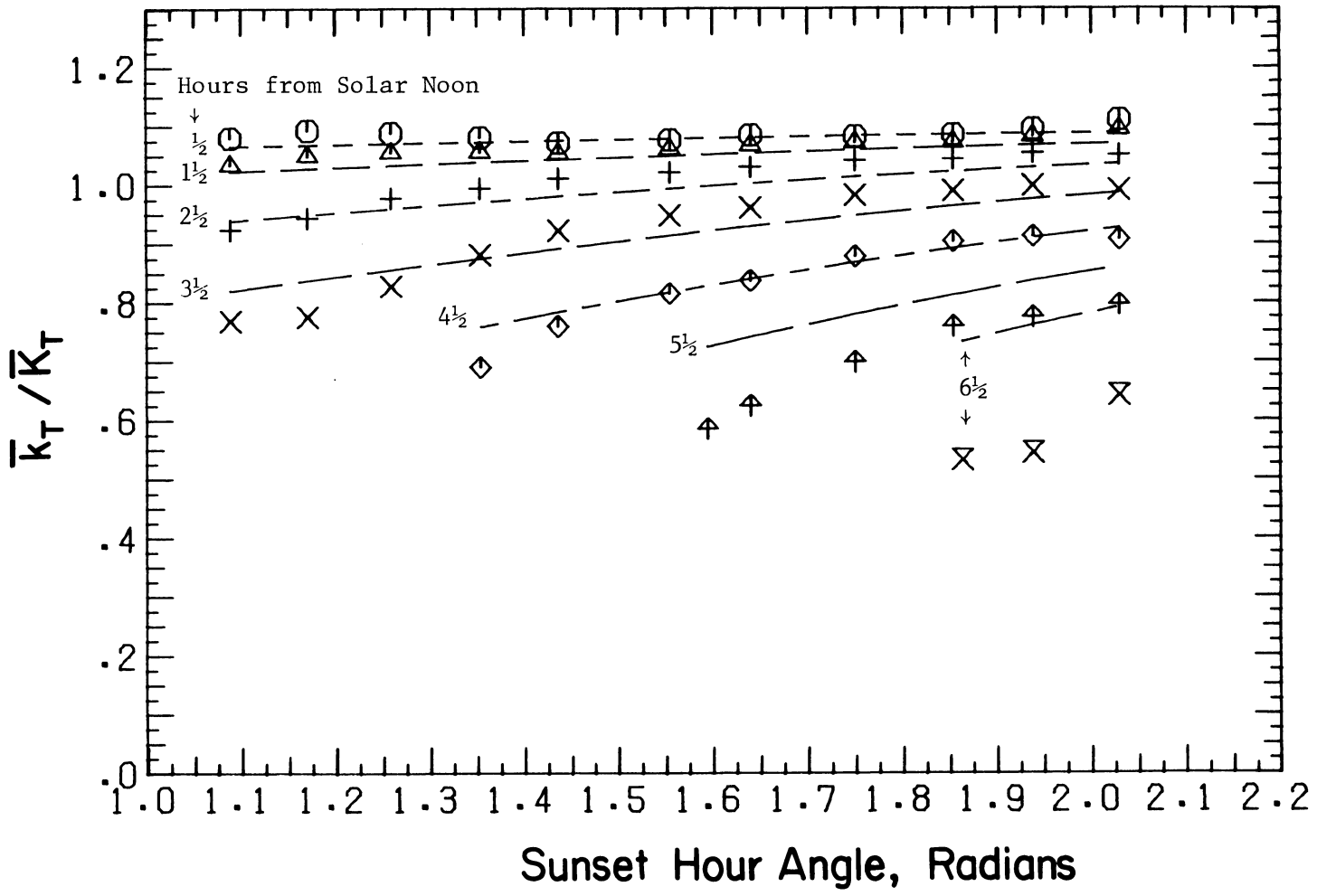

Figure 4.3 Diurnal Variation of the Monthly-Average Hourly Clearness Index as a Function of Time of Year

measurements for bins of γ_s 0.1 radians wide; the different symbol and line types are for different hours on either size of solar noon. The standard deviation of the measured data was calculated for each γ_s bin, and it was found that only for hours centered 6.5 hours from solar noon is the measured data statistically different from the relationship for a 95% confidence level, although the average difference for 5.5 hours from solar noon is also quite large. However, only a small amount of solar radiation occurs for these hours of the day.

4.2.3 Comparison of Measured and Estimated Bin Data

The procedure described above for the estimation of sol-air temperature/ambient temperature bin data was programmed. A listing of the program is given in Appendix B. Sol-air temperature/ambient temperature bin data were generated with this program for a south facing, sloped surface for each of the 9 SOLMET locations. A solar absorptance of 0.9, an outside film coefficient (h_o) of 28 W/m^2-°C and a slope consisting of the 5 degree multiple nearest in value to the latitude of the location were used. A bin size of 2°F was chosen for both the sol-air temperature difference and ambient temperature. Hourly bin data were estimated and summed for those hours of the day when the sun was above the horizon for the hour on the average day of the month. Measured values of the monthly-average daily clearness index and ambient temperature were used as input, with the monthly-average hourly values of these variables estimated in the

manner described above.

Sol-air temperature/ambient temperature bin data were also developed for each location from the hourly SOLMET data. The measured and estimated bin data were summed over all months, and the resulting annual bin data sets are compared in Figure 4.4. The three-dimensional surfaces shown were developed directly from the bin data, although some smoothing occurs in the process of interpolation between bins. The use of the difference between the sol-air temperature and the ambient temperature instead of the sol-air temperature as one of the independent variables allows for a more compact representation of the data, as explained above.

The estimated bin data look similar to the measured bin data for all of the locations, but there are noticeable differences. The measured data have sharper peaks and are more ragged looking. This is to be expected, as the mathematical functions used to model the distributions are smooth and continuous, while the data are discrete measurements. Skewness in the measured ambient temperature distributions shows up strongly in the colder locations as a peak near an ambient temperature of 32°F. The sol-air temperature for this peak is close to the ambient temperature, suggesting cloudy conditions or hours far from solar noon.

The estimated data also fail to reproduce a small but noticeable peak which occurs at low ambient temperatures and high sol-air temperatures (relative to the ambient temperature) in the Albuquerque and Phoenix data. Since the correlation coefficient between am-

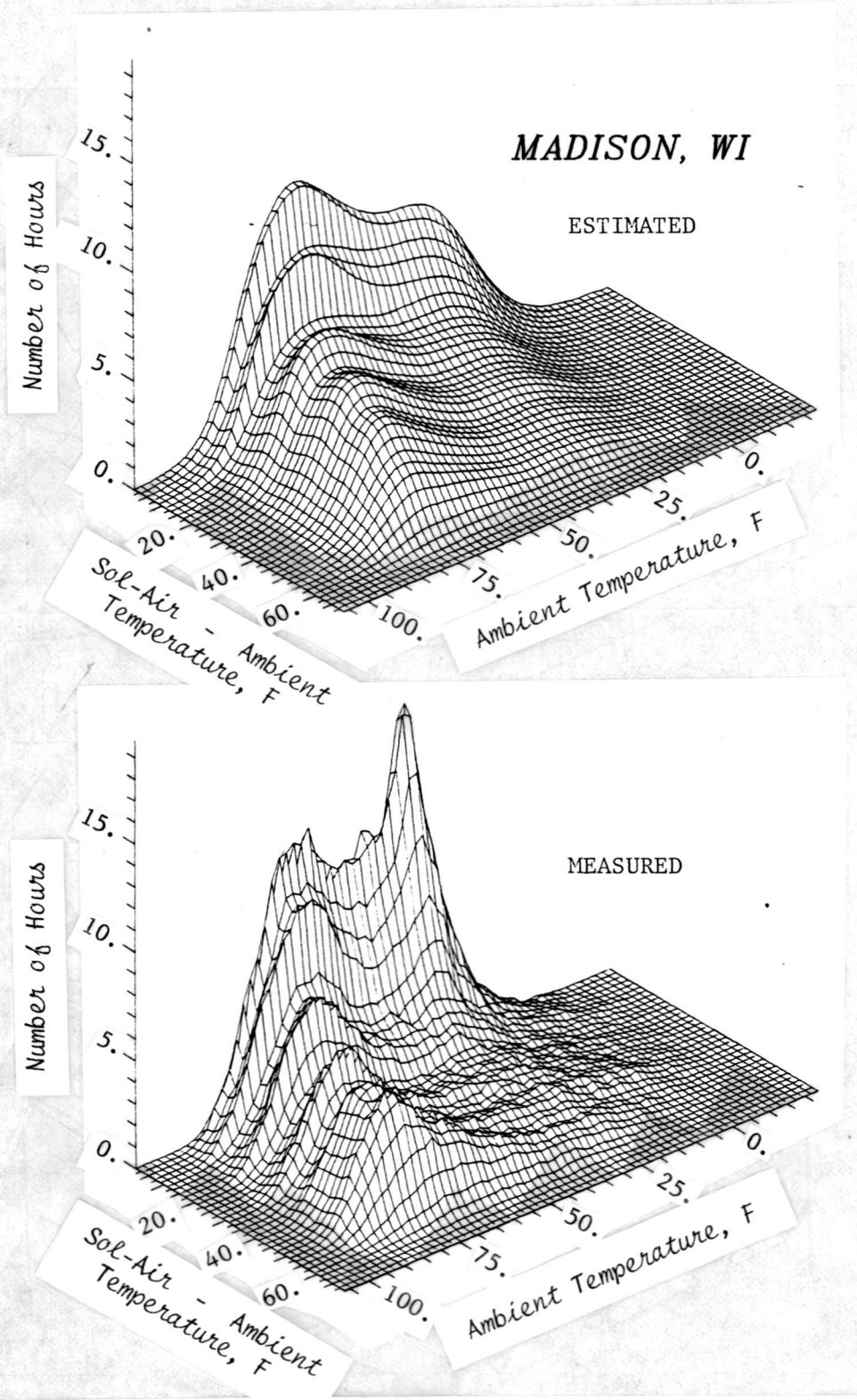

Figure 4.4 Estimated and Measured Sol-Air Temperature/Ambient Temperature Bin Data

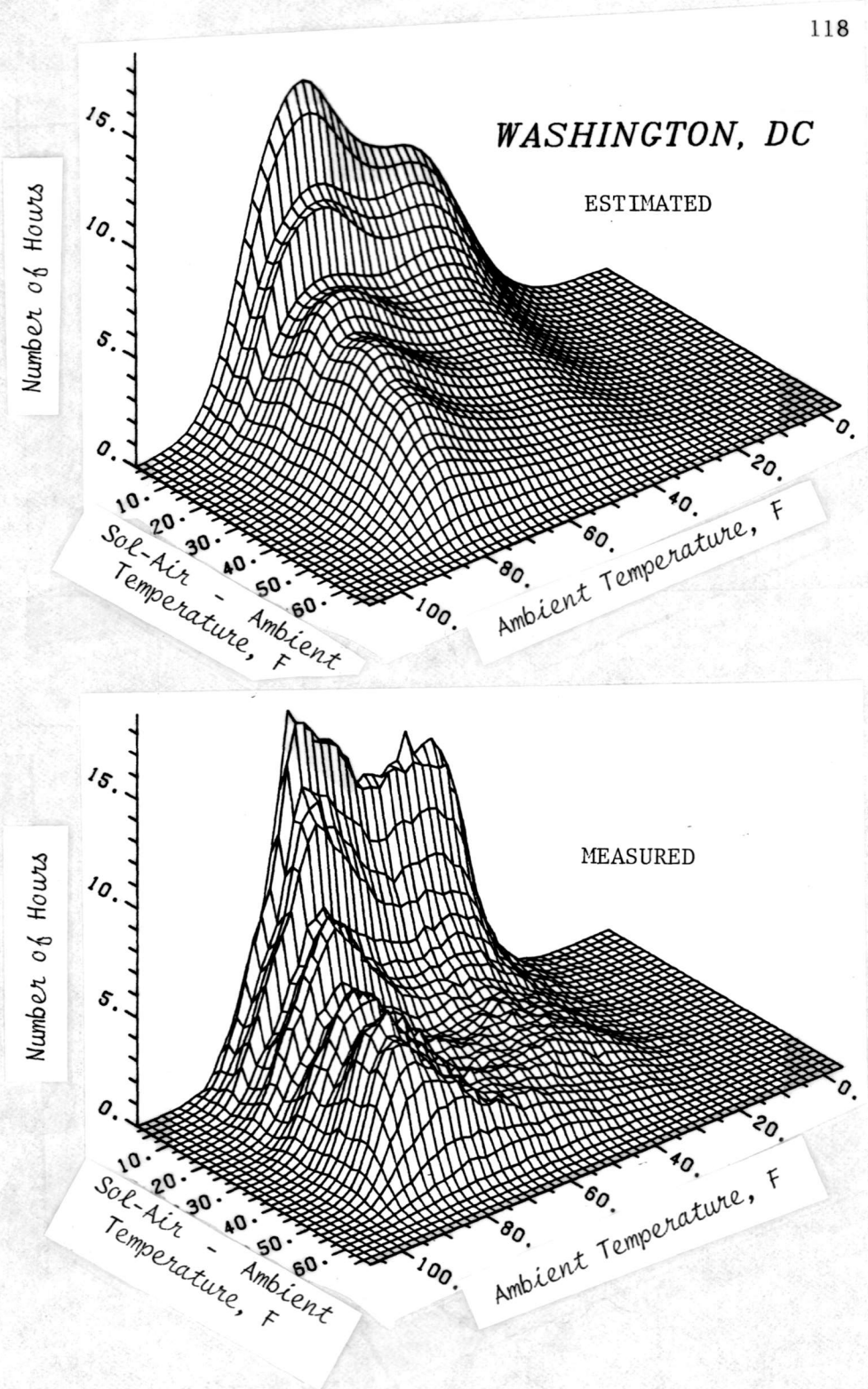

Figure 4.4 (cont.)

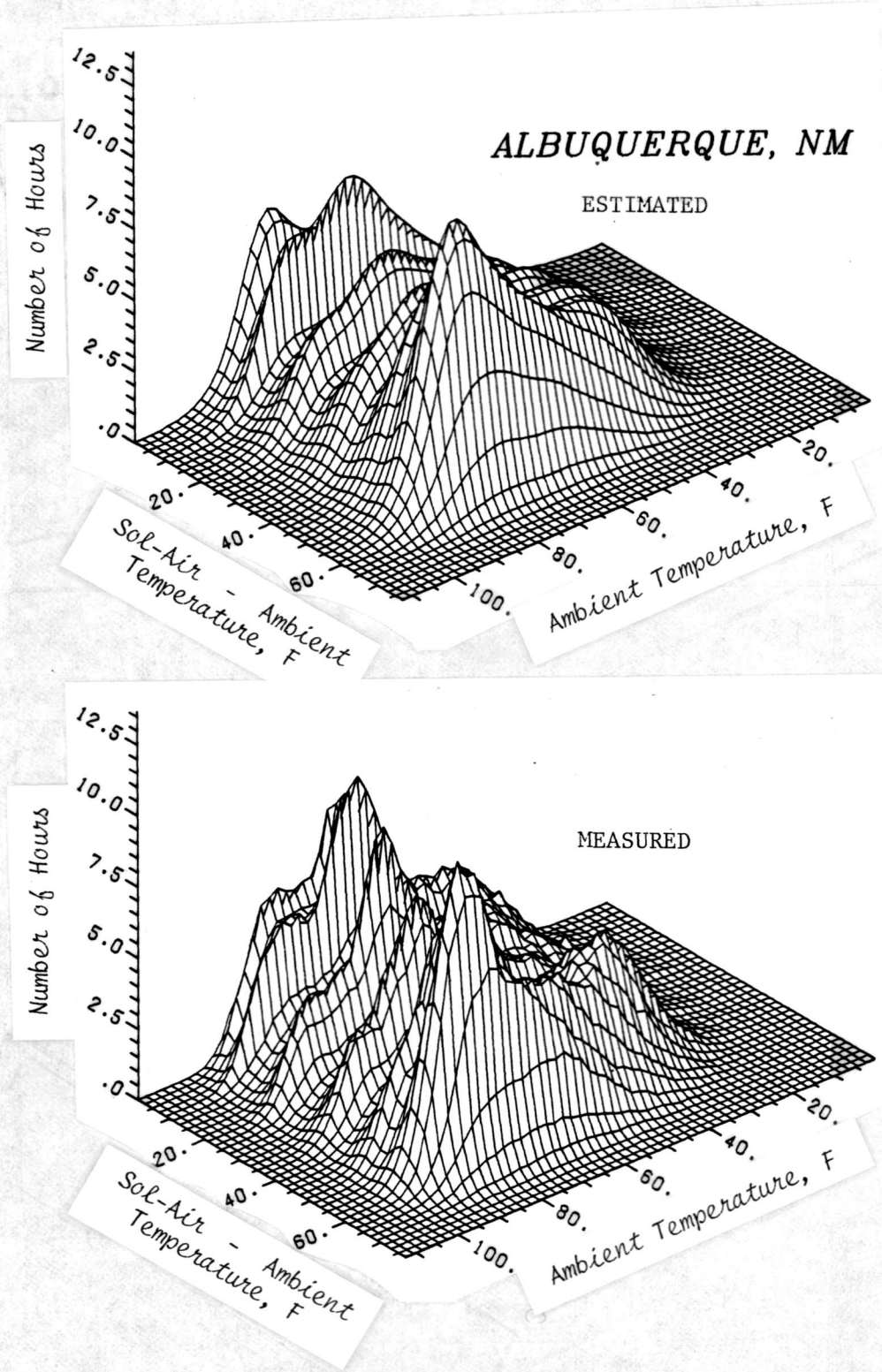

Figure 4.4 (cont.)

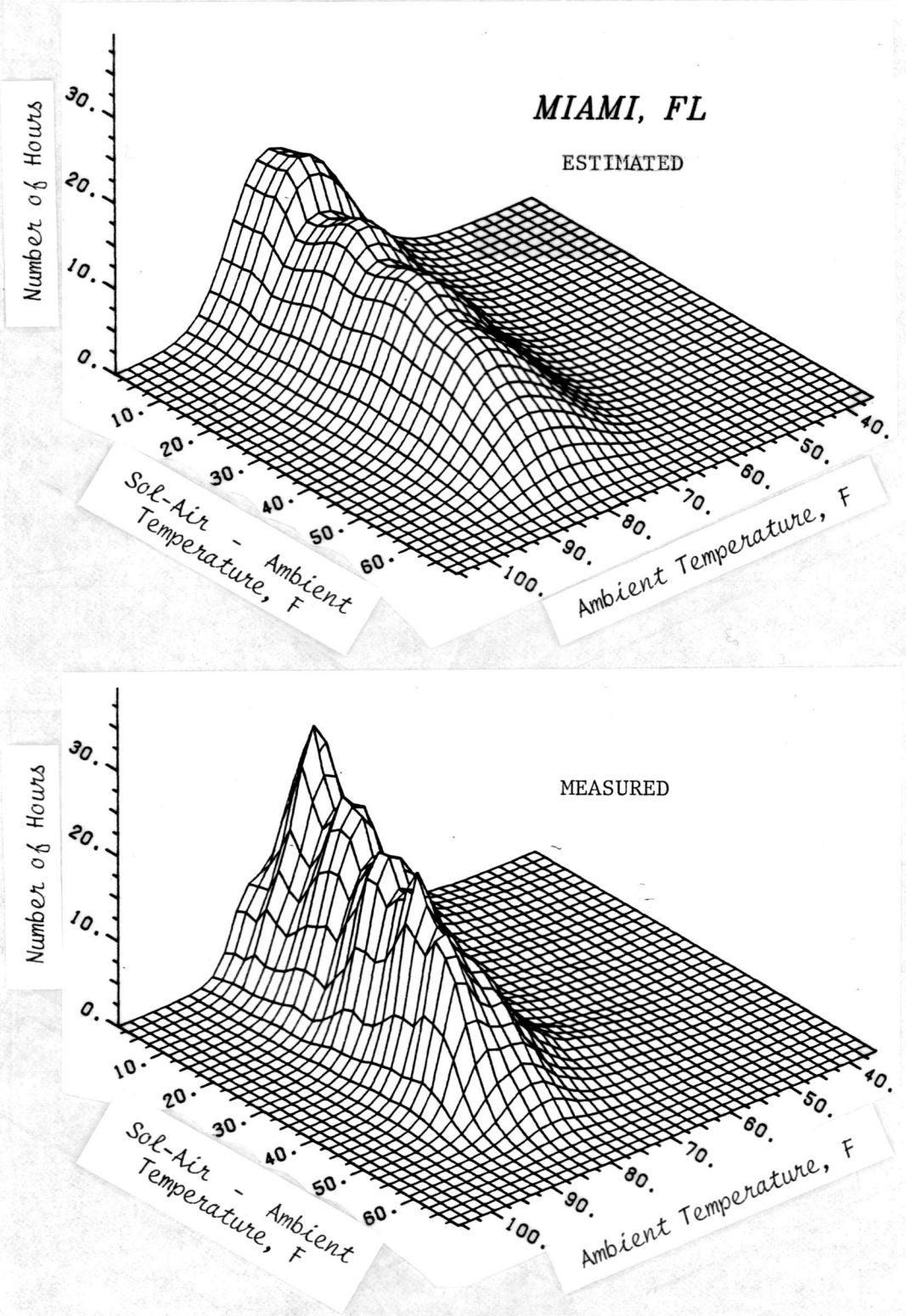

Figure 4.4 (cont.)

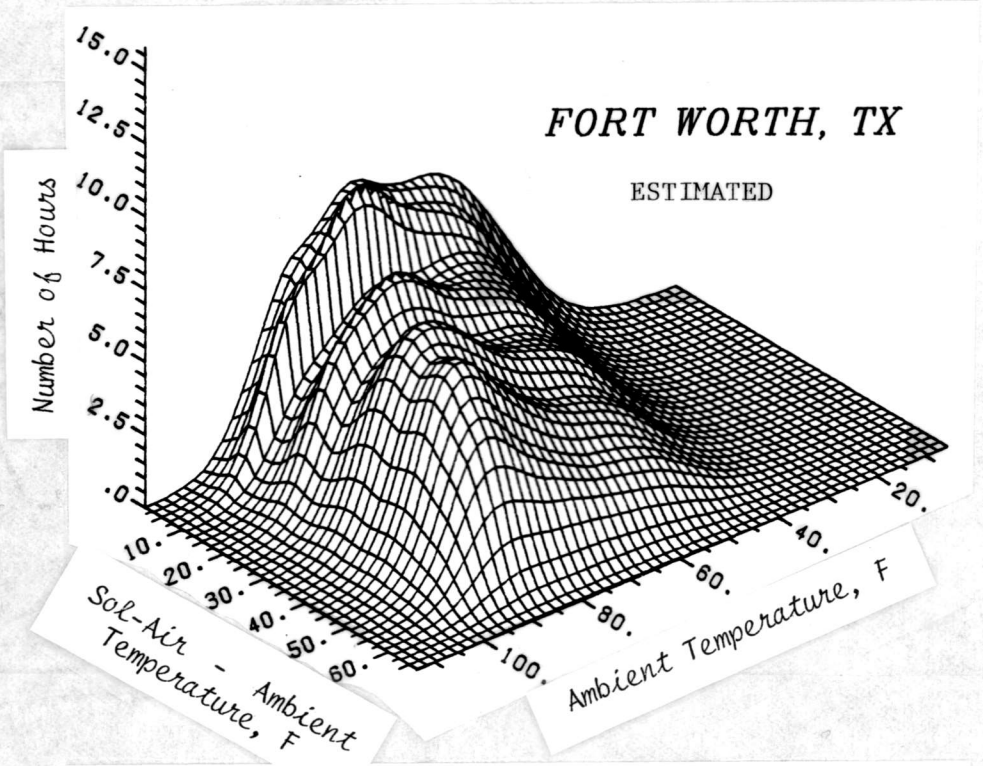

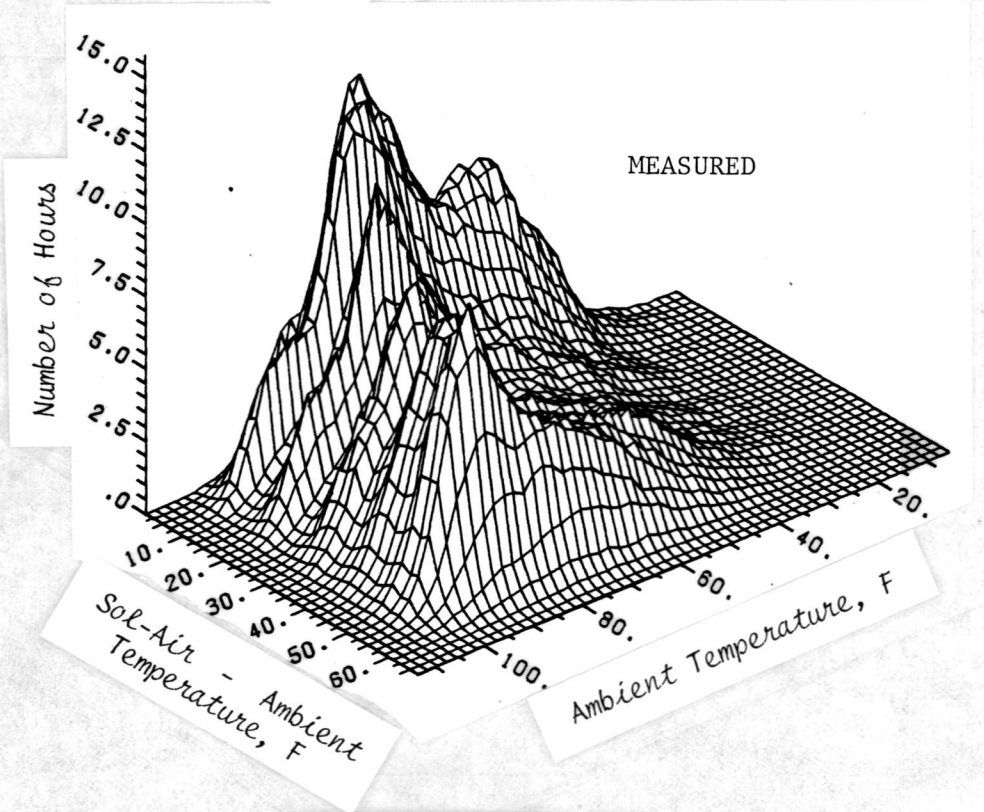

Figure 4.4 (cont.)

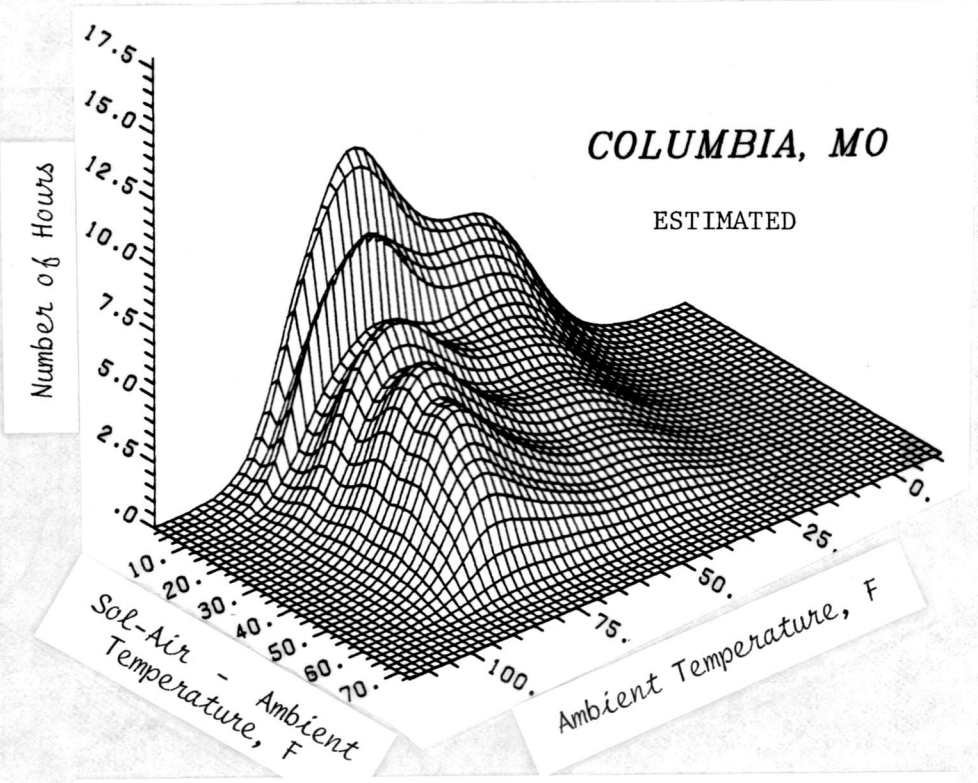

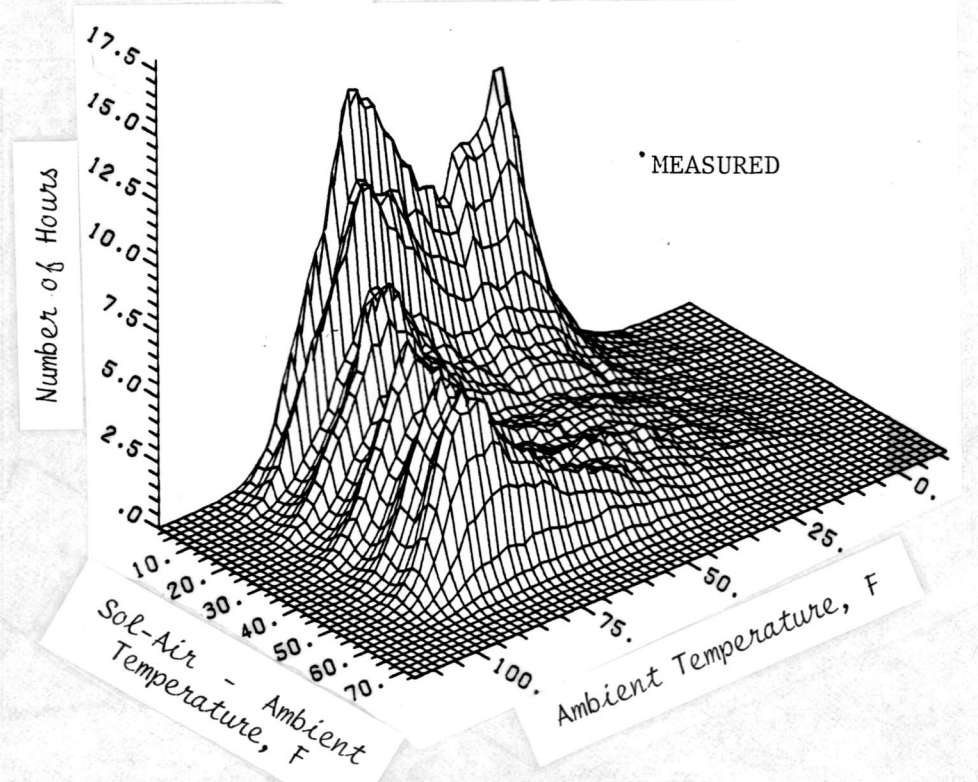

Figure 4.4 (cont.)

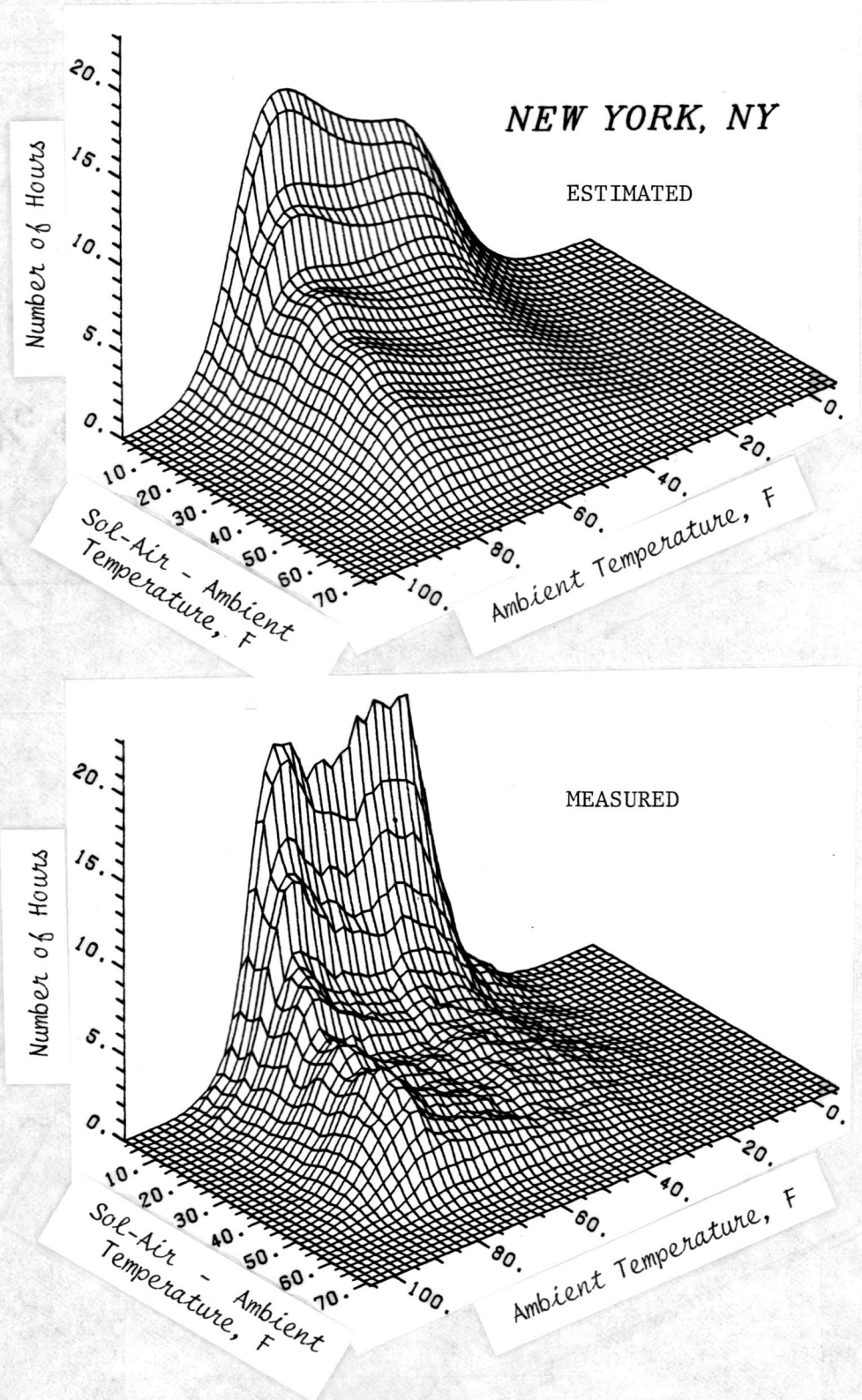

Figure 4.4 (cont.)

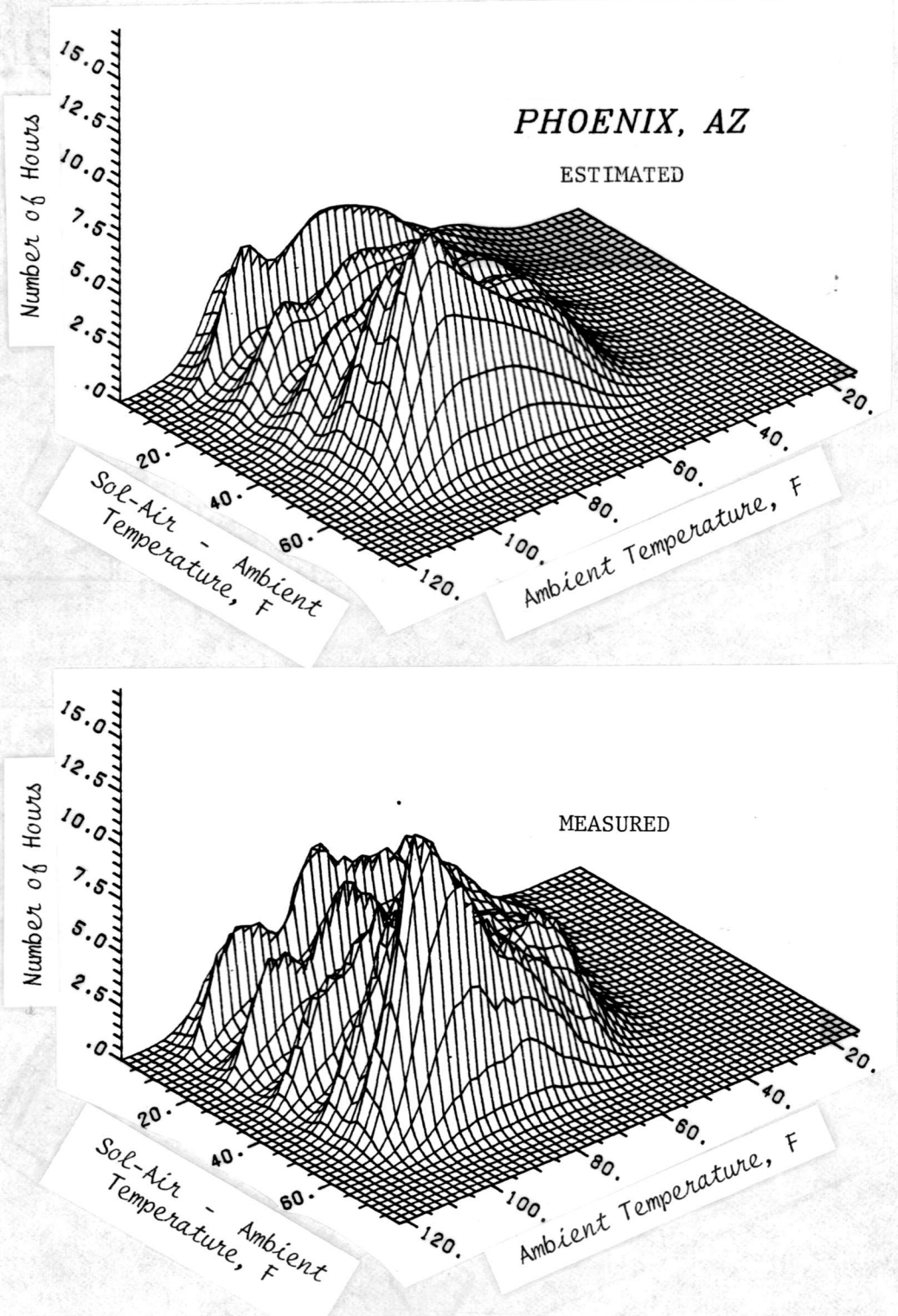

Figure 4.4 (cont.)

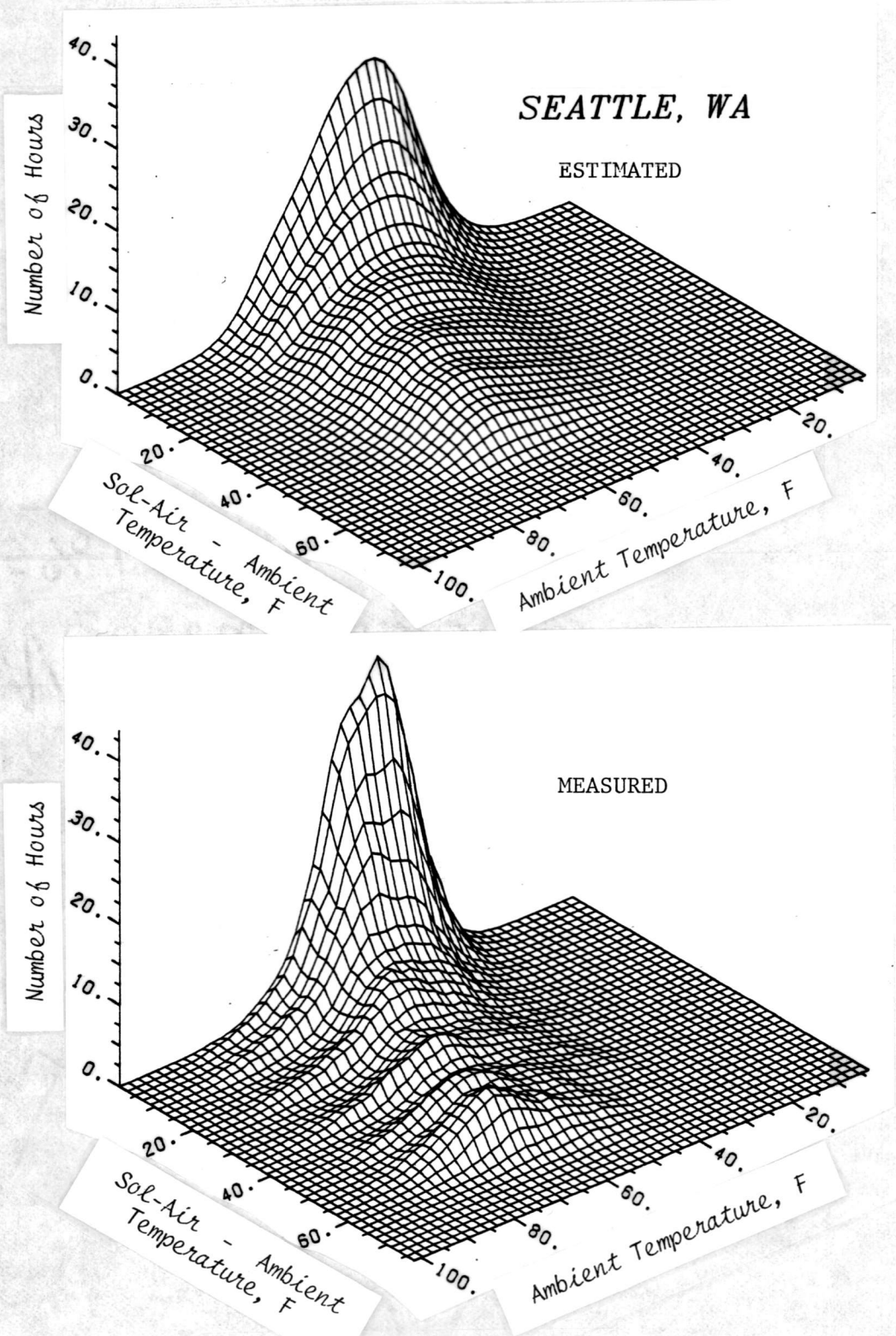

Figure 4.4 (cont.)

bient temperature and solar radiation is nearly zero for the winter months in these locations, the peak is not the result of a negative correlation between these variables. A possible cause is a very narrow range of clearness index values for the measured data. During the winter months in these two locations, the clearness of the atmosphere for hours near solar noon is nearly constant much of the time due to a lack of clouds and dust. Since the extraterrestrial radiation and the ratio of tilted to horizontal surface radiation are also nearly constant for these hours, the sol-air temperature difference is limited to a small range, and a peak forms.

The distribution function model for clearness index has a fairly broad range of clearness index values for which the probability of occurrence is significant (for a monthly-average hourly clearness index of 0.7, the probability density is at least 10% of the maximum value over a clearness index range of 0.5). This relatively large range for clearness index results in a wider range of sol-air temperature difference than is found in the measured data for the same hours, and the estimation model does not reproduce the peak contained in the measured data.

A feature which is evident in both the measured and estimated data are ridges running parallel to the ambient temperature axis. The ridges are most pronounced in the data for Albuquerque, Phoenix and Fort Worth, which are the locations with the highest values of the monthly-average clearness index. The ridges are not the result of physical phenomena preventing the occurrence of certain values

of sol-air temperature; instead they can be traced to the discrete nature of the data.

The measured and estimated bin data shown were obtained by summing the bin data for each daylight hour. The tilted surface radiation for a given value of clearness index changes by discrete intervals for both the measured and estimated data as solar noon is approached hour-by-hour. The ridges are the result of the superpositioning of data for different hours of the day, with each hour having a limited range of sol-air temperature difference where most of the data lie. Sunny locations have more distinct ridges due to: 1. The narrow range of clearness index for which the probability density is significant for high values of the monthly-average clearness index when compared to the probability density function for low values of the monthly-average clearness index and 2. The stronger dependence of the tilted surface radiation on R_b for large values of clearness index coupled with the fact that R_b also changes discretely from one hour to the next. When bin data were plotted for a single hour of the day and month of the year, no ridges were observed.

4.3 Sol-Air Heating and Cooling Degree-Days

4.3.1 Models for an Individual Surface

The difference between the sol-air temperature and the interior temperature of a building is a closer approximation to the driving force for conduction heat transfer through a wall than is the dif-

ference between the ambient and inside temperatures. If the degree-day concept is extended to sol-air temperature, the rate of heat transfer through the wall is assumed to equal the product of the wall conductance, UA, and the difference between the sol-air and inside air temperatures. Sol-air heating and cooling degree-days can be used in place of ambient temperature degree-days, providing a more realistic estimate of heat transfer through the shell. This is particularly important in the estimation of cooling loads, where the load resulting from solar radiation is often a greater percentage of the total load than for heating due to increased solar radiation and smaller differences between the ambient and inside temperatures during the summer months.

The derivation of a model for the estimation of sol-air heating degree-days, D_{SH}, is based on the definition given in Equation (2-8)

$$D_{SH} = N \int_{T_{sa,min}}^{T_b} (T_b - T_{sa}) P(T_{sa}) dT_{sa} \qquad (4\text{-}15)$$

where N is the number of days in the month. $P(T_{sa})$ is a complex function of a number of variables, as described above. If the analysis is restricted to a particular hour of the day and h_o is assumed to be constant, the probability density function for sol-air temperature is much easier to model. The assumption that ambient

temperature and sol-air temperature variations are uncorrelated allows $P(T_{sa})$ to be replaced by the product of $P(k_T)$ and $P(T_a)$, and the integration over sol-air temperature is transformed into a double integration over clearness index and ambient temperature. The sol-air heating degree-days for an hour of the day is then given by

$$D_{SH,h} = (N/24) \int_{T_{a,min}}^{T_{a,max}} \left(\int_{o}^{k_{T,max}} [T_b - T_{a,h} - \alpha I_T/h_o]^+ \cdot P(k_T)dk_T \right) P(T_{a,h})dT_{a,h} \tag{4-16}$$

where the superscript "+" signifies negative values of the enclosed quantity are set equal to zero.

The integration over k_T in the above equation cannot be performed directly due to the discontinuity introduced by the "+" operator. This problem can be circumvented if a second integral is subtracted to counter the effect of including negative values of the integrand in the original integral.

$$D_{SH,h} = \frac{N}{24} \int_{T_{a,min}}^{T_{a,max}} \left(\int_{o}^{k_{T,max}} [(T_b - T_{a,h})^+ - \frac{\alpha I_T}{h_o}]P(k_T)dk_T - \int_{k_{Tc}}^{k_{T,max}} [(T_b - T_{a,h})^+ - \frac{\alpha I_T}{h_o}]P(k_T)dk_T \right) P(T_{a,h})dT_{a,h} \tag{4-17}$$

where k_{Tc} is the value of k_T where $\alpha I_T/h_o$ is equal to the difference between the base temperature and the hourly ambient temperature. The first integrand in Equation (4-17) is integrated over k_T. The second integral, after some rearrangement, represents the definition of the hourly utilizability function (see Clark et al. (1983)) for solar radiation, $\phi(I_c)$. Hourly utilizability is the fraction of the total hourly tilted surface radiation for the month which occurs at intensities greater than I_c, the critical level.

If the integrations over k_T are performed, Equation (4-17) becomes

$$D_{SH,h} = (N/24)\int_{T_{a,min}}^{T_{a,max}} [(T_b - T_{a,h})^+ - (\alpha\bar{I}_T/h_o)(1 - \phi(I_c))] \cdot P(T_{a,h})dT_{a,h} \qquad (4\text{-}18)$$

where

$$I_c = (h_o/\alpha)(T_b - T_{a,h})^+ \qquad (4\text{-}19)$$

The integral of the temperature difference term in Equation (4-18) is the ambient temperature heating degree-days. The integral of $\phi(I_c)$ over ambient temperature, however, cannot be evaluated analytically using the functions available for $\phi(I_c)$ and $P(T_{a,h})$.

As an approximation, the hourly ambient temperature is assumed to always be equal to the monthly-average value for the purpose of evaluating the integral of $\phi(I_c)$. This assumption is equivalent to assuming the mean value of ϕ over the range of critical levels en-

countered is equal to the utilizability for the mean critical level. The expression for sol-air heating degree-days then becomes

$$D_{SH,h} = D_{H,h} - (N\alpha\bar{I}_T/24h_o)(1 - \phi(\bar{I}_c)) \qquad (4\text{-}20)$$

where

$$\bar{I}_c = (h_o/\alpha)(T_b - \bar{T}_{a,h})^+ \qquad (4\text{-}21)$$

A similar development leads to a relationship for the estimation of sol-air cooling degree-days.

$$D_{SC,h} = D_{C,h} + (N\alpha\bar{I}_T/24h_o)\phi(\bar{I}_c) \qquad (4\text{-}22)$$

where $\bar{I}_c$ is defined above.

4.3.2 Extension of the Models to Multiple Surfaces

The relationships presented so far for sol-air heating and cooling degree-days are for a single surface. Buildings are composed of a number of distinct surfaces each having different orientations and properties. In addition to the solar radiation which is absorbed on outer surfaces, solar radiation is transmitted through glazings and absorbed internally. Energy may be flowing in through some of the surfaces while at the same time other surfaces are losing energy to the environment. To properly account for the net effect solar radiation and ambient temperature have on the heating and cooling loads, it is necessary to combine the sol-air heating and cooling degree-days for the entire structure into a single calcula-

tion.

Equation (4-16) can be expanded into a more general form to include all building surfaces and glazings. This expansion is accomplished by summing up the energy flow terms due to conduction heat transfer and the energy flow terms due to the transmission of solar energy through glazings and dividing the resulting net energy flow for the building by the overall building conductance. The result is:

$$D_{SH,h} = \frac{N}{24} \int_{T_{a,min}}^{T_{a,max}} \int_{o}^{k_{T,max}} \left(T_b - T_{a,h} - \frac{\sum_{j=1}^{ns} (UA)_j \alpha_j I_{Tsj}}{h_o (UA)_o} - \frac{\sum_{i=1}^{ns} (\tau\alpha)_i A_{gi} I_{Twi}}{(UA)_o} \right)^{+} P(k_T)dk_T \cdot P(T_{a,h})dT_{a,h} \tag{4-23}$$

where nw is the number of windows, ns is the number of absorbing surfaces, $(\tau\alpha)_i$ is the effective transmittance-absorptance product for the window-room system, A_{gi} is the glazing area, $(UA)_j$ is the thermal conductance for each surface, and $(UA)_o$ is the overall building conductance. If the glazings absorb a significant fraction of the incident solar radiation, they must be included in both the window summation (to account for the transmission of solar energy) and the surface summation (to account for the effect of the sol-air temperature for the window on the conduction of heat through the

window).

The available utilizability functions are designed for a single surface with an incident radiation level between zero and extra-terrestrial. Before Equation (4-23) can be simplified, it is necessary to combine the solar gain terms into a single term. This combined term is an "effective" surface which represents a superpositioning of all of the individual surface solar gains. The two summations are first placed over the common denominator $h_o(UA)_o$ and then normalized by dividing by Z, where Z is defined as:

$$Z = [\sum_{j=1}^{ns} (UA)_j \alpha_j + h_o \sum_{i=1}^{nw} (\tau\alpha)_i A_{gi}]/[(UA)_o h_o] \qquad (4\text{-}24)$$

The form of the integral becomes equivalent to that for a single surface (Equation (4-16)), and the final result for an arbitrary number of surfaces is

$$D_{SH,h} = D_{H,h} - Z(N/24)\bar{I}_{To}(1 - \phi(\bar{I}_{co})) \qquad (4\text{-}25)$$

where

$$\bar{I}_{co} = (T_b - \bar{T}_{a,h})^+/Z \qquad (4\text{-}26)$$

$$\bar{I}_{To} = \frac{[\sum_{j=1}^{ns} (UA)_j \alpha_j \bar{I}_{Tsj} + h_o \sum_{i=1}^{nw} (\tau\alpha)_i A_{gi} \bar{I}_{Twi}]}{[Z(UA)_o h_o]} \qquad (4\text{-}27)$$

If surface dependent properties are required in the evaluation

of ϕ, they should be radiation-weighted averages of the properties for the various surfaces.

Sol-air cooling degree-days for a building are modeled by the analogous relationship

$$D_{SC,h} = D_{C,h} + Z(N/24)\bar{I}_{To}\phi(\bar{I}_{co}) \qquad (4\text{-}28)$$

where Z, $\bar{I}_{To}$ and $\bar{I}_{co}$ are defined above.

4.3.3 Sol-Air Heating Degree-Days for No-Storage Solar Systems

A solar air heating system which has no thermal storage draws in room air and returns it directly to the heated space. Solar gains from a no-storage system can be treated in the same manner as direct gains through a window, with one important difference. When the radiation incident on the collector is less than the level required to result in a net gain for the collector, the collector critical level, the collector should not operate. If the gains due to transmission through windows and absorption by walls are sufficient to offset the heating requirements of the structure at a radiation level less than the collector critical level, the collector will not operate at all.

If the condition

$$I_{Tc} < [U_L/(\tau\alpha)_c](T_r - T_{a,h})^+ \qquad (4\text{-}29)$$

is satisfied for the clearness index value where there is no heating load, k'_{co}, the collector system will not run for the hour and month

under consideration, and sol-air degree-days can be calculated using Equation (4-25). I_{Tc} is the tilted surface radiation incident on the collector plane for an arbitrary value of clearness index. The following equation must be solved for k'_{co}:

$$\sum_{j=1}^{ns} (UA)_j \alpha_{sj} I_{Tsj} + h_o \sum_{i=1}^{nw} (\tau\alpha)_i A_{gi} I_{Tw_i} + A_c F_R (\tau\alpha)_c h_o I_{Tc} \tag{4-30}$$

$$= h_o UA_o (T_b - T_{a,h})^+ + h_o A_c F_R U_L (T_r - T_{a,h})^+$$

where F_R is the collector heat removal factor, U_L is the collector loss coefficient, $(\tau\alpha)_c$ is the effective transmittance-absorptance product for the collector (for a more complete definition of F_R, U_L and $(\tau\alpha)_c$, see Duffie and Beckman (1980)) and T_r is the interior air temperature.

When Equation (4-29) is not satisfied, the collector will be able to supply useful gains to the structure. If Equation (4-23) is modified to include the energy delivery by the collectors, the expression for sol-air heating degree-days becomes

$$D_{SH,h} = D_{H,h}(T_b) - \frac{N}{24} Z' \bar{I}'_{To} (1-\phi(\bar{I}'_{co})) \tag{4-31}$$

$$+ \frac{NA_c F_R (\tau\alpha)_c}{24(UA)_o} \bar{I}_{Tc} (1-\phi(\bar{I}_{cc}))$$

where

$$\bar{I}'_{co} = \frac{(T_b - \bar{T}_{a,h})^+}{Z'} + \frac{A_c F_R U_L}{Z'(UA)_o} (T_r - \bar{T}_{a,h})^+ ,$$

$$\bar{I}_{cc} = \frac{U_L}{(\tau\alpha)_c} (T_r - \bar{T}_{a,h})^+ ,$$

$$Z' = Z + \frac{A_c F_R (\tau\alpha)_c}{(UA)_o} ,$$

$$\bar{I}'_{To} = \frac{\left(\sum_{j=1}^{ns} (UA)_j \alpha_{sj} \bar{I}_{Tsj} + h_o \sum_{i=1}^{nw} (\tau\alpha)_i A_{gi} \bar{I}_{Twi} + A_c F_R (\tau\alpha)_c h_o \bar{I}_{Tc}\right)}{Z'(UA)_o h_o}$$

Equation (4-31) differs from Equation (4-25) by an additional term to account for the incident radiation which occurs at levels below the collector critical level.

4.3.4 Ventilation Sol-Air Cooling Degree-Days

The reduction in the cooling load for a structure when ambient air is used for cooling was discussed in Chapter 3. It is even more important to include the effect of ventilation when considering sol-air cooling degree-days, as the ambient temperature at which a cooling load first appears may be substantially below the room setpoint if there are significant solar gains.

The development of a relationship for the estimation of ventilation sol-air cooling degree-days, $D_{SCV,h}$, is similar to that for ventilation ambient temperature cooling degree-days. The rate at

which energy can be removed by ventilation is equal to the product of the air capacitance rate, $\dot{m}C_p$, and the inside-outside temperature difference. An expression similar to Equation (4-16) can be written for $D_{SCV,h}$

$$D_{SCV,h} = N \int_{T_{a,h,min}}^{T_r} \int_{o}^{k_{T,max}} (T_{a,h} + ZI_{To} - T_b - \frac{\dot{m}c_p(T_r - T_{a,h})}{(UA)_o}) +$$

$$\cdot P(k_T)\,dk_T P(T_{a,h})\,dT_{a,h} \qquad (4\text{-}32)$$

$$+ \int_{T_r}^{T_{a,h,max}} \int_{o}^{k_{T,max}} (T_{a,h} + ZI_{To} - T_b)\; P(k_T)\,dk_T P(T_{a,h})\,dT_{a,h}$$

where the integration over ambient temperature has been divided into the ranges where ventilation can and cannot be used.

After some algebraic simplification and the substitution of the ambient temperature distribution model presented in Chapter 3, an expression is obtained for $D_{SCV,h}$.

$$D_{SCV,h} = \left(\frac{N^{3/2}\sigma_m}{48}\right)\left(\frac{\dot{m}c_p + (UA)_o}{(UA)_o}\right)\left[\frac{\ell n\, cosh(Bh^*_b) - \ell n\, cosh(Bh^*_r)}{B}\right.$$

$$\left. + (h^*_r - h^*_b)\tanh(Bh^*_r)\right] + \frac{N}{24} Z\bar{I}_{To}\phi(\bar{I}''_{co}) + D_{C,h}(T_r) \qquad (4\text{-}33)$$

$$+ \frac{N}{24}(1 - Q(h_r))(T_r - T_b)$$

where

$$h^*_r = \frac{(\overline{T}_{a,h} - T_r)}{\sqrt{N}\sigma_m} ,$$

$$h^*_b = \frac{(\overline{T}_{a,h} - T'_b)}{\sqrt{N}\sigma_m} ,$$

$$h_r = \frac{(T_r - \overline{T}_{a,h})}{\sqrt{N}\sigma_m} ,$$

$$T'_b = \frac{(UA)_o}{(\dot{m}c_p+(UA)_o)} T_b + \frac{\dot{m}c_p}{(\dot{m}c_p+(UA)_o)} T_r,$$

$$\overline{I}''_{co} = \frac{(T_b + \dot{m}c_p(T_r-\overline{T}_{a,<h})/(UA)_o-\overline{T}_{a,h})}{Z} ,$$

where $\overline{T}_{a,<h}$ is the average value for ambient temperatures below the room thermostat setpoint, B is equal to 1.698 and Q is the cumulative distribution function for ambient temperature.

4.3.5 Comparisons with Measured Data

The models developed for the estimation of sol-air degree-days are based on a number of simplifying assumptions. The variations of hourly ambient temperature and hourly clearness index from their respective monthly-average values were assumed to be uncorrelated to allow the use of univariate distribution function models for these variables. The utilizable solar energy gains are estimated using the monthly-average hourly value of ambient temperature

instead of integrating over the monthly range of ambient temperature. The outside surface heat transfer coefficient was assumed constant to eliminate the need for a distribution function model for this variable. The sol-air degree-day models are functions of relationships which describe the distribution of solar radiation and ambient temperature, and the use of these relationships introduces additional error into the estimation procedure. Comparisons between measured and estimated sol-air degree-days provide an indication of the combined effect of these approximations on the accuracy of the model.

The hourly SOLMET data were used to generate sol-air heating and cooling degree-days. Base temperatures between 1 and 20°C for heating and 10 and 29°C for cooling were considered. Degree-days for hours when the sun was above the horizon were summed to obtain daylight sol-air degree-days. A ground reflectance of 0.2 was used for all months, and diffuse radiation was modeled as isotropic. The value used for α was 0.9, and h_o was 34 W/m^2-°C for heating degree-days and 23 W/m^2-°C for cooling degree-days.

Sol-air degree-days were calculated for six surface orientations: vertical surfaces facing the four compass directions, a horizontal surface and a south-facing surface with a slope equal to the latitude. Comparisons of measured and estimated sol-air degree-days for surfaces of different orientations indicate the effect of orientation on the accuracy of the estimation procedure. A surface which receives no solar radiation was included to indicate the rela-

tive importance of solar radiation for each of the surface orientations.

Sol-air heating and cooling degree-days were then estimated for the same locations, surfaces and hours of the day using the relationships provided in Equations (4-20) and (4-22). The hourly utilizability model of Clark et al. (1983) and the ambient temperature degree-day models given in Chapter 3 were used. The monthly-average hourly values of clearness index and ambient temperature were estimated from the monthly-average daily values.

Figure 4.5 is a comparison of measured and estimated sol-air heating degree-days for the 6 locations with the largest heating degree-day totals. The no solar curve indicates the accuracy of the ambient temperature degree-day estimates. In Columbia and Albuquerque, the ambient temperature degree-days are underpredicted, leading to an underprediction of the sol-air degree days for all surfaces in Columbia. In Albuquerque, a compensating error in the utilizability estimate leads to good agreement for the 5 surfaces which receive the most solar radiation. A more systematic error which shows up in all locations at low values of base temperature is the overprediction of sol-air heating degree-days. This overprediction can be attributed to the use of an average critical level, based on the monthly-average temperature, to evaluate ϕ. In all cases, however, the differences between the measured and estimated sol-air degree-days are small in magnitude.

Surface Orientation	Hourly SOLMET Data	Estimation Method
South, Vertical	⏀	- - - - - - - - - - -
West, Vertical	△	— — — — — — —
East, Vertical	×	— — — — — —
North, Vertical	+	- - - - - - - - - -
Horizontal	◇	— - — - — - —
South, Slope = Lat.	↑	— — — — —
No Solar	⧖	- — - — - —

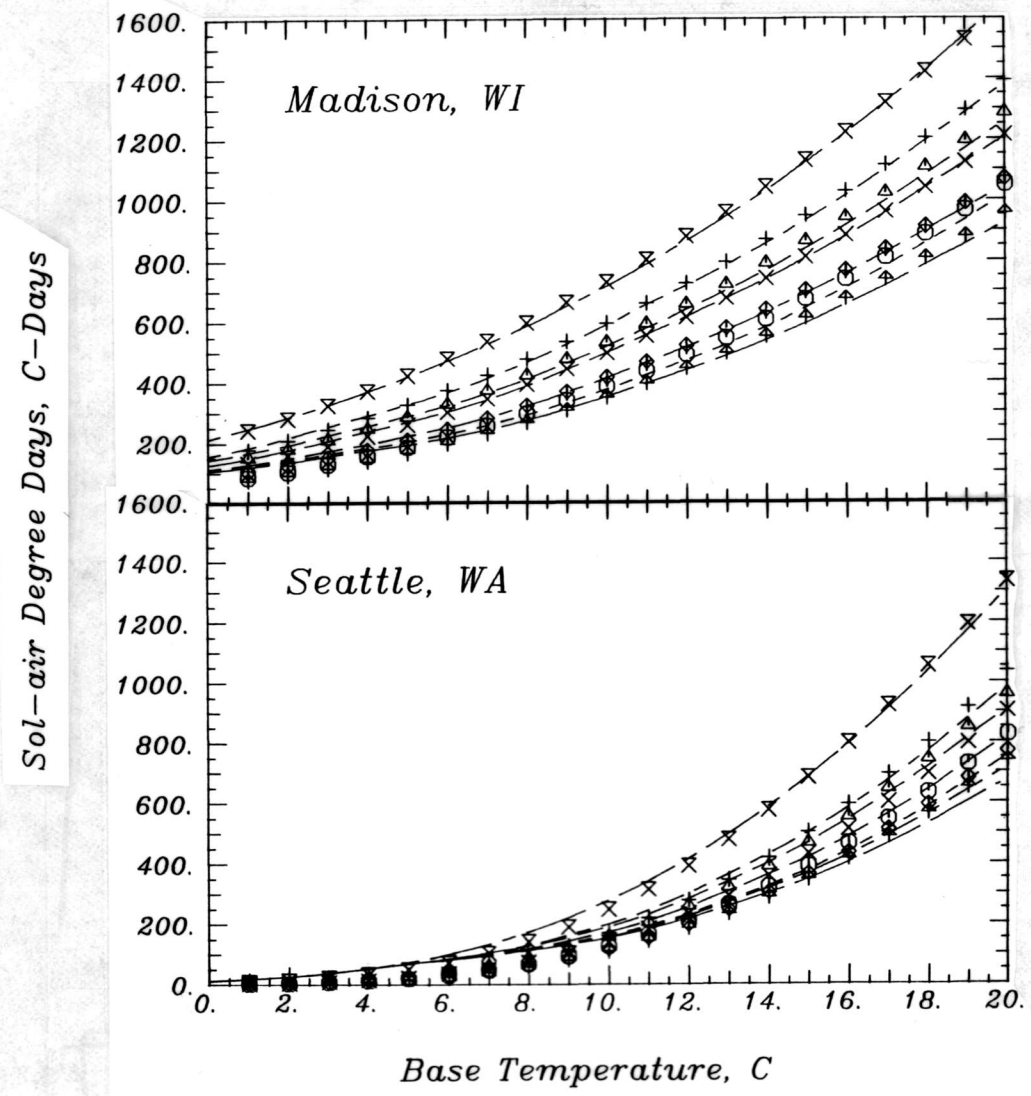

Figure 4.5 Measured and Estimated Sol-Air Heating Degree-Days for Different Surface Orientations with Constant Heat Transfer Coefficients

Surface Orientation	Hourly SOLMET Data	Estimation Method
South, Vertical	⏲	- - - - - - - - - - -
West, Vertical	△	— — — — — — —
East, Vertical	×	— — — — — —
North, Vertical	+	- - - - - - - - - -
Horizontal	◇	- — - — - — - —
South, Slope = Lat.	↟	— — — — — —
No Solar	⧖	- — - — - — -

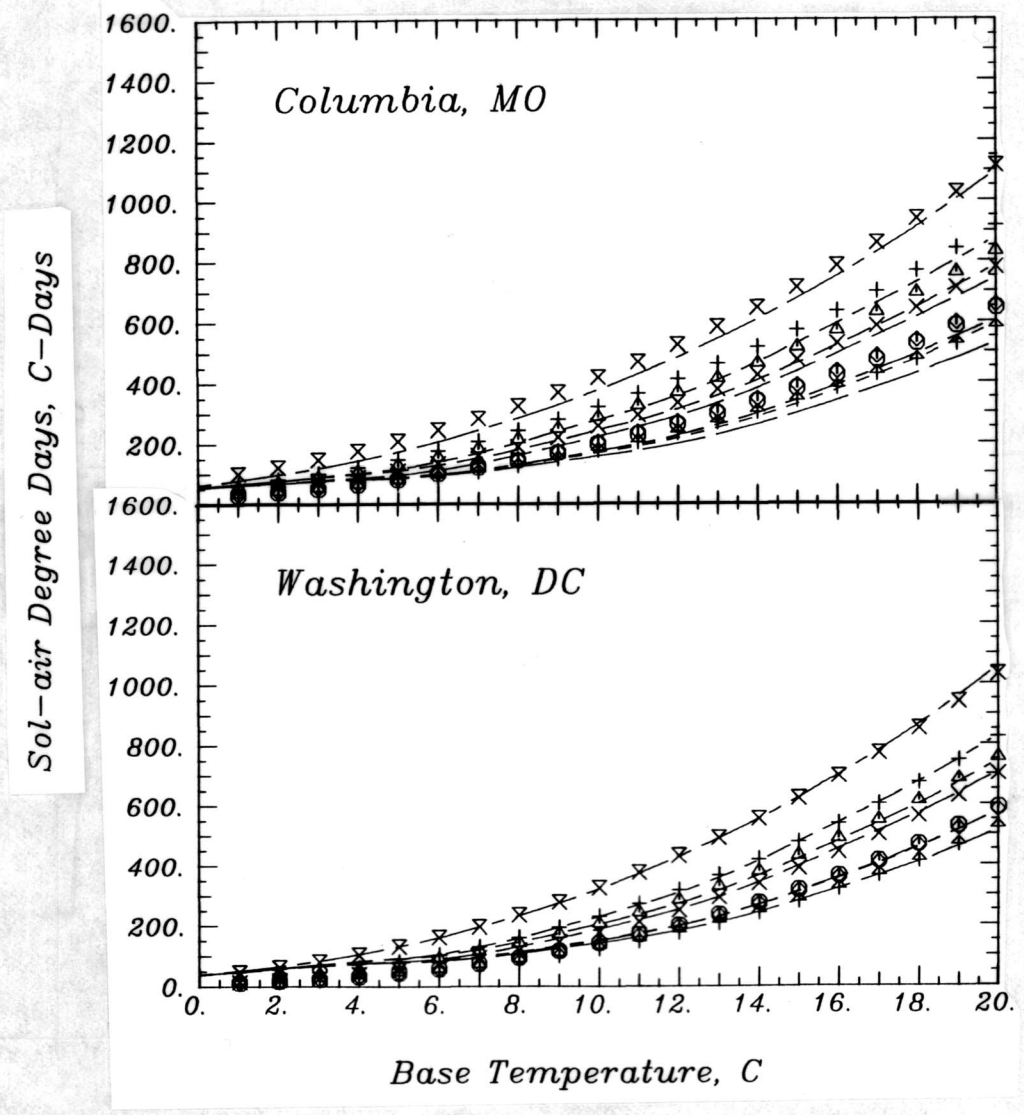

Figure 4.5 (cont.)

Surface Orientation	Hourly SOLMET Data	Estimation Method
South, Vertical	⏲	- - - - - - - - - - -
West, Vertical	△	— — — — — — —
East, Vertical	×	— — — — — —
North, Vertical	+	- - - - - - - - - -
Horizontal	◇	- — - — - — -
South, Slope = Lat.	↟	—— —— —— ——
No Solar	⧖	- —— - —— - ——

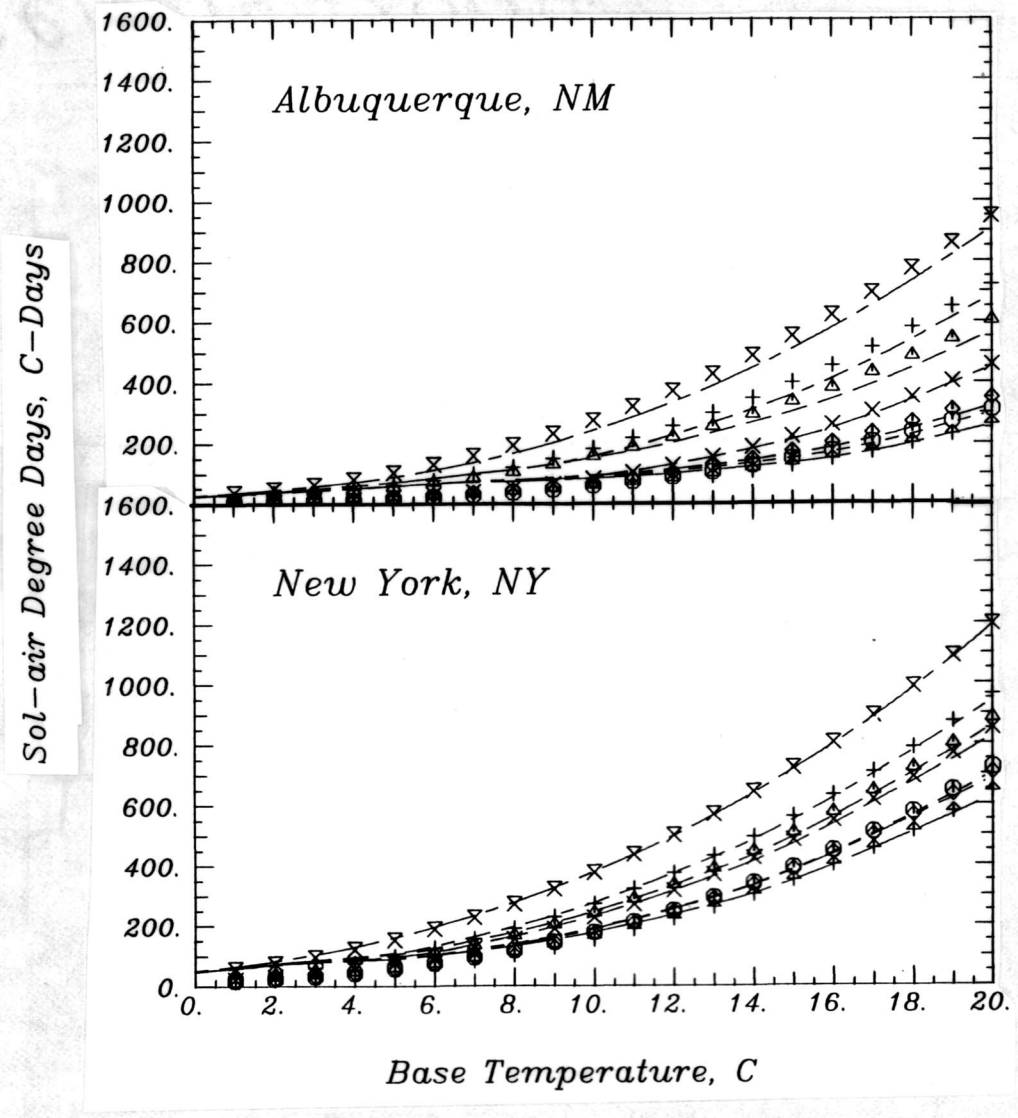

Figure 4.5 (cont.)

Figure 4.6 is a comparison of measured and estimated sol-air cooling degree-days for the 6 locations with the largest cooling degree-day totals. In this figure, the lowermost curve indicates the accuracy of the ambient temperature cooling degree-day estimates. The effect of solar radiation on the cooling degree-days is much larger on the average than the effect of solar radiation on the heating degree-days for the same surface. This is partly due to the smaller convection coefficient chosen for the calculation of D_{SC} (wind speeds are generally lower in the summer) and partly due to the larger fraction of the load which results from solar radiation for the cooling season. Again, the errors for the estimated sol-air degree-days are small.

The comparisons presented above were based on the assumption that h_o is constant. Time variations in h_o occur largely as a result of wind speed fluctuations. In order to test the effect of variations in h_o on the accuracy of the sol-air degree-day estimates, it is necessary to model the variation of h_o. An average value of the convective component of h_o for all surfaces of a building can be obtained from a relationship developed by Mitchell (1976) which treats the building as a sphere. A linearized infrared radiation heat transfer coefficient was calculated by assuming a surface emittance of 0.9 and a surface temperature equal to the ambient temperature (the surface temperature assumption is only for the purpose of linearizing the radiation heat transfer), and the radiative coefficient was added to the convective coefficient to obtain a

Surface Orientation	Hourly SOLMET Data	Estimation Method
South, Vertical	⏲	- - - - - - - - - - -
West, Vertical	△	— — — — — — — —
East, Vertical	×	— — — — — — —
North, Vertical	+	- - - - - - - - - -
Horizontal	◇	— - — — — - —
South, Slope = Lat.	⏲	— — — — — —
No Solar	⧖	- — - — - —

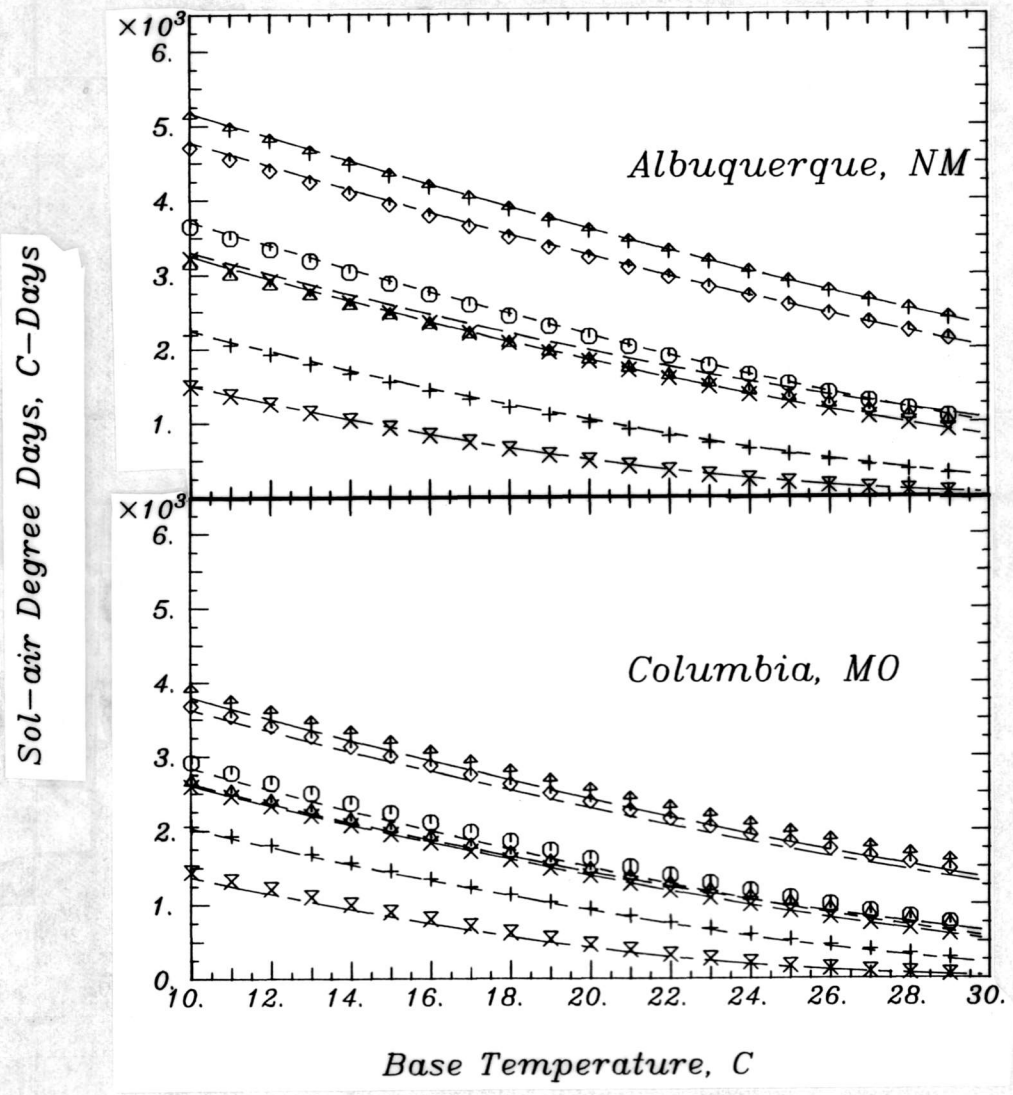

Figure 4.6 Measured and Estimated Sol-Air Cooling Degree-Days for Different Surface Orientations with Constant Heat Transfer Coefficients

Surface Orientation	Hourly SOLMET Data	Estimation Method
South, Vertical	⏀	- - - - - - - - - - -
West, Vertical	△	— — — — — — —
East, Vertical	×	— — — — — —
North, Vertical	+	- - - - - - - - - -
Horizontal	◇	- — - — - — - —
South, Slope = Lat.	↟	— — — — — —
No Solar	⧖	- — - — - —

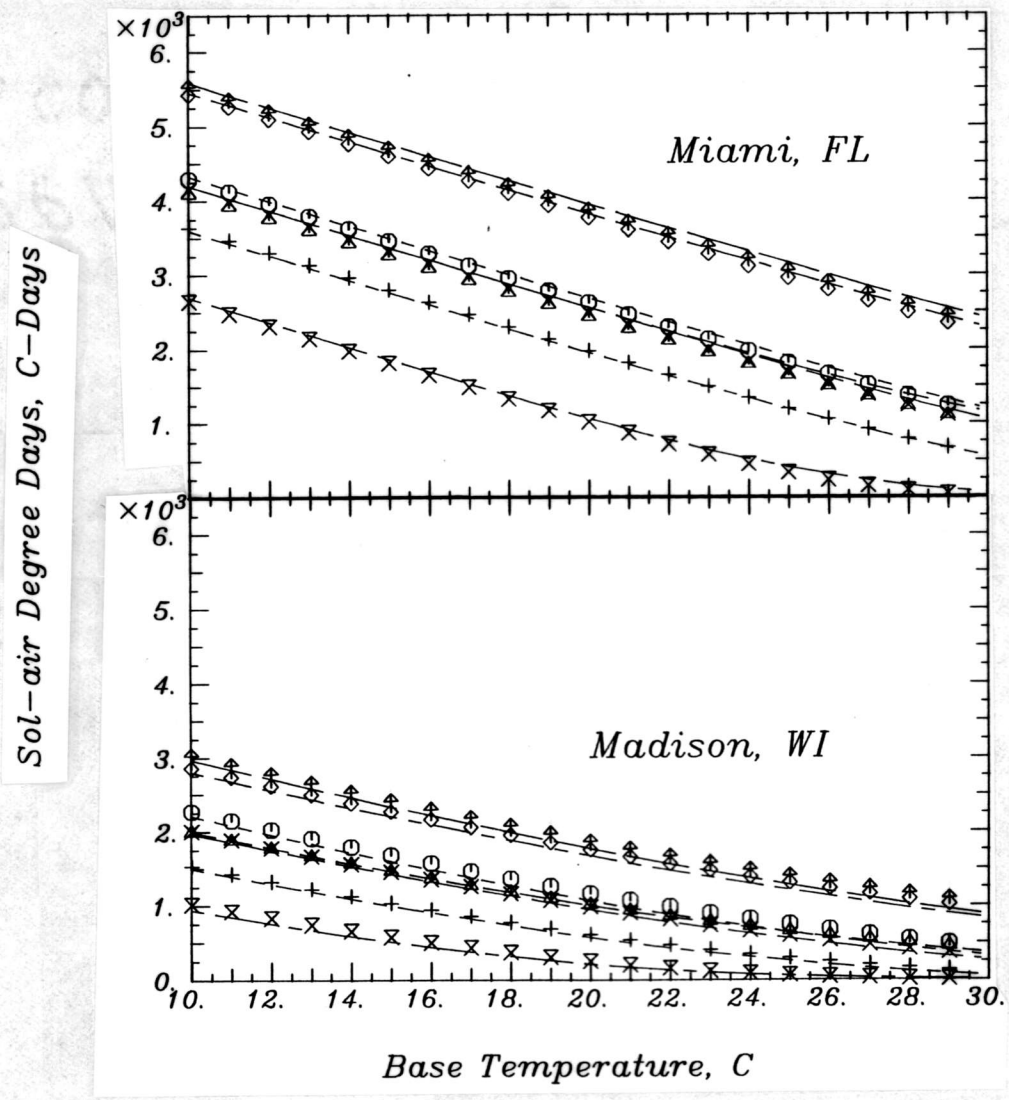

Figure 4.6 (cont.)

Surface Orientation	*Hourly SOLMET Data*	*Estimation Method*
South, Vertical	⏀	- - - - - - - - - - -
West, Vertical	△	— — — — — — —
East, Vertical	×	— — — — — —
North, Vertical	+	- - - - - - - - -
Horizontal	◇	- — - — - — -
South, Slope = Lat.	⏀	— — — —
No Solar	⧖	- — - — - —

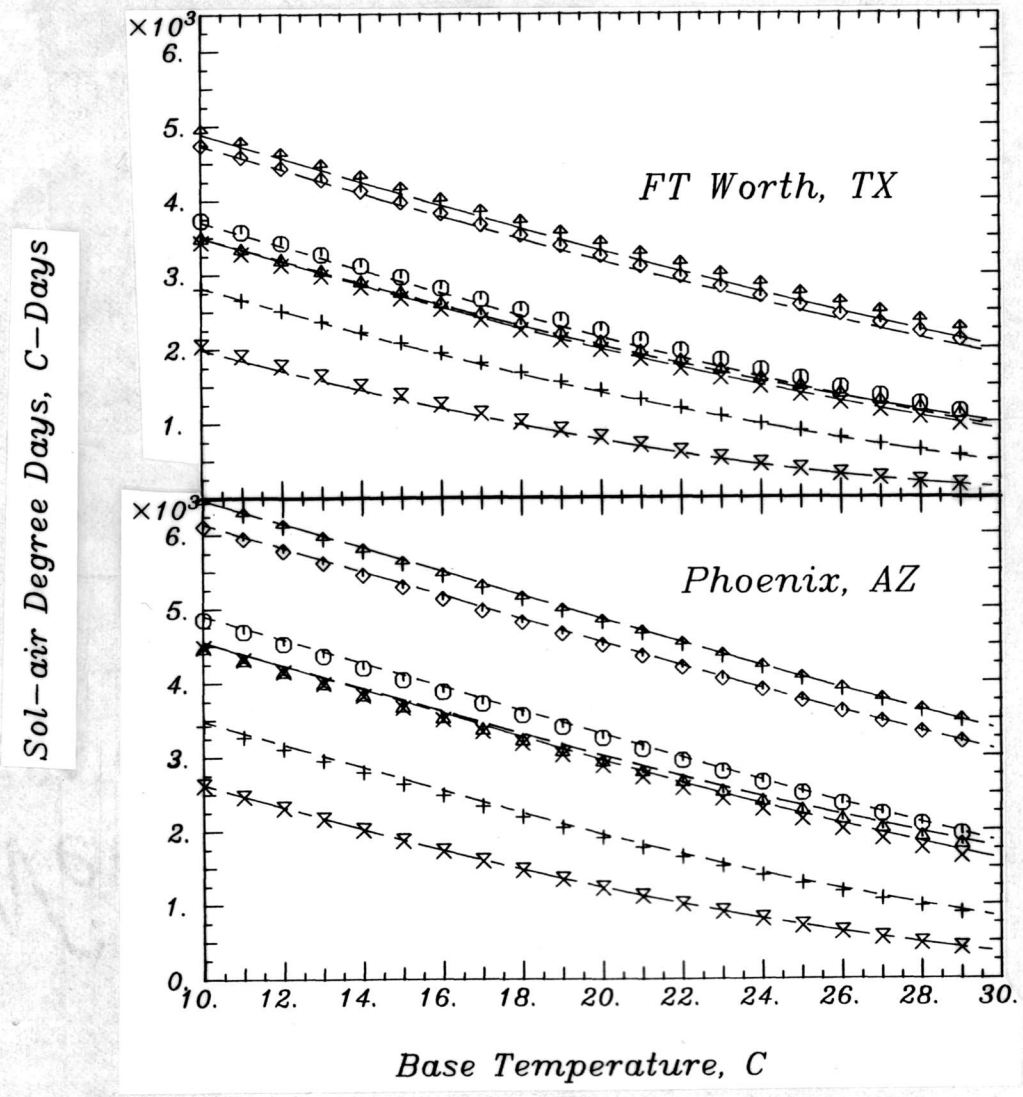

Figure 4.6 (cont.)

value for h_o. Although the value of h_o calculated from airport wind speed data may not be correct for the walls of a structure, the variation in the estimated values of h_o will hopefully be representative of the variation in the actual values of h_o.

Sol-air heating and cooling degree-days were recompiled from the long-term hourly data using values of h_o calculated with measured wind speed data. In order to reduce the computational effort, a single year of TMY [SOLMET (1978)] wind speed data was used repeatedly for each year in the long-term data sets. Only a south-facing surface with a slope equal to the latitude and an absorptance of 0.9 was considered. The average windspeed was also calculated for each month for the daytime period.

Sol-air heating and cooling degree-days were then estimated for this surface using a constant value of h_o for each month. The constant value of h_o for each month was obtained using the average daytime wind speed for the month and the model for h_o described above.

The sol-air heating degree-days estimated with the constant h_o values are compared in Figure 4.7 to the values compiled using hourly values of h_o for the same 6 locations as shown in Figure 4.5. The average value of h_o is smaller than the constant value of h_o originally used, and the difference between the no-solar degree-days and the sol-air degree-days is larger for the same surface than in Figure 4.5. The degree-day estimates based on a constant value of h_o are in good agreement with the sol-air degree-days

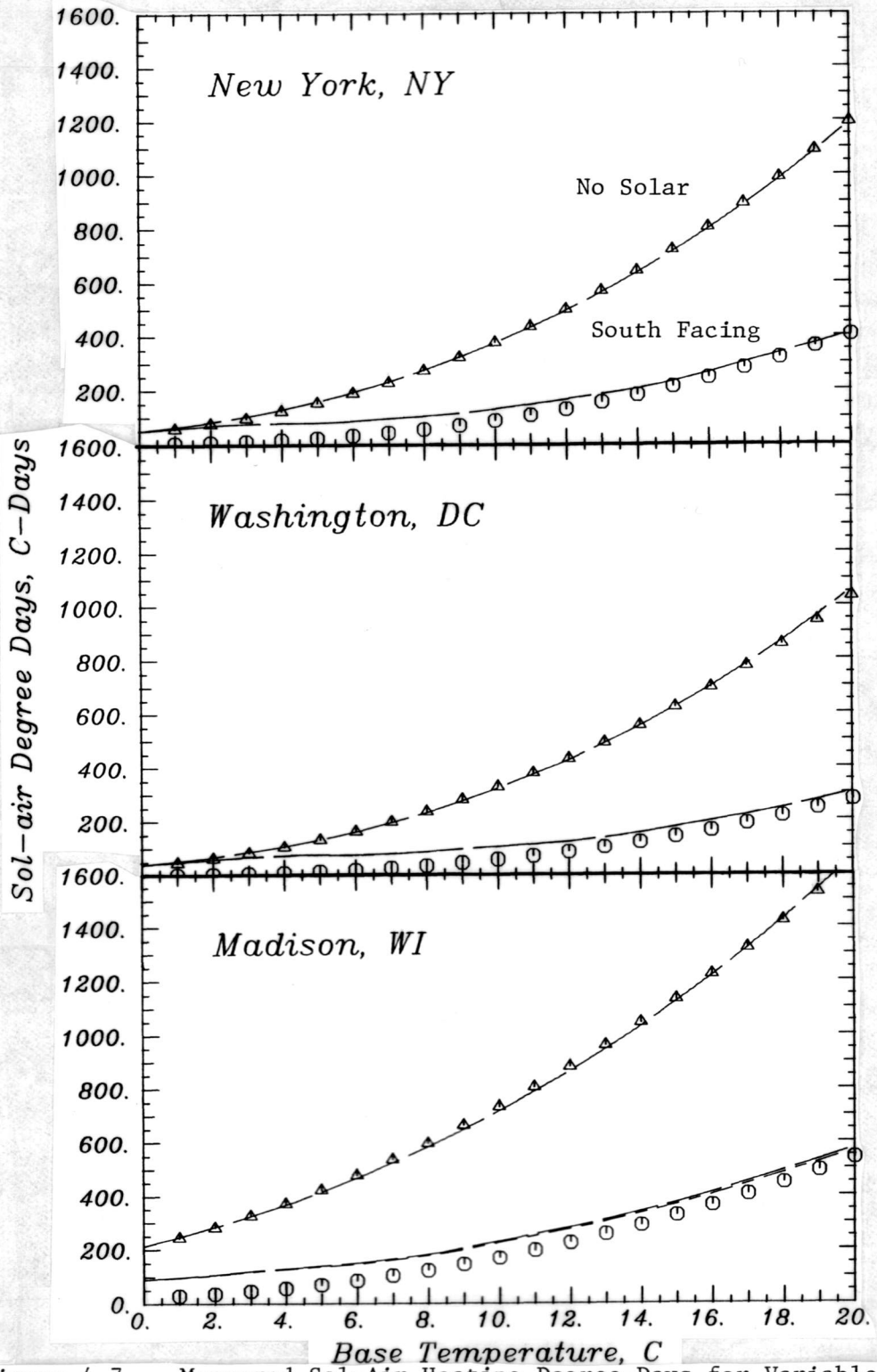

Figure 4.7 Measured Sol-Air Heating Degree-Days for Variable Heat Transfer Coefficients and Estimated Values for Constant Heat Transfer Coefficients

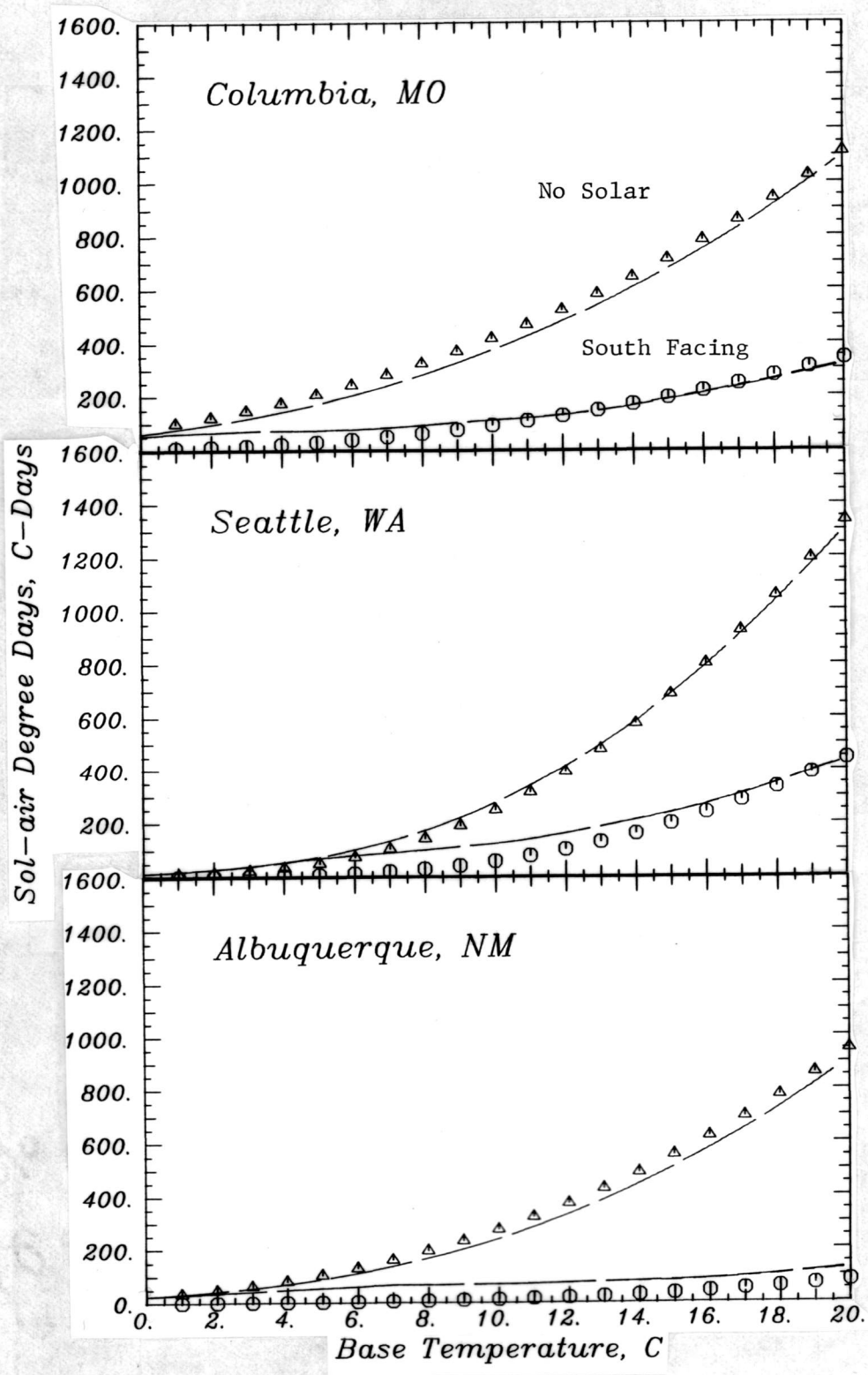

Figure 4.7 (cont.)

compiled from the hourly data with a variable h_o.

The corresponding comparison for sol-air cooling degree-days is shown in Figure 4.8. The effect of variations in the value of h_o is more significant for cooling degree-days than it is for heating degree-days. The data for Albuquerque exhibit the largest effect, possibly indicating a correlation between wind speed and solar radiation or wind speed and ambient temperature for this location. The agreement between the measured and estimated sol-air degree-days is still within 10% for Albuquerque and within 5% for the remaining locations.

4.4 Summary

A model was developed for the bivariate distribution of sol-air temperature and ambient temperature for an hour of the day using existing univariate distribution functions for ambient temperature and clearness index. This model is based on the assumption that the variations of hourly ambient temperature and hourly clearness index are uncorrelated. A procedure was described for the estimation of two-dimensional sol-air temperature/ambient temperature bin data which only requires the monthly-average daily clearness index and ambient temperature as input. Estimated and measured sol-air temperature/ambient temperature bin data for a south-facing tilted surface were compared for 9 U.S. locations, and the estimated bin data were found to be similar in appearance to the measured bin data.

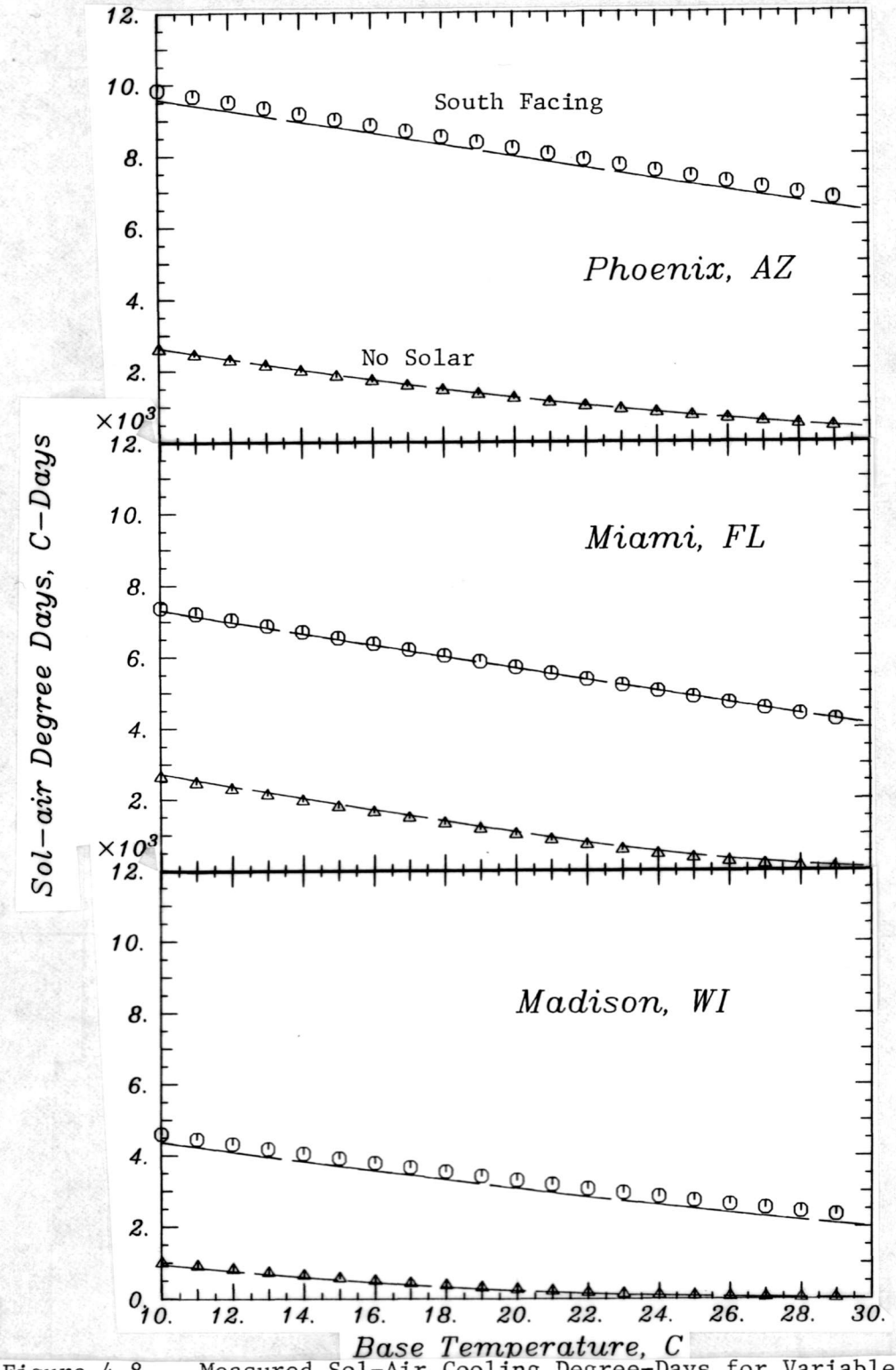

Figure 4.8 Measured Sol-Air Cooling Degree-Days for Variable Heat Transfer Coefficients and Estimated Values for Constant Heat Transfer Coefficients

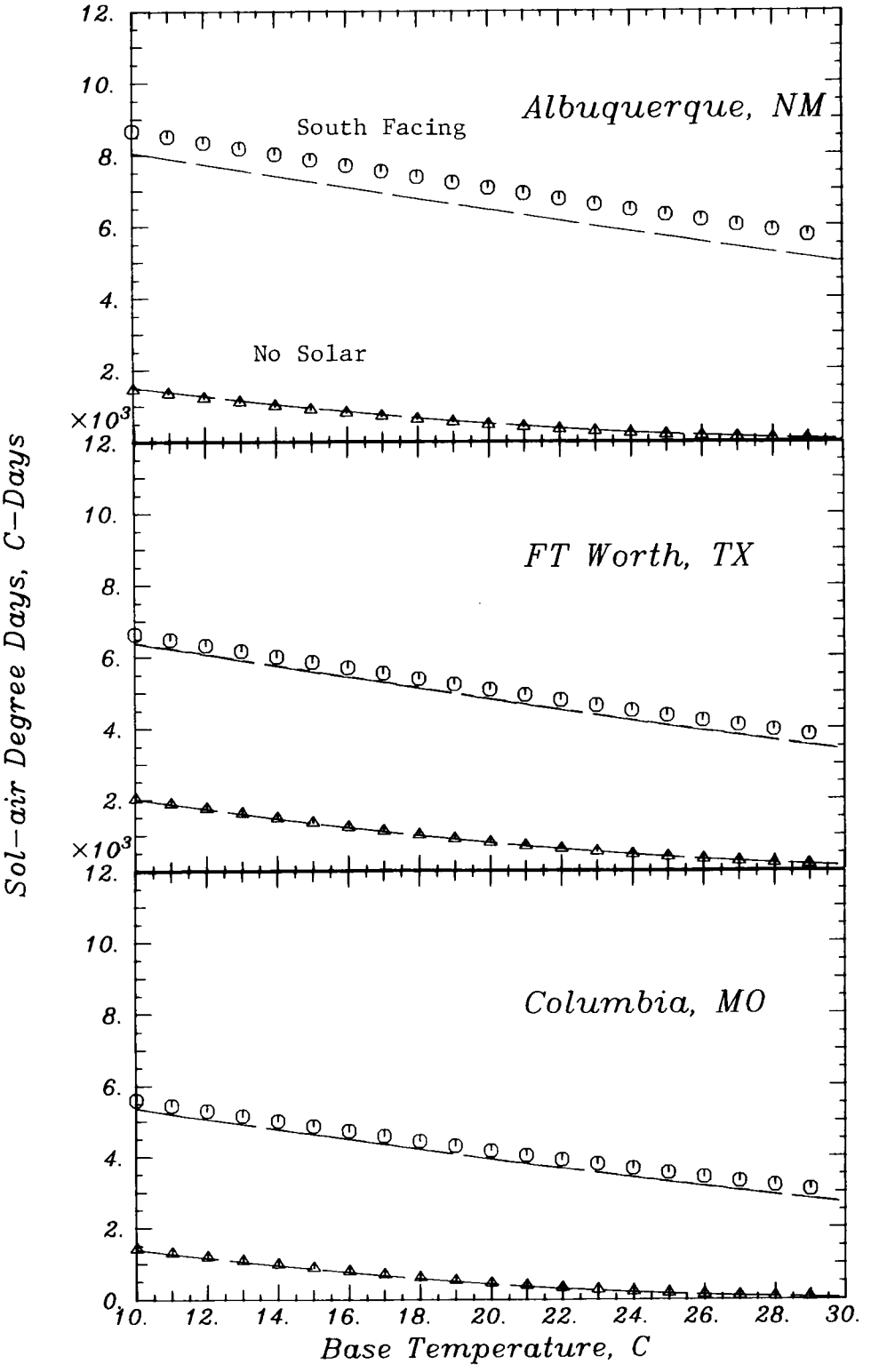

Figure 4.8 (cont.)

A set of relationships was also developed for the estimation of sol-air heating and cooling degree-days. The relationship for a single surface was extended to include an arbitrary number of absorbing and transmitting surfaces. A relationship was presented for sol-air heating degree-days when a no-storage solar system is used to heat the building, and a relationship was presented for sol-air cooling degree-days when ventilation with ambient air is used to cool the building. The relationship for a single surface was used to estimate heating and cooling sol-air degree-days for 6 surface orientations and a range of base temperature values, and comparisons were presented between the estimated sol-air degree-days and sol-air degree-day values compiled from the long-term hourly measurements. The agreement between the measured and estimated degree-day values is generally within 5% of the measured degree-days on an annual basis. Similar comparisons were presented for a south-facing surface for values of sol-air degree-days compiled using hourly values of the outside surface heat transfer coefficient. The sol-air degree-days estimated using a constant value of the heat transfer coefficient are still within 10% (and generally within 5%) of the compiled values based on a variable heat transfer coefficient.

CHAPTER 5

5. AMBIENT HUMIDITY STATISTICS

5.1 Literature Review

Ambient humidity is measured and recorded at most airports and weather stations in the U.S. Historical humidity data are available in both printed and magnetic tape [Butson and Hatch (1979)] form for several hundred locations, but the large amount of data required to provide a representation of long-term average conditions makes the use of such data impractical for most studies. Single year data sets have been created by selecting those months most representative of long-term average conditions from long-term historical data [SOLMET (1978)]. While these "typical year" data reduce the required computational effort, a possible source of inaccuracy is introduced, since it may not be possible to construct a single, continuous year of data which represents the long-term behavior of all weather variables. Also, "typical year" data are available for only 26 locations in the U.S.

Ambient temperature bin data are tabulated [Air Force (1978)] for a large number of locations. The mean wet-bulb temperature is given for each dry-bulb temperature bin, but no information is provided on the distribution of the wet-bulb temperatures. Although research efforts are underway to provide coincident dry-bulb and wet-bulb temperature bin data [ASHRAE (1983)], there are currently

no published sets of bin data which contain information on the distribution of air moisture content for a large number of locations.

There is also a lack of distribution models for measures of ambient humidity. Yao (1974) demonstrated that relative humidity follows the beta distribution, but the parameters which control the shape of the beta distribution are a strong function of the monthly-average relative humidity, $\overline{RH}$, and no means was provided for determining the correct shape parameter values for an arbitrary value of $\overline{RH}$. Dodd (1965) developed maps for the U.S. which show isolines of monthly-average dew point temperature and its standard deviation. No attempt was made to find a representative distribution function.

5.2 The Distribution of Humidity Ratio

Humidity ratio is the mass of water in a sample of air divided by the mass of the dry air in the sample. Changes in air temperature do not affect the humidity ratio provided that the dew point temperature is not reached. Because it is a direct measure of the mass of water in the air, humidity ratio is generally the most useful variable for the calculation of latent cooling loads. Initial modeling efforts for humidity data were therefore directed at developing a distribution function for humidity ratio. Hourly values of humidity ratio were calculated for the 9 SOLMET locations listed in Chapter 3, and probability density curves were developed for humidity ratio from the measured data for each hour of the day and for each month of the year.

When the various distribution functions were compared, strong locational, seasonal and even diurnal variations were observed in the distribution shapes. The development of a distribution function model which is general for all locations and months of the year requires that either the measured distribution curves for different months and locations all have the same shape (or at least be very similar) or that the model shape change with location and time of year. The variation of the distribution curves from one month to the next was too severe to justify fitting a function which does not change in shape, as was done with ambient temperature. The unusual shapes of some of the measured distribution curves and the initial lack of success in trying to quantify the variations in the distribution curves led to a more detailed investigation of the humidity data.

The hourly humidity ratio data were plotted as a function of both humidity ratio and dry-bulb temperature in an attempt to determine the reasons for the unusual shapes of the humidity ratio probability density functions. The temperature and humidity ratio scales were divided into intervals (bins), and the number of hours the ambient temperature and humidity ratio were in each of the two dimensional bins recorded. Contour plots were then developed from these two-dimensional bin data. Figure 5.1 is an example of one of the contour plots; the data are for 6 AM in June at Madison. The circular contours indicate the number of hours ambient conditions were within each of the temperature-humidity ratio bins (which form a

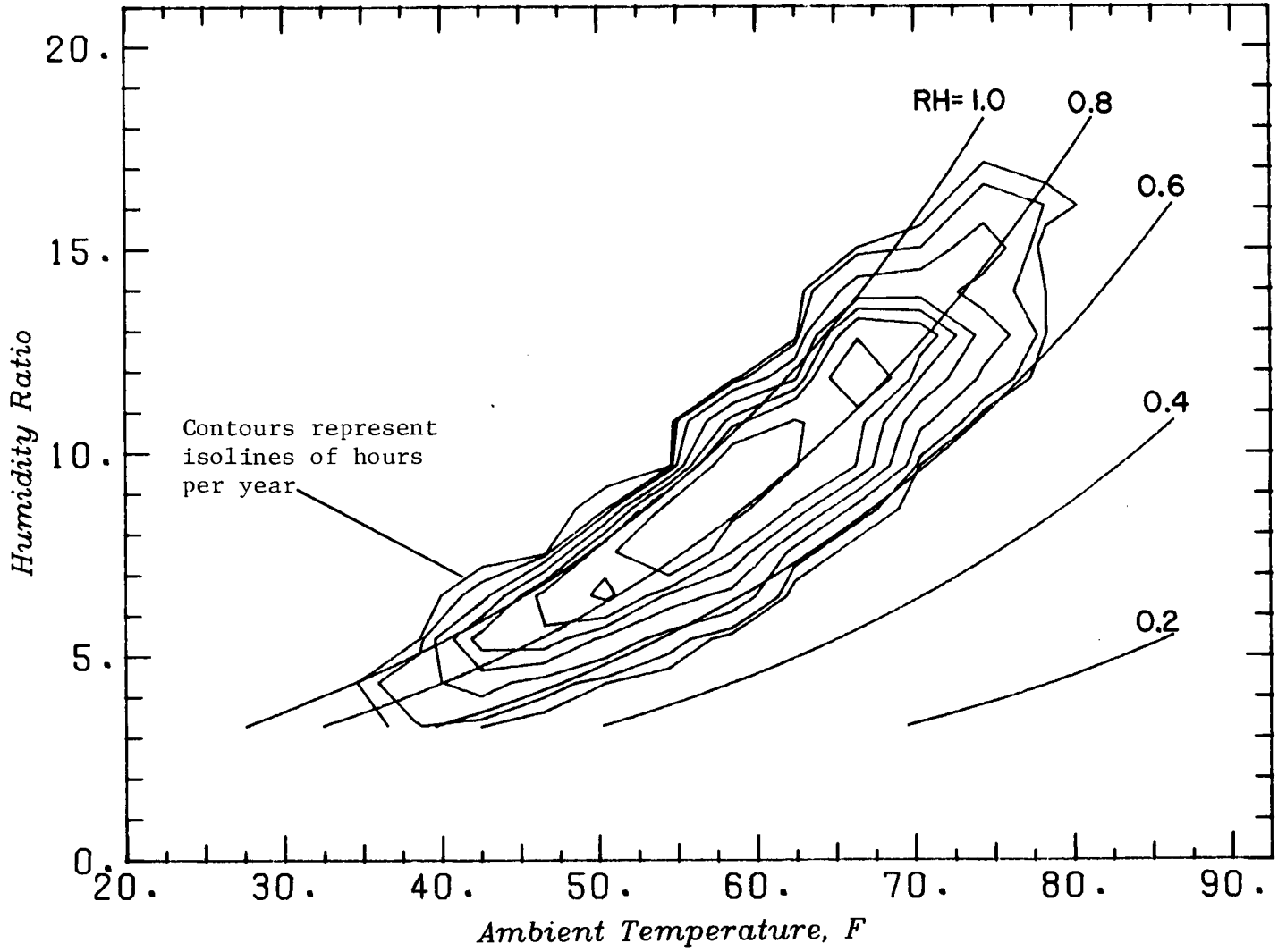

Figure 5.1 Contour Plot of Humidity Ratio/Dry-Bulb Temperature Bin Data

two dimensional grid). The data in each bin are associated with the midpoint value of dry-bulb temperature and humidity ratio for the bin, and the contour locations are established by linear interpolation between adjoining bins. The axes of the plot correspond to those of a psychometric chart, and contour lines of relative humidity are also shown. Some of the bin data contours indicate relative humidities in excess of 100%. This is a result of both the interpolation procedure, which redistributes the hours, and the finite bin size, which causes some bins to contain the saturation line. The measured data never exceeded a relative humidity of 100%.

The bin data contours in Figure 5.1, which represent the two-dimensional probability density function for dry-bulb temperature and humidity ratio, are bounded by relative humidity isolines, and the highest probability density also tends to follow a line of constant relative humidity. The same trend was observed for nearly all of the bin data sets. The curvature of the bivariate PDF for dry-bulb temperature and humidity ratio, as demonstrated in Figure 5.1, explains the unusual and variable nature of the PDF for humidity ratio alone. The relationship between humidity ratio and dry-bulb temperature for a constant value of relative humidity is nonlinear, and the variation in the dry-bulb temperature range from month-to-month causes the shape of the bivariate PDF for dry-bulb temperature and humidity ratio to change significantly for different times of the year.

The ranges of humidity ratio and dry-bulb temperature vary as a function of location, season, and time of day, but the shape of the bivariate distribution of dry-bulb temperature and humidity ratio is qualitatively similar in all cases. A dry-bulb temperature cross-section of the bivariate distribution shown in Figure 5.1 has a similar shape for all values of dry-bulb temperature. The distribution function for relative humidity does not appear to be a strong function of temperature for a particular hour of the day and month of the year. The distribution function for humidity ratio, on the other hand, is strongly influenced by the distribution of dry-bulb temperature. This suggests that relative humidity may be a better variable for the development of a generalized distribution function than humidity ratio.

5.3 A Distribution Model for Relative Humidity

5.3.1 Model Development

The probability density function for relative humidity is required to satisfy several constraints. The range for relative humidity is between 0 and 1 on a fractional basis, and the total area under the PDF curve and the average value of relative humidity for the curve must satisfy Equations (2-4) and (2-5). These constraints do not uniquely determine the shape of the probability density function for relative humidity, but they do require the shape to be different for different average values of relative

humidity. This is different from the situation for dry-bulb temperature, where the mean can vary over a wide range without the temperature range running into physical limits, allowing the shape to remain the same when the mean changes.

The monthly-average hourly relative humidity, $\overline{RH}_h$, has a large diurnal variation for many locations. For the 9 SOLMET locations, peak to peak amplitudes are as large as 0.40. The large diurnal variation of the monthly-average hourly relative humidity requires that the probability density function for relative humidity be significantly different for different hours of the day. The measured hourly RH data were separated by month of the year and hour of the day, and a probability density curve was developed for each data set. This resulted in 288 (12 X 24) PDF curves for each location. PDF curves for different hours, months and locations having the same nominal value of $\overline{RH}$ were compared to determine whether the distribution function for relative humidity could be generalized in terms of $\overline{RH}$. Nominal values of $\overline{RH}$ from 0.2 through 0.9 in increments of 0.1 were defined to include values of $\overline{RH}$ within plus and minus 0.01 of each incremental value. Although some differences exist among individual curves with the same nominal value of $\overline{RH}$, the shapes were found to be remarkably similar for the range of climate types represented.

Figure 5.2 shows the average PDF's for the 8 nominal values of $\overline{RH}$, where the curves represent the combined data of all 9 locations. Figure 5.3 contains the cumulative distributions for the same

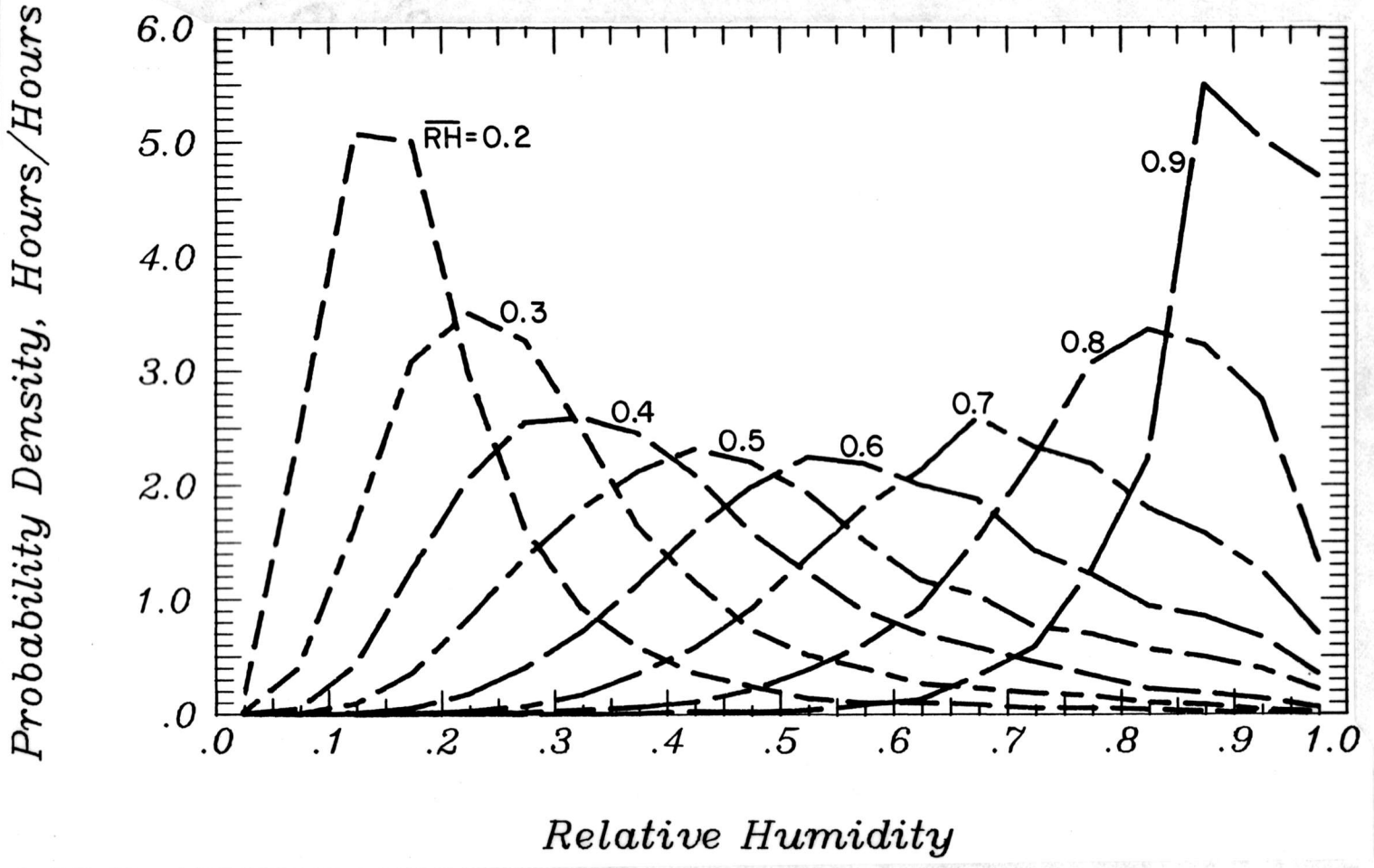

Figure 5.2 Relative Humidity Probability Density Curves for Nominal Values of Monthly-Average Hourly Relative Humidity

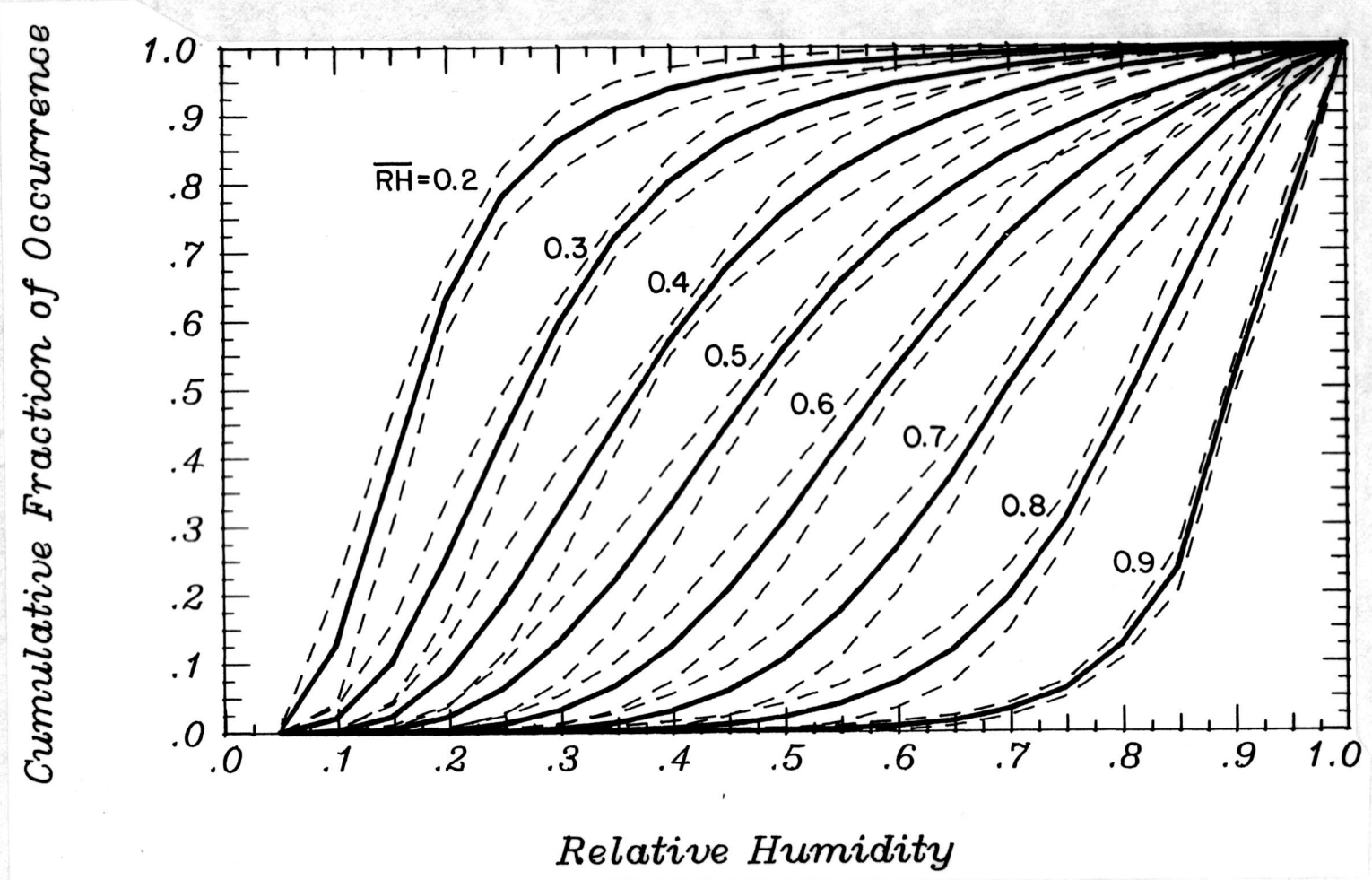

Figure 5.3 Relative Humidity Cumulative Distribution Curves for Nominal Values of Monthly-Average Hourly Relative Humidity

nominal values of $\overline{RH}$. Also shown in Figure 5.3 are dashed lines representing plus and minus one standard deviation of the monthly-average hourly distributions which make up each average curve. Part of the variation of the individual curves from the average is due to seasonal dependence within each location, part is due to locational dependence and part is due to the range of $\overline{RH}$ for the individual curves which make up each nominal average curve. The seasonal and locational standard deviations were also calculated separately, and it was found that the locational dependence is slightly larger than the seasonal dependence. The variation in the cumulative distribution curves is not large enough to justify the inclusion of seasonal or locational dependence in a model.

A number of standard probability density functions were curve fit to the probability density data for the nominal values of $\overline{RH}$, and it was found that a Weibull function [Hines and Montgomery (1980)] could represent any of the curves by varying the function parameters. Functional forms were then found for the estimation of the two shape parameters for the Weibull function. A nonlinear regression routine was used to fit the set of relationships for the distribution model to all 2592 (9 X 288) PDF curves.

$$P(RH) = (\theta_2/\theta_1)(RH/\theta_1)^{(\theta_2-1)} \exp(-(RH/\theta_1)^{\theta_2})/(1-\exp(-1/\theta_1)^{\theta_2})) \quad (5\text{-}1)$$

and

$$Q(RH) = (1-\exp(-(RH/\theta_1)^{\theta_2}))/(1-\exp(-(1/\theta_1)^{\theta_2})) \quad (5\text{-}2)$$

where

$$\theta_1 = -0.02691 + 1.2276\overline{RH} - 0.14880\overline{RH}^2 \qquad (5\text{-}3)$$

$$\theta_2 = 0.08165\exp(5.3801\overline{RH}) + 2.2747\exp(-0.59958\overline{RH}) \qquad (5\text{-}4)$$

and where P(RH) is the probability density function, and Q(RH) is the cumulative distribution of RH obtained by integration of P(RH) according to Equation (2-6).

The relationships provided in Equations (5-1) through (5-4) can be used to model the distribution of relative humidity for any value of $\overline{RH}$. Figure 5.4 shows the PDF model for values of $\overline{RH}$ between 0.2 and 0.9 in increments of 0.1. The agreement between the curves in Figure 5.4 and the curves for the measured data given in Figure 5.2 is good for all values of $\overline{RH}$, with the best agreement at the higher values of $\overline{RH}$. The model is smoother than the measured data, and the modeled PDF curves for the lower values of $\overline{RH}$ are broader and have lower peaks than the measured PDF curves. Figure 5.5 compares the cumulative distribution functions for the model with those for the measured data for nominal values of $\overline{RH}$ between 0.2 and 0.9. The agreement between the model and the measured data is within the one standard deviation bounds shown in Figure 5.3.

5.3.2 Relationships for Monthly-Average Relative Humidity

The only input required to use the relative humidity distribution model is the monthly-average relative humidity. Long-term

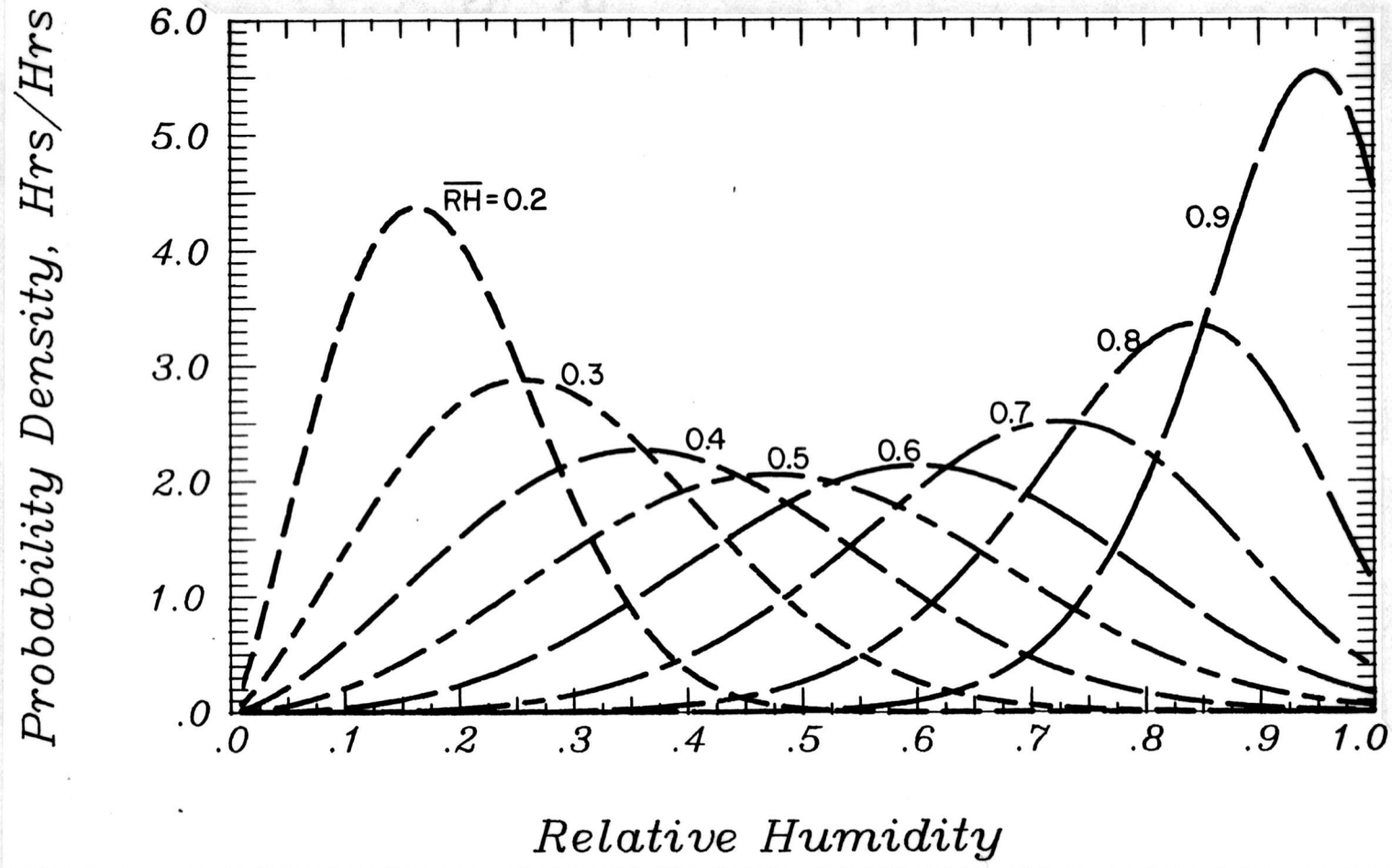

Figure 5.4 Probability Density Function Model for Relative Humidity

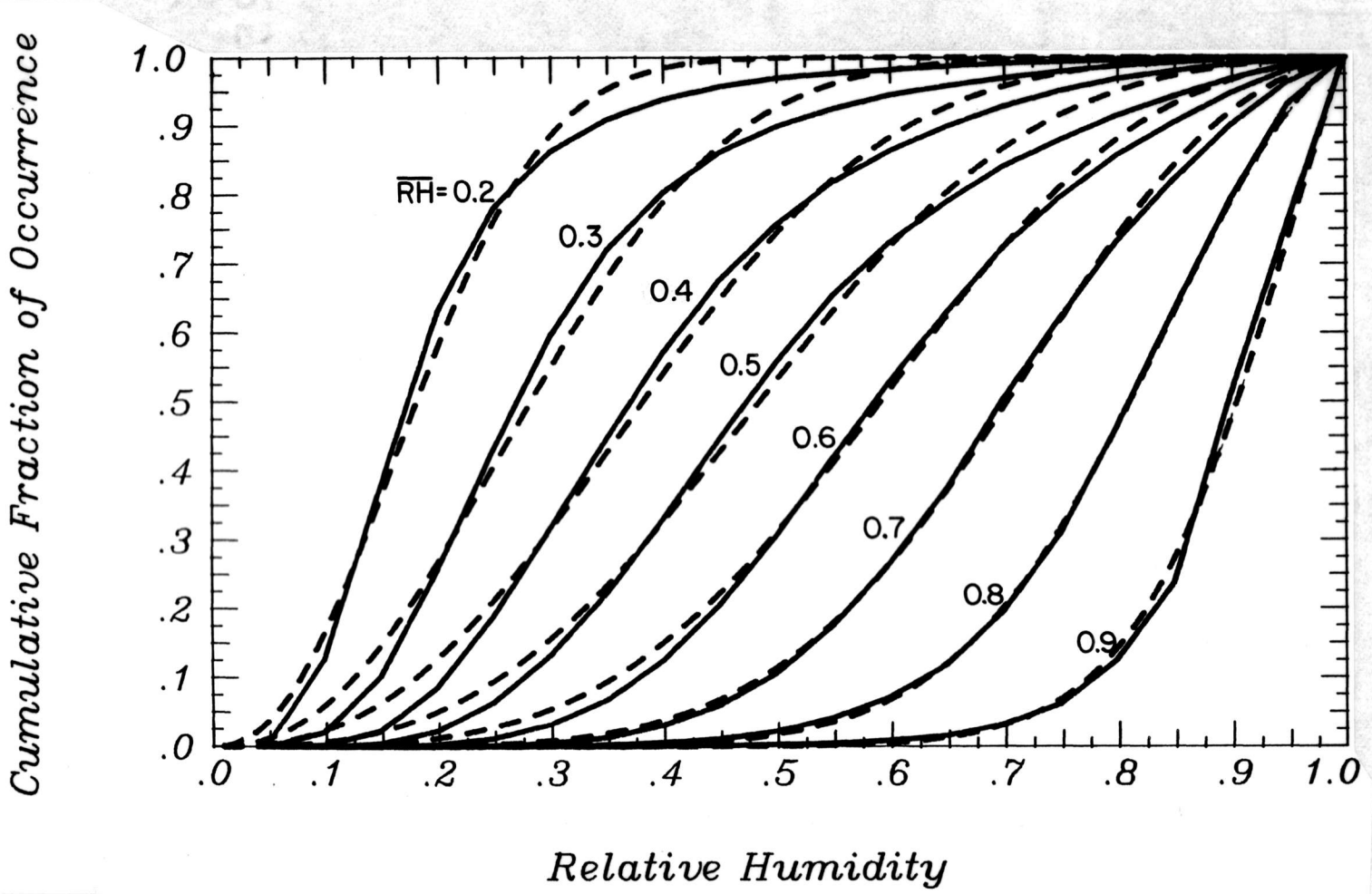

Figure 5.5 Cumulative Distribution Function Model and Measured Data Curves for Relative Humidity

average values of $\overline{RH}$ are tabulated in annual local climatological data (LCD) summaries for several hundred locations in the U.S. [Butson and Hatch (1979)]; the observations are for 4 hours of the day equally spaced 6 hours apart, but the 4 hours used are different for each time zone. Figure 5.6 compares the monthly-average daily relative humidities for the 9 locations used in the present study, obtained by averaging the hourly data for each month, with the averages of the 4 hourly monthly-average values (normals) given in the annual LCD summaries. The excellent agreement in Figure 5.6 is evidence that the average of the 4 hourly values given in a LCD annual summary represents a good approximation to the monthly-average daily relative humidity. These summaries provide a convenient source of input data for the relative humidity distribution model.

A relationship was also developed which allows the monthly-average daily relative humidity to be estimated from the monthly-average daily dry-bulb temperature and the monthly-average clearness index. The relationship between atmospheric clearness and $\overline{RH}$ is primarily the result of cloud cover and haze, both of which are strongly dependent on the presence of atmospheric moisture. The correlation of $\overline{RH}$ with $\overline{T}_a$ may be the result of seasonal weather patterns.

$$\overline{RH} = 0.53 + 0.799\overline{K}_T - 2.2039\overline{K}_T^3 + 0.00315\overline{T}_a \qquad (5\text{-}5)$$

where $\overline{T}_a$ is in degrees Celsius. The comparison between measured

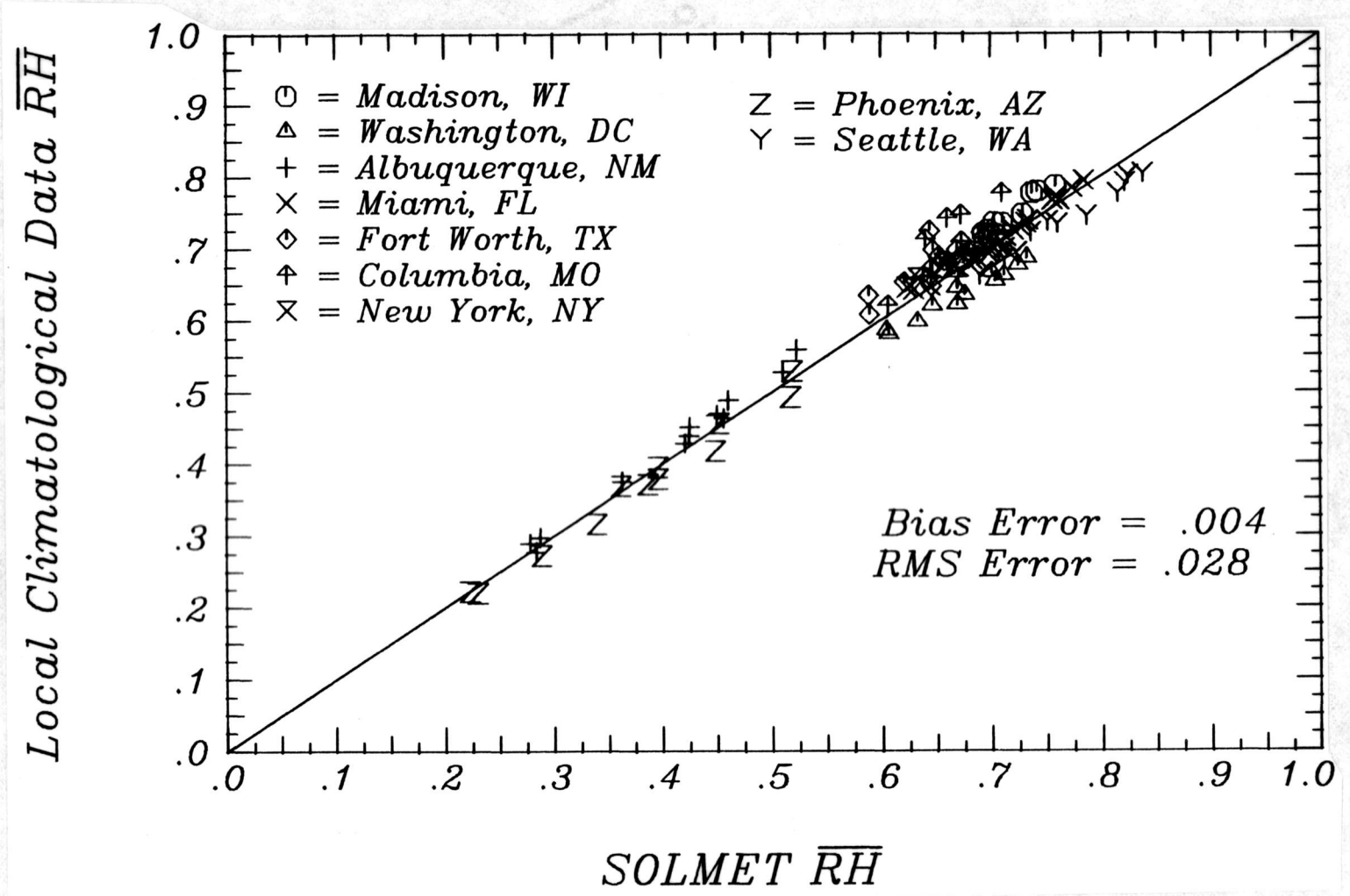

Figure 5.6 Comparison of SOLMET and Local Climatological Data Monthly-Average Daily Relative Humidity Values

and estimated values of $\overline{RH}$, shown in Figure 5.7, is not as good as the agreement in Figure 5.6. However, the RMS error for values of $\overline{RH}$ estimated using Equation (5-5) is less than 10% of a typical value for $\overline{RH}$ (0.6) at most locations.

The diurnal variation of the monthly-average hourly relative humidity in many locations is 20 to 40% of the total possible range for RH. The monthly-average hourly relative humidity is required to use the distribution model for RH on an hourly basis, but only daily values of $\overline{RH}$ are generally available. The following Fourier series was fit to the monthly-average diurnal variation of the hourly SOLMET data:

$$(\overline{RH}_h - \overline{RH})/A = 0.4672\cos(t^* - 0.666) + 0.0958\cos(2t^* - 3.484) + 0.0195\cos(3t^* - 4.147) + 0.0147\cos(4t^* - 0.452) \quad (5\text{-}6)$$

where

$$t^* = 2\pi(t-1)/24 \quad (3\text{-}10)$$

and t is in hours with 1 corresponding to 1 AM and 24 to midnight. Figure 5.8 shows Equation (5-6), the average data for the 9 locations and plus and minus one standard deviation of the 108 monthly curves (12 months X 9 locations). The amplitude of the diurnal swing, A, is given by

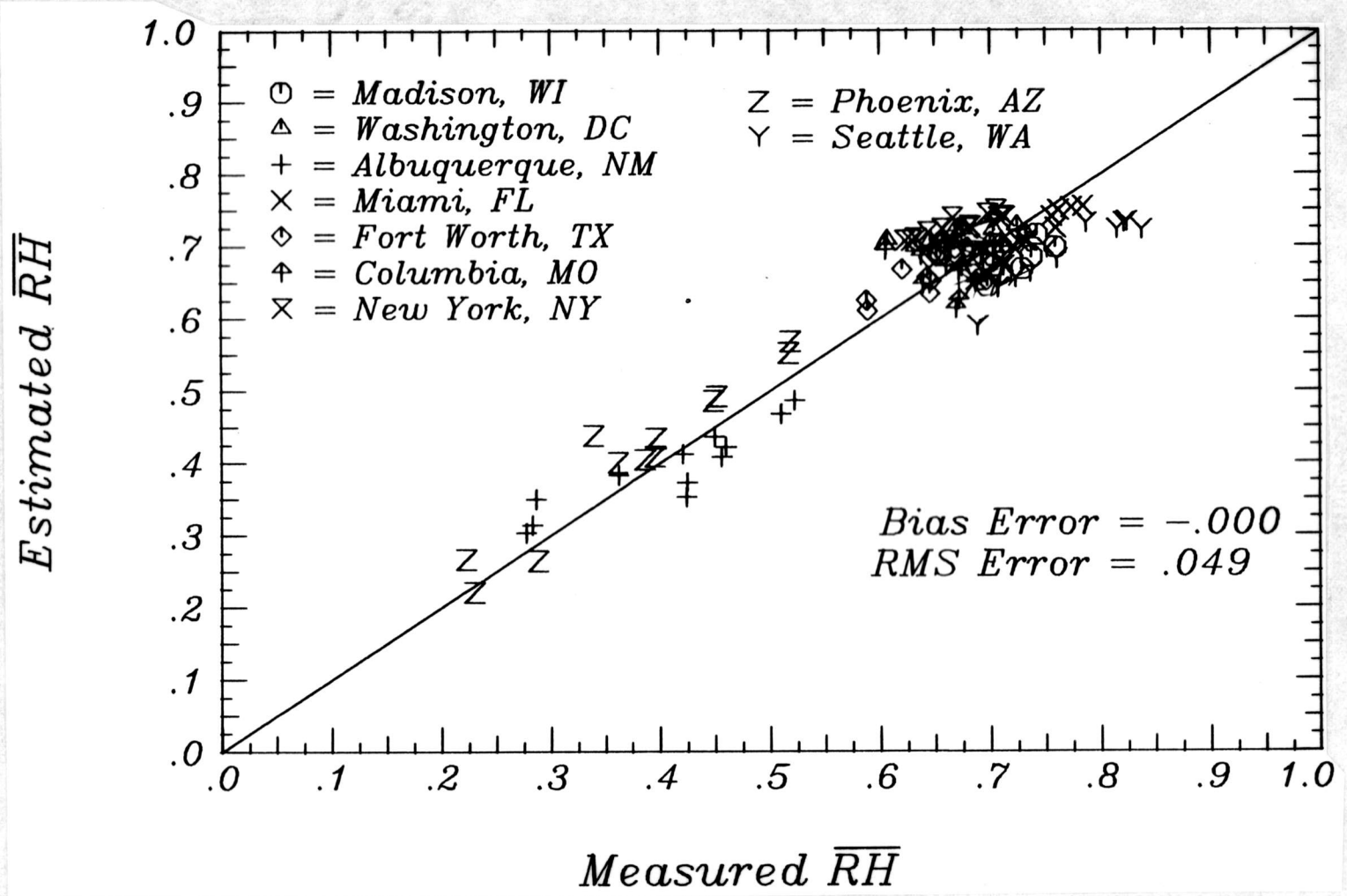

Figure 5.7 Comparison of Measured and Estimated Monthly-Average Daily Relative Humidity

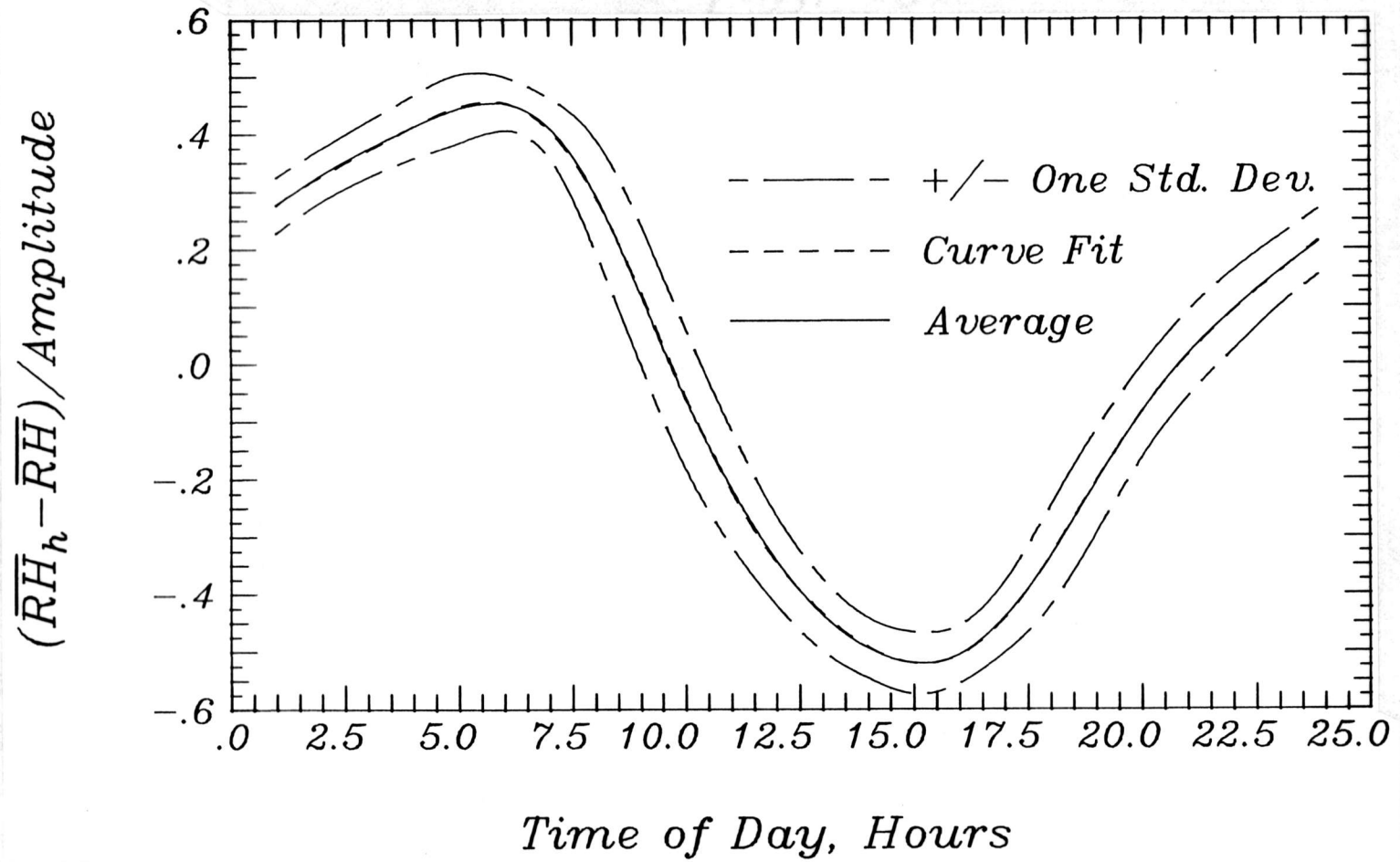

Figure 5.8 Standardized Diurnal Variation of Monthly-Average Hourly Relative Humidity for 9 U.S. Locations

$$A = -0.516 + 1.933\overline{K}_T - 1.663\overline{K}_T^3 + 0.00669\overline{T}_a - 1.993X10^{-4}\,\overline{T}_a^2 \qquad (5\text{-}7)$$

where $\overline{T}_a$ is in degrees Celsius. The diurnal variation of RH is caused by the diurnal variation of dry-bulb temperature, as the humidity ratio is relatively constant over the course of a day. The dry-bulb diurnal temperature swing is related to the clearness index, and the change in relative humidity which results from a change in dry-bulb temperature is a function of the dry-bulb temperature. Equation (5-7) is compared to the measured diurnal amplitude of $\overline{RH}$ in Figure 5.9. Although there is some scatter evident, the use of estimated values of the monthly-average hourly relative humidity is an improvement over using the monthly-average daily value for all hours of the day.

5.4 A Distribution Function for Wet-Bulb Temperature

5.4.1 Model Development

The distribution of wet-bulb temperature was also investigated. The distribution model for relative humidity presented above and the distribution model for ambient (dry-bulb) temperature developed in Chapter 3 can be used to model the distribution of wet-bulb temperature, but it is computationally simpler to directly use a distribution function for T_{wb}. A wet-bulb temperature distribution model also provides a second variable with which RH can be paired

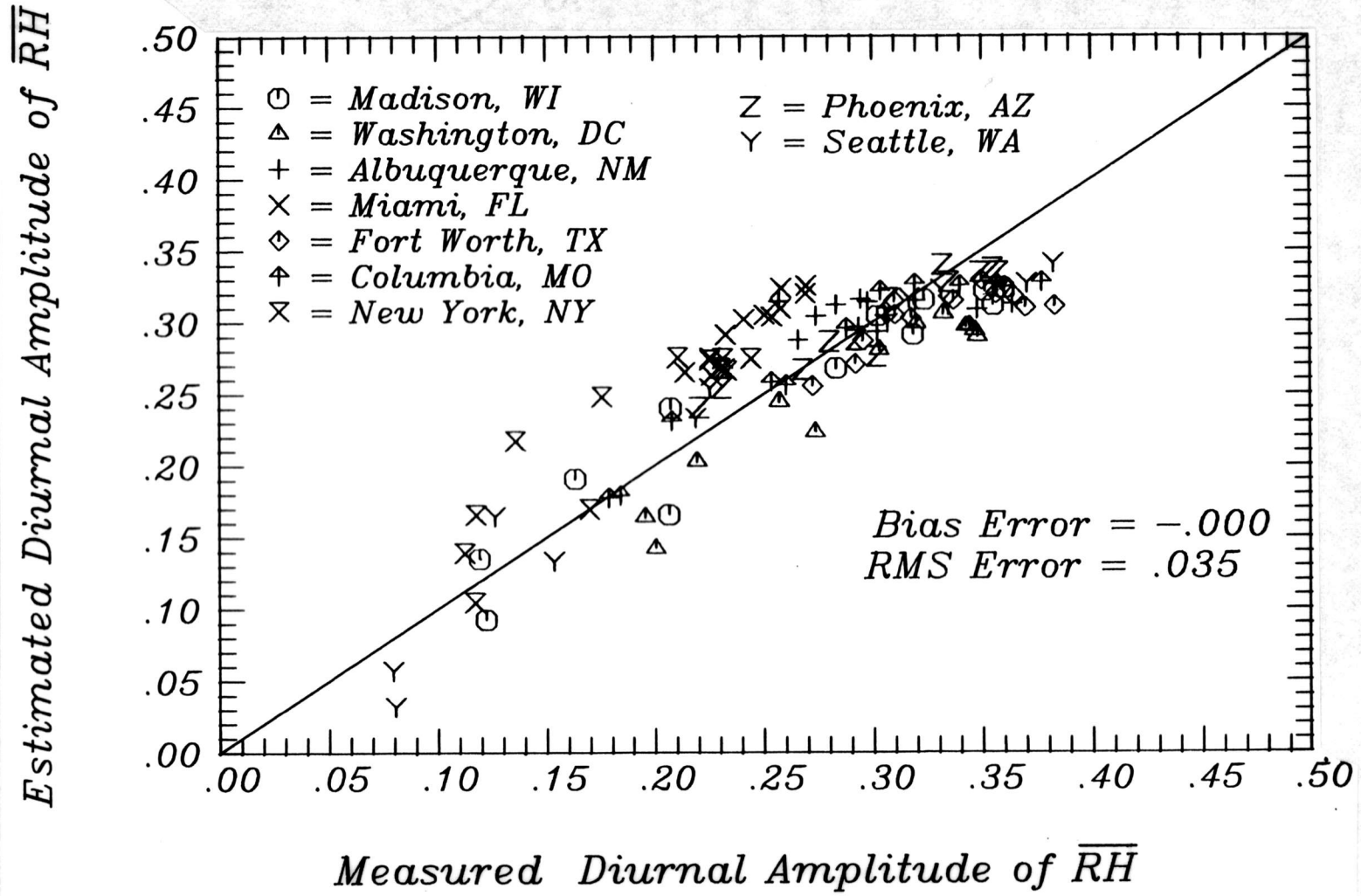

Figure 5.9 Estimated and Measured Values of the Peak-to-Peak Amplitude for the Diurnal Variation of Monthly-Average Hourly Relative Humidity

to estimate dry-bulb temperature/humidity ratio bin data.

Hourly wet-bulb temperatures were calculated for each of the 9 locations. Since the range of wet-bulb temperature observed for a particular hour of the day and month is a function of the time of year and location, the nondimensional scale variable h_{wb}, where

$$h_{wb} = (T_{wb} - \overline{T}_{wb,h})/\sigma_{wb} \qquad (5\text{-}8)$$

was introduced to remove the dependence of the distribution on the mean and variance of the data. The standard deviation of the hourly wet-bulb temperature, σ_{wb}, was calculated from the hourly data. Probability density curves were developed for each hour of the day for each month. Inspection of the distribution curves revealed that for most of the locations the distributions are skewed towards higher (than average) values of wet-bulb temperature, although the degree of skewness is often small. This skewness is a result of a corresponding skewness in the dry-bulb temperature distributions and a tendency for higher than average dry-bulb temperatures to be accompanied by lower than average relative humidities.

The skewness in the wet-bulb temperature distributions is not easily correlated with any of the readily available monthly-average meteorological variables. A symmetric distribution function model was fit to the hourly PDF curves for the 9 locations. A symmetric distribution function for wet-bulb temperature has the advantages of simplicity and consistency with the PDF model developed for dry-bulb temperature. The fitted model is compared in Figure 5.10 with

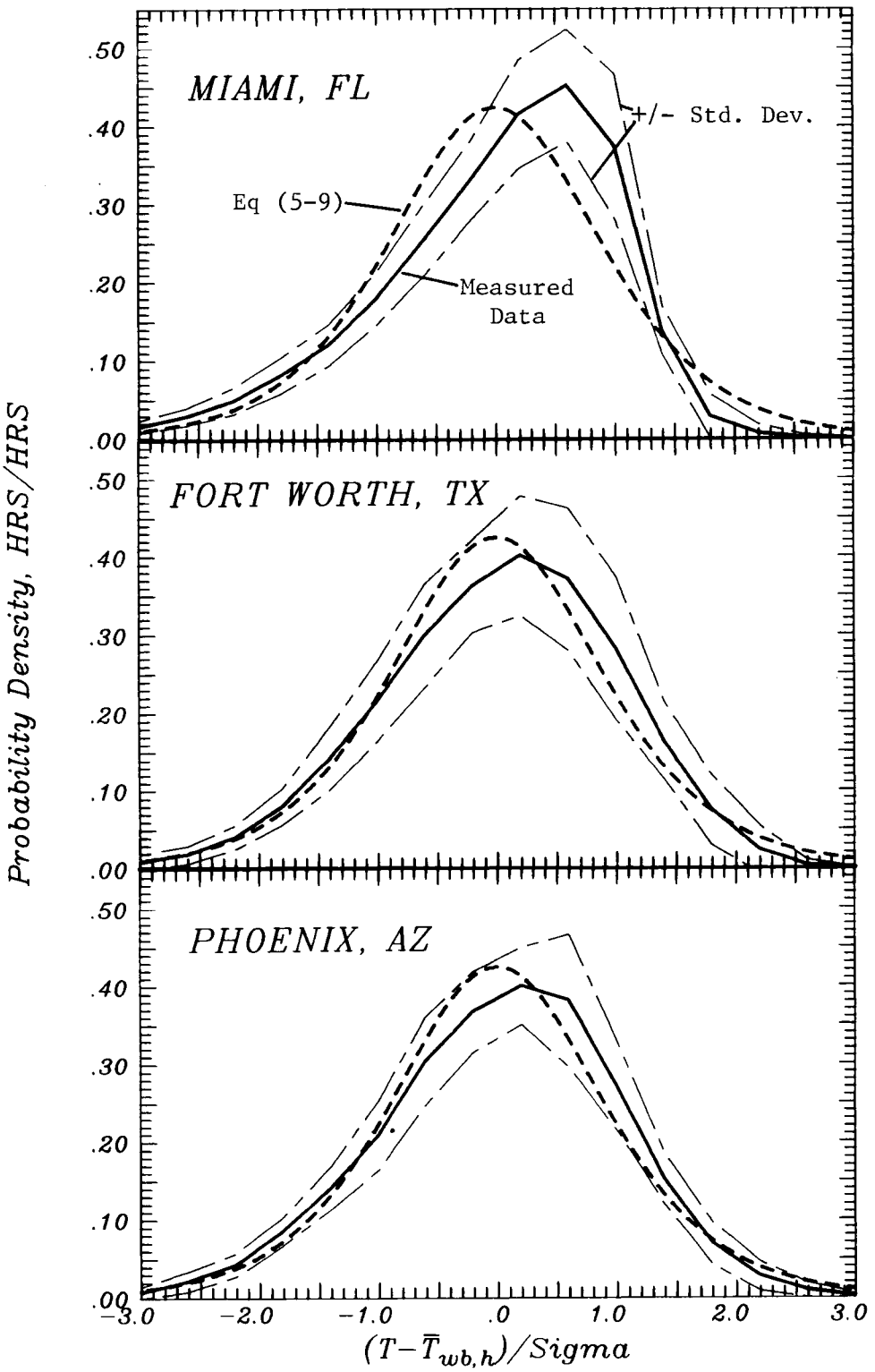

Figure 5.10 Probability Density Function Model and Measured Curves for Wet-Bulb Temperature

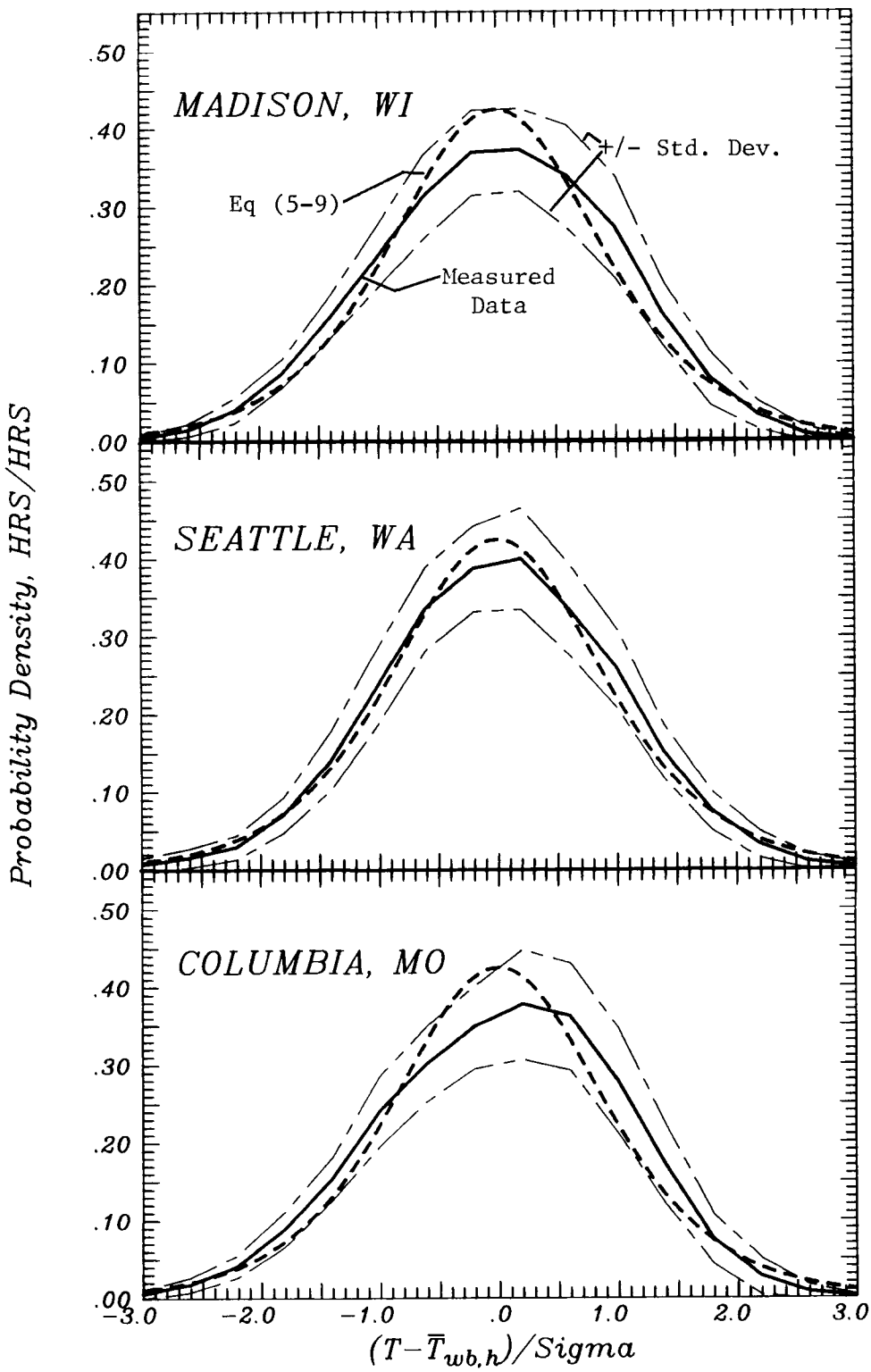

Figure 5.10 (cont.)

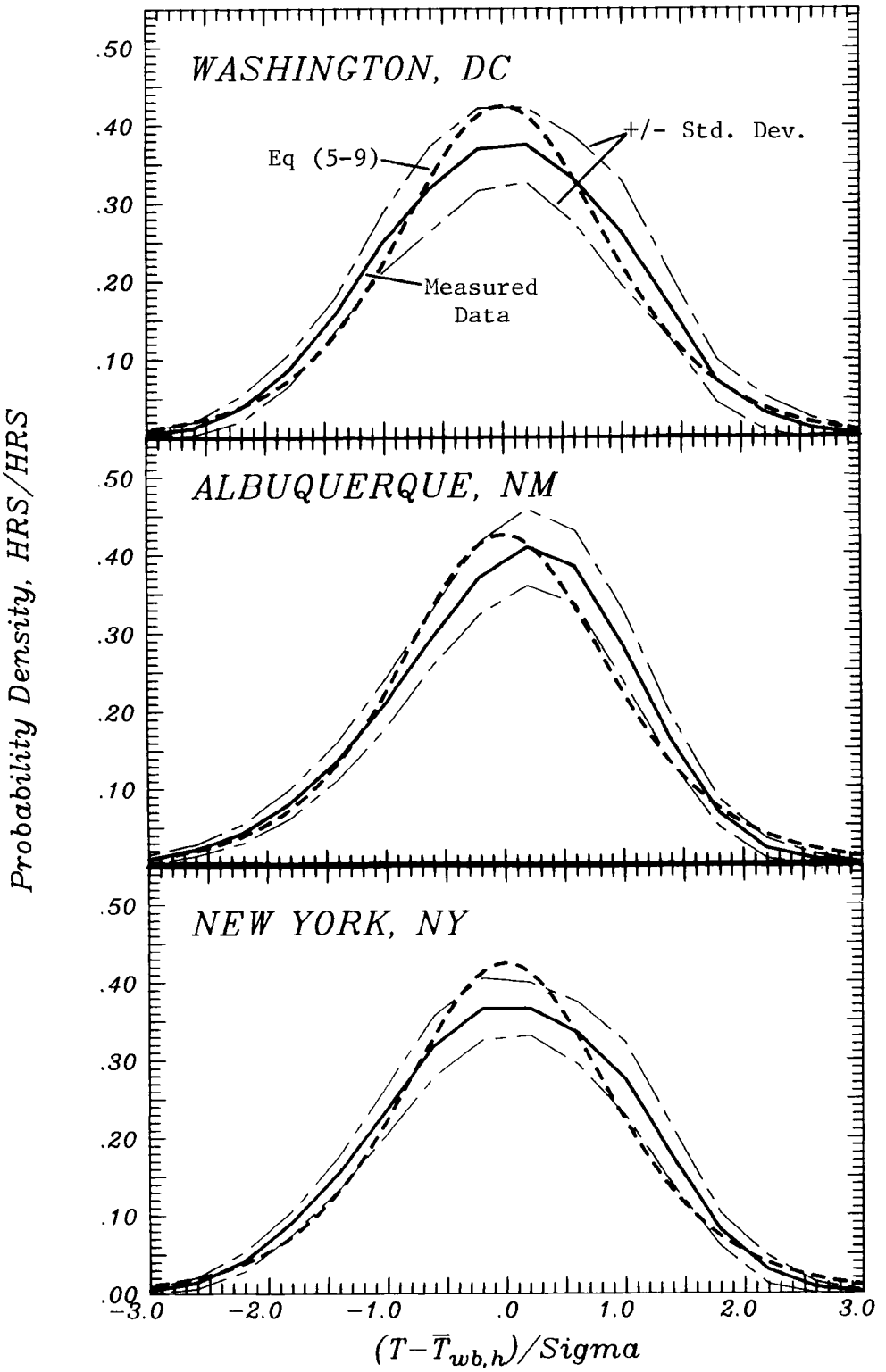

Figure 5.10 (cont.)

the measured data for the 9 SOLMET locations. The heavy solid line is the average of the 288 hourly PDF curves for each location, the heavy dashes are the fitted model and the light broken lines are plus and minus a standard deviation of the 288 individual curves. Only in Miami is the difference between the fitted line and the annual average data larger than the standard deviation of the hourly curves. The model developed for the wet-bulb temperature PDF is

$$P(h_{wb}) = 0.4244/[\cosh^2(0.8488h_{wb})] \qquad (5\text{-}9)$$

and the corresponding cumulative distribution function is

$$Q(h_{wb}) = (1+\tanh(0.8488h_{wb}))/2. \qquad (5\text{-}10)$$

5.4.2 Relationships for the Mean and Variance of Wet-Bulb Temperature

Monthly-average wet-bulb temperature and the standard deviation of the wet-bulb temperature are required to use the distribution model. Long-term values of $\overline{T}_{wb}$, calculated by averaging the hourly values of T_{wb} for each month, are compared in Figure 5.11 to the wet-bulb temperatures which correspond to the measured values of $\overline{RH}$ and $\overline{T}_a$ for the same data. The excellent agreement between the two sets of monthly-average wet-bulb temperature allows the monthly-average wet-bulb temperature to be estimated from the monthly-average dry-bulb temperature and the monthly-average relative humidity without introducing additional uncertainty into the wet-bulb temper-

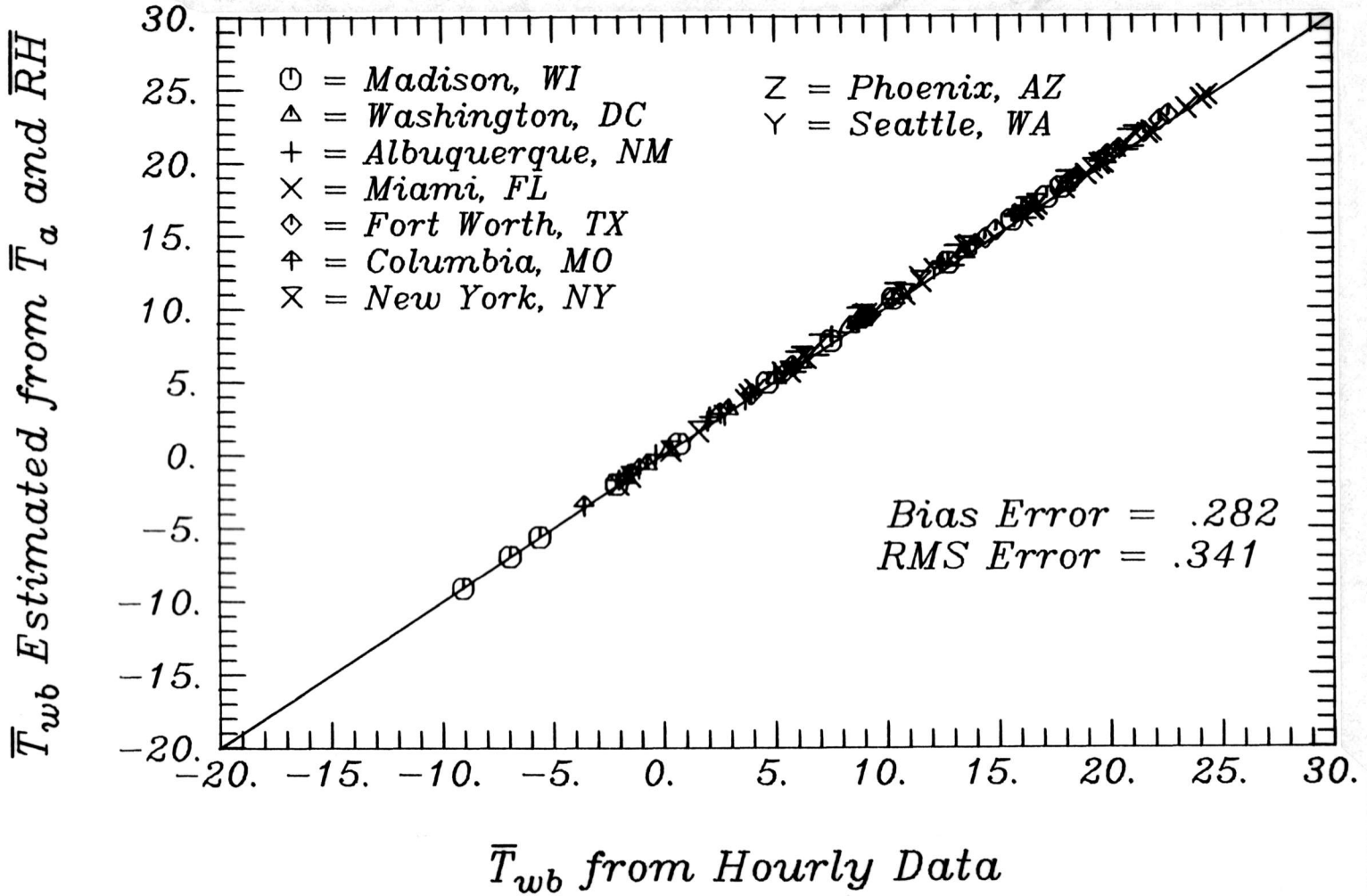

Figure 5.11 Measured and Estimated Values of Monthly-Average Daily Wet-Bulb Temperature for 9 U.S. Locations

ature distribution model.

The standard deviation of the hourly wet-bulb temperature was also calculated for each hour of the day for each month using the 20 year data sets of T_{wb}. A relationship was developed for the estimation of σ_{wb} from more commonly available information. Although this relationship is similar to the relationship for σ_m given in Chapter 3, $\overline{K}_T$ was found to be significantly correlated with σ_{wb} and was included as an independent variable.

$$\sigma_{wb} = 6.419 - 0.0700\overline{T}_a - 0.316\sigma_{yr} + 0.0405\sigma_{yr}^2 - 3.685\overline{K}_T \qquad (5\text{-}11)$$

The units for σ_{wb}, $\overline{T}_a$ and σ_{yr} are degree Celsius and σ_{yr} is the standard deviation of the 12 monthly values of $\overline{T}_a$. Measured values of σ_{wb} are compared in Figure 5.12 with values estimated from Equation (5-11).

The diurnal variation of the monthly-average hourly wet-bulb temperature can be determined from the diurnal variations of the monthly-average dry-bulb temperature and relative humidity, but again a more direct approach was desired. A Fourier series was fit to the average diurnal variation of $\overline{T}_{wb,h}$ for the 9 U.S. locations.

$$(\overline{T}_{wb,h} - \overline{T}_{wb})/A_{wb} = 0.4563\cos(t^*-3.804) + 0.0923\cos(2t^*+0.0252) + 0.0267\cos(3t^*-0.834) + 0.0138\cos(4t^*-3.085) \qquad (5\text{-}12)$$

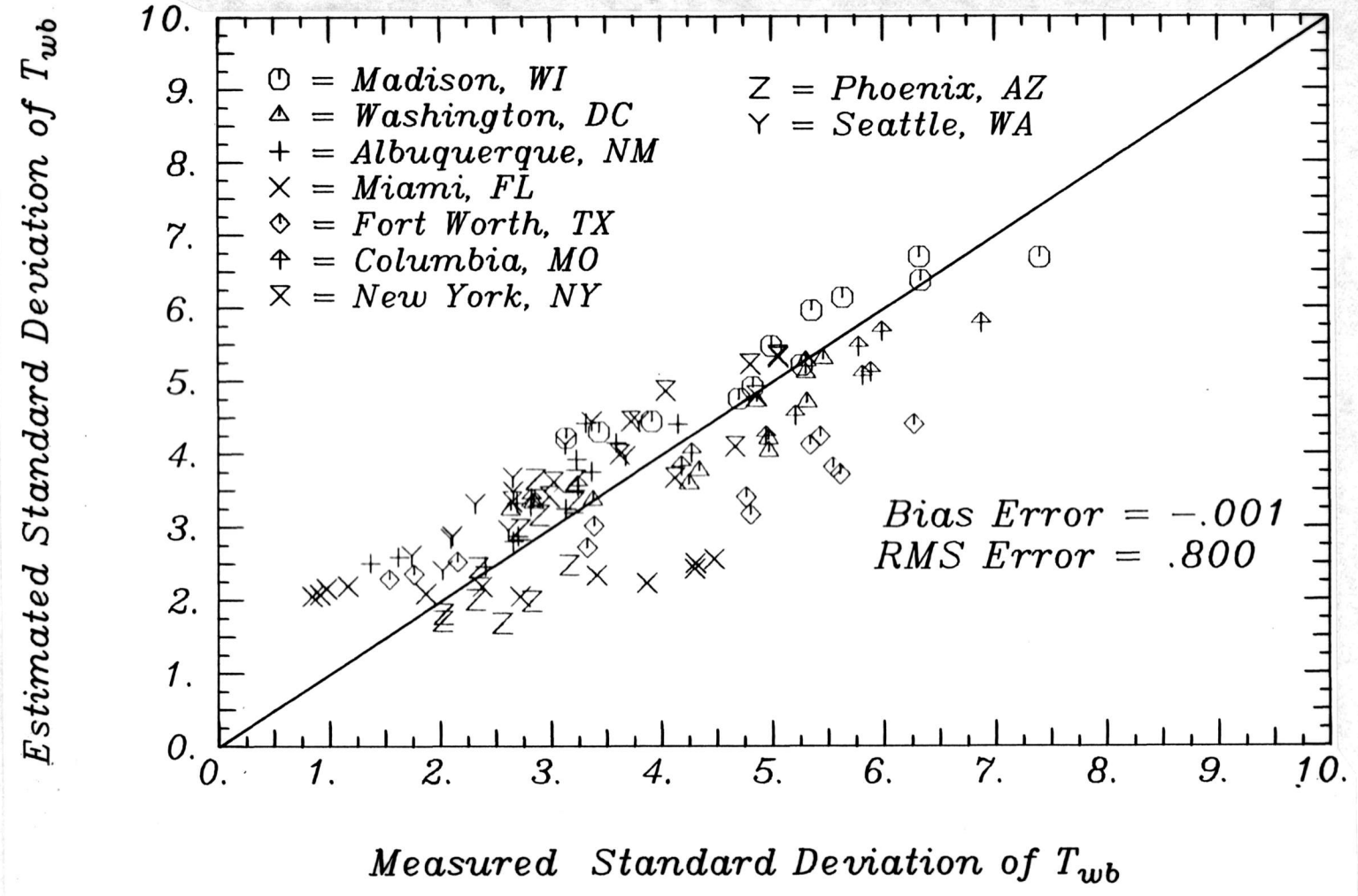

Figure 5.12 Measured and Estimated Values of Standard Deviation for Wet-Bulb Temperature

where t^* is defined by Equation (3-10). The average curve for the measured data and plus and minus one standard deviation of the monthly curves for each location from the average are shown in Figure 5.13 along with Equation (5-12). The amplitude of the diurnal swing for $\bar{T}_{wb,h}$, A_{wb}, is found from the relationship

$$A_{wb} = -5.177 + 24.64\bar{K}_T - 16.54\bar{K}_T^3 - 0.0363\bar{T}_a - 0.00551\bar{T}_a^2 \quad (17)$$

where A_{wb} and $\bar{T}_a$ are in degrees Celsius. Estimated and measured values of A_{wb} appear in Figure 5.14.

5.5 The Estimation of Dry-Bulb Temperature/Humidity Ratio Bin Data

5.5.1 The Use of Single-Variable Distribution Models

The humidity distributions described and modeled so far have only considered a single meteorological variable at a time. The energy required to maintain comfort within a building is often a function of both the dry-bulb temperature and the humidity ratio of the ambient air. Accurate estimation procedures for building loads may require information about the coincidence of temperature and humidity. Two-dimensional dry-bulb temperature/humidity ratio bin data provide a representation of the coincidence and the distributions for temperature and humidity. Two-dimensional bin data require a three-dimensional representation, as described in Chapter 2.

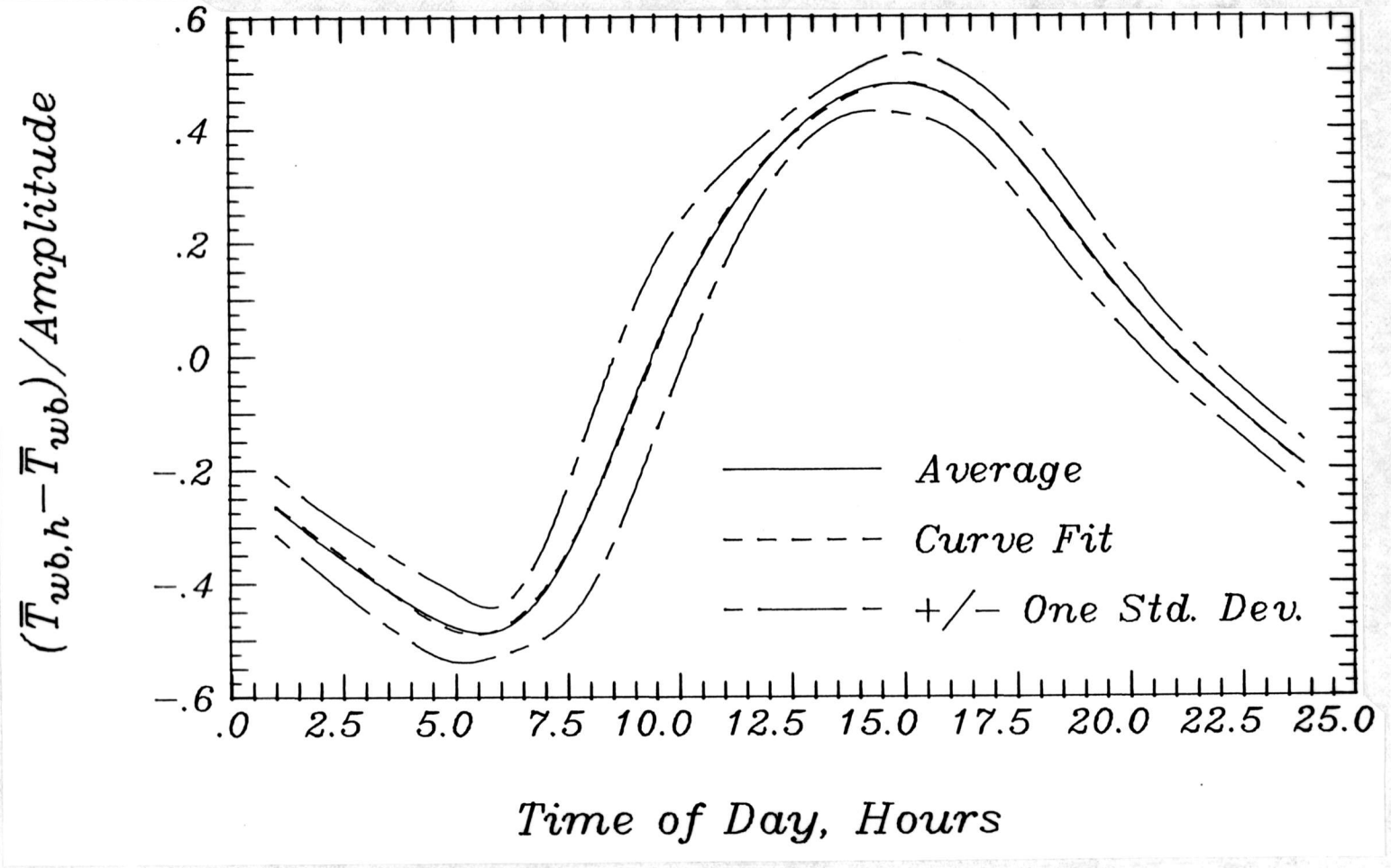

Figure 5.13 Standardized Diurnal Variation of Monthly-Average Hourly Wet-Bulb Temperature for 9 U.S. Locations

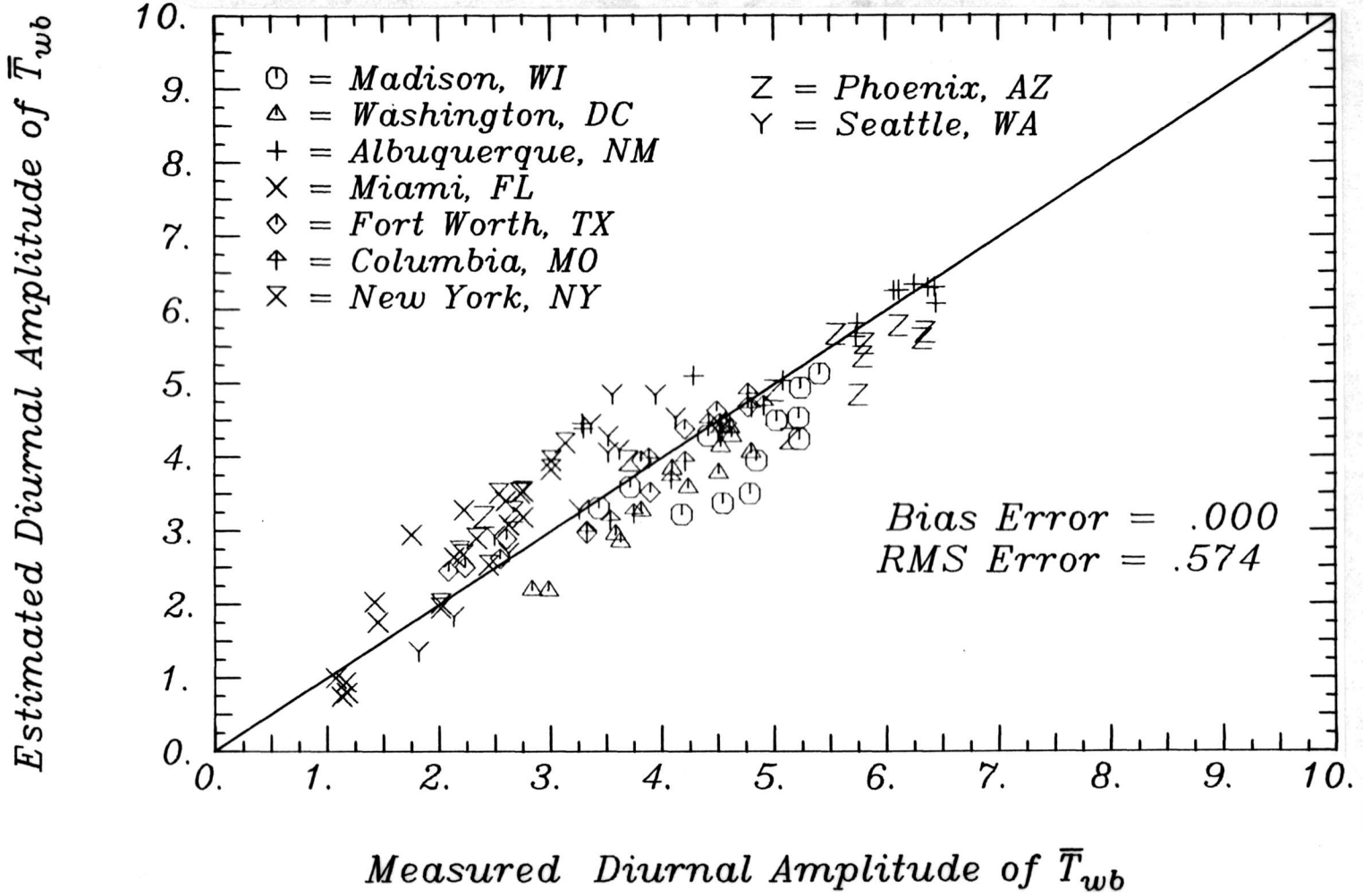

Figure 5.14 Estimated and Measured Peak-to-Peak Amplitudes for the Diurnal Variation of Monthly-Average Wet-Bulb Temperature

A two-dimensional dry-bulb temperature/humidity ratio bin represents a particular interval of dry-bulb temperature and a particular interval of humidity ratio. The dependent variable for a two-dimensional dry-bulb temperature/humidity ratio bin is the number of hours (or the fraction of the time) that the temperature and humidity ratio were both within the intervals of dry-bulb temperature and humidity ratio which define the bin.

The estimation of two-dimensional bin data requires a bivariate distribution function describing the probability of occurrence for any particular combination of values for the two independent variables. If the two independent variables are not correlated, it is possible to use two single variable distribution functions (one for each variable) in place of the bivariate distribution function. When the independent variables are not correlated, the probability of occurrence for one variable is the same for all values of the other variable, and the joint probability of occurrence for the two variables is given by the product of the probabilities for each of the variables considered separately.

The correlation of two variables can be measured by the cross-correlation coefficient, ρ_{xy}, which was defined in Chapter 2. The definition for ρ_{xy} is based on deviations of the variables x and y from their average values, and so ρ_{xy} does not provide any information on the correlation of the average values for x and y. Correlations between the average values of the variables do not affect the validity of using two univariate distribution models in place of a bi-

variate distribution model, since the averages are input to the distribution models.

Distribution models have been developed and presented for dry-bulb (ambient) temperature, relative humidity, and wet-bulb temperature. Any two of these three distributions can be used to estimate two-dimensional dry-bulb temperature/humidity ratio bin data, but since all of the distributions are univariate, the two variables chosen should be uncorrelated. The combination of dry-bulb temperature and relative humidity and the combination of wet-bulb temperature and relative humidity were chosen as the most likely candidates for variable pairs which are uncorrelated.

Monthly values of the cross-correlation coefficients for dry-bulb temperature and relative humidity (ρ_{Ta-RH}) and for wet-bulb temperature and relative humidity (ρ_{Twb-RH}) were calculated from the long-term hourly data for each location. The cross-correlation coefficients for dry-bulb temperature and relative humidity are given in Table 5.1 and the coefficients for wet-bulb temperature and relative humidity are given in Table 5.2.

During the summer months, ρ_{Ta-RH} is negative at all 9 locations, with magnitudes ranging from 0.2 to 0.85. The negative cross-correlation coefficients indicate that when the dry-bulb temperature is above normal, the relative humidity is below normal, and vice versa. During the fall, winter and spring months the cross-correlations between deviations of dry-bulb temperature and relative humidity are of both signs, with magnitudes generally less than 0.4.

Table 5.1 Cross-Correlation Coefficients Between Variations of Hourly Dry-Bulb Temperature and Relative Humidity from their Respective Monthly-Average Values.

	Cross-Correlation Coefficients								
Month	Madison	Washington	Albuquerque	Miami	Fort Worth	Columbia	New York	Phoenix	Seattle
Jan	0.55	0.18	-0.22	0.27	0.05	0.15	0.48	-0.14	0.21
Feb	0.43	0.14	-0.38	0.29	-0.09	0.02	0.46	-0.22	-0.10
Mar	0.08	-0.04	-0.48	0.26	-0.11	-0.25	0.17	-0.50	-0.31
Apr	-0.21	-0.16	-0.54	0.05	-0.03	-0.21	-0.13	-0.52	-0.50
May	-0.24	-0.18	-0.44	-0.36	-0.34	-0.20	-0.23	-0.46	-0.60
June	-0.32	-0.35	-0.46	-0.74	-0.66	-0.39	-0.35	-0.29	-0.67
July	-0.37	-0.42	-0.80	-0.85	-0.78	-0.42	-0.37	-0.66	-0.75
Aug	-0.34	-0.36	-0.70	-0.82	-0.73	-0.43	-0.17	-0.65	-0.74
Sep	-0.22	-0.15	-0.49	-0.77	-0.42	-0.30	0.13	-0.34	-0.60
Oct	-0.07	0.02	-0.40	-0.12	-0.06	-0.13	0.36	-0.34	-0.44
Nov	0.13	0.07	-0.36	0.12	0.07	-0.06	0.44	-0.40	0.02
Dec	0.42	0.20	-0.33	0.25	0.03	-0.04	0.46	-0.32	0.00

Table 5.2 Cross-Correlation Coefficients Between Variations of Hourly Wet-Bulb Temperature and Relative Humidity from their Respective Monthly-Average Values.

	Cross-Correlation Coefficients								
Month	Madison	Washington	Albuquerque	Miami	Fort Worth	Columbia	New York	Phoenix	Seattle
Jan	0.60	0.38	0.03	0.55	0.32	0.29	0.64	0.46	0.46
Feb	0.51	0.38	-0.07	0.59	0.27	0.22	0.65	0.43	0.26
Mar	0.25	0.30	-0.10	0.62	0.29	-0.00	0.53	0.19	0.15
Apr	0.11	0.26	-0.03	0.61	0.47	0.17	0.40	0.11	-0.00
May	0.14	0.31	0.26	0.51	0.22	0.26	0.36	0.13	-0.16
June	0.10	0.22	0.45	0.14	0.06	0.13	0.35	0.44	-0.19
July	0.13	0.33	0.43	-0.11	0.32	0.28	0.52	0.67	-0.35
Aug	0.10	0.29	0.49	-0.06	0.33	0.22	0.57	0.62	-0.24
Sep	0.12	0.28	0.42	0.07	0.38	0.22	0.58	0.54	-0.03
Oct	0.22	0.36	0.25	0.52	0.46	0.28	0.67	0.37	-0.05
Nov	0.32	0.35	0.04	0.52	0.42	0.20	0.68	0.26	0.29
Dec	0.50	0.43	-0.01	0.55	0.35	0.14	0.64	0.31	0.27

The cross-correlation coefficients for wet-bulb temperature and relative humidity are almost always positive for the 9 locations. The magnitude of ρ_{Twb-RH} is largest during the winter for most of the 9 locations, Albuquerque and Phoenix being exceptions, with values typically between 0.2 and 0.5. Seattle is the only location out of the 9 where a significant negative correlation is observed.

Neither of the variable pairs is completely uncorrelated, although of the two, relative humidity and wet-bulb temperature have a smaller average correlation. The additional complexity required to model the correlation between either pair of independent variables would result in methods which are too difficult to use. It was assumed that both independent variable pairs could be treated as uncorrelated, with the errors introduced by this assumption becoming part of the overall errors of the estimation procedures.

The estimation of dry-bulb temperature/humidity ratio bin data with the distribution models of dry-bulb temperature and relative humidity or the distribution models of wet-bulb temperature and relative humidity are described below. The large diurnal variation of the monthly-average hourly relative humidity results in significant differences in the relative humidity distribution function for different hours of the day, and the procedures described are intended for the estimation of bin data for an individual hour of the day. The bin data are summed for all hours in the day to obtain daily bin data. It is possible to use the procedures to estimate bin data for

the entire day by using daily average inputs in place of the hourly average values, but there is a loss of accuracy.

5.5.2 Dry-Bulb Temperature and Relative Humidity Distribution Pair

The estimation of dry-bulb temperature/humidity ratio bin data from the distribution functions for dry-bulb temperature and relative humidity begins with the distribution of the total number of hours in the month (for either an hour of the day or the entire day) into the dry-bulb temperature bins. The estimation of dry-bulb (ambient) temperature bin data is described in Chapter 3.

The hours in a dry-bulb temperature bin contain the distribution of humidity ratio for that dry-bulb temperature. The next step in the estimation procedure is to distribute the hours for each temperature bin among the humidity ratio bins. The humidity ratio bins and the dry-bulb temperature bins can be represented on a psychometric chart as sets of parallel lines, with the spacings between the lines equal to the bin sizes. The lines for dry-bulb temperature are orthogonal to those for humidity ratio, and their intersection results in a grid of rectangles. The intersection of a bin for dry-bulb temperature and a bin for humidity ratio is illustrated in Figure 5.15.

Each dry-bulb temperature bin has a set of humidity ratio bins corresponding to it, and the values of humidity ratio defining the humidity ratio bins are the same for each dry-bulb temperature bin. Since a distribution function model is not available for humidity

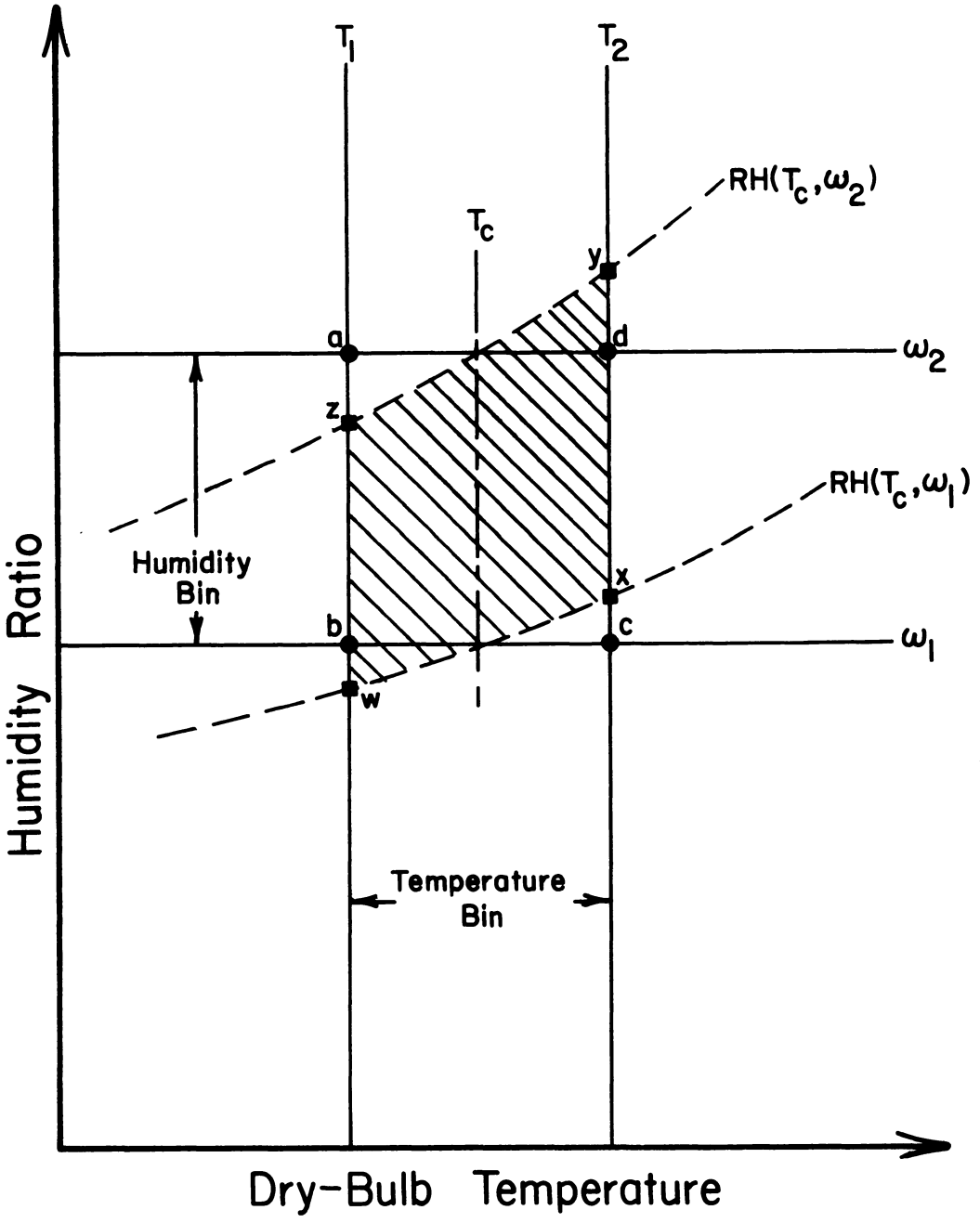

Figure 5.15 A Two-Dimensional Humidity Ratio/Dry-Bulb Temperature Bin

ratio, the dry-bulb temperature/humidity ratio bins must be approximated by dry-bulb temperature/relative humidity bins. This approximation is shown in Figure 5.15, where the area $\overline{abcd}$ is replaced by the area $\overline{wxyz}$. The accuracy of this approximation improves as the dry-bulb temperature bin size is made smaller. Because relative humidity is a function of both humidity ratio and dry-bulb temperature, the set of relative humidity values which corresponds to the set of humidity ratio bins is different for each dry-bulb temperature bin.

The relative humidity for each value of humidity ratio is calculated from

$$RH = \omega(0.62198 + \omega_s)/\omega_s(0.62198 + \omega) \qquad (5\text{-}14)$$

The saturation humidity ratio, ω_s, is a function of dry-bulb temperature. Simple relationships for the estimation of ω_s are provided in Appendix A. The average dry-bulb temperature for each temperature bin is used to find ω_s, and the set of values of relative humidity defining the humidity ratio bins for each temperature bin are determined using Equation (5-14). If RH is greater than 1 for any of the bins, it is set equal to 1. The relative humidity distribution function is then used to estimate the fraction of the total hours in a temperature bin which is in each relative humidity bin for that temperature.

5.5.3 Wet-Bulb Temperature and Relative Humidity Distribution Pair

The estimation of dry-bulb temperature/humidity ratio bin data from the distribution functions for wet-bulb temperature and relative humidity requires first the estimation of wet-bulb temperature/relative humidity bin data. A dry-bulb temperature/humidity ratio bin may include portions of a number of wet-bulb temperature/relative humidity bins, as illustrated in Figure 5.16. It is not possible to match a single wet-bulb temperature/relative humidity bin to each dry-bulb temperature/humidity ratio bin in a consistent manner.

The number of hours in each wet-bulb temperature bin is found using Equations (5-10) through (5-13). The procedure is identical to the procedure described in Chapter 3 for the estimation of dry-bulb temperature bin data. A wet-bulb temperature range of

$$\overline{T}_{wb} - 4\sigma_{wb} < T_{wb} < \overline{T}_{wb} + 4\sigma_{wb} \qquad (5\text{-}15)$$

includes 99.8% of all hours in the month. The hours in each wet-bulb temperature bin are then distributed among the relative humidity bins using the distribution model for relative humidity. The bin sizes selected for wet-bulb temperature and relative humidity are dependent on the bin sizes for humidity ratio and dry-bulb temperature. Too large a bin size for wet-bulb temperature and relative humidity will decrease the accuracy of the resulting dry-bulb temperature/humidity ratio bin data estimates, while too small

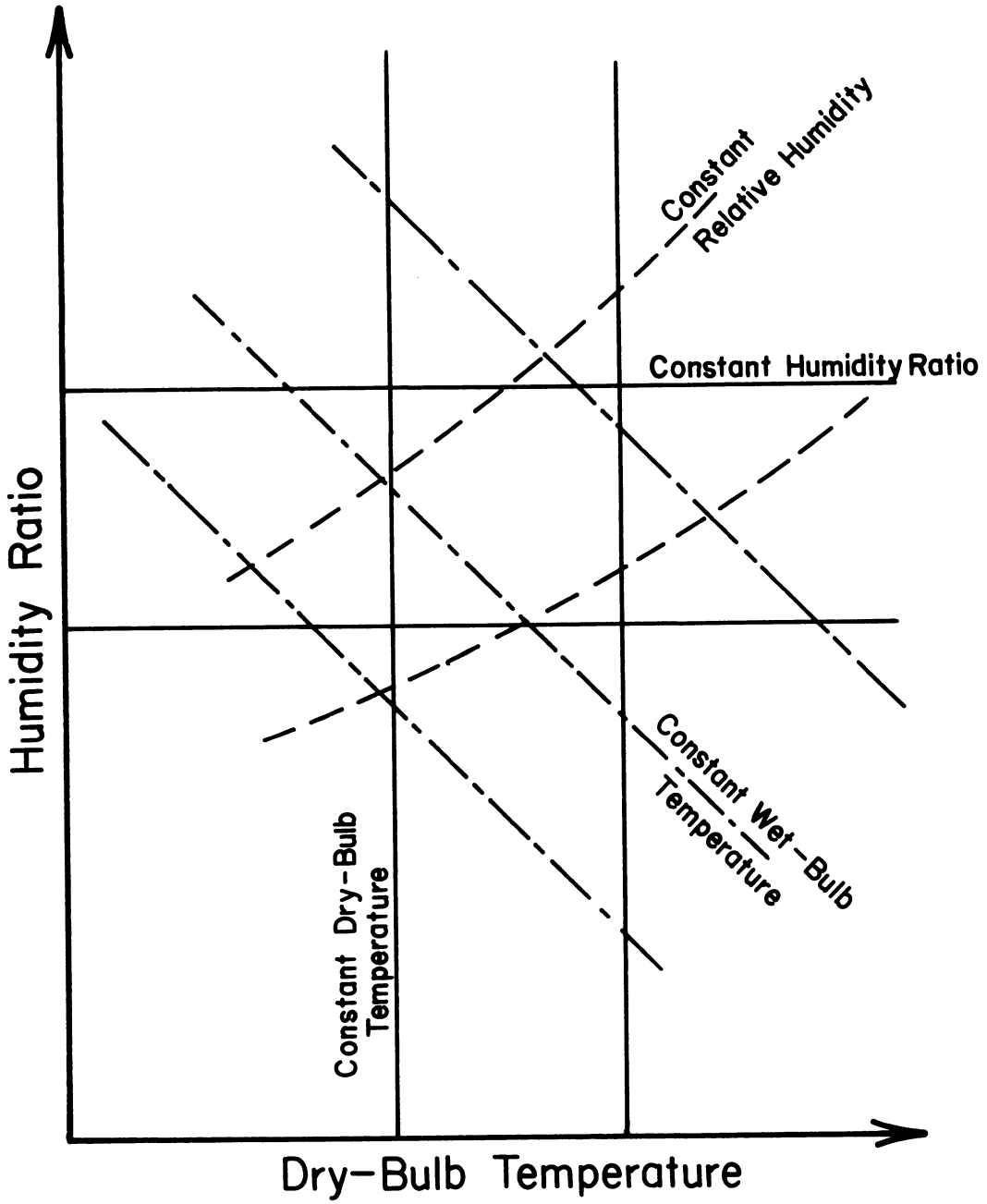

Figure 5.16 Two-Dimensional Relative Humidity/Wet-Bulb Temperature Bins

a bin size will unnecessarily increase the computational effort required.

Once the wet-bulb temperature/relative humidity bin data have been determined, the dry-bulb temperatures and humidity ratios which correspond to the values of wet-bulb temperature and relative humidity at the center of each wet-bulb temperature/relative humidity bin are calculated. The number of hours in a dry-bulb temperature/humidity ratio bin is the sum of the hours in all wet-bulb temperature/relative humidity bins whose midpoint lies within the dry-bulb temperature/humidity ratio bin.

5.5.4 Comparisons of Measured and Estimated Bin Data

Dry-bulb temperature/humidity ratio bin data were generated from the long-term hourly SOLMET data sets on both a monthly and annual basis. A bin size of 4°F was chosen for dry-bulb temperature. The humidity ratio bin size was varied so that approximately 20 bins covered the range of occurrence for humidity ratio for both monthly and annual bin data. Monthly and annual bin data were also estimated for each of the 9 locations using both of the estimation procedures outlined above. Measured values of monthly-average hourly dry-bulb temperature and relative humidity were used as input to each estimation procedure. The annual measured bin data are compared in Figure 5.17 with the two sets of estimated bin data for the 9 locations. The bin size shown in the figures is for twice the interval of both dry-bulb temperature and humidity ratio as the bin

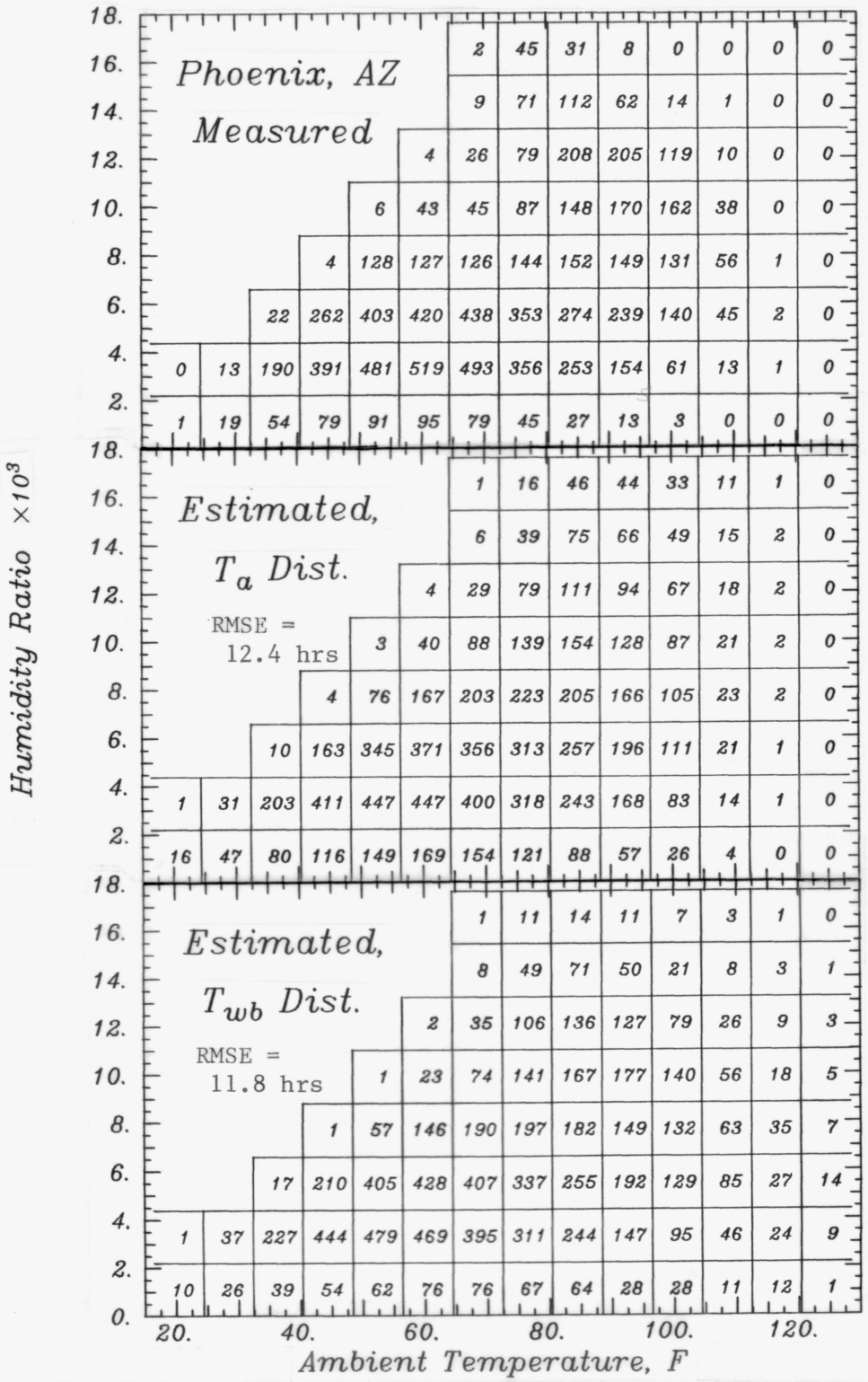

Figure 5.17 Measured and Estimated Annual Dry-Bulb Temperature/ Humidity Ratio Bin Data

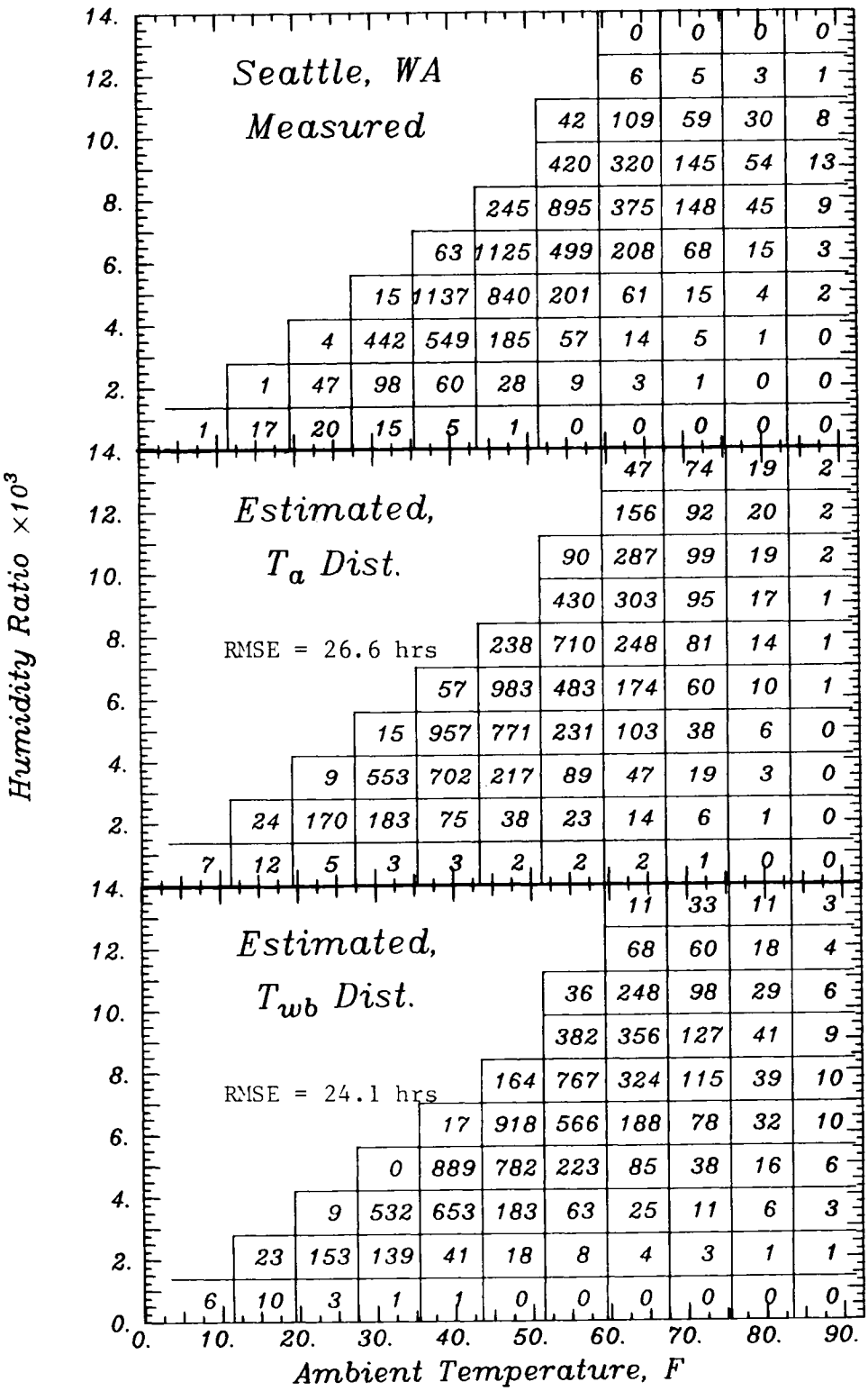

Figure 5.17 (cont.)

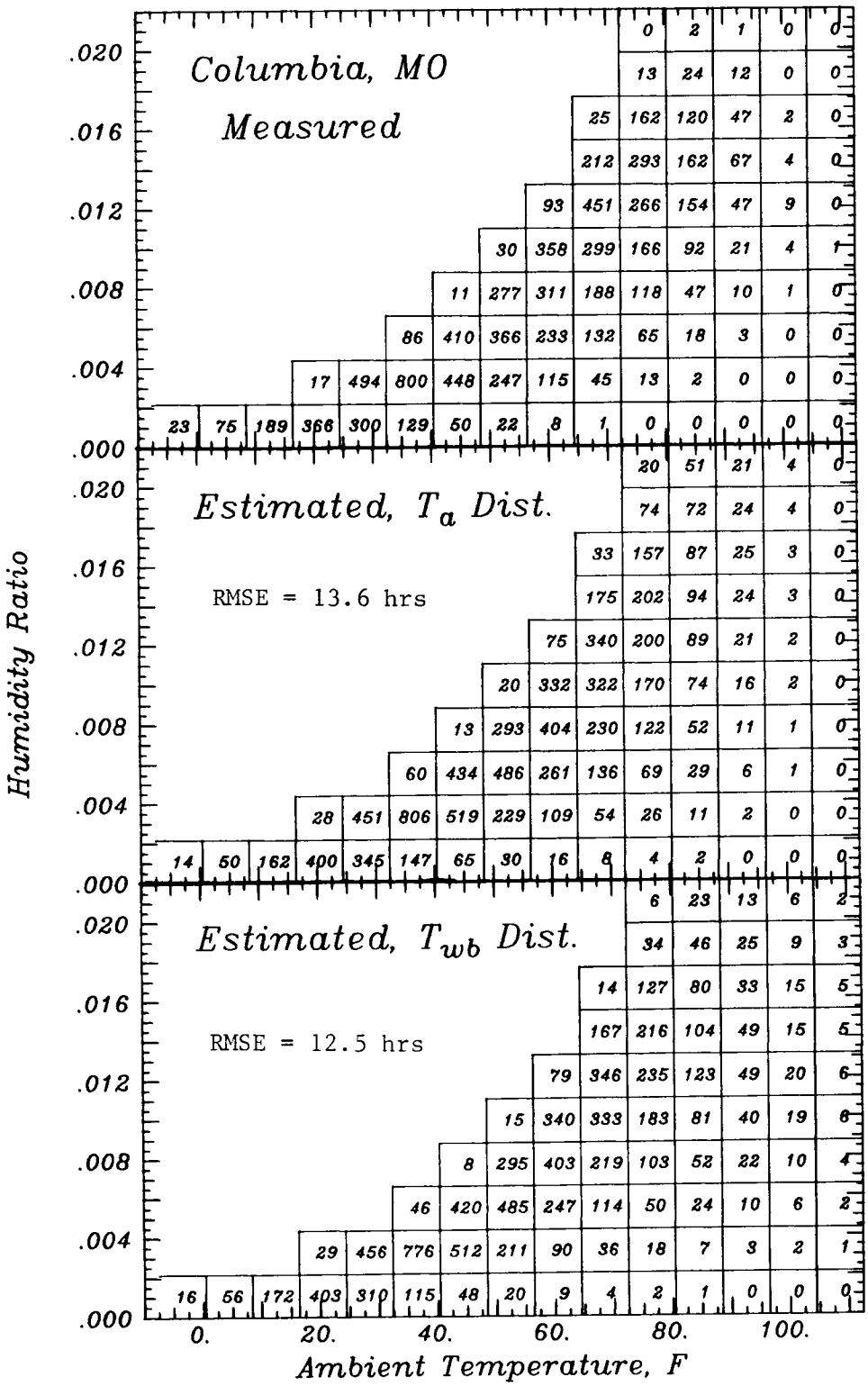

Figure 5.17 (cont.)

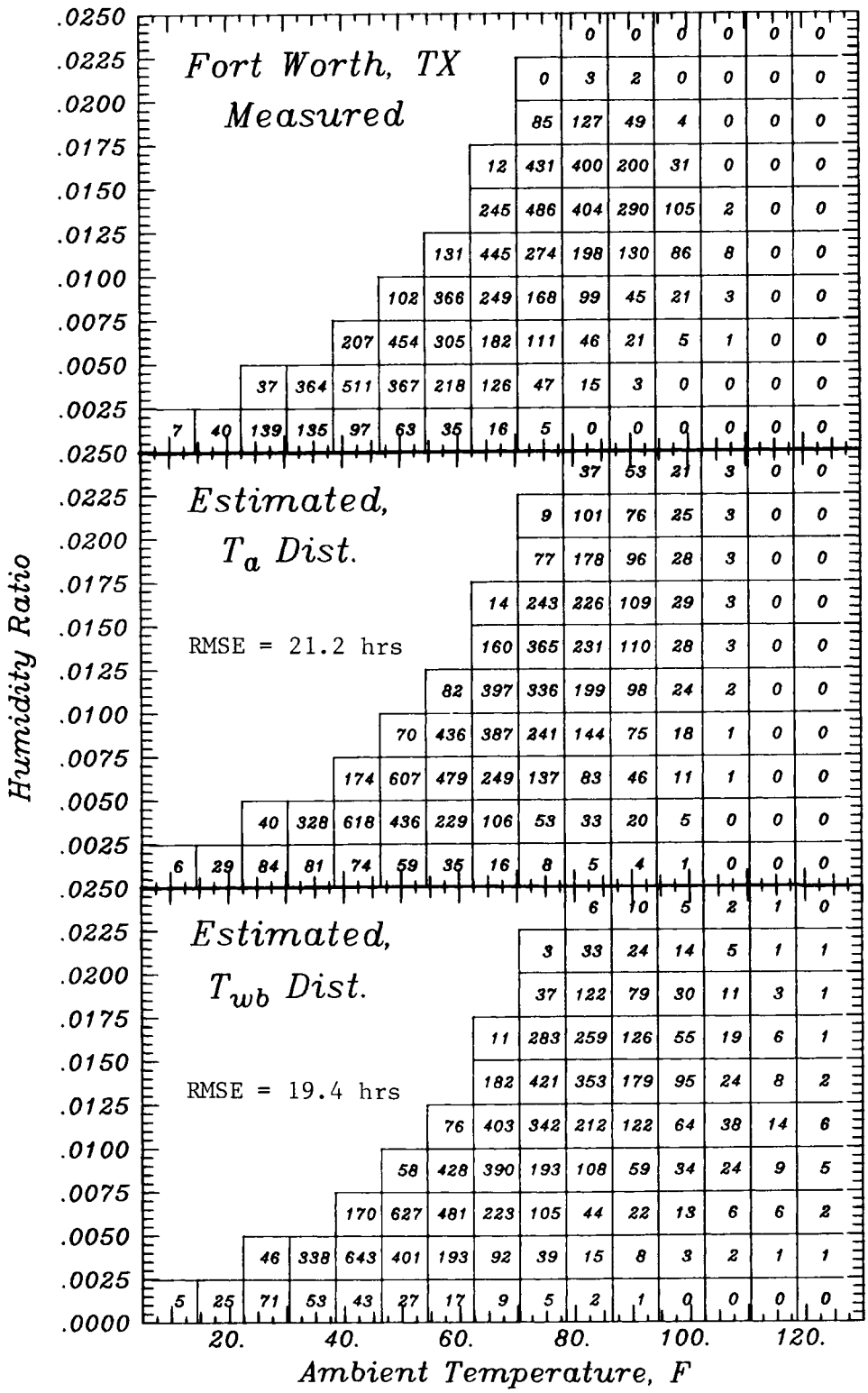

Figure 5.17 (cont.)

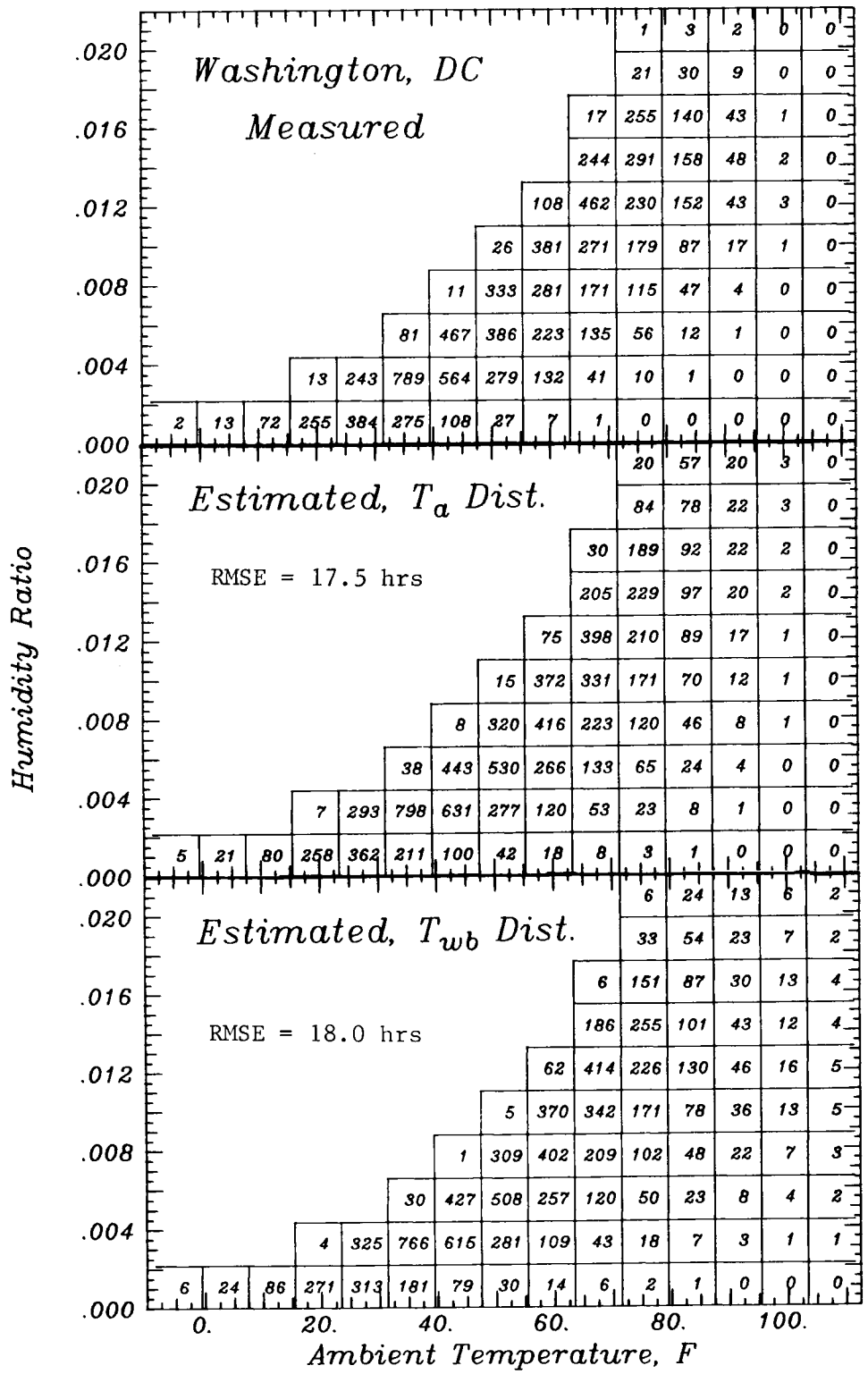

Figure 5.17 (cont.)

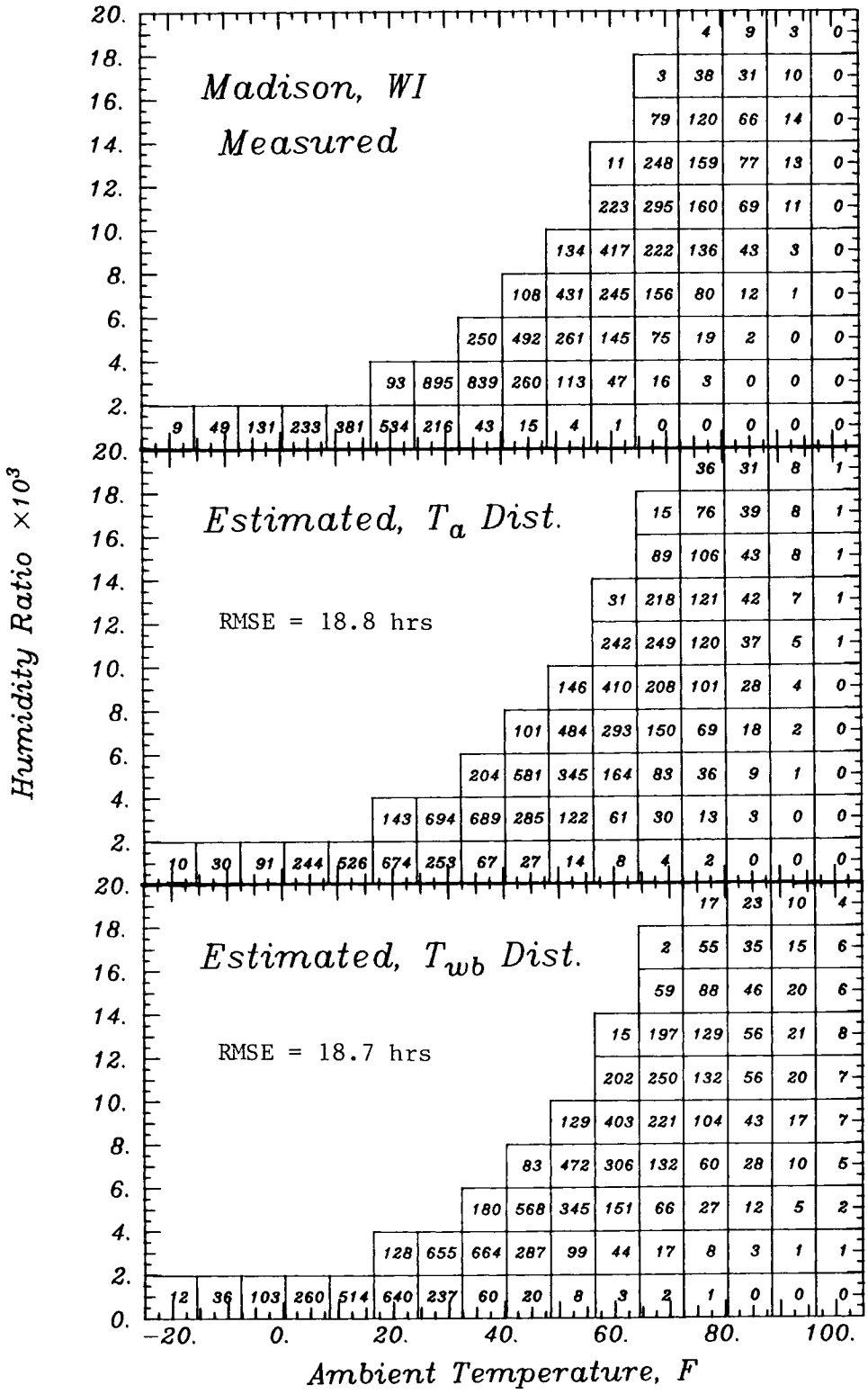

Figure 5.17 (cont.)

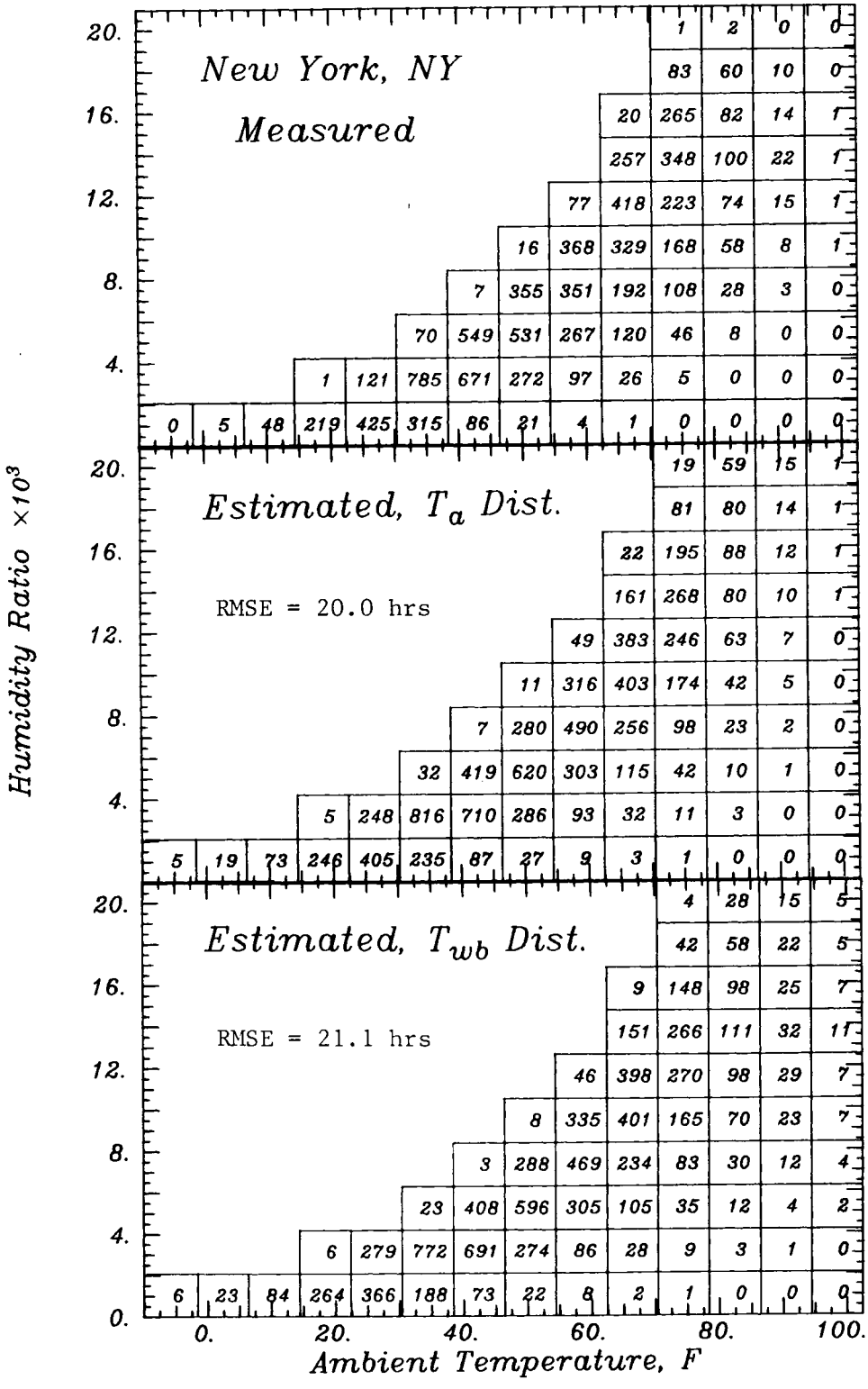

Figure 5.17 (cont.)

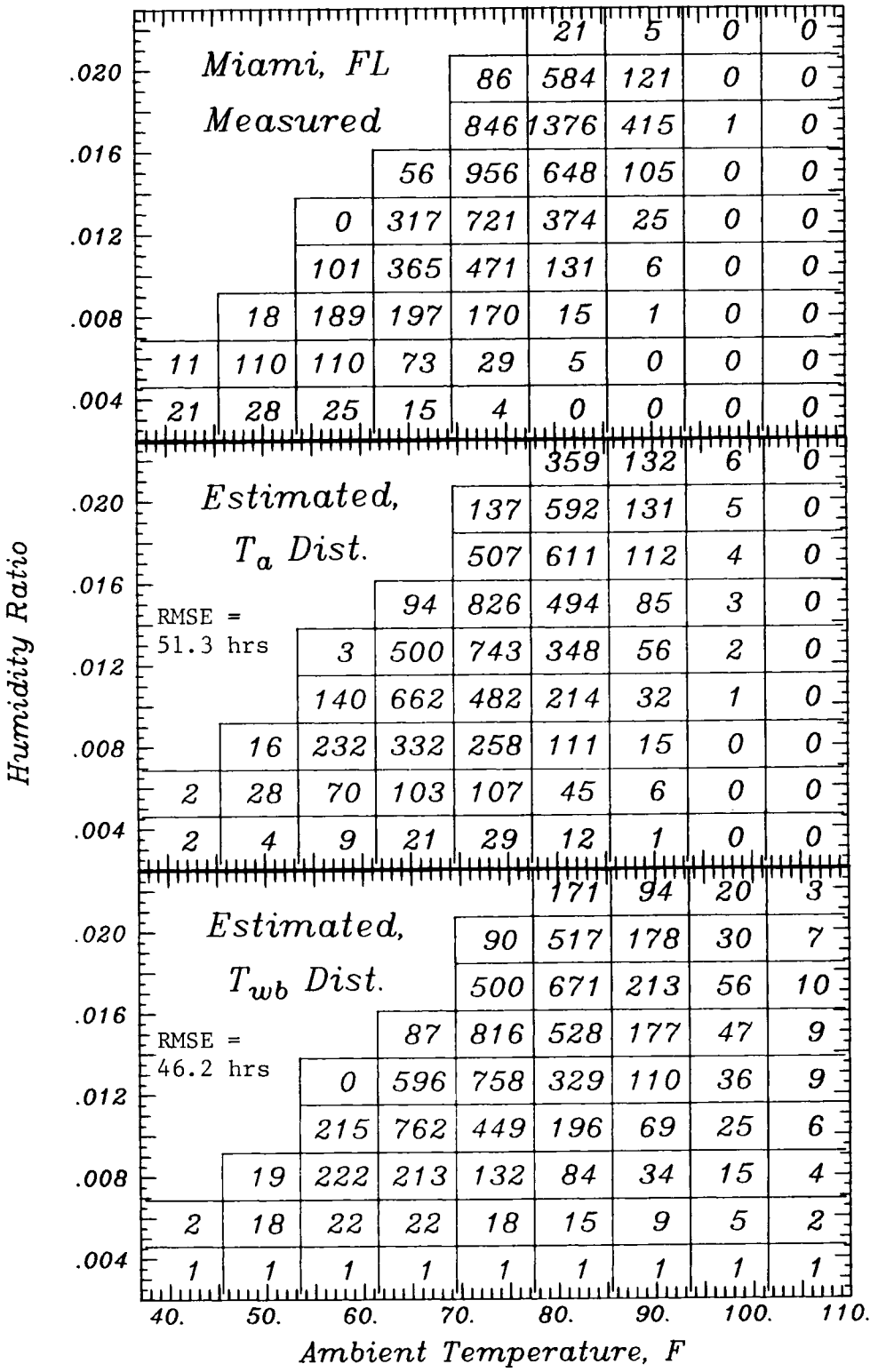

Figure 5.17 (cont.)

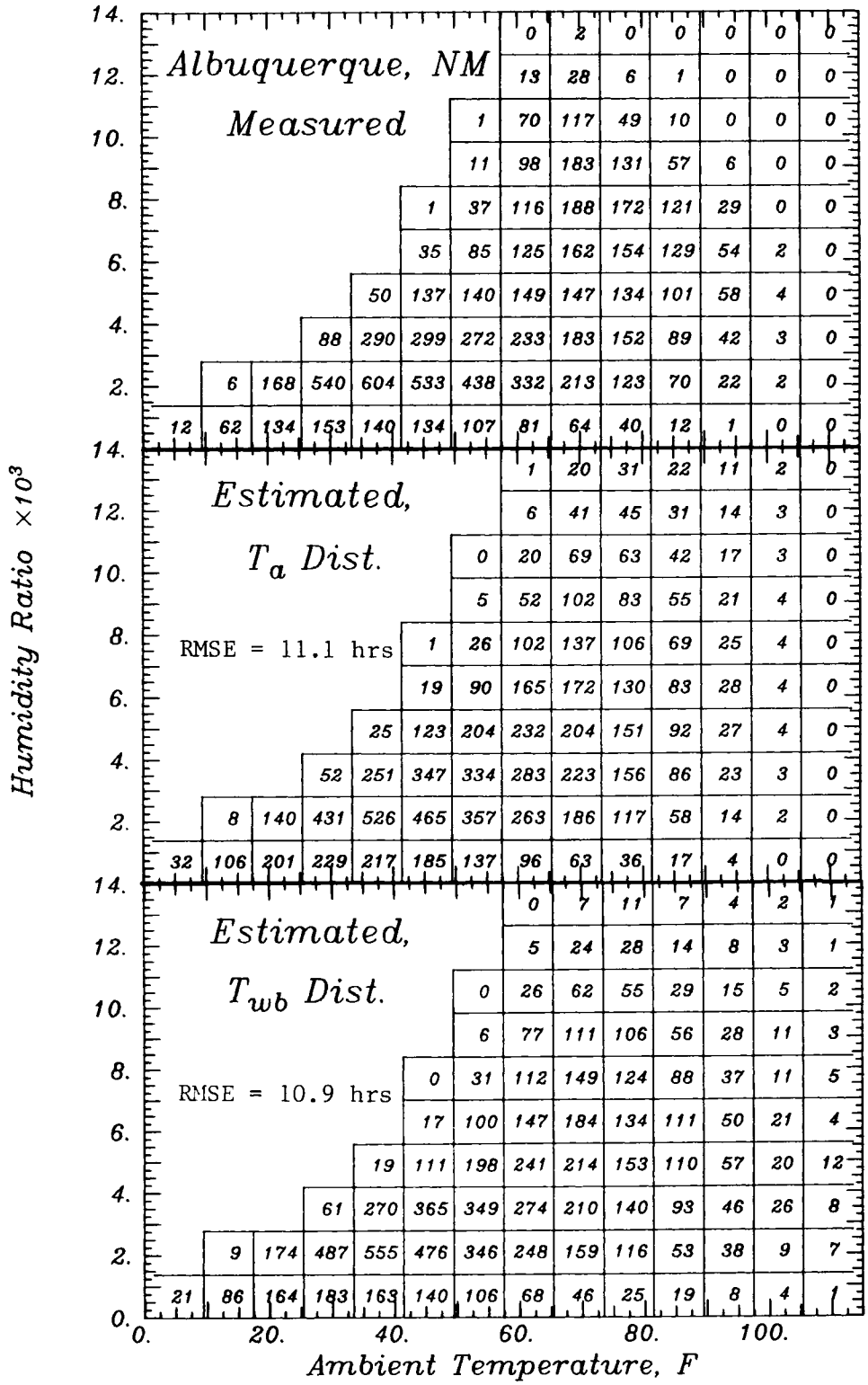

Figure 5.17 (cont.)

size used in generating the measured and estimated data. Thus, each of the bins shown contains 4 of the original bins. The RMS errors given in the figure were calculated using the data in the original bins. The errors are based on the differences in the number of hours between the measured data and the estimated data for each bin where either the measured or estimated value for a bin contained 1 or more hours.

A significant error in the number of hours estimated for an individual dry-bulb temperature/humidity ratio bin may occur with either estimation method. Both estimation procedures tend to overestimate the number of hours at high values of humidity ratio, and the procedure based on the wet-bulb temperature distribution function also tends to overpredict the number of hours at high values of dry-bulb temperature. The estimated bin data are more spread out than the measured bin data, and the gradients in the number of hours between adjacent bins are generally not as large in the estimated bin data.

The cross-correlation between dry-bulb temperature and relative humidity or between wet-bulb temperature and relative humidity, which are not included in the estimation methods, is one possible source of error. Other possible sources of error are differences between the distribution models and the measured data for T_a, T_{wb} and RH. The temperature distributions are scaled using estimates of the standard deviation, introducing another source of uncertainty. The estimates were based on measured values of monthly-average hourly

wet-bulb temperature, dry-bulb temperature and relative humidity; the estimation of the diurnal variations of these variables and the estimation of monthly-average relative humidity from other variables may increase the size of the errors over those in the comparisons shown.

A second set of comparisons between the measured and estimated dry-bulb temperature/humidity ratio bin data was devised to consider only the accuracy of the humidity ratio distributions as represented by the estimated bin data. Humidity-hours, W, is the accumulated difference of all positive differences between ambient humidity ratio and the base humidity ratio, ω_b, as defined in Equation (2-8). W can be calculated using bin data by summing the product of the difference between the humidity ratio for the bin and the base humidity ratio and the number of hours in the bin over all bins where ω is larger than ω_b.

Six different sets of monthly and annual bin data were estimated for each location. The first set was estimated using the distribution function for dry-bulb temperature and the distribution function for relative humidity in the manner described above. Measured values of the monthly-average hourly dry-bulb temperature and relative humidity were used as input. The second set was estimated using the distribution function for wet-bulb temperature and relative humidity as described above. Measured values of the monthly-average hourly dry-bulb temperature and relative humidity were again used as input, with the monthly-average wet-bulb temper-

ature and the standard deviation of the wet-bulb temperature estimated with the relationships presented in Section 5.4.

The third bin data set was estimated with the dry-bulb temperature and relative humidity distribution models, but the monthly-average hourly values of dry-bulb temperature and relative humidity were estimated from measured daily values with the diurnal variation relationships presented. The fourth set was estimated in the same manner as the third set, but in addition to estimating the diurnal variation of the monthly-average dry-bulb temperature and relative humidity, the monthly-average daily relative humidity was also estimated.

The fifth and sixth sets were estimated with the distribution function for dry-bulb temperature, but the distribution function for relative humidity was not used. In the fifth set, the relative humidity was assumed to always be equal to the monthly-average hourly relative humidity for each hour of the day. The monthly-average hourly relative humidity and dry-bulb temperature were estimated from the monthly-average daily values. In the sixth set, the relative humidity was assumed to equal the monthly-average daily relative humidity for all hours of the day, and the monthly-average hourly dry-bulb temperatures were all set equal to the monthly-average daily value.

Humidity-hours were calculated for the measured bin data and for each of the 6 sets of estimated dry-bulb temperature/humidity ratio bin data for a value of base humidity ratio corresponding to

dry-bulb temperature of 24°C and a relative humidity of 50%. The monthly and annual humidity-hour totals for each of the bin data estimation procedures were compared to the values obtained using the measured data. The monthly and annual bias errors and RMS errors for the combined errors of the 9 locations are given in Table 5.3.

The monthly and annual humidity-hours for the measured bin data and for the first set of estimated bin data are also compared in Figure 5.18. Similar comparisons are shown in Figure 5.19 for the second set of estimated bin data and in Figure 5.20 for the sixth set of estimated bin data.

The first two estimation procedures for bin data result in humidity-hour estimates of comparable accuracy. The estimation of the diurnal variations of monthly-average dry-bulb temperature and relative humidity increases the annual RMS and bias errors somewhat, and the estimation of the monthly-average daily relative humidity results in an even larger increase in the size of the errors. Surprisingly, the simplest of the estimation procedures (used for the sixth bin data set) was the most accurate on an annual basis and comparable in accuracy to the more complex methods on a monthly basis.

5.6 Summary

Distribution function models were developed for relative humidity and wet-bulb temperature. Additional relationships are presented

Table 5.3 Monthly and Annual Bias and RMS Errors for Humidity-Hours Estimated with Dry-Bulb Temperature/Humidity Ratio Bin Data

Description of Bin Data Estimation Procedure	Monthly Humidity-Hours		Annual Humidity-Hours	
	RMS Error, hrs	Bias Error, hrs	RMS Error, hrs	Bias Error, hrs
T_a and RH distributions, measured $\overline{T}_{a,h}$ and $\overline{RH}_h$	0.156	0.021	1.23	0.25
T_{wb} and RH distributions, measured $\overline{T}_{a,h}$ and $\overline{RH}_h$	0.165	-0.046	1.20	-0.55
T_a and RH distributions, $\overline{T}_{a,h}$ and $\overline{RH}_h$ estimated from T_a and $\overline{RH}$	0.163	-0.031	1.65	-0.37
T_a and RH distributions, $\overline{T}_{a,h}$ and $\overline{RH}_h$ estimated from T_a and K_T	0.320	0.004	2.71	0.04
T_a distribution, RH = $\overline{RH}_h$, $\overline{T}_{a,h}$ and $\overline{RH}_h$ estimated from T_a and $\overline{RH}$	0.189	-0.081	1.58	-0.98
T_a distribution, RH = $\overline{RH}$, no diurnal variation of T_a or RH, measured $\overline{T}_a$ and $\overline{RH}$	0.175	-0.039	1.02	-0.47
Average humidity-hours from measured bin data	0.98 hrs-Kg/Kg		11.7 hours-Kg/Kg	

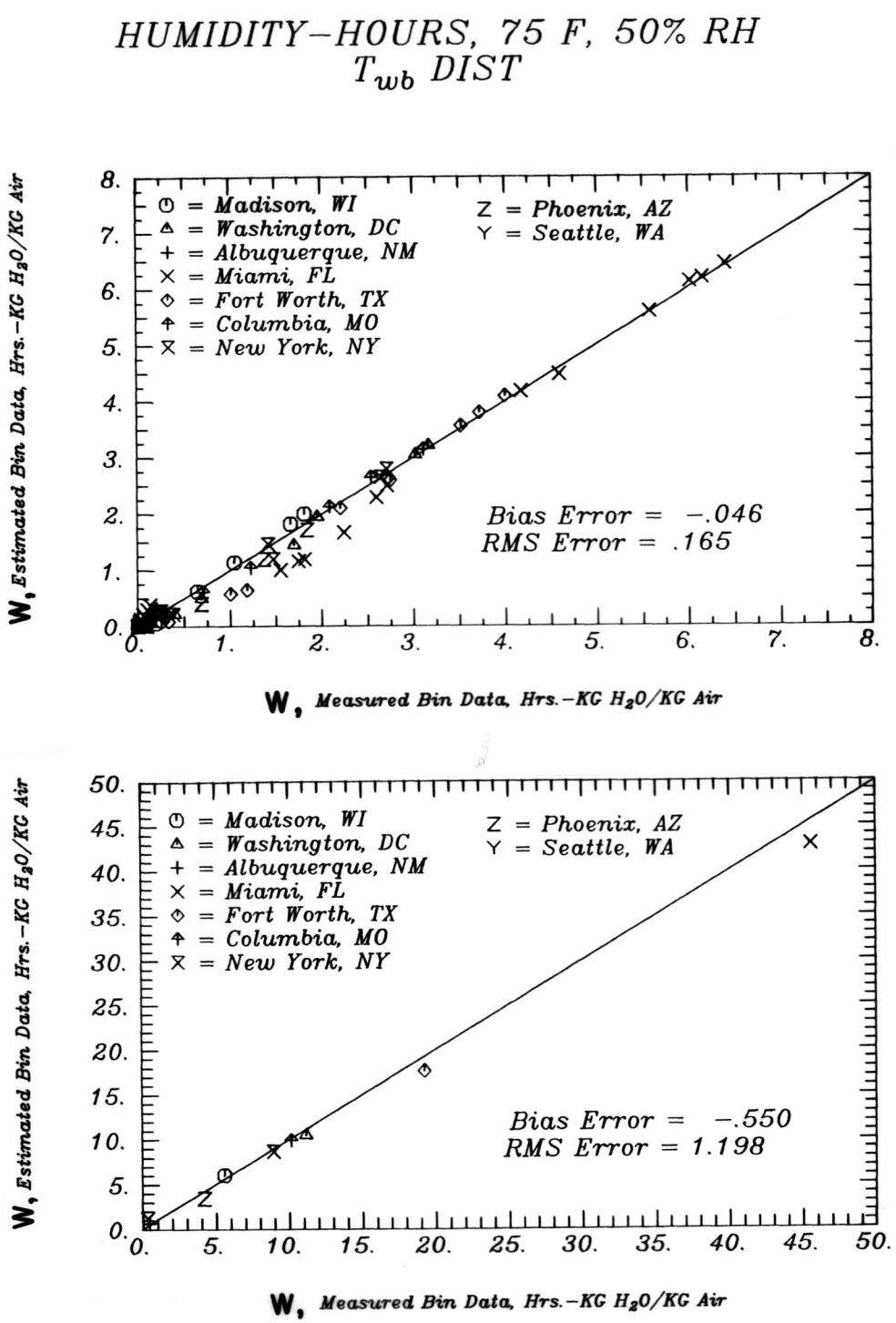

Figure 5.18 Comparison of Humidity-Hours for Measured Bin Data with Humidity-Hours for Bin Data Estimated with the Distribution Functions for Dry-Bulb Temperature and Relative Humidity

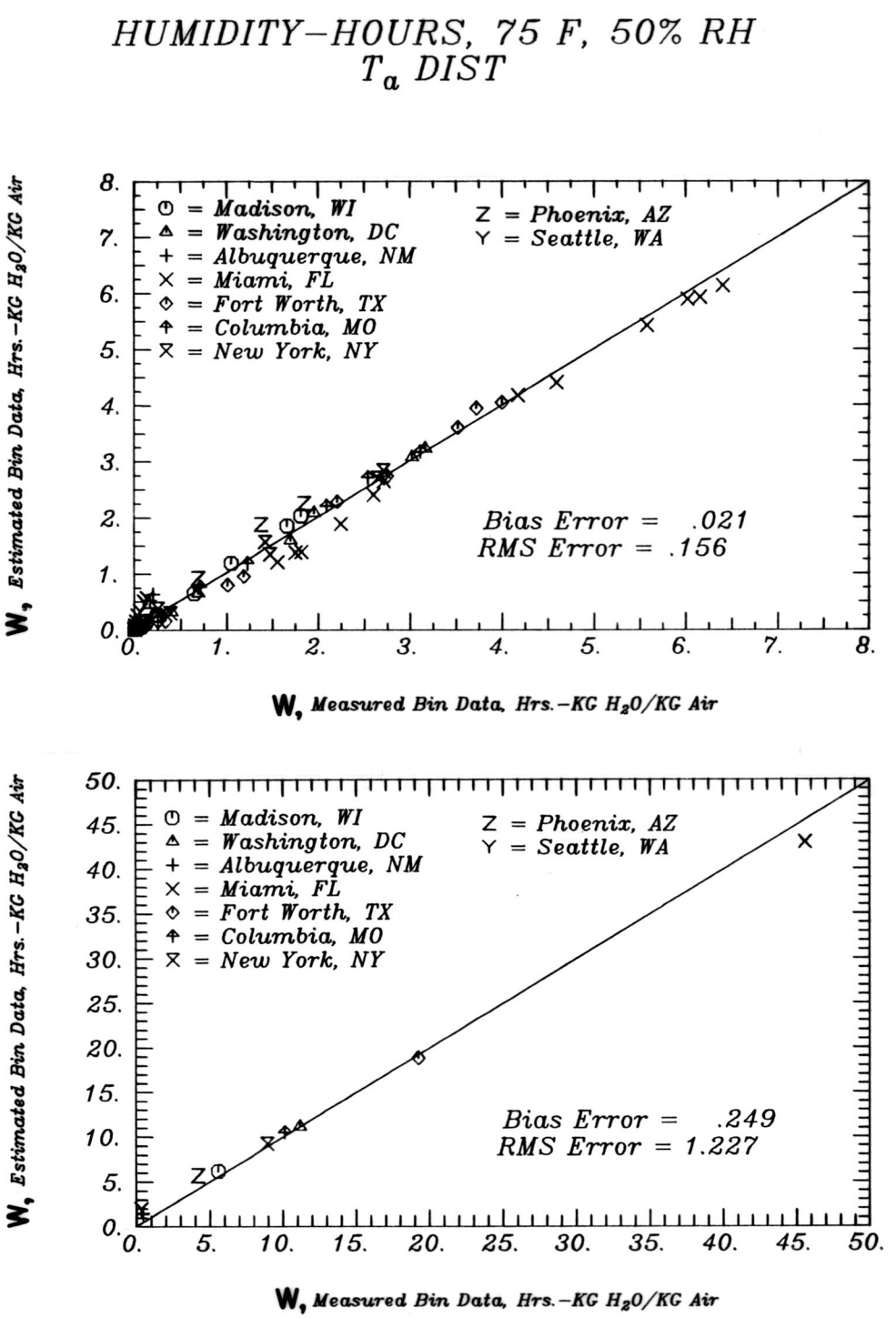

Figure 5.19 Comparison of Humidity-Hours for Measured Bin Data with Humidity-Hours for Bin Data Estimated with the Distribution Functions for Wet-Bulb Temperature and Relative Humidity

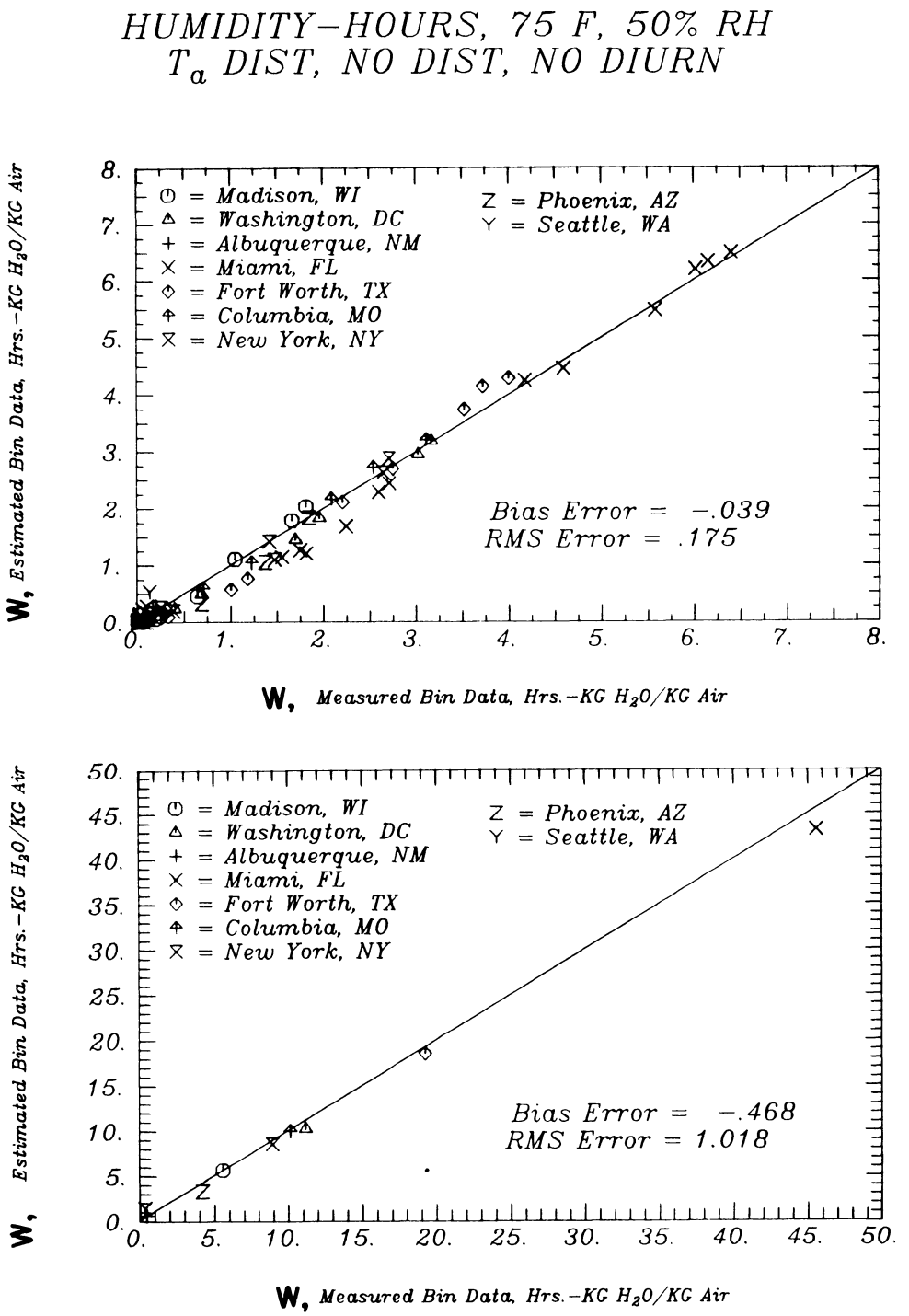

Figure 5.20 Comparison of Humidity-Hours for Measured Bin Data with Humidity-Hours for Bin Data Estimated with the Distribution Function for Dry-Bulb Temperature and with Relative Humidity Constant at the Monthly-Average Daily Value

which allow the distribution models to be used with only monthly-average daily dry-bulb temperature and clearness index as input.

Relative humidity and wet-bulb temperature are convenient variables to work with when modeling the distribution of ambient air moisture content. Since neither variable uniquely determines the humidity ratio, it is necessary to use more than a single variable for the estimation of ω or other measures of absolute water vapor content. Dry-bulb temperature/humidity ratio bin data estimated with the distribution models for relative humidity and wet-bulb temperature are slightly more accurate than the estimates obtained using the distribution models for relative humidity and dry-bulb temperature.

Humidity-hours for 24°C and 50% relative humidity are estimated equally well by either set of distribution model pairs. Replacing the distribution of RH with the monthly-average daily value and ignoring the diurnal variation of T_a improves the estimates for humidity-hours slightly on an annual basis when compared to estimates based on both distribution functions. The accuracy of the estimated dry-bulb temperature/humidity ratio bin data in air conditioner performance calculations is demonstrated in Chapter 7.

CHAPTER 6

6. A CORRECTION PROCEDURE FOR BUILDING THERMAL CAPACITANCE EFFECTS

The weather statistics which have been described and modeled in Chapters 3, 4 and 5 neglect the effects of energy and moisture storage in the materials which make up a building and its contents. For some building types and weather conditions, the storage of energy in the building mass can have a significant effect on the heating and cooling loads, so that it may be necessary to model the dependence of building loads on thermal capacitance when using weather statistics for load estimation. The effect of thermal capacitance on the heating and cooling loads for buildings has been studied extensively, particularly for structures which are passively heated by the sun. The storage of moisture in building materials can also conceivably affect the energy required to heat or cool a building, but there is very little information on the importance of moisture storage or the effective capacity for storage in common materials. Only the storage of thermal energy will be addressed in this chapter.

6.1 Literature Review

Methods which account for the effect building thermal capacitance has on heating and cooling loads can be classified as either empirical or theoretical in nature. The Solar Savings Fraction method (Solar Load Ratio method), developed by Balcomb et al. (1983),

is a building load model which empirically determines the effect of thermal capacitance on the heating loads for a structure. The relationship between the building load and weather statistics describing ambient temperature and solar radiation is different for different building types in this method. A large number of relationships are presented to make the method applicable for most common building constructions. The SSF method only allows for the estimation of heating loads, and the constructions represented are primarily passive solar heating applications.

The procedures developed by Monsen et al. (1981, 1982) are also empirical in nature, as they are based on simulated heating loads for a wide range of direct gain and collector-storage wall passively heated buildings. A single relationship is used to estimate the heating load for a finite capacitance building, making it less cumbersome than the Solar Savings Fraction method. The correction is a function of the solar fraction for a building with infinite thermal capacitance, the utilizable solar radiation for a building which has no thermal storage and the size of the storage capacity of the building relative to the excess solar gains available for storage. The storage capacity of the building is based on the "effective" lumped thermal capacitance of the structure (discussed in the next section) and the allowable interior temperature swing. As with the Solar Savings Fraction method, the correction procedures of Monsen et al. are only for heating load calculations, and the data on which they were based and tested are for passive solar heating applica-

tions.

The building capacitance correction procedure developed by Kusuda and Saitoh (1980) also makes use of the lumped building capacitance concept, but the corrections are based on an analytical solution for the interior temperature for an "average" day of the month. The method is very general in that any combination of thermostat setbacks or setups can be treated (provided the pattern is constant for all days in the month), but because only a single "average" day is considered, the distributions of ambient temperature and solar radiation are not represented. The reduction in the heating or cooling load for a building is determined from the amount of time it takes for the interior temperature to decay to the set-point temperature. No heating or cooling energy is required while the interior temperature is floating.

Sonderegger and Garnier (1981) also developed a method which models the interior air temperature variation for the average day of the month, but they only consider interior temperature variations due to thermostat setbacks and setups. The temperature swings due to excess solar and conduction gains or excess conduction losses are not modeled, and the method is unable to account for the reduction in the heating and cooling loads which result from the storage of excess gains and losses by the building. Heating and cooling auxiliary energy is found by evaluating the heating and cooling degree-days with a base temperature which varies according to time of day and which is determined using the average day interior air

temperature profile.

6.2 An Analysis of Building Thermal Energy Storage on a Diurnal Basis

6.2.1 Building Capacitance and Excess Gains and Losses

The thermal capacitance of a building is well distributed spatially, and the storage of energy in the distributed capacitance of a building is in general very nonuniform. If there is a net flow of energy into a building, the temperature of some building components is likely to increase more than others. In addition, components which are massive will not be uniform in temperature. The change in the temperature of the air inside a building will tend to fall within the range of temperature changes for the structural components of the building, but significant variations in the total internal energy change for the building can occur for the same change in inside air temperature. To correctly model the thermal capacitance of a building, it is necessary to break the building up into nodes, with each node small enough so that it can be considered uniform in temperature. A set of equations describing the energy transfer between nodes must be written and the resulting set of coupled first order ordinary differential equations solved.

The lumped "effective" thermal capacitance for a building is a single node which is always at the inside air temperature and which correctly describes the storage of energy by the distributed build-

ing mass. If the lumped "effective" thermal capacitance value is known for a building, the modeling of energy storage and internal air temperature variations for the building is greatly simplified. The "effective" capacitance for a building, however, is not strictly a building property. The "effective" capacitance for a given building is dependent on the weather patterns which occur and the internal temperature swing which is allowed. The estimation of the lumped "effective" capacitance for a building has been investigated by Horn (1982) and more recently by Evans (1983). A method was developed by Evans which allows the effective capacitance of a building to be determined from detailed simulations for short time periods. The correction procedures which are developed in this chapter are all based on the use of a lumped "effective" thermal capacitance to represent the storage of energy in a building.

The heating and cooling loads for a building refer to the energy which must be supplied by the heating and cooling equipment. The heating and cooling loads are integrated quantities, generally for the period of a month or more. The energy gains and losses for a building are used to refer to the actual flow of energy into and out of the building. Since there may be simultaneous gains and losses, the integrated gains and losses for a building can be quite different from the heating and cooling loads for the same time periods. The excess gains and excess losses are the net rate of energy flow into or out of a building, and at any instant of time, there can only be excess gains or excess losses. The integrated excess gains and ex-

cess losses still differ from the heating and cooling loads as a result of the building thermal capacitance effects.

6.2.2 Building Response

Thermal energy storage in a building occurs when the rate of energy gain exceeds the rate of energy loss and the interior air temperature is allowed to float. Energy gains can be the result of internal generation, solar radiation or conduction and infiltration. Losses, on the other hand, can only be the result of conduction and infiltration when ambient temperature falls below the interior temperature value.

When there are excess gains, there is a net influx of energy into the building. An energy balance requires that either cooling be provided or the interior temperature allowed to rise. Similarly, when there are excess losses, the interior temperature will decrease unless heating is supplied. If there is either a net energy loss or gain for an extended period of time (several days or more), the interior temperature is fixed at the heating or cooling setpoint for most of the period, and the thermal capacitance of the building has little or no effect on the loads. It is only when there are alternating periods of excess gains and losses that thermal capacitance acts to significantly reduce or eliminate the heating and cooling loads.

The manner in which a building responds to excess gains and losses and the degree to which these excess gains and losses are

utilized in offsetting the building heating and cooling loads depends on the time constant of the building, the time period associated with the fluctuation of the net energy flow between excess gains and excess losses, and the storage capacity of the building (relative to the load). The thermal storage capacity of a building is the product of the "effective" thermal capacitance and the allowable room temperature swing. The allowable room temperature swing (ΔT_{set}) is assumed to be the difference in thermostat setpoint for heating (T_{rh}) and cooling (T_{rc}). The thermal time constant of the building, τ, is the ratio of the "effective" building thermal capacitance, MC, to the building conductance, UA. The time constant determines how fast the building responds to excess gains and losses.

The reversal of the net building energy transfer rate from losses to gains or vice versa can be the result of either diurnal or day-to-day variations in the weather and internal generation rate. Variations in internal generation are the result of many factors, most of which are due to the habits of the occupants, and they are difficult to model. Variations in the weather are also difficult to model on a short time basis, but some general observations can be made. Solar gains occur only during the daytime hours. Gains due to ambient temperature can occur over the entire day, but on the average they are larger during the daytime hours as a result of the diurnal variation of ambient temperature. On a diurnal basis, when there are both excess heat gains and losses for a day, the excess

gains occur during the daytime and the excess losses occur at night. However, the day-to-day variation of ambient temperature and solar radiation also make it possible for there to be excess gains for the entire day for one or more days in a row, followed by excess losses for the entire day for one or more days in a row.

Reported time constants for houses [Kusuda and Saitoh (1980)] are typically on the order of one day. A house which has a time constant of one day will be able to utilize alternating excess heat losses and gains most effectively when they alternate over a diurnal or shorter time period. Excess gains at the beginning of a month cannot be used to offset heating loads at the end of a month. Since weather variations which lead to diurnal fluctuations of the net energy flow for a building between net gains and losses are generally more important than weather variations which lead to heat flow reversals with a period of several days, the analyses which follow will be concerned with the characterization of diurnal weather variation and building response patterns.

6.2.3 Patterns of Variation for Ambient Temperature and Solar Radiation

The variation of ambient temperature can be divided into variations which take place within the period of a day and variations which occur from day-to-day. The monthly-average amplitude of the diurnal variation of ambient temperature was presented in Figure 3.3 for 9 SOLMET locations. The range of amplitude for these loca-

tions is from 3 to 15°C, with larger amplitudes observed during summer months and in sunny locations. The persistence of ambient temperature from one day to the next for the period of an hour was investigated by calculating autocorrelation coefficients for a lag of 24 hours using the hourly temperature measurements for the 9 SOLMET locations. The ambient temperature autocorrelation coefficient for a lag of 24 hours, $\rho_{Ta}(24)$, is defined by Equation (2-16). The coefficients given in Table 6.1 are the averages of the 24 hourly values of autocorrelation coefficient for each month. The values are between 0.5 and 0.7 for most months and locations, indicating that on the average, ambient temperature changes slowly from day to day.

The diurnal variation of solar radiation is more variable than the diurnal variation of ambient temperature. The radiation intensity for a building surface varies from 0 at night to as much as 1000 W/m^2 during the day. The shape of the diurnal solar radiation profile for a surface is a function of location, time of year and surface orientation. Autocorrelation coefficients were also calculated from the hourly values of clearness index for a time lag of 24 hours to measure the day-to-day persistence of solar radiation. Only those hours of the day when the sun was above the horizon were used for each month. The averages of the hourly autocorrelation coefficients for each of the daytime hours are given in Table 6.2. The autocorrelation coefficients are much smaller for clearness index than they are for ambient temperature, indicating that solar

Table 6.1 Autocorrelation Coefficients for Hourly Ambient Temperature for a Lag of 24 Hours

Month	Madison	Washington	Albuquerque	Miami	Fort Worth	Columbia	New York	Phoenix	Seattle
Jan	.67	.55	.72	.64	.58	.59	.58	.71	.74
Feb	.57	.53	.69	.61	.52	.52	.53	.73	.67
Mar	.62	.54	.63	.61	.61	.62	.56	.67	.62
Apr	.59	.56	.55	.57	.55	.57	.47	.71	.52
May	.58	.56	.62	.56	.63	.61	.51	.74	.65
June	.62	.62	.67	.47	.68	.62	.52	.80	.57
July	.50	.55	.50	.42	.68	.59	.52	.58	.67
Aug	.54	.58	.52	.43	.62	.57	.51	.54	.55
Sep	.57	.68	.63	.52	.65	.63	.63	.72	.59
Oct	.60	.62	.66	.61	.65	.62	.57	.75	.60
Nov	.60	.56	.65	.61	.58	.60	.56	.74	.69
Dec	.60	.56	.67	.65	.55	.60	.58	.66	.61

Table 6.2 Autocorrelation Coefficients for Hourly Clearness Index (k_T) for a Lag of 24 Hours

Month	Madison	Washington	Albuquerque	Miami	Fort Worth	Columbia	New York	Phoenix	Seattle
Jan	.21	.12	.22	.24	.33	.21	.06	.34	.32
Feb	.21	.14	.25	.17	.24	.24	.16	.26	.21
Mar	.24	.16	.17	.21	.26	.21	.17	.24	.21
Apr	.18	.18	.21	.32	.28	.13	.15	.26	.21
May	.26	.24	.19	.38	.31	.21	.21	.19	.22
June	.19	.27	.30	.44	.32	.21	.26	.39	.18
July	.16	.28	.22	.35	.37	.25	.25	.27	.32
Aug	.18	.25	.22	.32	.23	.20	.20	.18	.27
Sep	.23	.35	.33	.34	.39	.28	.27	.40	.27
Oct	.34	.30	.34	.29	.37	.31	.25	.31	.23
Nov	.19	.15	.28	.22	.37	.24	.13	.36	.21
Dec	.23	.16	.25	.23	.36	.24	.12	.31	.26

radiation levels vary more from one day to the next than does ambient temperature.

6.3 Heating Load Correction Factor

6.3.1 Excess Daytime Gains

Excess daytime gains are the result of a net flow of energy into the building. The interior temperature (which is the temperature associated with the effective capacitance of the building) increases as the excess gains are stored in the thermal mass. The increase in the interior temperature leads to a higher rate of conduction loss through the shell, reducing the rate of excess gain. If the conditions resulting in the excess gains were held constant for a long enough period of time, the interior temperature would eventually reach a steady-state equilibrium temperature, T_{eq}, where the increased losses due to the higher inside temperature offset the original rate of excess gains. The rate of excess gains is usually variable for days during which excess gains occur, but the concept of an equilibrium temperature can still be applied at any instant of time.

The energy stored by a building during a period of excess gains is equal to the product of the "effective" thermal capacitance and the internal temperature rise of the building. In order to calculate the energy storage, it is necessary to find the interior temperature at the end of the excess gains period. The solu-

tion for the change in internal temperature over the excess gains period is simplified if it is assumed the equilibrium temperature is constant over the daytime period, where the daytime period is defined from sunrise to sunset.

Although the rate of excess gain is usually variable during the daytime period, the time constant of most buildings (typically 24 hours) is large compared to the time period for significant variations in the rate of excess gains (typically 2 to 4 hours). The interior temperature of the building changes slowly with respect to changes in the excess gain rate, and it will tend to approach the average equilibrium temperature for the excess gains period. The temperature rise for a building in this situation is close to the temperature rise which results from a constant rate of excess gain equal to the average daytime value of the actual excess gain rate. The development which follows approximates the temperature response of a building during a period of excess gains with the response of the building to the average rate of excess gain.

It is assumed that internal generation gains can be treated as constant over the daytime period. The total excess gains for a day, E_{eg}, are found by integrating the instantaneous rate of excess gains ($\dot{E}_{eg}$) over the daytime period. If the interior temperature is held at the heating setpoint, the total excess gains are given by

$$E_{eg} = \int_{\Delta t_d} [\dot{E}_s - (UA)(T_{bh,d} - T_a)]^+ dt \qquad (6\text{-}1)$$

where

$$T_{bh,d} = T_{rh} - \dot{E}_{int}/UA \qquad (6\text{-}2)$$

$\dot{E}_s$ is the rate of solar gains and $T_{bh,d}$ is the daytime balance temperature based on the heating setpoint and constant daytime rate of internal generation, $\dot{E}_{int}$. E_{eg} is distributed evenly across the daylight hours, and the difference between the heating setpoint and the equilibrium temperature, denoted by ΔT_{eq}, is constant. ΔT_{eq} is equal to $\dot{E}_{eg}$ divided by the house conductance, UA. Figure 6.1 shows a typical daily profile for $\dot{E}_{eg}$ and the constant value for $\dot{E}_{eg}$ which results in the same total daily excess gains as the actual profile.

The average daily value of ΔT_{eq} represents a forcing function for the interior temperature of the building, which is assumed to be at the heating setpoint at the start of the daytime period. The response of a lumped capacitance building as a function of time is given by

$$\Delta T_f(t) = \Delta T_{eq,dh}[1 - \exp(-(t - t_d)/\tau)] \qquad (6\text{-}3)$$

where $\Delta T_f(t)$ is the increase in the room temperature above the heating setpoint, $\Delta T_{eq,dh}$ is the average value of ΔT_{eq} over the daytime hours, and t_d is the beginning hour for the daytime period. The interior temperature rise at the end of the daytime period is represented by the symbol $\Delta T_{f,d}$. Two possible shapes for the profile of $\Delta T_f(t)$ are shown qualitatively in Figure 6.2. The maximum

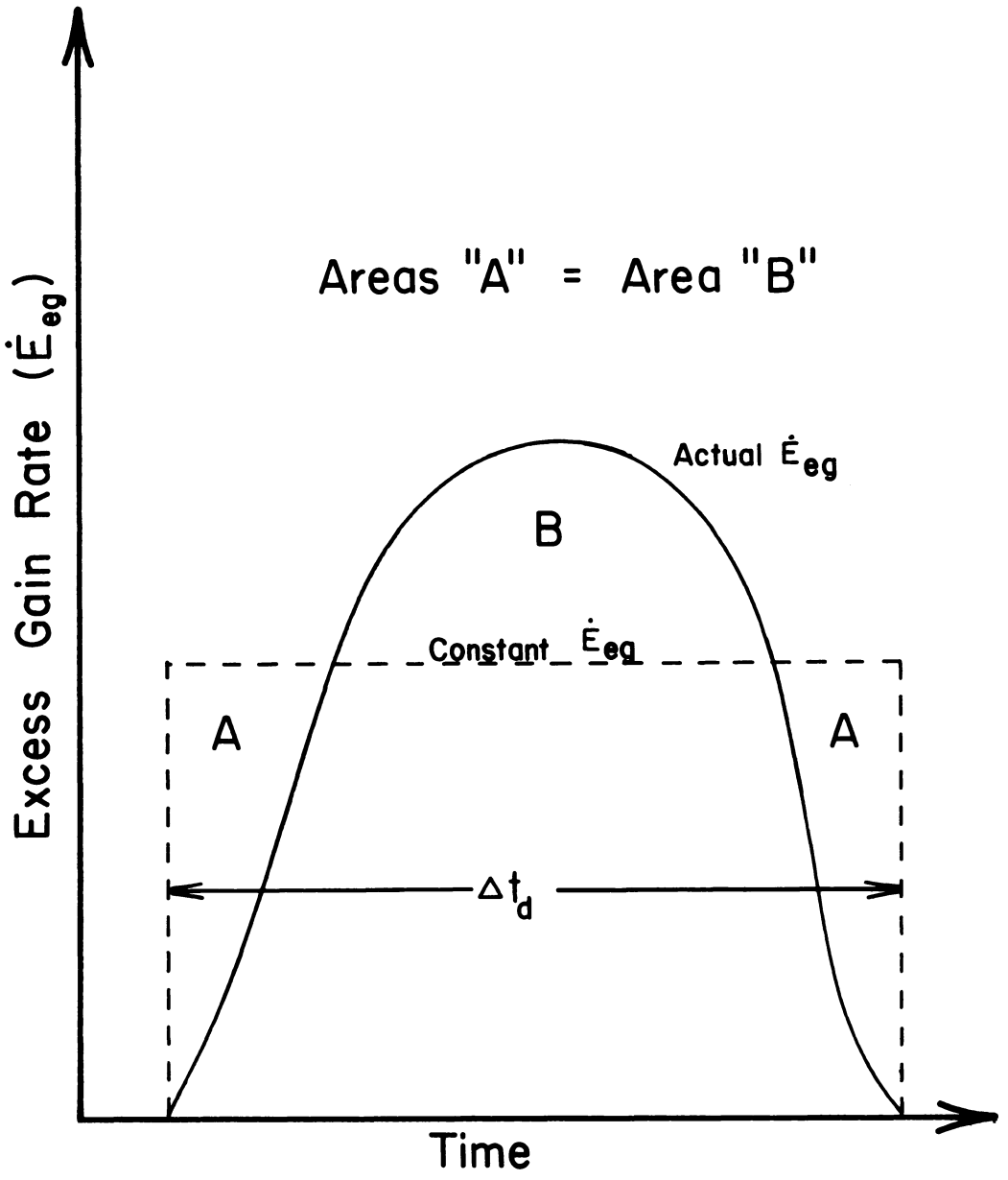

Figure 6.1 Variable Excess Gain Rate and Constant Excess Gain Rate Having the Same Daily Total Excess Gains

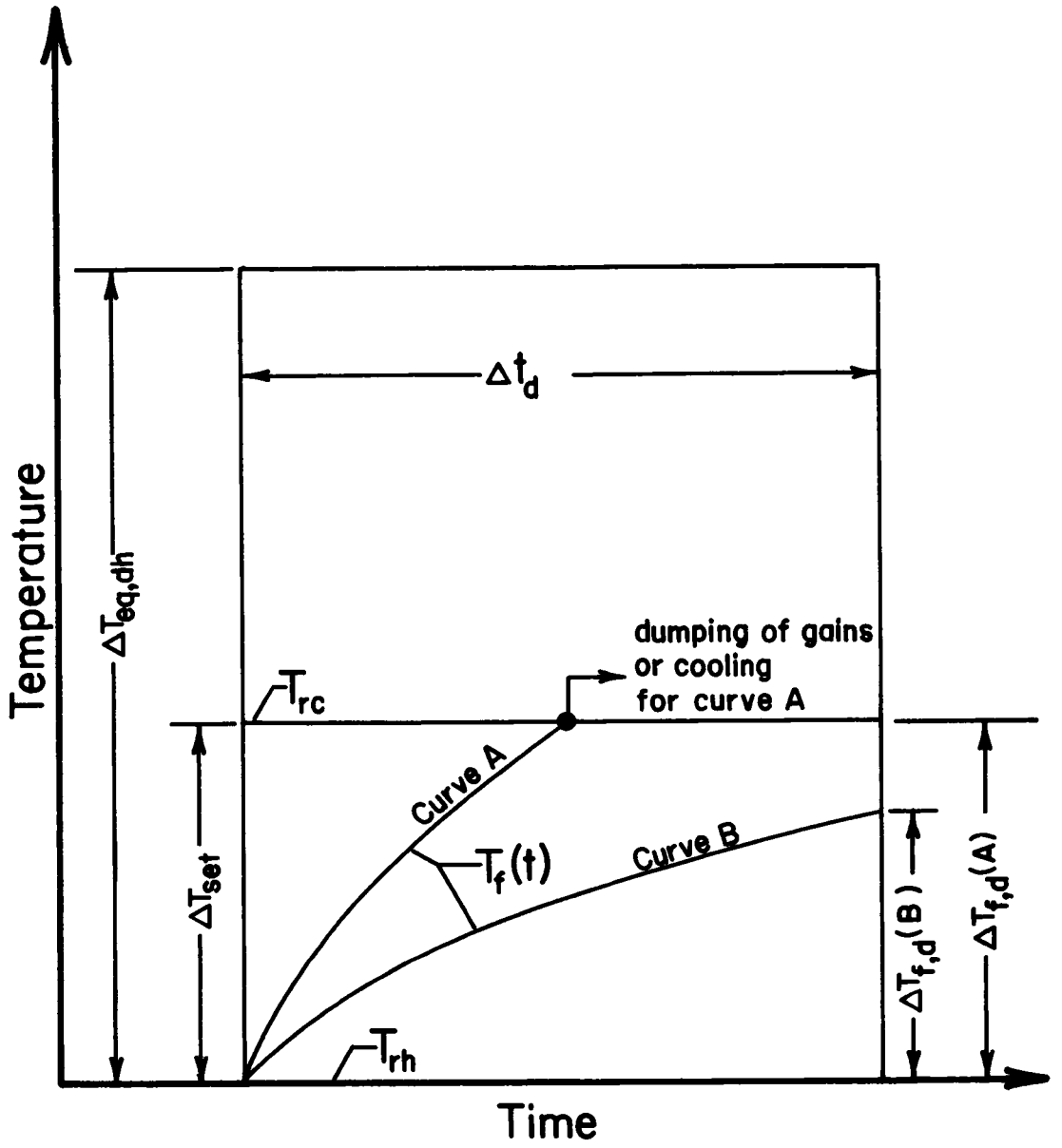

Figure 6.2 Building Temperature Response to a Constant Daytime Excess Gain Rate

interior temperature rise allowed is assumed to equal the difference between the cooling and heating setpoints; once this value is reached, the interior temperature is held at the cooling setpoint.

There are 3 solutions for the thermal energy stored by the building for a day:

1. For $\Delta T_{eq,dh} = 0$,

$$E_{stor} = 0$$

2. For $0 < \Delta T_{eq,dh} < \Delta T_{eq,dump}$,

$$E_{stor} = MC[1 - \exp(-\Delta t_d/\tau)](1/\Delta t_d) \int_{\Delta t_d} [\dot{E}_s/UA - (T_{bh,d} - T_a)]^+ dt \qquad (6\text{-}4)$$

3. For $\Delta T_{eq,dh} > \Delta T_{eq,dump}$,

$$E_{stor} = MC\Delta T_{set}$$

where $\Delta T_{eq,dump}$ is the value of $\Delta T_{eq,dh}$ which results in a value of $\Delta T_{f,d}$ equal to ΔT_{set}. $\Delta T_{eq,dump}$ is given by

$$\Delta T_{eq,dump} = \Delta T_{set}/[1 - \exp(-\Delta t_d/\tau)] \qquad (6\text{-}5)$$

The average daily energy storage for the period of a month, $\overline{E}_{stor}$, is found by integrating E_{stor} over the ranges of clearness index and ambient temperature for the month. On a diurnal basis, the

storage of excess daytime gains is only useful when there are excess losses during the following nighttime period. If the diurnal variation of ambient temperature is included, excess nighttime losses only occur when the average ambient temperature for the daytime period is less than $T_{a,nht}$, given by

$$T_{a,nht} = T_{bh,n} + \Delta T_a, \qquad (6\text{-}6)$$

where $T_{bh,n}$ is the heating balance temperature for the nighttime period and ΔT_a is the difference between the average ambient temperature for the daytime period, $\hat{T}_{a,d}$, and the average ambient temperature for the nighttime period, $\hat{T}_{a,n}$. The balance temperature for the nighttime period is found from Equation (6-2) by replacing the internal energy generation rate of the daytime period with the nighttime internal generation rate. The difference between the average temperatures for the daytime and nighttime periods can be approximated with the difference between the monthly-average daytime and nighttime temperatures, which can be found using relationships given in Chapter 3.

The ambient temperature integration is only carried out over the temperature range from $T_{a,min}$ to $T_{a,nht}$ so that only those excess gains which occur when there are nighttime losses are considered. Restricting the temperature integration in this manner neglects the ability of the building to use energy stored on one day to offset loads occurring on a later day, but it was shown above that ambient temperature changes relatively slowly, and if there is

no heating load one day, the load the next day will generally be small (if one exists).

The discontinuity introduced by the fact that $\Delta T_{f,d}$ cannot exceed ΔT_{set} requires the integration of E_{stor} to be performed in two parts.

$$\overline{E}_{stor} = (MC/UA)(1/\Delta t_d)[1-\exp(-\Delta t_d/\tau)]$$

$$\cdot\int_{T_{a,min}}^{T_{a,nht}}\int_{o}^{K_{TD}}\int_{\Delta t_d}(\dot{E}_s - UA(T_{bh,d} - T_a))^{+}dt \cdot P(K_T)dK_T P(T_a)dT_a \qquad (6\text{-}7)$$

$$+\int_{T_{a,min}}^{T_{a,nht}}\int_{K_{TD}}^{K_{Tmax}} MC\Delta T_{set}P(K_T)dK_T P(T_a)dT_a$$

K_{TD} is the clearness index value which results in a value of $\Delta T_{f,d}$ equal to ΔT_{set}. Since K_{TD} is a function of ambient temperature, it is advantageous to change the limits of integration for K_T in the above integrals to cover the entire range of K_T. The first integral can be expanded as follows

$$\int_{o}^{K_{TD}} \int_{\Delta t_d} [\dot{E}_s - UA(T_{bh,d} - T_a)]^{+} dtP(K_T)dK_T$$

$$= \int_{o}^{K_{T,max}} \int_{\Delta t_d} [\dot{E}_s - UA(T_{bh,d} - T_a)]^{+} dtP(K_T)dK_T \qquad (6\text{-}8)$$

$$- \int_{K_{TD}}^{K_{T,max}} \int_{\Delta t_d} [\dot{E}_s - UA(T_{bh,d} - T_a)]^{+} dtP(K_T)dK_T$$

The second integral on the right hand side of Equation (6-8) can be expanded, yielding

$$\int_{K_{TD}}^{K_{T,max}} \int_{\Delta t_d} [\dot{E}_s - UA(T_{bh,d} - T_a)]^{+} dtP(K_T)dK_T$$

$$= \int_{K_{TD}}^{K_{T,max}} \int_{\Delta t_d} (UA\Delta T_{set})/[1 - \exp(-\Delta t_d/\tau)]dtP(K_T)dK_T \qquad (6\text{-}9)$$

$$+ \int_{K_{TD}}^{K_{T,max}} \int_{\Delta t_d} [\dot{E}_s - (UA(T_{bh,d} - T_a) + \frac{UA\Delta T_{set}}{[1-\exp(-\Delta t_d/\tau)]})]^{+}$$

$$dtP(K_T)dK_T$$

The lower limit for K_T in the second integral on the RHS of Equation (6-9) can be changed to 0, since the integrand is equal to 0 for K_T less than K_{TD} (due to the "+" sign and the definition of K_{TD}).

Equation (6-9) is substituted into Equation (6-8), and Equation (6-8) is substituted into Equation (6-7). After some simplification, the result is

$$\bar{E}_{stor} = (\tau/\Delta t_d)(1 - \exp(\Delta t_d/\tau))$$

$$\cdot \int_{T_{a,min}}^{T_{a,nht}} \int_{o}^{K_{T,max}} \int_{\Delta t_d} [\dot{E}_s - UA(T_{bh,d} - T_a)]^+ dt$$

$$\cdot P(K_T) dK_T P(T_a) dT_a \qquad (6\text{-}10)$$

$$- \int_{T_{a,min}}^{T_{a,nht}} \int_{o}^{K_{T,max}} \int_{\Delta t_d} [\dot{E}_s - UA((T_{bh,d} - T_a) + \Delta T_{set}/(1 - \exp(-\Delta t_d/\tau)))]^+$$

$$\cdot dt P(K_T) dK_T P(T_a) dT_a$$

The solar gains for a building are discussed in Chapter 4, where the concept of an effective surface was introduced to allow the use of utilizability relationships in the estimation of sol-air degree-days. If the solar gains in Equation (6-10) are normalized using Z or Z', as defined in Equations (4-24) and (4-31), the integrals in Equation (6-10) represent daily utilizability [Klein

(1978)]. Daily utilizability, like hourly utilizability, is the fraction of the radiation incident on a surface which occurs at intensities in excess of the critical level. Daily utilizability, or $\overline{\phi}$, however, is for all daylight hours combined instead of a particular hour of the day.

Equation (6-10) can then be written as

$$\overline{E}_{stor} = (\tau/\Delta t_d)(1 - \exp(-\Delta t_d/\tau))(UA)Z\overline{H}_{To} \int_{T_{a,min}}^{T_{a,nht}} [\overline{\phi}(I_{cg}) - \overline{\phi}(I_{cd})]P(T_a)dT_a \qquad (6\text{-}11)$$

where

$$I_{cg} = (T_{bh,d} - T_a)/Z \qquad (6\text{-}12)$$

$$I_{cd} = I_{cg} + \Delta T_{set}/[(1 - \exp(-\Delta t_d/\tau))Z] \qquad (6\text{-}13)$$

and where $\overline{H}_{To}$ is found from Equation (4-27) by replacing $\overline{I}_T$ for each surface with $\overline{H}_T$.

The remaining integration in Equation (6-11) cannot be evaluated analytically using the functions available for $\overline{\phi}$ and $P(T_a)$. The same problem was encountered in Chapter 4, where it was assumed that the ambient temperature is always equal to the monthly-average temperature for the purpose of evaluating the integral over ambient temperature. The ambient temperature is again assumed to be con-

stant for the purpose of evaluating the integral of the utilizability function, but instead of using the monthly-average ambient temperature, the average ambient temperature for temperatures less than $T_{a,nht}$ (denoted by $\overline{T}_{a,<nht}$) is used.

Since the integration is only over a portion of the ambient temperature range, the expression for the total energy storage for a month must account for the fact that not all days in the month can be used. This is accomplished by multiplying the expression obtained for $\overline{E}_{stor}$ by the fraction of the time the ambient temperature is less than $T_{a,nht}$. The final expression is:

$$\overline{E}_{stor} = Q(T_{a,nht})(UA)(\tau/\Delta t_d)(1 - \exp(-\Delta t_d/\tau)) \qquad (6\text{-}14)$$
$$Z\overline{H}_{To}(\overline{\phi}(\overline{I}_{cg}) - \overline{\phi}(\overline{I}_{cd}))$$

where $\overline{I}_{cg}$ and $\overline{I}_{cd}$ are found by replacing T_a in Equation (6-12) with $\overline{T}_{a,<nht}$. If a no-storage air collector is used, Z' replaces Z, $\overline{I}_{cg}$ is changed to $\overline{I}'_{cg}$ in the same manner as $\overline{I}_{co}$ was changed to $\overline{I}'_{co}$ in Chapter 4 (but $\overline{T}_{a,<nht}$ is used instead of $\overline{T}_{a,h}$), $\overline{I}'_{cd}$ is calculated by replacing $\overline{I}_{cg}$ in Equation (6-13) with $\overline{I}'_{cg}$, and $\overline{H}_{To}$ is calculated from Equation (4-31) by replacing $\overline{I}_T$ with $\overline{H}_T$. The total useful energy storage for a month is the product of $\overline{E}_{stor}$ and the number of days in the month.

The energy stored in the structure is usually released during the nighttime period. In the development presented above, it is assumed that the house cools down to the heating setpoint before the start of the next daytime period. This implies that all of the

energy stored during a daytime period is used to offset heating requirements which occur during the following nighttime period. If the interior temperature is still greater than the heating setpoint at the end of the nighttime period, some of the excess gains stored during one daytime period will be carried into the next daytime period.

When there is energy carryover from one daytime period to the next daytime period, the temperature response of the building for the second daytime period is different from what it would have been without the carryover of energy. There are 3 possible situations which can occur for this second daytime period. In the first situation, there are no excess gains on the second daytime period, and the house will continue to cool down over the second daytime period. The carryover energy is used to offset part of the load for the second day in this situation. In the second situation, the excess gains are small enough so that the interior temperature will not reach the cooling setpoint during the second daytime period, and the carryover energy can be used to help offset the heating load for the evening following the second daytime period. In the third situation, however, the excess gains for the second daytime period are such that the interior temperature would have reached the cooling setpoint even if it had started out at the heating setpoint. The stored energy at the end of the second daytime period is not increased by the presence of carryover energy at the start of the day. The carryover energy is not useful in this last situation, but at the same time,

there is no heating load. Although the relationship for $\overline{E}_{stor}$ given above overestimates the amount of energy stored by the building when carryover energy is not usable, the heating load for weather conditions where there is significant amounts of carryover energy which cannot be utilized is generally quite small (or nonexistent), and the effect of this error on the estimated heating load is minimized.

6.3.2 Additional Nighttime Losses

The fact that the house warms up in the process of storing excess gains during the daytime period leads to greater heat losses during the following nighttime period than would result if there was no storage of gains. Two possible nighttime cooldown profiles are shown qualitatively in Figure 6.3. Both profiles have an average nighttime interior temperature which is greater than the heating setpoint. The difference between the average nighttime interior temperature, $\hat{T}_{f,n}$, and the heating setpoint is dependent on the temperature rise for the preceeding daytime period, the time constant of the house, and the difference between the nighttime balance temperature and the ambient temperature, $\Delta T_{eq,nh}$. The increased losses for a night due to the daytime warmup are given by

$$E_{loss} = UA(\hat{T}_{f,n} - T_{rh})\Delta t_n \qquad (6\text{-}15)$$

where Δt_n is the length of the nighttime period.

The average interior temperature for the nighttime period can be found by integrating the equations describing the interior temp-

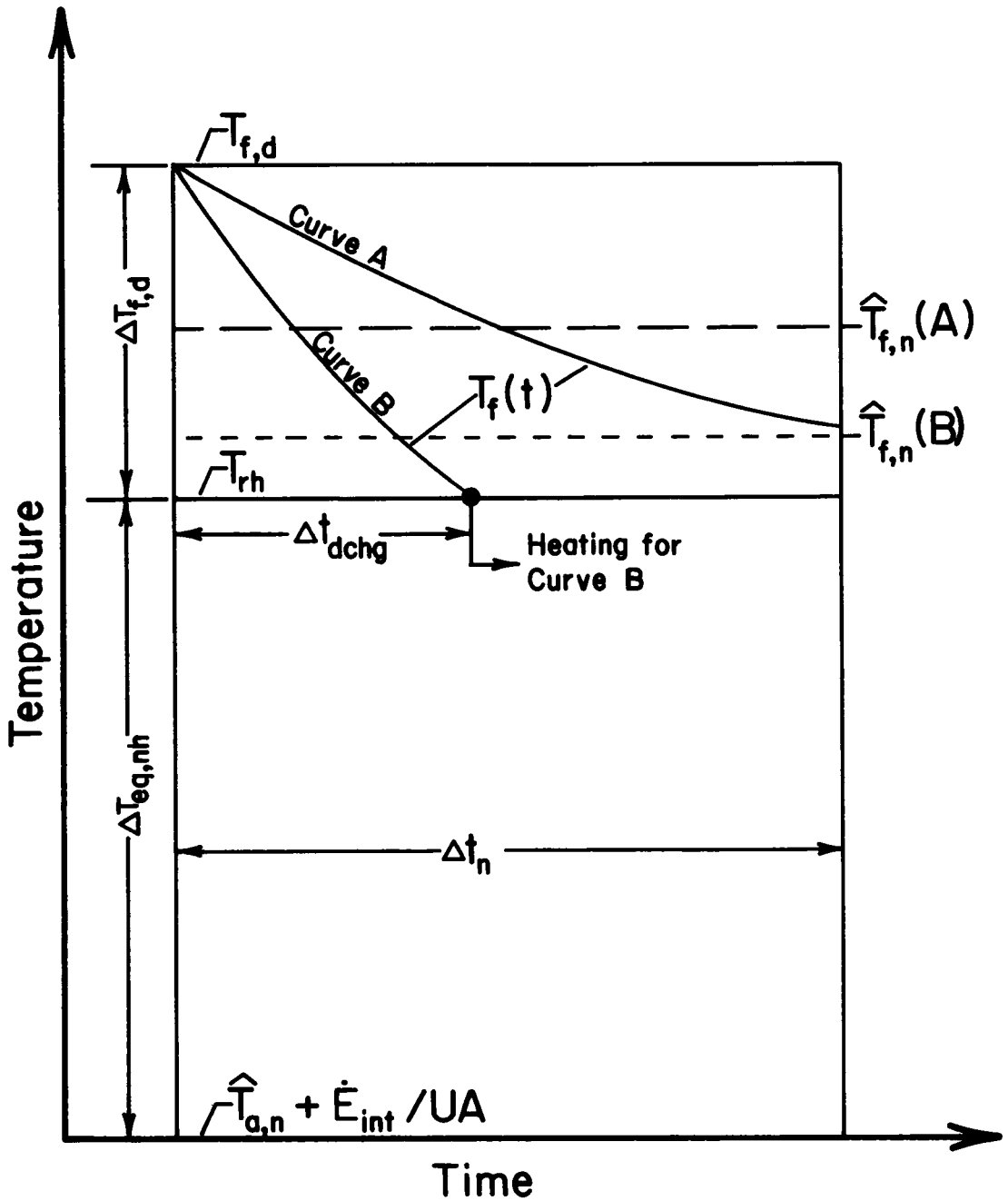

Figure 6.3 Nighttime Building Cool-Down Following Storage of Excess Gains

erature as a function of time. The two different profile shapes shown in Figure 6.3 lead to two different relationships for $\hat{T}_{f,n}$. If the time required for the building to reach the heating setpoint, Δt_{dchg}, is less than Δt_n,

$$\hat{T}_{f,n} - T_{rh} = (\Delta T_{eq,nh}/\Delta t_n)(\tau X - \Delta t_{dchg}) \tag{6-16}$$

where

$$X = \Delta T_{f,d}/\Delta T_{eq,nh} \tag{6-17}$$

If the building temperature is still above the heating setpoint at the end of the night, Δt_{dchg} is larger than Δt_n, and

$$\hat{T}_{f,n} - T_r = (\Delta T_{eq,nh}/\Delta t_n)[\tau(1 + X)(1 - \exp(-\Delta t_n/\tau)) - \Delta t_n] \tag{6-18}$$

The time required for the interior temperature to reach the heating setpoint is given by

$$\Delta t_{dchg} = \tau \ln(1 + X) \tag{6-19}$$

The additional nighttime losses for a month are a function of the distributions of solar radiation and ambient temperature during the day and the distribution of ambient temperature during the night. The additional nighttime losses for the month are based on $\overline{T}_{f,n}$, the monthly-average value of the nighttime interior temperature for

those days of the month when there are excess losses for the nighttime period. The integration of the expressions given above for the average nighttime interior temperature over the ranges of solar radiation and ambient temperature is complicated by the form of Equations (6-16) and (6-18) and by the discontinuities which result when $\Delta T_{f,d}$ reaches ΔT_{set} and when Δt_{dchg} reaches Δt_{n}. It is not possible to analytically evaluate the resulting integrals using the available distribution functions for ambient temperature or clearness index or to rearrange the integrals so that they represent an accumulated difference statistic for which there are models, as was done for the daytime period. The effect of variations in ambient temperature and solar radiation for a month on the additional nighttime losses cannot be fully represented.

The monthly-average interior temperature for the nighttime period is approximated with a single nighttime interior temperature profile which is representative of the days in a month when there are excess nighttime losses. The use of a single, average nighttime period to estimate the additional nighttime losses requires the average value for $\Delta T_{f,d}$. The average daytime temperature rise is found from the average excess gains stored by the building,

$$\overline{\Delta T}_{f,d} = \overline{E}_{stor} / [(MC) \cdot Q(T_{a,nht})] \qquad (6\text{-}20)$$

where $\overline{E}_{stor}$ is estimated using Equation (6-14). The temperature rise calculated with Equation (6-20) is the average value for those days when there are excess nighttime losses, which is consistent

with the relationship for $\overline{E}_{stor}$. The average value of $\Delta T_{eq,nh}$ is given by

$$\overline{\Delta T}_{eq,nh} = T_{bh,n} - \overline{T}_{a,<bh,n} \qquad (6\text{-}21)$$

where $\overline{T}_{a,<bh,n}$ is the monthly-average ambient temperature for the nighttime period for ambient temperatures below $T_{bh,n}$.

The average values for $\Delta T_{f,d}$ and $\Delta T_{eq,nh}$ are used in Equation (6-16) or (6-18) to calculate the average value of $\hat{T}_{f,n} - T_{rh}$. The additional nighttime losses for the average day of the month (for those days with heating loads) are then given by

$$\overline{E}_{loss} = Q(T_{a,nht})\Delta t_n UA(\overline{T}_{f,n} - T_{rh}) \qquad (6\text{-}22)$$

Equation (6-22) does not include increased losses due to the carry-over of energy from one day to the next.

The product of the difference between $\overline{E}_{stor}$ and $\overline{E}_{loss}$ and the number of days in the month provides an estimate of the reduction in the heating requirements for a finite capacitance building when compared to a zero capacitance building. The heating load for a zero capacitance building, which is given by the sol-air heating degree-days as described in Chapter 4, is corrected by subtracting $N(\overline{E}_{stor} - \overline{E}_{loss})$ to give the heating load for a finite capacitance building.

6.4 Cooling Load Correction Factor

6.4.1 Excess Nighttime Losses

Although the physical processes by which the building cools down at night are no different when cooling loads are considered than when heating loads are considered, the effect of nighttime losses on the cooling load differs from the effect of nighttime losses on the heating load. In the preceeding section, excess gains are only considered useful if there are excess losses during the nighttime period. Similarly, nighttime losses are only useful during the cooling season when there are excess gains during the next daytime period.

The nighttime temperature response of a building is shown in Figure 6.4, where the two curves represent two possible profiles for $T_{f,n}$. It is assumed that the interior temperature is initially at the cooling setpoint, indicating there was a cooling load for the preceeding daytime period, and it is assumed a cooling load also will occur during the next daytime period. The ambient temperature and the internal generation rate are assumed constant during the nighttime period, which results in a constant value of $\Delta T_{eq,nc}$. $\Delta T_{eq,nc}$ is the difference between $T_{bc,n}$ and $\hat{T}_{a,n}$ for the nighttime period; the change in the definition for the nighttime equilibrium temperature difference from the previous section is due to the different thermostat settings for heating and cooling. The change in the interior temperature over the nighttime period, $\Delta T_{f,n}$, is given by

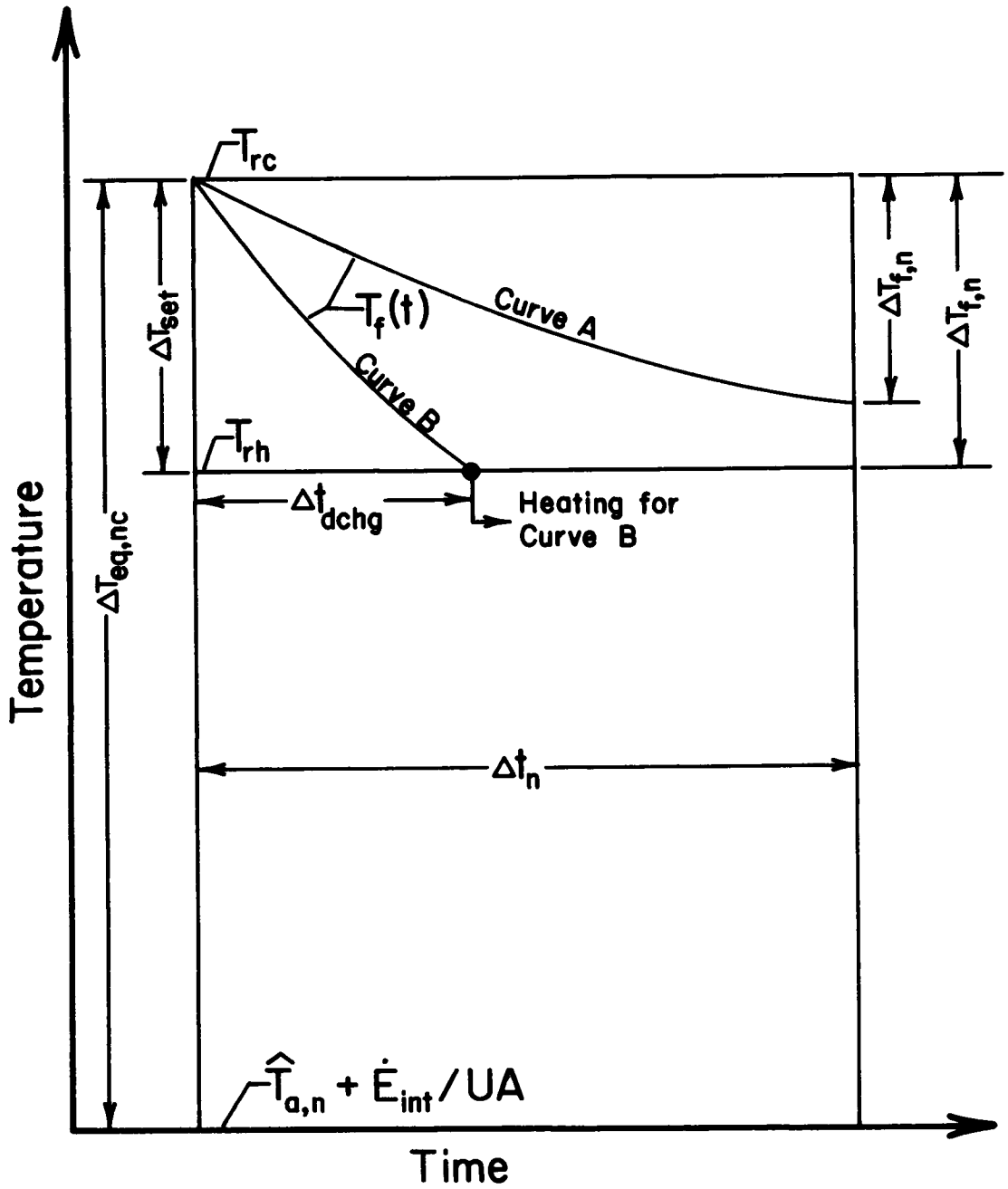

Figure 6.4 Nighttime Building Cool-Down Following Daytime Cooling Load

$$\Delta T_{f,n} = \text{MIN} \begin{cases} \Delta T_{eq,nc}[1 - \exp(-\Delta t_n/\tau)] \\ \\ \Delta T_{set} \end{cases} \qquad (6\text{-}23)$$

The energy loss by the building during the night is equal to the product of MC and $\Delta T_{f,n}$. This change in internal energy represents a cooling source for the daytime period. The effect of internal capacitance on the cooling load is found by integrating the product of MC and $\Delta T_{f,n}$ over the portion of the month for which there are excess daytime gains. Excess daytime gains occur if the following condition is satisfied:

$$\dot{E}_s/(UA) - (T_{bc,d} - \hat{T}_{a,d}) > 0 \qquad (6\text{-}24)$$

where the subscript d indicates the temperatures are averages for the daytime period. If average conditions over the daytime and nighttime periods are used and the difference between the average daytime and nighttime ambient temperatures is included, Equation (6-24) can be rearranged to yield the equivalent condition

$$\hat{T}_{a,n} > T_{bc,d} - (1/\Delta t_d)\int_{\Delta t_d} (\dot{E}_s/(UA))dt - \Delta\overline{T}_a \qquad (6\text{-}25)$$

where $\Delta\overline{T}_a$ is the difference between the average ambient temperature for the daytime and nighttime periods.

If the minimum value of $\hat{T}_{a,n}$ which still results in excess daytime gains (i.e., just satisfies Equation (6-24)) is denoted as T_{ac},

the integration of $\Delta T_{f,n}$ over the fraction of the month when there is both daytime excess gains and excess nighttime losses is given by

$$\overline{\Delta T}_{f,n} = (1 - \exp(-\Delta t_n/\tau)) \int_0^{K_{T,max}} \left[\int_{T_{a,ht}}^{T_{bc,n}} (T_{bc,n} - T_a) \cdot P(T_a) dT_a - \int_{T_{ac}}^{T_{a,ht}} \Delta T_{set} P(T_a) dT_a \right] P(K_T) dK_T \quad (6\text{-}26)$$

The second integral is only required when T_{ac} is less than $T_{a,ht}$, the ambient temperature value where the interior temperature just reaches the heating setpoint at the end of the night.

$$T_{a,ht} = T_{bc,n} - \Delta T_{set}/(1 - \exp(-\Delta t_n/\tau)) \quad (6\text{-}27)$$

If T_{ac} is greater than or equal to $T_{a,ht}$, the lower limit in the first integral of Equation (6-26) is T_{ac} and the second integral is eliminated.

Not only is one of the limits of integration for ambient temperature in Equation (6-26) a function of the value of K_T, but whether there are one or two integrals over ambient temperature is also dependent on the value of K_T.

The ambient temperature integrals can be expressed in terms of heating degree-day functions. For example,

$$\int_{T_{ac}}^{T_{bc,n}} (T_{bc,n} - T_a)P(T_a)dT_a$$

$$= \int_{T_{a,min}}^{T_{bc,n}} (T_{bc,n} - T_a)P(T_a)dT_a$$

$$- \int_{T_{a,min}}^{T_{ac}} (T_{ac} - T_a)P(T_a)dT_a \qquad (6\text{-}28)$$

$$- \int_{T_{a,min}}^{T_{ac}} (T_{bc,n} - T_{ac})P(T_a)dT_a$$

which when evaluated yields

$$\int_{T_{ac}}^{T_{bc,n}} (T_{bc,n} - T_a)P(T_a)dT_a \qquad (6\text{-}29)$$

$$= D_H(T_{bc,n})/N - D_H(T_{ac})/N$$

$$- Q(T_{ac})[(1/\Delta t_d)\int_{\Delta t_d} (\dot{E}_s/(UA))dt - \Delta\overline{T}_a]$$

The other ambient temperature integrals are evaluated in a similar manner, and after some simplification, the solution for $\overline{\Delta T}_{f,n}$ becomes

If $T_{ac}\ (K_{T,max}) > T_{a,ht}$,

$$\overline{\Delta T}_{f,n} = (1 - \exp(-\Delta t_n/\tau)) \int_{o}^{K_{T,max}} [D_H(T_{bc,n})/N - D_H(T_{ac})/N - Q(T_{ac})[(1/\Delta t_d) \int_{\Delta t_d} (\dot{E}_s/(UA))dt - \overline{\Delta T}_a]]P(K_T)dK_T \tag{6-30}$$

and if $T_{ac}(K_{T,max}) < T_{a,ht}$,

$$\overline{\Delta T}_{f,n} = (1 - \exp(-\Delta t_n/\tau)) \int_{o}^{K_{TDH}} [D_H(T_{bc,n})/N - D_H(T_{ac})/N - Q(T_{ac})[(1/\Delta t_d) \int_{\Delta t_d} (\dot{E}_s/(UA))dt - \overline{\Delta T}_a]]P(K_T)dK_T + \int_{K_{TDH}}^{K_{T,max}} [D_H(T_{bc,n})/N - D_H(T_{a,ht})/N - Q(T_{ac})(T_{bc,n} - T_{a,ht})]P(K_T)dK_T \tag{6-31}$$

where $T_{ac}(K_{T,max})$ is T_{ac} for a value of K_T equal to $K_{T,max}$ and K_{TDH} is the value of K_T when T_{ac} is equal to $T_{a,ht}$.

The integrations over K_T in the equations presented above cannot be solved analytically using the models available for D_H and $P(K_T)$. Once again, it is necessary to replace the integrals with functions evaluated at an appropriate average value of the independent variable. Since all values of K_T represent a gain, $\overline{\Delta T}_{f,n}$ is found by evaluating either the integrand in Equation (6-30) or the integrand in the second integral of Equation (6-31) with $\overline{K}_T$. The relationships obtained in this manner are:

If $T_{ac}(\overline{K}_T) > T_{a,ht}$,

$$\overline{\Delta T}_{f,n} = (1 - \exp(-\Delta t_n/\tau))[D_H(T_{bc,n})/N - D_H(T_{ac})/N - Q(T_{bc,n})\overline{ZH}_{To}] \quad (6\text{-}32)$$

If $T_{ac}(\overline{K}_T) < T_{a,ht}$,

$$\overline{\Delta T}_{f,n} = (1 - \exp(-\Delta t_n/\tau))[D_H(T_{bc,n})/N - D_H(T_{a,ht})/N - Q(T_{bc,n})(T_{bc,n} - T_{a,ht})] \quad (6\text{-}33)$$

where

$$T_{ac}(\overline{K}_T) = T_{bc,n} - \overline{ZH}_{To} - \overline{\Delta T}_a \quad (6\text{-}34)$$

The average daily useful nighttime energy loss for the month which

is stored by the building, $\overline{E}_{cool}$, is given by the product of MC and $\overline{\Delta T}_{f,n}$. The expressions given in Equations (6-32) and (6-33) include the effects of variations of ambient temperature, but the variation of solar radiation is not accounted for.

6.4.2 Additional Daytime Gains

The interior temperature at the end of the nighttime period is between the heating and cooling setpoints when there are nighttime excess losses. During the time it takes the interior temperature to reach the cooling setpoint in the daytime period following a nighttime period in which there was a cooldown of the building, the rate of excess gains for the building is higher than it would have been if the interior temperature always remained at the cooling setpoint. The increase in the excess daytime gains which results from the lower average interior temperature must be subtracted from the energy loss stored by the building during the nighttime to find the net change in the building cooling load (when compared to a zero capacitance building) which is caused by building capacitance.

Figure 6.5 shows two representative interior temperature profiles for the daytime warmup of the building during the cooling season. The profiles for the storage of excess gains during the heating season, which were shown in Figure 6.2, are qualitatively similar to those shown in Figure 6.5, but $\Delta T_{eq,dc}$, the difference between the cooling setpoint and the daytime equilibrium temperature for the building, is not the same as $\Delta T_{eq,dh}$. There may be

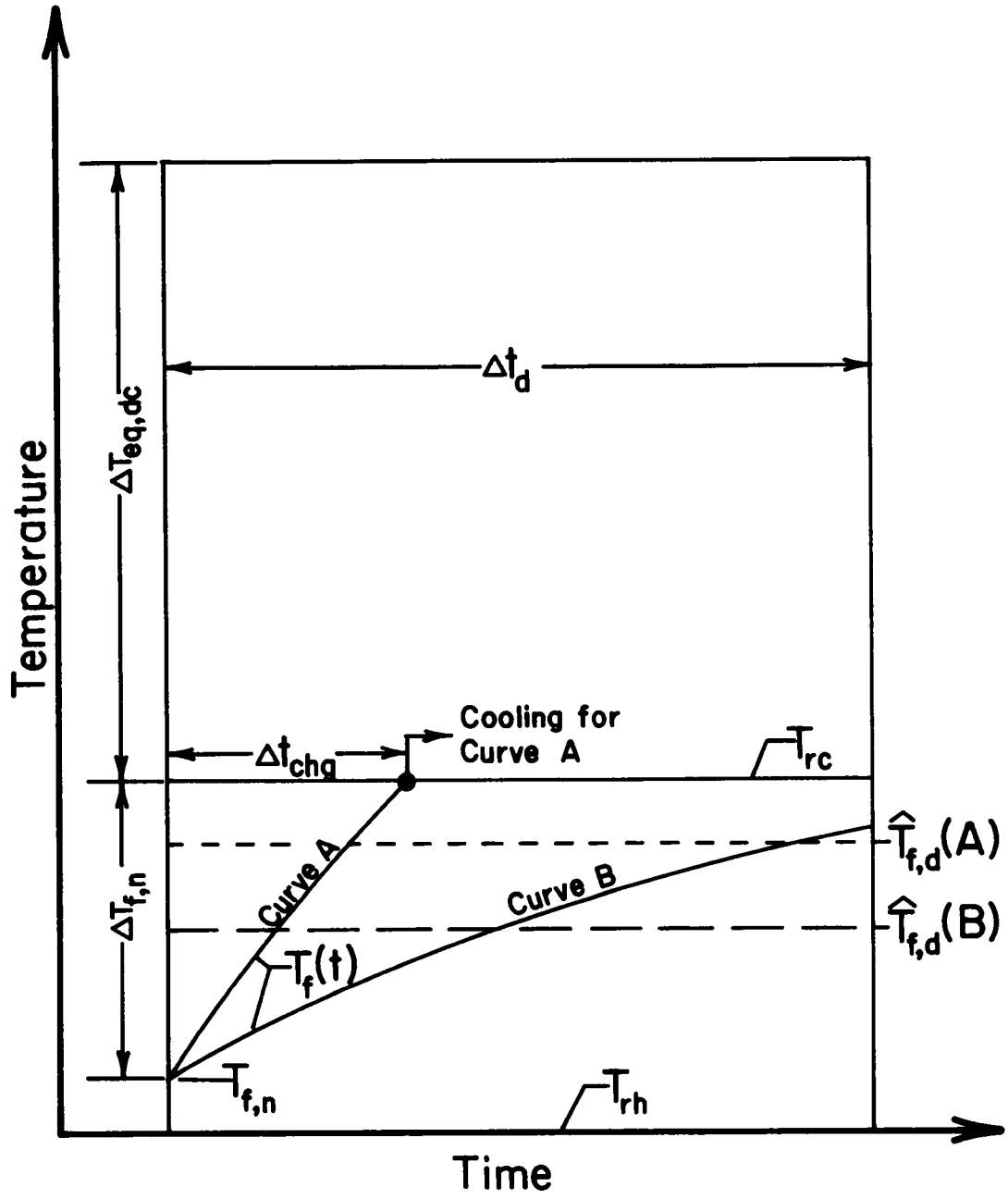

Figure 6.5 Daytime Warm-Up of Building Following Nighttime Cool-Down

days when there are excess gains for the heating setpoint ($\Delta T_{eq,dh}$ is greater than zero), but there are no excess gains for the cooling setpoint ($\Delta T_{eq,dc}$ is equal to or less than zero).

The increase in daytime excess gains which results from nighttime cooldown is equal to the product of UA and the difference between the cooling setpoint and the average daytime interior temperature. The interior temperature profile for a single day is used to estimate the monthly-average interior temperature for the daytime period for days when there are both excess daytime gains and excess nighttime losses. The monthly-average warm up time period, $\overline{\Delta t}_{chg}$, is calculated from

$$\overline{\Delta t}_{chg} = \tau \ln(1 + \overline{X}_c) \tag{6-35}$$

where

$$\overline{X}_c = \overline{\Delta T}_{f,n} / \overline{\Delta T}_{eq,dc} \tag{6-36}$$

The value for $\overline{\Delta T}_{f,n}$ is calculated from Equation (6-32) or Equation (6-33). The average value for $\overline{\Delta T}_{eq,dc}$ is based on an integration over all values of K_T and the average value of T_a for the range of temperature over which there are excess daytime gains and excess nighttime losses.

$$\overline{\Delta T}_{eq,dc} = (1/\Delta t_d) Z \overline{H}_{To} \overline{\phi} (\overline{I}_{cgc}) \tag{6-37}$$

where

$$\overline{I}_{cgc} = (T_{bc,d} - \overline{T}_{a,Tbc-Tac})/Z \qquad (6\text{-}38)$$

and where $\overline{T}_{a,Tbc-Tac}$ is the average value for daytime ambient temperatures between $T_{bc,d}$ and $T_{ac} + \Delta\overline{T}_a$.

If the value of $\overline{\Delta t}_{chg}$ is less than or equal to the daytime length,

$$T_{rc} - \overline{T}_{f,d} = (\overline{\Delta T}_{eq,dc}/\Delta t_d)(\tau\overline{X}_c - \overline{\Delta t}_{chg}) \qquad (6\text{-}39)$$

If the value of $\overline{\Delta t}_{chg}$ is greater than the daytime length,

$$T_{rc} - \overline{T}_{f,d} \qquad (6\text{-}40)$$

$$= (\overline{\Delta T}_{eq,dc}/\Delta t_d)(\tau(1 + \overline{X}_c)(1 - \exp(-\Delta t_d/\tau))$$

The average daily increase in the daytime excess gains which results from nighttime cooldown is given by

$$\overline{E}_{gain} = (Q(T_{bc,d}) - Q(T_{ac} + \Delta\overline{T}_a)) \cdot (UA)(T_{rc} - \overline{T}_{f,n})\Delta t_d \qquad (6\text{-}41)$$

where $(Q(T_{bc,d}) - Q(T_{ac} + \Delta\overline{T}_a))$ represents the fraction of the month when there are both daytime excess gains and nighttime excess losses.

The cooling load for a finite capacitance building can be estimated by subtracting $N(\overline{E}_{cool} - \overline{E}_{gain})$ from the zero capacitance cooling load. The zero capacitance load is estimated from sol-air cooling degree-days as described and modeled in Chapter 4.

6.5 Summary

Approximate relationships were developed which allow the heating and cooling loads for a finite capacitance building to be estimated from the loads for a zero capacitance building. These capacitance correction relationships are a function of the building UA, the lumped "effective" capacitance of the building, the allowable internal temperature swing, and weather statistics describing the distributions of solar radiation and ambient temperature. The corrections were derived by assuming the effect of capacitance on heating and cooling loads is primarily due to diurnal variations in the building load and that the excess gains and losses that occur can be treated as constant over the period of the day during which they occur.

It was not possible to fully account for the distributions of both solar radiation and ambient temperature in the final forms of the correction relationships. However, it was possible to incorporate the solar radiation distribution in the correction for heating loads and the ambient temperature distribution in the correction for cooling loads. In addition, the distribution functions for ambient temperature and solar radiation were used to determine representative average values for ambient temperature and solar radiation when it was necessary to replace the distribution of either variable with an average value. The correction procedures developed in previous analytic solutions do not account for any of the variations in ambient temperature or solar radiation, and they fail to

account for the fact that there may be useful excess gains (for the heating season) or losses (for the cooling season) during a month even though there are none for the average day of the month. The procedures developed in this chapter overcome this problem to a large extent. The accuracy of the correction procedures developed in this chapter is tested in Chapter 7 by comparing building loads estimated with the sol-air degree-day methods of Chapter 4 and the correction procedures against loads obtained with the hourly simulation program TRNSYS.

CHAPTER 7

7. EXAMPLES OF THE USE OF WEATHER STATISTICS FOR LOAD ESTIMATION

7.1 Ambient Temperature Bin Data

7.1.1 Heat Pump Performance Calculations

The use of the ambient temperature cumulative distribution function for the estimation of ambient temperature bin data is discussed in Chapters 2 and 3, and estimated and measured bin data are compared for a number of locations in Chapter 3. While the comparison of measured and estimated bin data indicates the accuracy of the estimation procedure for each bin, it is difficult to foresee what effect these errors have on the accuracy of loads and HVAC equipment performance calculated using bin data. The performance of an air-to-air heat pump represents a common application for ambient temperature bin data. Since the coefficient of performance and the capacity of the heat pump are functions of ambient temperature, degree-days cannot be used to determine equipment performance. A comparison of the seasonal heat pump performance calculated using measured bin data with the heat pump performance calculated using estimated bin data provides an indication of the usefulness of the bin data estimation procedure for building load calculations involving ambient temperature bin data.

The steady-state performance of a heat pump is a function of the condenser and evaporator temperatures. When the heating load required by the building is less than the capacity of the machine, it is necessary to cycle the heat pump on and off to match the average heat output of the heat pump to the building load. Cycling reduces the performance of the heat pump, and so the capacity and COP are also dependent on the ratio of the building load to the capacity of the machine when it is used to condition a building. In the comparisons which follow, it was assumed that the dependence of COP and capacity on the cycling rate could be neglected. The effect of cyclic operation on the seasonal performance of the equipment can be considered using the "degradation coefficient" method described in the Federal Register (1979). The effect of this assumption is the same for calculations based on measured and estimated bin data.

The condenser temperature is relatively constant for the heating mode of a heat pump, as it represents the delivery temperature for the air used to heat the building. Since the evaporator temperature is primarily a function of the ambient temperature, the capacity and COP of the heat pump can be represented as simple functions of ambient temperature. Tabular data for a Carrier Weathermaster 2 ton multiple package heat pump were fit with the following linear equations:

For $-24 < T_a < -4°C$,

$$\dot{E}_{del} = 16.13 + 0.490T_a$$

$$\dot{E}_{w} = 1.92 + 0.0077T_a \qquad (7\text{-}1)$$

For $T_a > -4°C$,

$$\dot{E}_{del} = 17.60 + 0.830T_a$$

$$\dot{E}_{w} = 1.38 + 0.0283T_a$$

where $\dot{E}_{del}$ is the capacity of the heat pump in KJ/hr and $\dot{E}_{w}$ is the electrical consumption in Kw. When the ambient temperature is below -24°C, the heat pump is not run.

The building load was modeled using the UA-degree hour approach. The effect of thermal capacitance was neglected to further simplify the analysis and to more clearly show the comparison between heat pump performance calculated with bin data compiled from measured hourly data and heat pump performance calculated with estimated bin data. A constant heating base temperature of 15.6°C (60°F) was used with house UA values of 160, 240, 320, 400, 475, 550, 630, 740, 850 and 950 W/°C.

The energy delivery and electrical demand for each bin, given by the product of the number of hours in the bin, the fraction of each hour in the bin the heat pump must run to meet the load, and the rate for $\dot{E}_{del}$ or $\dot{E}_{w}$ were calculated using both measured and estimated bin data. The fraction of each hour in a bin that the

heat pump must run is equal to the ratio of the building load to the heat pump capacity for the midpoint value of ambient temperature for the bin (assuming steady-state behavior). When the heat pump capacity is less than the house load, the heat pump runs 100% of the time and auxiliary heaters supply the deficit. The results for each bin in the heating season are then summed to yield the seasonal performance.

7.1.2 Performance Predictions for Measured and Estimated Bin Data

One measure of the heat pump performance is the fraction of the house heating load which is met with energy extracted from the ambient air, referred to as the fraction by nonpurchased energy (FNP). A second measure of performance is the fraction of the load which is met by the electrical energy used to run the heat pump, referred to as the fraction by work (FBW). The COP can be found by adding one to the ratio of the FNP to the FBW. Annual values of FNP and FBW were obtained by summing the monthly energy quantities over all months.

The annual fractions by nonpurchased energy and fractions by work calculated with bin data compiled from the long-term hourly SOLMET data are compared to those calculated with estimated bin data in Figure 7.1 for the 6 SOLMET locations with the largest heating load. The bin size used was 5°F, and the estimated bin data are based on values of σ_m estimated from Equation (3-12). The scatter for the FNP comparisons is larger than for the FBW comparisons. The

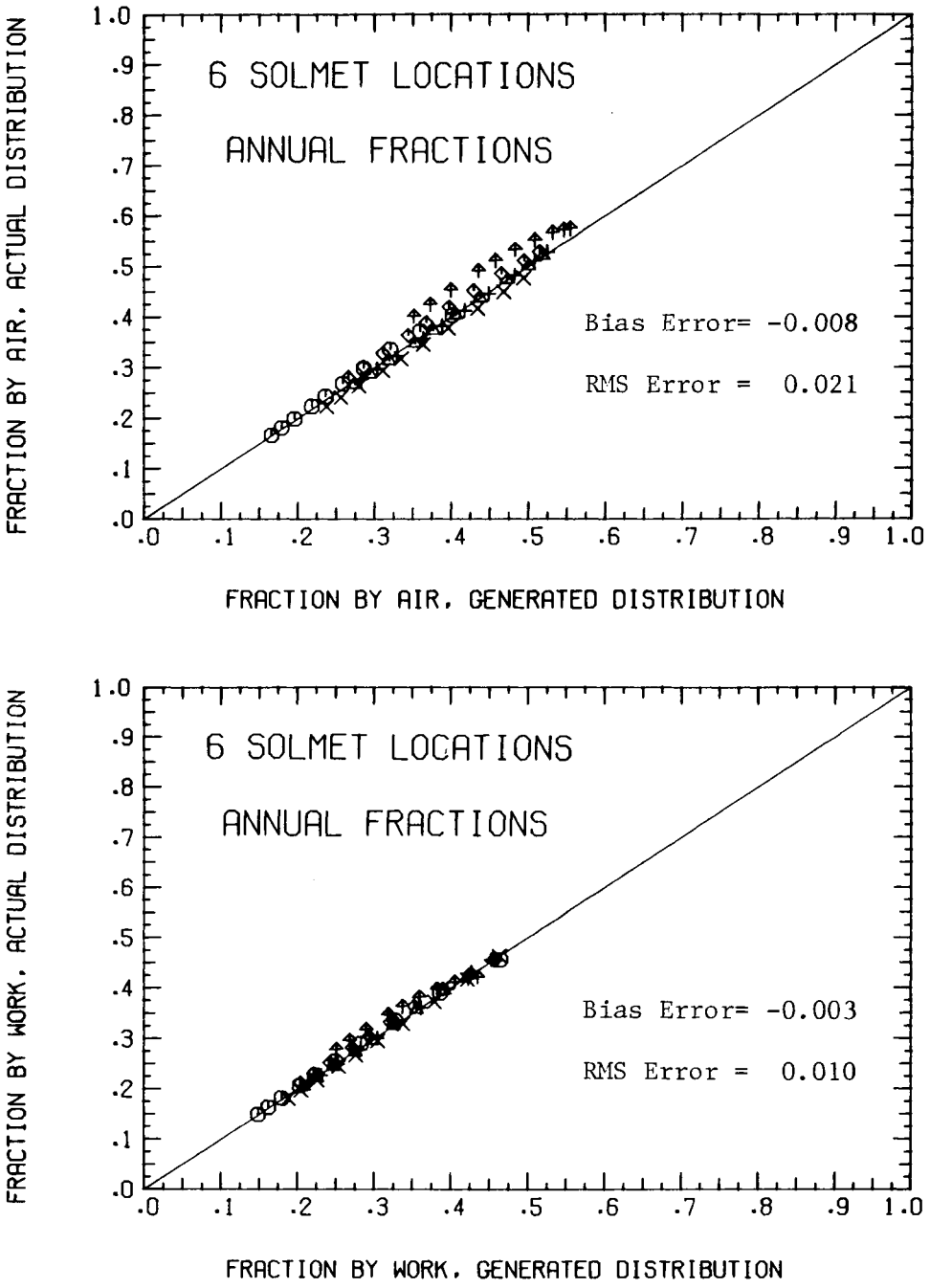

Figure 7.1 Performance of an Air-to-Air Heat Pump with Measured and Estimated Ambient Temperature Bin Data for 6 SOLMET Locations

largest errors occur in Seattle, where the estimated bin data result in an underprediction of the heat pump performance. The agreement between the values of FNP for the measured data and the values of FNP for the estimated data is within five percentage points for all locations.

Ambient temperature bin data were also estimated for 12 locations contained in the Air Force Manual 88-29 bin data set. The locations are: Denver, CO, Glascow, MT, Reno, NV, Albany, NY, Harrisburg, PA, Knoxville, TN, Dayton, OH, Grand Island, NB, Greensboro, NC, Sacramento, CA, Lewiston, ID and Bismark, ND. The values of FNP and the fractions by work for the estimated and measured bin data are compared for these locations in Figure 7.2. The scatter for the fraction by nonpurchased energy is again larger than the scatter for the fraction by work, and the values of FNP for the estimated bin data are within five percentage points of those for the measured bin data.

7.2 Sol-Air Temperature/Ambient Temperature Bin Data

7.2.1 Solar-Source Heat Pump Performance

The accuracy of the two-dimensional sol-air temperature/ambient temperature bin data model presented in Chapter 5 was demonstrated in Chapter 5 by comparing the estimated and measured bin data for a south-facing surface. Differences were noted between the measured and estimated bin data, but the effect of these differences on the

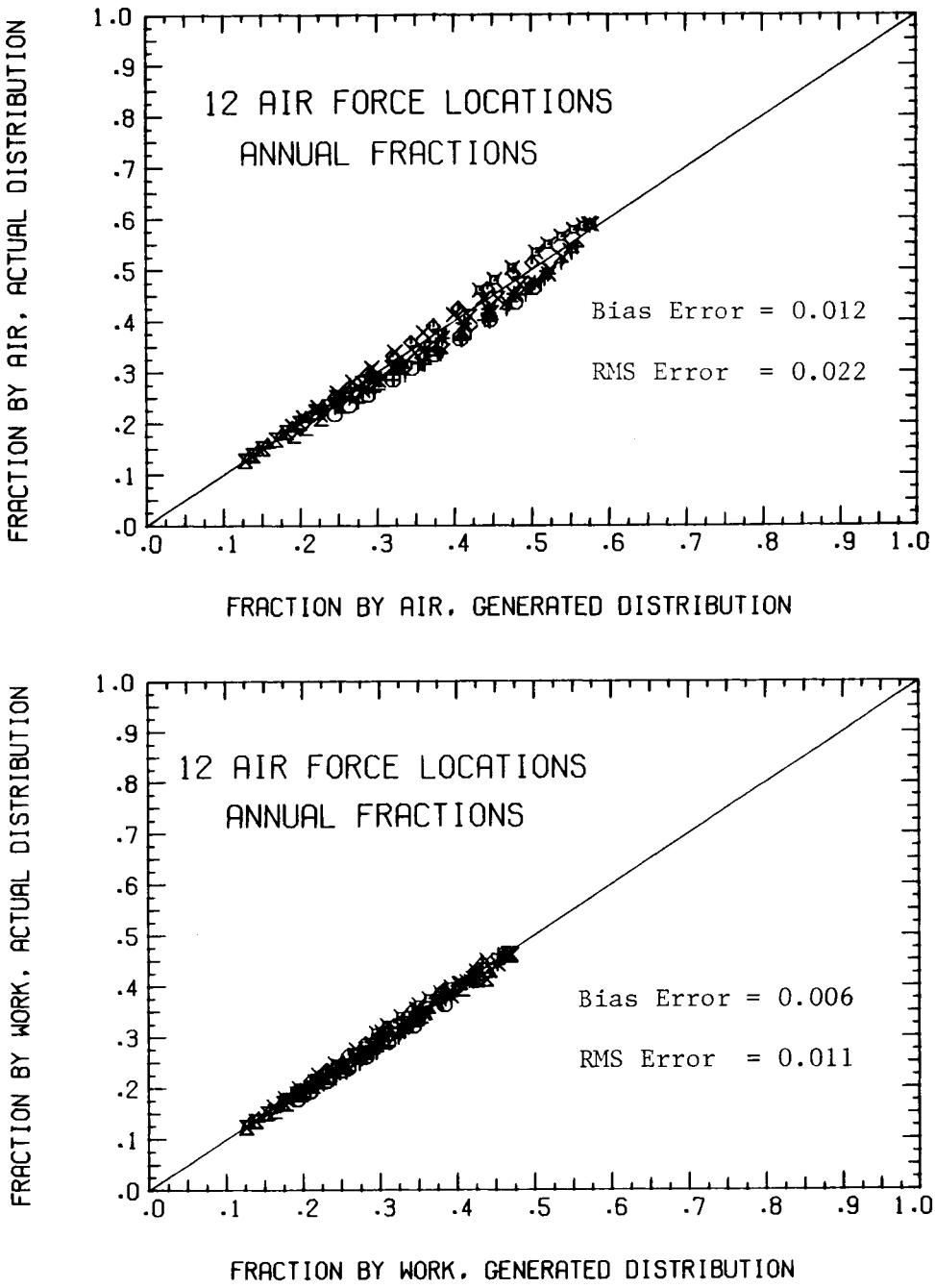

Figure 7.2 Performance of an Air-to-Air Heat Pump with Measured and Estimated Ambient Temperature Bin Data For 12 Air Force Locations

accuracy of heating and cooling loads or equipment performance calculated with the estimated bin data is of perhaps greater interest than the actual differences between the measured and estimated bin data.

Estimating the performance of a solar-source heat pump is an application for sol-air temperature/ambient temperature bin data and a test of the accuracy of equipment performance calculations based on the estimated bin data. A solar-source heat pump utilizes a refrigerant-filled solar collector as the evaporator, and its performance is a function of the sol-air temperature for the collector. The house load is modeled as a function of the ambient temperature (direct solar gains are not considered), and the monthly performance of the heat pump system in heating the house is a function of both the sol-air and ambient temperatures.

Solar-source heat pump systems were studied by Odell (1982), and the performance models developed as part of his research were used. A thorough description of the models, including a listing of a FORTRAN program which performs the necessary bin calculations, is provided by Odell. The calculation technique is analagous to that described in Section 7.1 for the estimation of air-to-air heat pump performance. The house load and heat pump performance are estimated for each bin assuming there is no dependence on the time sequence of the weather and no performance penalty for cycling of the heat pump. The capacity and COP of the heat pump are modeled as functions of evaporator temperature using polynomial fits to

data for a conventional heat pump.

7.2.2 Solar Source Heat Pump Performance Results

The systems chosen for study consist of a solar source heat pump in combination with house UA values of 230, 420, 700 and 1100 W/°C. Heating base temperatures of 20 and 15°C were considered, and the performance was calculated for both the daytime period only and the entire day. An uncovered collector with an area of 10 m^2 was mounted facing south with a tilt angle equal to the 5 degree multiple closest to the latitude. The solar absorptance for the collector was 0.9, and the loss coefficient was assumed to be constant at 28 W/m^2-°C.

The seasonal performance of the solar source heat pump systems described above is compared in Figure 7.3 for the measured and estimated two-dimensional bin data. These results are for the 6 SOLMET locations with the largest heating loads. For solar-source heat pumps, the nonpurchased energy includes both absorbed solar radiation and energy extracted from the ambient air. The months of October through May were used to define the heating season. The accuracy of the FNP values calculated with the estimated bin data changes only slightly when the heating base temperature is varied and when the bin data for the entire day are used instead of the bin data for the daylight hours. No strong locational trends are present, and the difference in FNP for the measured and estimated bin data is always within 5 percentage points.

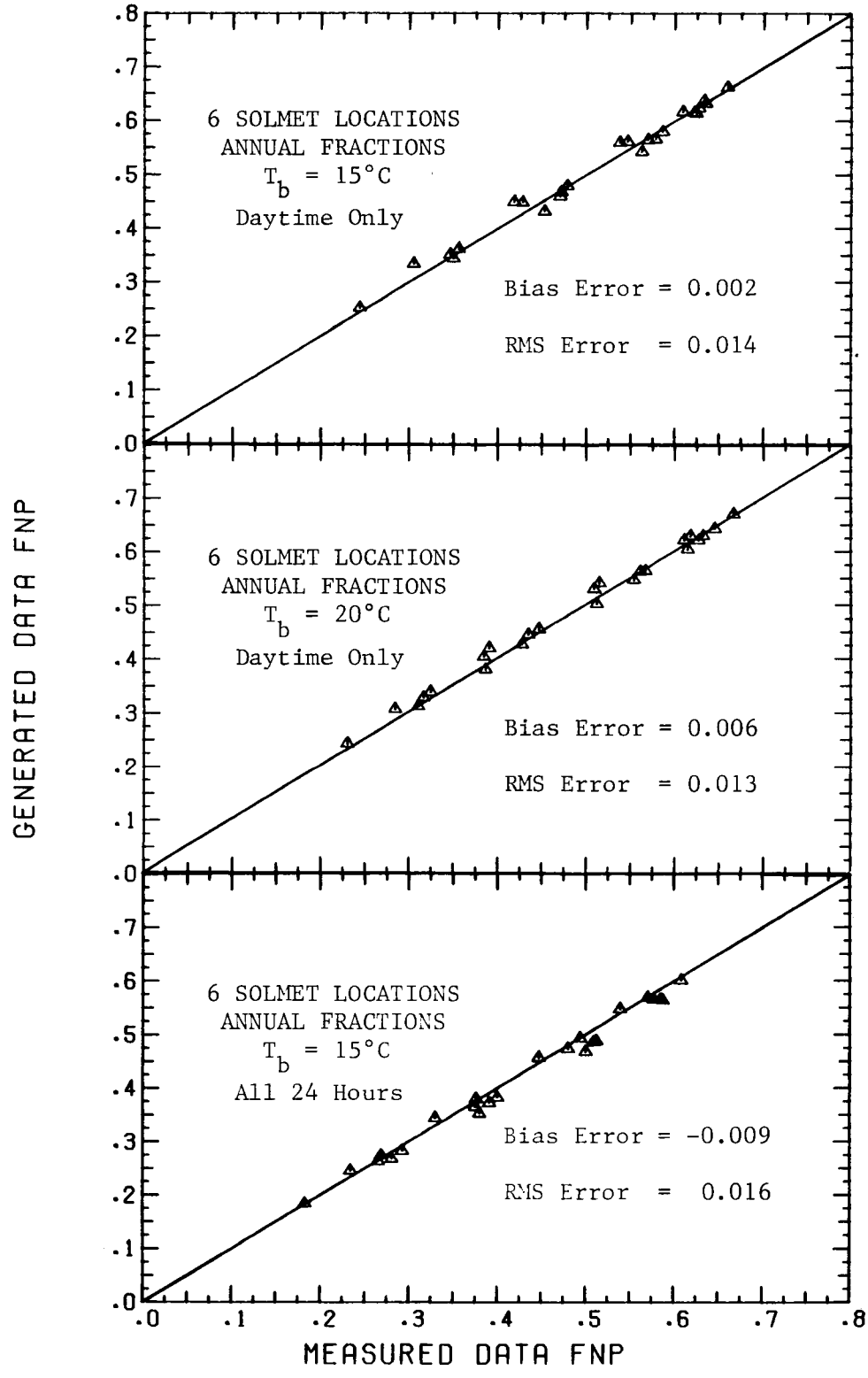

Figure 7.3 Performance Comparisons for a Solar-Source Heat Pump at 6 SOLMET Locations

Two other sources of sol-air temperature/ambient temperature bin data were investigated to test the sensitivity of the seasonal heat pump performance estimates to the accuracy of the bin data. Bin data compiled from Typical Meteorological Year data [SOLMET (1978)] for the 6 locations provide a close approximation to the bin data compiled from the long-term SOLMET records, since the TMY data were created from these long-term data sets with the goal of representing the long-term distributions of solar radiation and ambient temperature. The major drawbacks to the use of TMY data for the calculation of sol-air temperature/ambient temperature bin data are the limited number of locations for which these data are available and the effort required to process the data.

Another source of sol-air temperature/ambient temperature bin data is based on the Air Force Manual 88-29 ambient temperature bin data. The monthly-average daily solar radiation on the collector plane for each month was estimated from measured values of the monthly-average daily clearness index, and these incident radiation values were divided by the number of hours in the daytime period (8 for all months). The resulting constant values of incident monthly-average hourly solar radiation were used along with a loss coefficient of 28 W/m^2 - °C and a solar absorptance of 0.9 to calculate a constant sol-air temperature difference for each month. These monthly-average sol-air temperature differences were used for all ambient temperatures in the daytime period (9 AM to 4 PM) for each month to generate the two-dimensional bin data. The bin data esti-

mated in this manner do not represent any variation in the intensity of the incident solar radiation. All of the hours for a given ambient temperature bin are contained in a single sol-air temperature bin, and the temperature difference between this sol-air temperature bin and the ambient temperature bin is the same for all ambient temperature bins for each month. The two-dimensional Air Force bin (AFB) data are less accurate than the bin data estimated with the method described in Chapter 4, but they also require less effort to estimate.

The annual values of FNP for the TMY bin data and for the AFB data are compared to those for the measured bin data in Figure 7.4. The results of the TMY data are nearly identical to the results for the long-term bin data. The results for the AFB data, however, show a significant bias. The use of an average solar radiation intensity for all hours and days leads to a consistent underprediction of the heat pump performance. Although the errors are still within 5 percentage points for the AFB data, the systematic nature of the errors are evidence of model inadequacy. The bin data estimated with the sol-air temperature/ambient temperature model of Chapter 4 are between the TMY and AFB data both in terms of accuracy and computational effort. The input data required for either the TMY or AFB method are substantially greater than for the estimation procedure of Chapter 4.

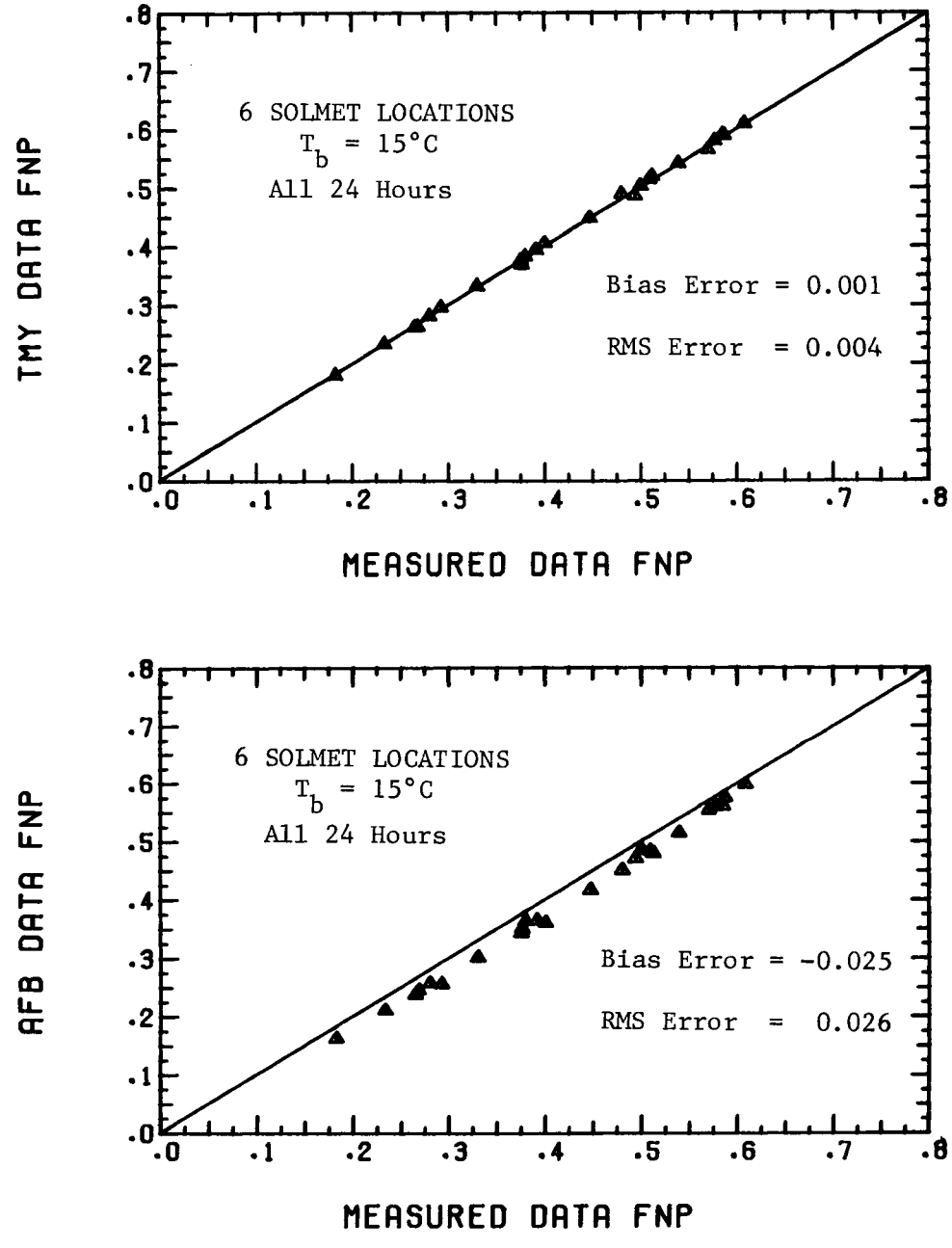

Figure 7.4 Performance Comparisons for a Solar-Source Heat Pump at 6 SOLMET Locations Using Alternate Bin Data Estimation Procedures

7.3 Sol-Air Heating and Cooling Degree-Days

The sol-air heating and cooling degree-day relationships were compared in Chapter 4 to sol-air heating and cooling degree-days compiled from the measured hourly data for a wide range of base temperatures and surface orientations. The heating and cooling loads for a building, however, are the combined result of the sol-air degree-days for all of the surfaces. Comparisons of building heating and cooling loads calculated with estimated sol-air degree-days and building heating and cooling loads calculated with measured hourly data are a more direct test of the usefulness of the sol-air degree-day models than are comparisons of measured and estimated sol-air degree-days for individual surfaces.

7.3.1 A Description of the Design Procedure and Simulation Models for Building Loads Estimation

The transient simulation program TRNSYS [Klein et al. (1981)] was used to establish reference loads for four different buildings. Since TRNSYS simulates the transient behavior of the buildings, any effects due to the sequence in which the weather occurs will be included in the TRNSYS building loads. The buildings were modeled as lumped capacitance systems with UA-degree hour loads. The heating and cooling equipment was assumed to meet the instantaneous load at all times, maintaining the interior temperature at exactly the heating setpoint when heating was required and at exactly the cool-

ing setpoint when cooling was required. The manner in which the buildings were modeled with TRNSYS is not completely representative of the physical processes which actually occur, but it is consistent with the assumptions built into the sol-air degree-day load estimation procedures, and it represents a reasonable approximation to the actual building load. Heating and cooling loads were also calculated for zero and infinite capacitance buildings having the same characteristics as the finite capacitance buildings. TMY data were supplied to TRNSYS.

The buildings considered all have floor areas of 140 m^2. Two of the buildings have 6 m^2 of glazing on each of the four walls, which face the four compass directions, and the other two have 24 m^2 of south-facing glazing only. The building UA is 320 W/°C for all four buildings, and the "effective" capacitance value is 17,100 KJ/°C for two of the buildings and 74,100 KJ/°C for the other two. These values for UA and MC result in house time constants of 15 hours and 65 hours. The thermostat settings are 18.3°C for heating and 25.6°C for cooling, with the base temperatures 2.8°C lower to account for internal generation. The effective transmittance-absorptance product for the glazings is 0.70. Solar radiation absorption on the outer surfaces of the building was neglected to simplify the use of TRNSYS.

The relationships presented in Chapter 4 for the estimation of sol-air heating and cooling degree-days and the relationships pre-

sented in Chapter 6 for the correction of zero capacitance loads to account for building capacitance effects were used to estimate heating and cooling loads for the buildings described above. A listing of a FORTRAN program written for this purpose is given in Appendix B. The weather data input to the design method program consisted of values of $\overline{K}_T$ and $\overline{T}_a$ obtained by averaging the hourly values of the TMY data used in the TRNSYS simulations.

7.3.2 Comparison of TRNSYS and Design Method Loads

The monthly and annual heating loads for TRNSYS and the loads for the design method are compared in Figure 7.5 for Madison, Albuquerque, Seattle, Phoenix and New York. The comparison of the zero capacitance loads indicates the accuracy of the sol-air degree-day procedure developed in Chapter 4, while the comparison of the finite capacitance loads indicates the combined accuracy of the degree-day and capacitance correction algorithms. The infinite capacitance loads are only a function of average values of ambient temperature and incident solar radiation, and so any differences between the TRNSYS and design method values for infinite building capacitance are solely the result of differences in the monthly-average tilted surface radiation values.

While the design method estimates for light capacitance buildings (τ = 15 hours) are less accurate (where accuracy refers to the difference between the design method and TRNSYS) than the estimates for zero capacitance, the heavy capacitance design method estimates

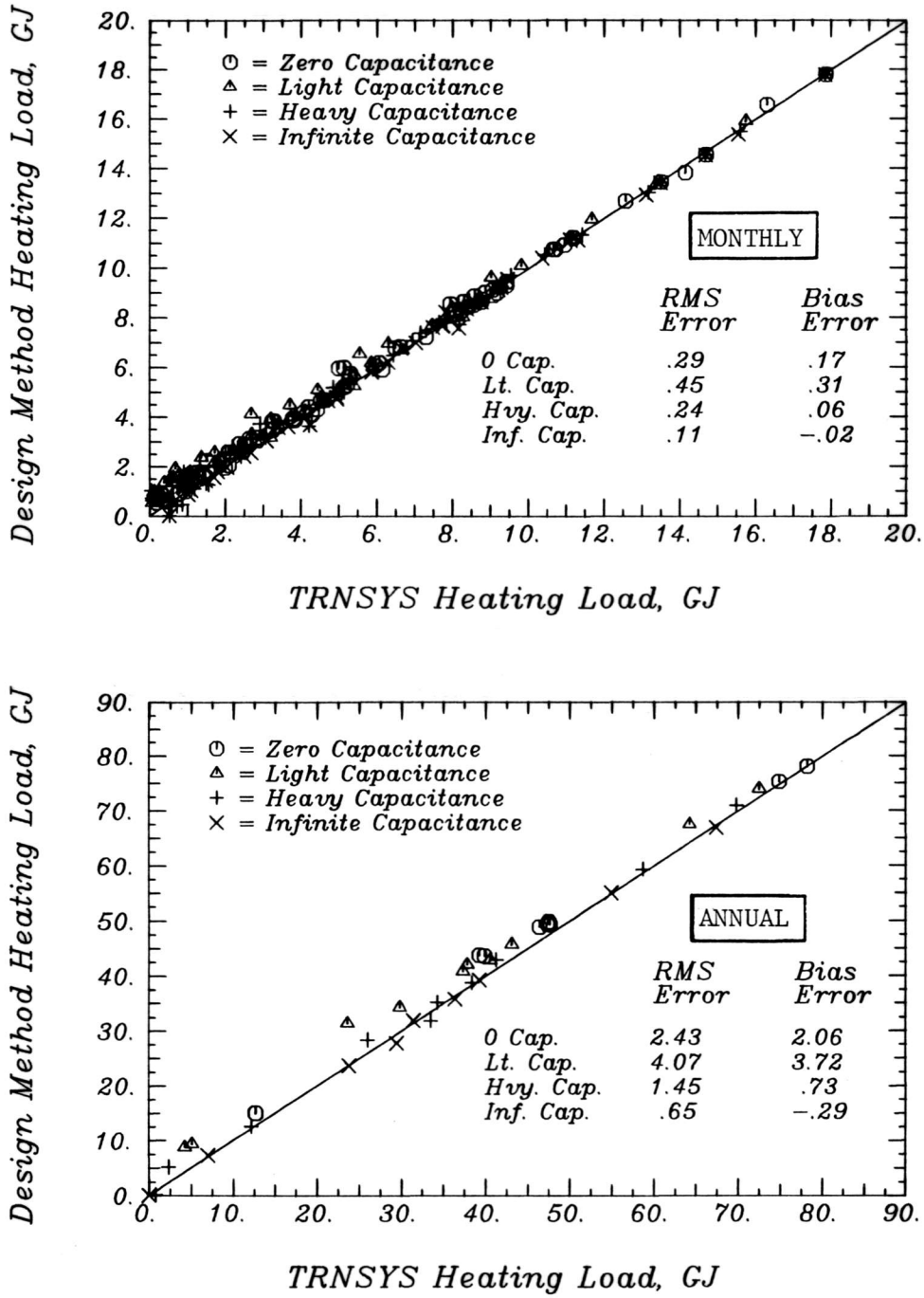

Figure 7.5 Monthly and Annual Heating Loads for TRNSYS and the Design Method for 5 U.S. Locations

are, on the average, more accurate than the zero capacitance estimates. The large size of the zero capacitance bias error relative to the size of the RMS error is the result of a systematic tendency of the design method to overestimate the heating load and underestimate the solar radiation which can be used to meet the heating load. The bias errors for the light capacitance buildings are larger in size than the bias errors for the zero capacitance buildings, which indicates that in addition to the systematic error for the sol-air degree calculation noted above, there is also a tendency of the design method to underestimate the storage of excess gains by the building. The reduction of the magnitude of the bias error for the heavy capacitance buildings when compared to the zero capacitance buildings is the result of the design method overpredicting the storage of excess gains.

The monthly and annual cooling loads for the same 5 locations are compared in Figure 7.6. The bias and RMS errors for zero capacitance and light capacitance cooling loads are nearly the same as the bias and RMS errors for zero capacitance and light capacitance heating loads. The errors for the zero and finite capacitance buildings are again largely systematic in nature, indicating overestimation of the gains due to ambient temperature and solar radiation and underestimation of the storage of useful night losses. The accuracy of the design method does not improve for heavy capacitance buildings, however, as was the case with heating loads. Instead, the underprediction of energy storage by the design method is larger

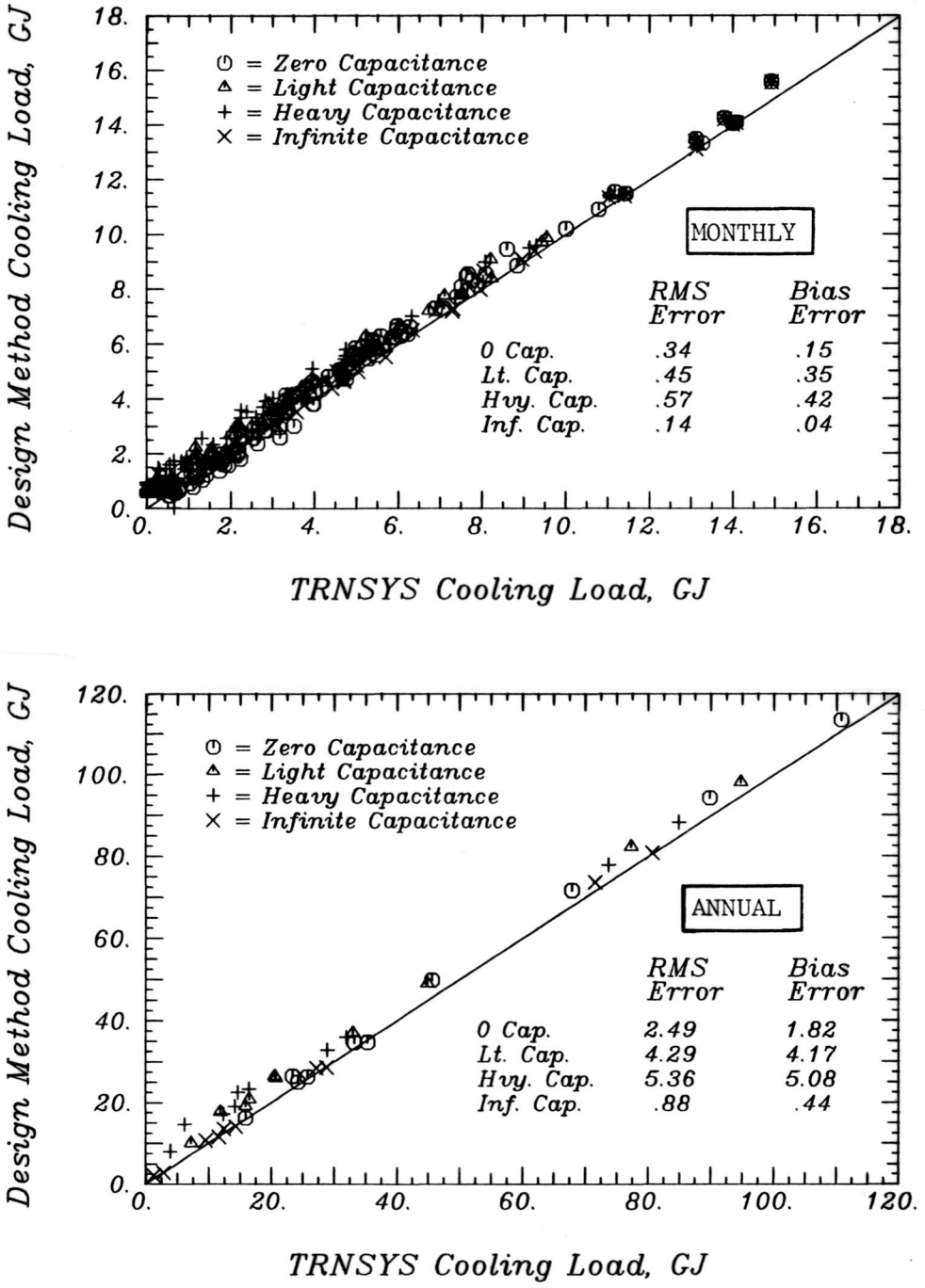

Figure 7.6 Monthly and Annual Cooling Loads for TRNSYS and the Design Method for 5 U.S. Locations

for heavy capacitance buildings than it is for light capacitance buildings when cooling loads are modeled.

The errors for the finite capacitance buildings are the combined result of errors in the sol-air degree-day estimates and errors in the capacitance correction procedure. The accuracy of the capacitance correction procedure is isolated in Figure 7.7, where the change in heating load when building capacitance is included is compared for TRNSYS and the design method on both a monthly and an annual basis. The results shown include both light and heavy capacitance buildings. A trend which is present in the data is an underprediction of the effect of capacitance for light capacitance structures and overprediction of the effect for heavy capacitance structures, as noted above.

The change in monthly and annual cooling loads when building capacitance is included is compared for TRNSYS and the design method in Figure 7.8. The comparison for the annual data exhibits a very distinct pattern. The correction procedure works extremely well in Phoenix and Albuquerque, while in the other three locations, the errors increase linearly with the size of the change in the cooling load. The correction procedure for cooling loads involves an assumption which is correct only when the solar radiation intensity is the same each day in the month. This assumption is used to determine which days in the month result in useful night losses. The consistently clear weather in Phoenix and Albuquerque makes this a good assumption for these two locations. In the remaining locations,

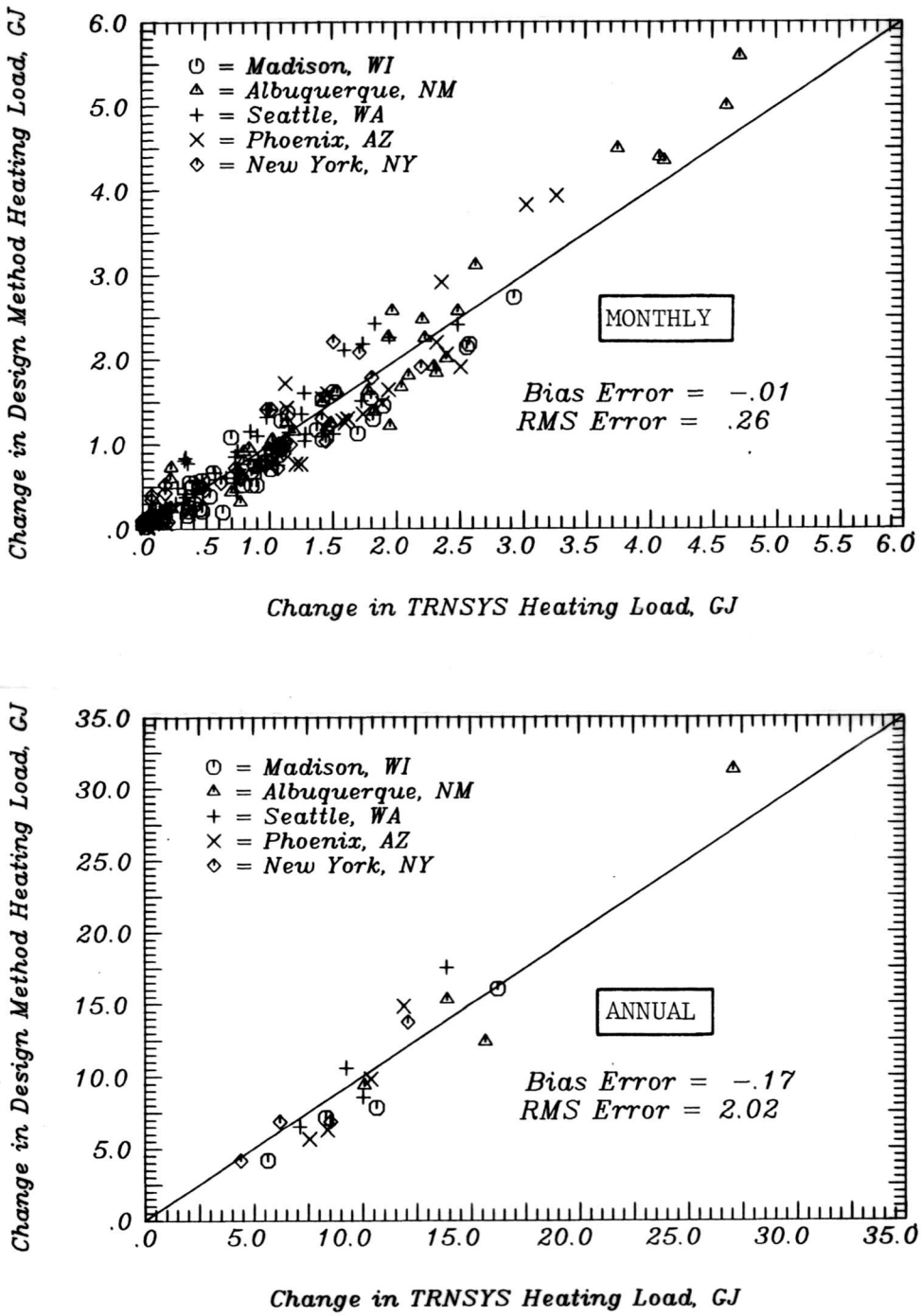

Figure 7.7 The Effect of Building Capacitance on Heating Loads as Predicted by TRNSYS and the Design Method

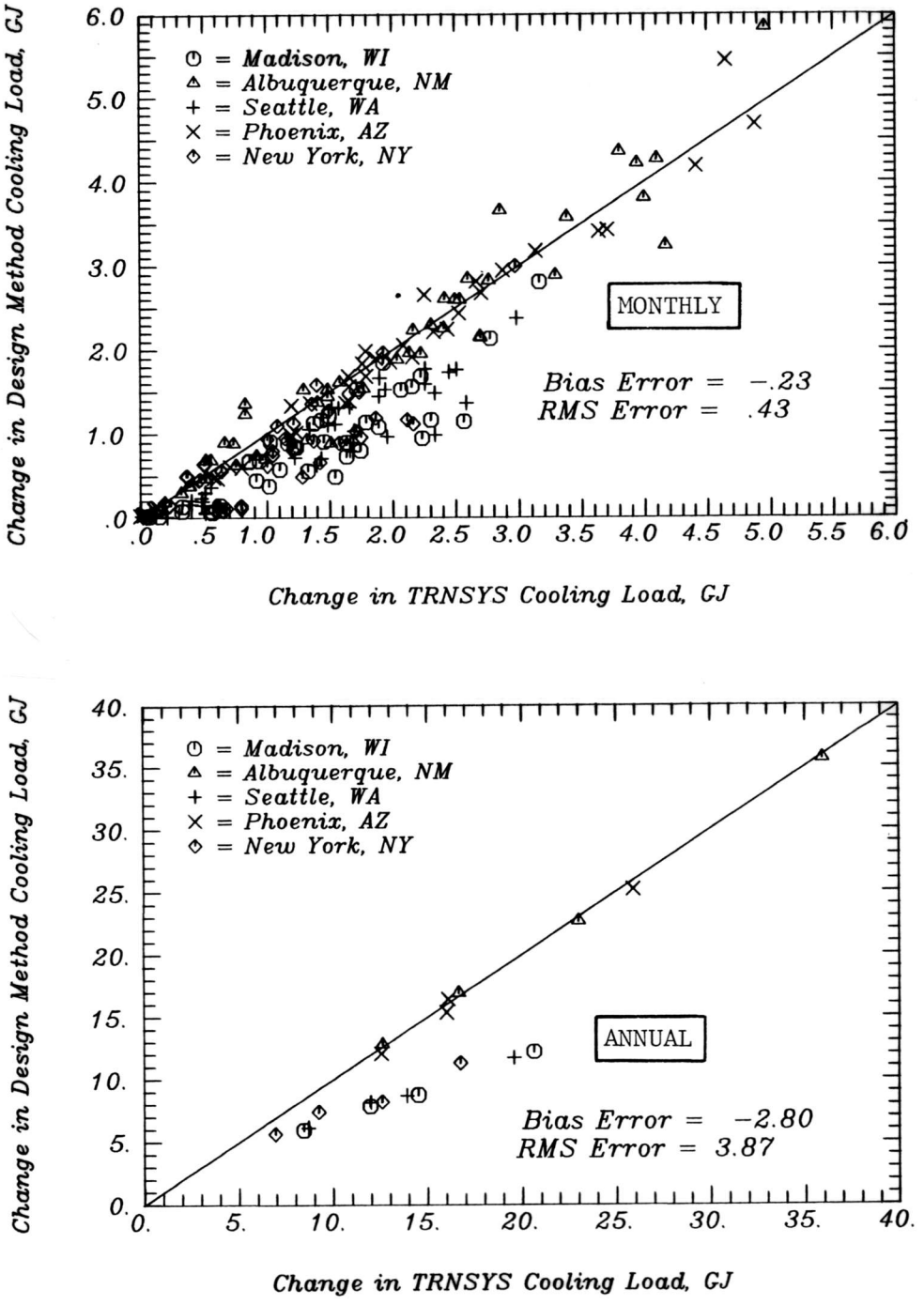

Figure 7.8 The Effect of Building Capacitance on Cooling Loads as Predicted by TRNSYS and the Design Method

the solar radiation, and thus the cooling load, is more variable. This allows day-to-day carryover of night losses and cool days with large solar gains to become important factors in determining the cooling load, and the effects of these weather patterns are not properly accounted for in the correction procedure.

7.4 Humidity Ratio/Dry-Bulb Temperature Bin Data

7.4.1 A Design Procedure for Residential Air Conditioner Performance

An application for two-dimensional humidity ratio/dry-bulb temperature bin data is the estimation of the performance of a residential air conditioner. The capacity and COP of an air conditioner are functions of the indoor and outdoor dry-bulb temperatures and the indoor humidity ratio. Although interior humidity is generally not controlled directly in a residence, moisture is removed from the air when its temperature is brought below the dew point. Thus, there can be both a sensible and a latent load on the air conditioner coil. When an air conditioner is operated to control the temperature inside a building, the fraction of each hour the air conditioner must run is equal to the ratio of the sensible building cooling load to the sensible cooling capacity of the machine. The sensible load on the air conditioner is assumed to always be equal to the instantaneous load for the house, unless the house load exceeds the steady-state capacity of the air conditioner.

The latent load on an air conditioner is dependent on a number

of factors. If the dew point of the air inside a building is below the evaporator coil temperature, there is no condensation of moisture and no latent load. When there is condensation, the latent load is determined by the instantaneous water removal rate and the fraction of the time the air conditioner is operating to meet the sensible load. The problem is complicated by the fact that the sensible capacity of the machine, and thus the fraction of the time it is running, is dependent on the latent load. Moisture enters the building through air infiltration or as internal generation due to cooking and transpiration from people, animals and plants. Moisture is removed by condensation on the evaporator coil.

Performance data were obtained for a Carrier single-package heat pump with a nominal total (sensible plus latent) capacity of 10.64 KW (3 tons). The tabular data provided by Carrier give the steady-state sensible capacity, latent capacity, and power consumption as a function of outdoor dry-bulb temperature and indoor wet-bulb temperature for an indoor dry-bulb temperature of 27°C. The sensible load for the house was calculated using the UA-degree hour approach with a cooling base temperature of 20°C, a cooling thermostat setpoint of 27°C, and a UA of 306 W/°C. The difference between the setpoint and base temperatures accounts for internal heat generation and gains due to solar radiation. Infiltration rates of 0.5 and 5.0 air changes per hour were considered with an internal volume of 340 cubic meters. Internal generation of moisture and the effect of cycling of the heat pump on its perfor-

mance were not considered. Ventilation with ambient air was assumed to satisfy the cooling load when the outdoor dry-bulb temperature was less than 24°C.

An iterative procedure is required determine the performance of the air conditioner when it is operating. The inside dry-bulb temperature, the outside dry-bulb temperature and the outside humidity ratio are known and fixed for a given bin. What remains is to solve for the inside humidity ratio for each bin (when the air conditioner is operating). A moisture balance for the interior air can be written as:

$$\dot{m}_{a,infil}(\omega_a - \omega_{r,f}) = \dot{m}_{a,coil}(\omega_{r,f} - \omega_{coil})(PLF) \qquad (7\text{-}2)$$

where PLF, the part load factor, is the ratio of the sensible building load to the sensible air conditioner capacity (with an upper limit of one), $\dot{m}_{a,infil}$ is the mass flow rate of infiltration air, $\omega_{r,f}$ is the inside humidity ratio, ω_a is the outside air humidity ratio, $\dot{m}_{a,coil}$ is the mass flow rate of air past the evaporator and ω_{coil} is the exit humidity ratio of the air flowing over the evaporator. Since the sensible capacity of the machine and the humidity ratio at the coil exit are a function of the room humidity ratio, it is necessary to solve Equation (7-2) numerically for room humidity ratio at each humidity ratio/dry-bulb temperature bin. The sensible load, latent load and power consumption of the air conditioner are found by summing the product of the PLF, the number of hours in the bin and the steady-state rate for each of these varia-

bles over those bins having an ambient temperature greater than 24°C.

7.4.2 Air Conditioner Performance Using Measured and Estimated Bin Data

A number of different procedures were discussed in Chapter 5 for the estimation of humidity ratio/dry-bulb temperature bin data. The estimation procedures differ in the distribution functions and inputs used, and it is not obvious from the comparisons given in Chapter 5 which results in the most accurate performance estimates for residential cooling loads. The estimation procedures (which are described in more detail in Chapter 5) are: 1. Distribution functions for T_a and RH, with measured values of $\overline{T}_{a,h}$ and $\overline{RH}_h$ as input; 2. Distribution functions for T_{wb} and RH, with measured values of $\overline{T}_{a,h}$ and $\overline{RH}_h$ as input, $\overline{T}_{wb,h}$ estimated from $\overline{T}_{a,h}$ and $\overline{RH}_h$; 3. Distribution functions for T_a and RH, with measured values of $\overline{T}_a$ and $\overline{RH}$ as input, $\overline{T}_{a,h}$ and $\overline{RH}_h$ estimated; 4. Distribution function for T_a, the distribution function for RH, measured values of $\overline{T}_a$ and $\overline{K}_T$ as input, $\overline{T}_{a,h}$ and $\overline{RH}_h$ estimated; 5. Distribution function for T_a, RH always equal to the value of $\overline{RH}_h$ for each hour of the day (no hourly distribution), measured $\overline{T}_a$ and $\overline{RH}$, $\overline{T}_{a,h}$ and $\overline{RH}_h$ estimated; and 6. Distribution function of T_a, RH always equal to $\overline{RH}$ for the day (no hourly distribution or diurnal variation), no diurnal variation for T_a, measured $\overline{T}_a$ and $\overline{RH}$.

The loads for the air conditioner-house systems described above were calculated using two-dimensional humidity ratio/dry bulb temperature data estimated with each of the procedures listed above. The loads were also determined with the bin data compiled from the measured hourly values of dry-bulb temperature and humidity ratio.

The monthly and annual cooling coil loads (sensible plus latent) calculated from the measured bin data are compared in Figure 7.9 to those determined with the bin data estimated using procedure 1. The monthly and annual cooling coil loads for bin data estimated with method 2 and the loads for the measured bin data are compared in Figure 7.10. Figure 7.11 shows the same comparison, but for bin data estimated with method 6. There are two annual loads shown for each location in each of the figures, one for an infiltration rate of 0.5 air changes per hour and one for an infiltration rate of 5.0 air changes per hour. The difference in the two loads for each location is an indirect indication of the importance of latent loads.

Bin data estimated with the distribution functions for T_a and RH (Procedure 1) give the most accurate performance estimates. The bin data estimated in the simplest manner, procedure 6, yield performance estimates which are less accurate than the load estimates based on estimation procedure 1. In Chapter 5 it was found that the bin data estimated with procedure 6 gave the most accurate values of humidity-hours. The least accurate loads are those calculated with the bin data estimated with the T_{wb} and RH distribution functions (procedure 2).

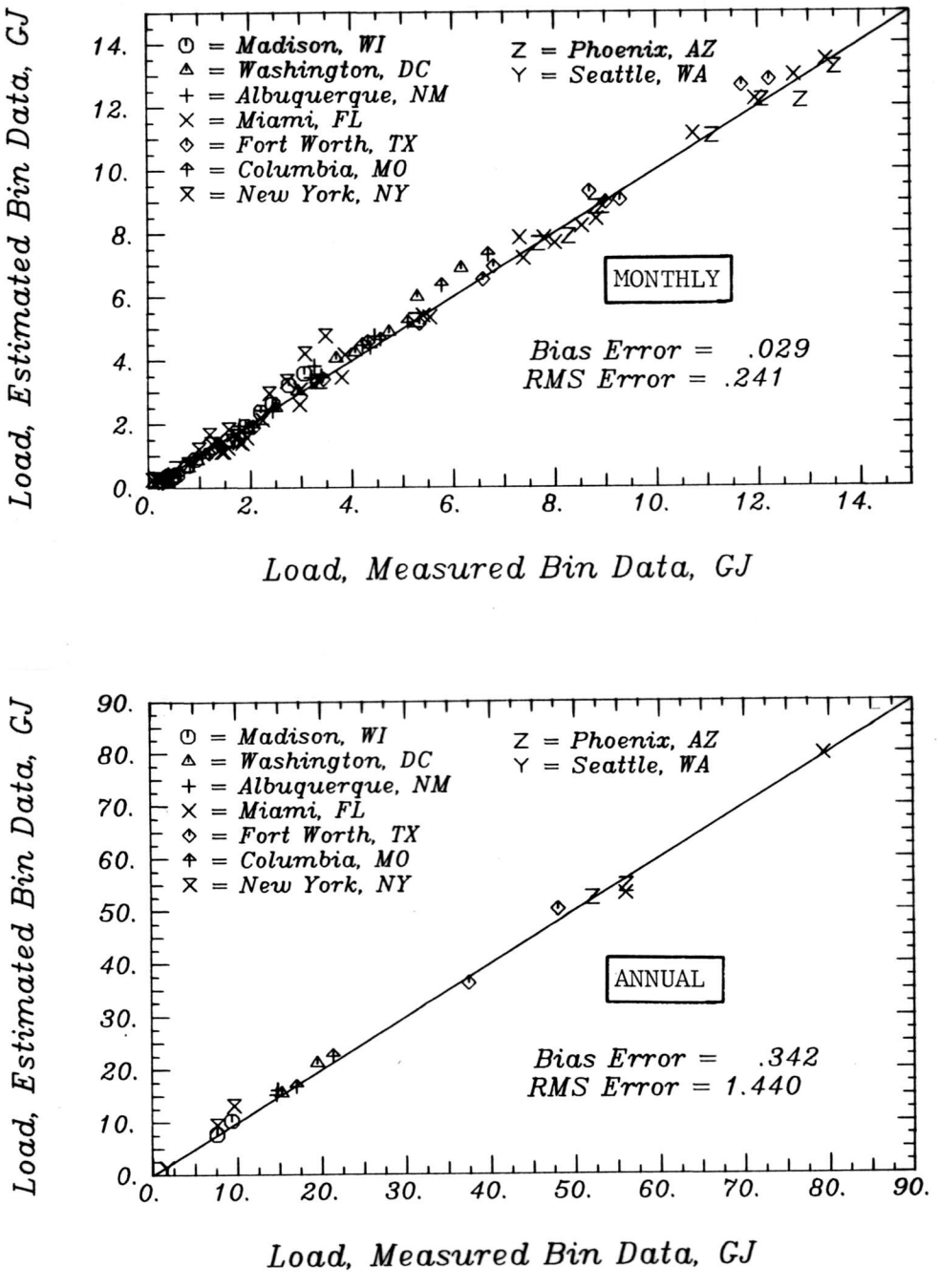

Figure 7.9 Air Conditioner Coil Loads for Measured Bin Data and for Bin Data Estimated with the Distribution Functions for Dry-Bulb Temperature and Relative Humidity

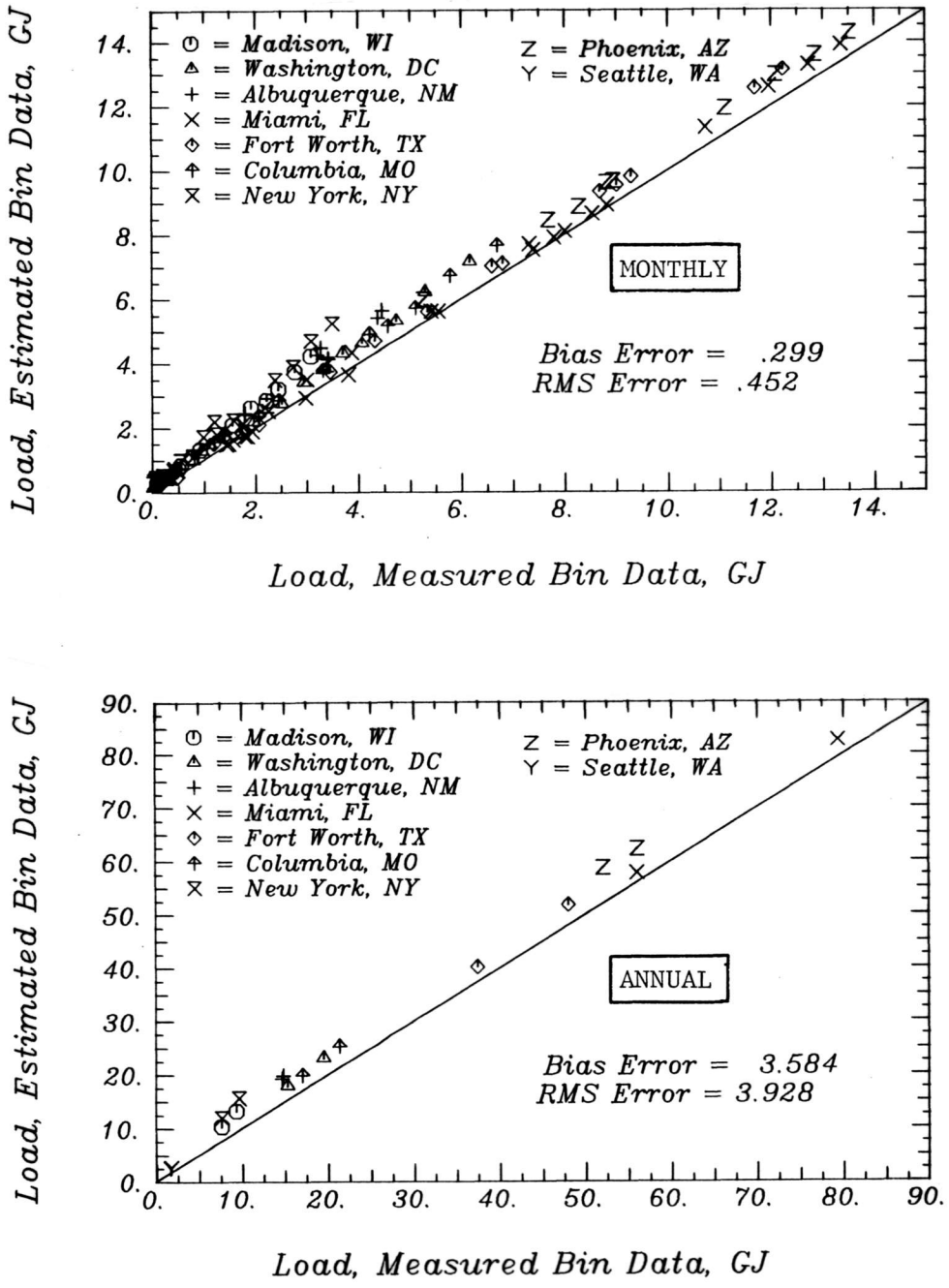

Figure 7.10 Air Conditioner Coil Loads for Measured Bin Data and for Bin Data Estimated with the Distribution Functions for Wet-Bulb Temperature and Relative Humidity

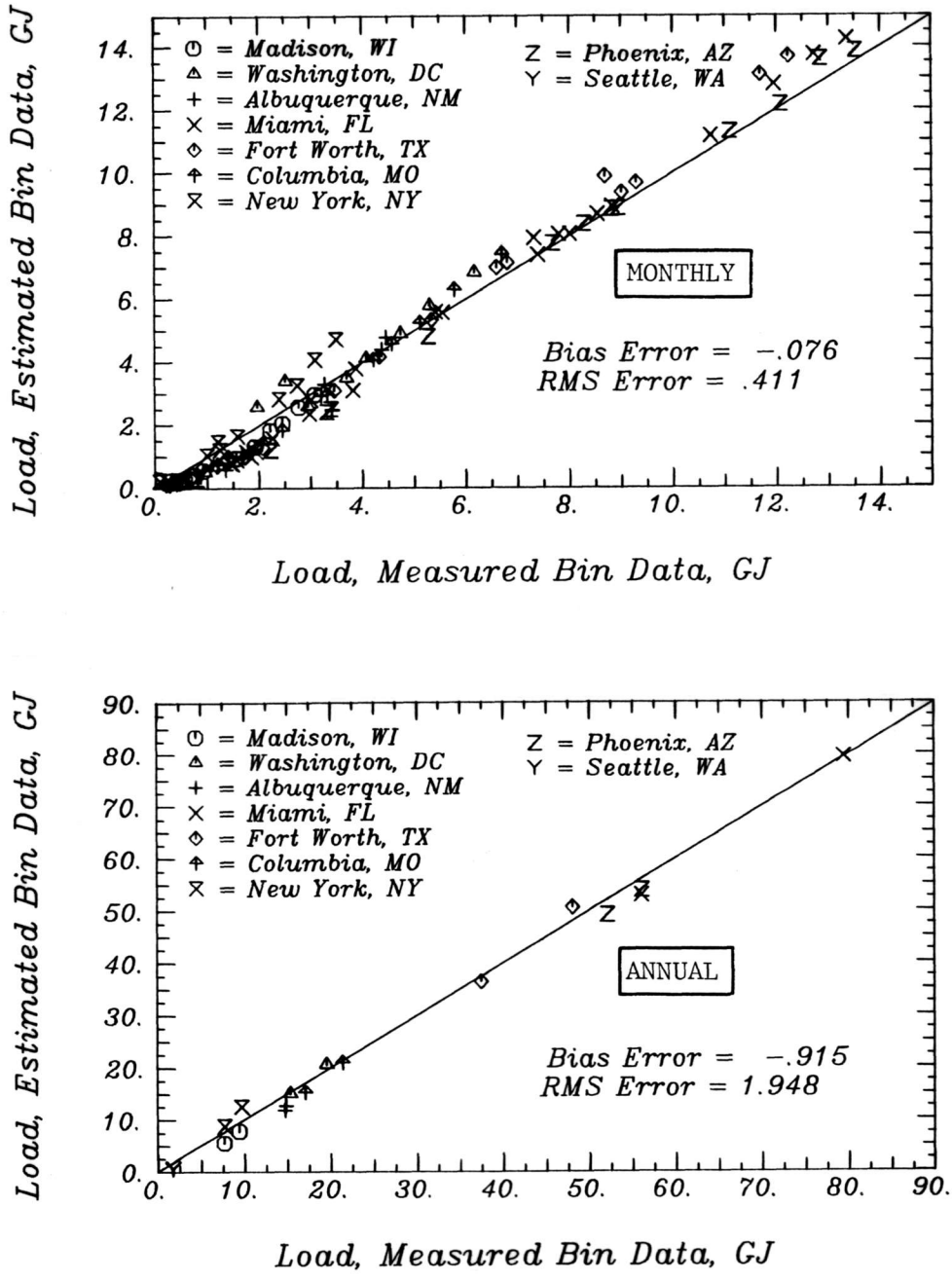

Figure 7.11 Air Conditioner Coil Loads for Measured Bin Data and for Bin Data Estimated with the Distribution Function for Dry-Bulb Temperature and with Relative Humidity Constant at the Monthly-Average Daily Value

The loads for the bin data estimated with procedure 2 are consistently overpredicted. The distribution of dry-bulb temperature for these bin data is not represented as well as in the other bin data sets, which are based directly on the distribution function for T_a. The use of the T_{wb} and RH distribution functions leads to significant numbers of hours at dry-bulb temperatures which are higher than the values contained in the measured data sets.

The monthly and annual values of the bias and RMS errors are given in Table 7.1 for all of the bin data estimation procedures. Replacing the measured values of $\overline{T}_{a,h}$ and $\overline{RH}_h$ with values estimated using the relationships given in Chapters 3 and 5 and measured values of $\overline{T}_a$ and $\overline{RH}$ has little effect on the accuracy of the load estimates. When $\overline{RH}$ is estimated from $\overline{T}_a$ and $\overline{K}_T$, however, there is a significant increase in the RMS error when compared to the results obtained with measured values of RH. The load estimates for estimation procedure 5 are more accurate than those for estimation procedure 6, indicating that it may be important to at least include the diurnal variation of RH when estimating humidity bin data. The accuracy of the loads based on estimation procedure 5 is only slightly worse than the accuracy for estimation procedure 1.

7.5 Summary

The performance of an air-to-air heat pump was calculated using measured and estimated ambient temperature bin data for 18 locations. The fraction of the heating load which was nonpurchased

Table 7.1 Monthly and Annual Bias and RMS Errors for Air Conditioning Loads Estimated with Humidity Ratio/Dry-Bulb Temperature Bin Data

Description of Bin Data Estimation Procedure	Monthly Loads		Annual Loads	
	RMS Error, GJ	Bias Error, GJ	RMS Error, GJ	Bias Error, GJ
T_a and RH distributions, measured $T_{a,h}$ and RH_h	0.241	0.029	1.44	0.34
T_{wb} and RH distributions, measured $T_{a,h}$ and RH_h	0.452	0.299	3.93	3.58
T_a and RH distributions, $T_{a,h}$ and RH_h estimated from $\overline{T}_a$ and $\overline{RH}$	0.254	0.016	1.43	0.19
T_a and RH distributions, $\overline{T}_{a,h}$ and RH_h estimated from $\overline{T}_a$ and K_T	0.353	0.035	2.02	0.42
T_a distribution, RH = $\overline{RH}_h$, $\overline{T}_{a,h}$ and RH_h estimated from $\overline{T}_a$ and RH	0.279	0.061	1.56	0.74
T_a distribution, RH = $\overline{RH}$, no diurnal variation of T_a or RH, measured $\overline{T}_a$ and $\overline{RH}$	0.411	-0.076	1.95	-0.92
Average Load Calculated with Measured Bin Data	2.18 GJ		26.11 GJ	

energy and the fraction of the load which was electricity used to run the heat pump were compared for the measured and estimated bin data, and it was found that the results for the estimated bin data were always within 5 percentage points of the results for the measured bin data on a seasonal basis.

A similar set of comparisons were made for a solar-source heat pump. The bin data for the solar-source heat pump are two-dimensional sol-air temperature/ambient temperature bin data. Once again, the nonpurchased energy fractions were found to be within 5 percentage points on a seasonal basis when the results for the measured and estimated bin data were compared. Sol-air temperature/ambient temperature bin data compiled from hourly TMY data were found to give slightly more accurate results than bin data estimated using the models given in Chapter 4. A simple procedure for the estimation of sol-air temperature/ambient temperature bin data, one which does not include any distribution of solar radiation, was also compared to the measured bin data; the results for this estimation method were still within 5 percentage points of the results for the measured data, but the performance was consistently low for the estimated bin data.

The sol-air degree-day relationships of Chapter 4 and the building capacitance correction models of Chapter 6 were combined to estimate the heating and cooling loads for zero, finite and infinite capacitance buildings. Light and heavy capacitance buildings with both distributed and south-facing only glass were considered. TRNSYS

was used to establish reference loads for the buildings. The design method was found to be somewhat more accurate for heating loads than for cooling loads. The errors in the load estimates for finite capacitance buildings are the result of errors in both the zero capacitance loads and the corrections for the effects of capacitance. The design method loads are generally within 10% of the TRNSYS loads.

A method for calculating the load on a residential air conditioner was outlined and used to compare the accuracy of several different procedures for estimating two-dimensional humidity ratio/dry-bulb temperature bin data. The most accurate load estimates, when compared to the loads obtained using bin data compiled from hourly measurements, were calculated using bin data estimated with the distribution functions for dry-bulb temperature and relative humidity. The least accurate load estimates were calculated using bin data estimated with the distribution functions for wet-bulb temperature and relative humidity. The poor accuracy of the load estimates for bin data based on the wet-bulb temperature distribution is the result of representing the ambient temperature distribution in an indirect manner. When the distribution function for relative humidity is replaced with the monthly-average hourly value of relative humidity, the accuracy of the load estimates decreases only slightly.

CHAPTER 8

8. CONCLUDING REMARKS AND RECOMMENDATIONS

8.1 Improvements in the Statistics Available for the Estimation of Loads

The ambient temperature distribution model presented in Chapter 3 permits the estimation of ambient temperature bin data from more readily available inputs, expanding the number of locations where bin data calculations can be performed. Although numerous models exist for the estimation of ambient temperature degree-days, the estimation of ventilation cooling degree-days has not been possible until now. The relationships presented for the diurnal variation of ambient temperature allow bin data and degree-days to be estimated for individual hours or portions of the day; the average ambient temperature for the daytime or nighttime periods is also useful for estimating the monthly performance of equipment which is dependent on ambient temperature.

The procedure developed for the estimation of sol-air temperature/ambient temperature bin data provides an alternative to the use of measured data. Bin data can be developed for more locations and with less effort when compared to the use of hourly measurements. The availability of these two-dimensional bin data permits the performance of equipment or loads which are nonlinear functions of ambient temperature and solar radiation to be calculated on a monthly

basis. The sol-air degree-day relationships presented combine the effects of ambient temperature and solar radiation on building loads in a manner which is more general than existing methods. Solar gains which result from absorption on outer surfaces, transmission through windows or the operation of no-storage solar systems can be included in the analysis. The diurnal variations of ambient temperature and solar radiation are incorporated, and it is possible to consider the effect of ventilation on the cooling load.

The distribution models developed for relative humidity and wet-bulb temperature represent the first distribution functions for air moisture content which can be used with input data which are widely available. The estimation of two-dimensional dry-bulb temperature/humidity ratio bin data with these distribution models greatly expands the number of locations where latent cooling loads and humidity-dependent equipment performance can be calculated through the use of weather statistics.

The correction procedures for the effect of building capacitance on heating and cooling loads were developed from an energy balance on a building which has a single node "effective" capacitance. The relationships are based on existing distribution functions for solar radiation and ambient temperature, and they can be used for the same wide range of building types as the sol-air degree-day models. Because the relationships were developed from an analytical treatment of the building energy flows and temperature response, they satisfy the limits for zero and infinite capacitance. Unlike empirical

approaches, there is no conditioning of the correction to a particular type of building or climate. The effects of variations in solar radiation and ambient temperature were included in the development of the correction relationships, which has not been done in previous analytic solutions.

The models developed in this study were tested in several ways. In the case of distribution models for weather statistics, estimated values were compared to the measured data they are designed to replace, both for the locations used to develop the models and also for locations not contained in the original data set. The bin data estimates were also tested by comparing load and equipment performance calculations made using estimated bin data against those made using measured bin data. The sol-air degree-day models and the capacitance correction relationships were tested by comparing building loads estimated with these models to those obtained by simulating the buildings with TRNSYS. The comparisons given provide some indication of the typical accuracy which can be expected when using the different models. They also point out any locational or seasonal dependencies and demonstrate the use of the relationships.

8.2 Simplified Estimation Models

The most important feature of the models which have been developed and presented is that the only input meteorological data required are the monthly-average daily temperature and the monthly-average daily clearness index, both of which are available for hund-

reds of locations in the United States. As a result of the simple nature of the required input, the relationships can be used on a widespread basis. A second advantage is the small amount of data which must be entered and stored to represent climatic conditions in many locations.

All of the weather statistics models presented are of a form which allow the accuracy of the estimated statistics to be improved if monthly-average meteorological data in addition to the monthly-average clearness index and ambient temperature are available. For example, the estimation of humidity data is improved if the measured monthly-average relative humidity, which is also tabulated for a large number of locations, is used in place of the monthly-average relative humidity estimated with Equation (5-5). The ability to supply more detailed weather data as input if they are available provides flexibility in the use of the models.

The mathematical forms for the models were chosen to be as simple as possible without compromising their ability accurately represent the measured data. The relationships are all in terms of functions which are found on most calculators and computers. The probability density function, cumulative distribution function and accumulated difference models are all consistent with each other for each variable. Seasonal and locational dependence were not included in the model forms, which avoids the problems associated with defining and quantifying seasons and location types.

8.3 Directions for Further Study

The distribution functions developed from the measured data for the different meteorological variables exhibit varying degrees of seasonal and locational dependence. The topography surrounding a location, the proximity of the location to large bodies of water and other prominent geographical features, and the dependence of weather patterns on the time of year all affect the distributions of the meteorological variables. Trends were identified in the seasonal and location dependence for many of the variables, and possible physical explanations were offered for these trends. The errors in the models presented could be reduced somewhat if a means were found to quantity the effect of locational and seasonal factors and if models were developed which are functions of these factors.

Significant correlation exists between some of the weather variables, such as ambient temperature and relative humidity. This cross-correlation was ignored in the two-dimensional distribution models developed. The effect of the correlation of two or more variables on the loads for a building and the performance of conditioning equipment needs to be investigated in more detail. Bivariate models which correctly model the coincidence of a pair of weather variables would improve the accuracy of estimated two-dimensional bin data over the methods based on two one-dimensional models.

The distributions of solar radiation and ambient temperature could not be fully incorporated into the relationships developed for the effect of building capacitance on heating and cooling loads. The accuracy of the corrections could be improved, particularly for cooling loads, if it were possible to fully account for the variations of both ambient temperature and solar radiation. The effect of ambient temperature and solar radiation persistence on the size of the corrections should also be investigated. The methods need to be extended to include the effect of thermostat setbacks and setups on the building loads, and much work remains to be done in establishing a simple methodology for determining the "effective capacitance" of a building.

Procedures were presented in Chapter 5 for the estimation of two-dimensional humidity ratio/dry-bulb temperature bin data, and humidity-hours were numerically determined for the bin data. Humidity-hours may be useful for load and equipment performance estimation, and a more direct and less complex method of estimating humidity-hours is needed.

Although wind speed affects the infiltration rate and the sol-air temperature for a building, the distribution of wind speed was not investigated and no distribution models were presented. The effects of variations in wind speed on the load for a building need to be investigated more fully, and if the effects are found to be significant, appropriate statistics should be defined and modeled.

APPENDIX A

RELATIONSHIPS FOR SATURATION HUMIDITY RATIO

A mixture of water vapor and air can be approximated as a mixture of ideal gases for the ranges of temperature and pressure which are found in the atmosphere near the surface of the earth. The ratio of the mass of water vapor to the mass of dry air for saturation conditions, ω_s, can be expressed in terms of the ratio of pressures for the two constituents.

$$\omega_s = 0.622 \frac{P_{ws}}{(P - P_{ws})} \qquad \text{(A-1)}$$

P is the total pressure of the air-water vapor mixture (normally 14.7 psia) and P_{ws} is the saturation vapor pressure for water.

The Clausius-Clapeyron Equation was used along with published data[1] for the properties of saturated water vapor to derive the following relationships for the saturation vapor pressure of water:

a) Over water (T greater than 492 °R),

$$P_{ws} = 2.4074 \times 10^{7} \exp(-9548/T) \qquad \text{(A-2)}$$

b) Over ice (T less than 492 °R),

$$P_{ws} = 4.933 \times 10^{8} \exp(-11040/T) \qquad \text{(A-3)}$$

where T is in °R and P_{ws} is in psia. These equations are compared to tabulated data[1] in Tables A.1 and A.2.

[1] J.H. Keenan, F.G. Keyes, P.G. Hill and J.G. Moore, Steam Tables, John Wiley and Sons, New York, (1969).

Table A.1. Comparison of Estimated and Measured Saturation Vapor Pressure for Liquid Water.

Temperature, °F	Equation (A-2), psi	Steam Table, psi
32	0.090	0.089
50	0.178	0.178
68	0.338	0.339
86	0.613	0.616
104	1.070	1.070
122	1.808	1.793
140	2.954	2.895

Table A.2. Comparison of Estimated and Measured Saturation Vapor Pressure for Ice.

Temperature, °F	Equation (A-3), psi	Steam Table, psi
32	0.0888	0.0886
23	0.0583	0.0582
14	0.0379	0.0378
5	0.0241	0.0240
-4	0.0151	0.0150
-13	0.0093	0.0092
-22	0.0056	0.0055

APPENDIX B

COMPUTER PROGRAM LISTINGS

PROGRAM SOL-AIR

```
C     THIS PROGRAM DETERMINES THE HEATING AND COOLING LOADS FOR
C     A BUILDING.  THE LOAD FOR A BUILDING WITH NO THERMAL CAPACITANCE
C     IS DETERMINED USING THE SOL-AIR DEGREE-DAY RELATIONSHIPS DEVELOPED
C     IN CHAPTER 4 OF THIS THESIS.  THE LOAD FOR A FINITE CAPACITANCE
C     BUILDING IS CALCULATED FROM THE ZERO CAPACITANCE LOAD AND THE
C     CAPACITANCE CORRECTION PROCEDURES DEVELOPED IN CHAPTER 6.  A
C     DESCRIPTION OF EACH INDIVIDUAL SURFACE WHICH MAKES UP THE BUILDING
C     SHELL IS INPUT TO THE PROGRAM, ALONG WITH GENERAL INFORMATION
C     ABOUT THE BUILDING.  MONTHLY-AVERAGE DAILY VALUES OF SOLAR
C     RADIATION AND AMBIENT TEMPERATURE ARE THE ONLY WEATHER DATA INPUT
C     REQUIRED.  THE PROGRAM HAS THE CAPABILITY OF ESTIMATING HEATING
C     LOADS FOR A BUILDING WITH A NO-STORAGE SOLAR SYSTEM AND COOLING
C     LOADS FOR A BUILDING WHICH IS COOLED BY VENTILATION WITH AMBIENT
C     AIR.  BUILDING LOADS FOR ZERO AND INFINITE THERMAL CAPACITANCE
C     ARE OUTPUT IN ADDITION TO THE LOADS FOR THE FINITE CAPACITANCE
C     VALUE INPUT TO THE PROGRAM.
C
C
C
      DIMENSION SNDC(12),CSDC(12),XKTB(12,25),SGMA(12),RCRIT(4,12,24),
     *XIMLT(12,24),ROBAR(12,24),RTILDA(12,24),BETA(12,24),DSH(12),
     *DDC(12,24),COLCRT(12,24),QTMP(12,24),NDY(12),HSTR(12,24),
     *HSTB(12,24),TMBP(12,24),RADTLT(12,24,20),DDH(12,24),HBAR(12),
     *TBAR(12),RDCL(12,24),ITITLE(4),DSC(12),DSH2(12),DSC2(12),
     &DSH3(12),DSC3(12),QTMP2(12,24),AVTSWG(12),DTEQN(12,24)
     *,DDH2(12,24),DDC2(12,24)
      COMMON /BLOCK1/ THBAR(12,24),IHSTP(12),IHSTRT(12)
      COMMON /BLOCK2/ BTA(20),AZM(20),UA(20),ALPH(20),ETR(12,24)
     *,IDX(12),ALAT,RHO
C
C       INITIALIZATION
C
      DATA PI/3.1415927/,RC/.0174533/,IDX/17,47,75,105,135,162,198,228,
     *258,288,318,344/,NDY/31,28,31,30,31,30,31,31,30,31,30,31/,
     *SGYR/0./,THT/1.698/,RHO/.2/,DSH/12*0./,DSC/12*0./,
     &TAV/0./,SGYR/0./,DSC3/12*0./,DSH3/12*0./
C
C       READ IN THE NUMBER OF ABSORBING SURFACES (NWALLS) AND THE
C       NUMBER OF TRANSMITTING SURFACES (NWNDWS).  A SURFACE CONSISTS
C       OF A PLANAR SECTION OF THE SHELL WHICH HAS CONSTANT SURFACE
C       PROPERTIES.  SINCE GLAZINGS ABSORB AND TRANSMIT SOLAR RADIATION,
C      EACH WINDOW IS BOTH AN ABSORBING AND TRANSMITTING SURFACE.
      READ(-,-) NWALLS,NWNDWS
C
C     READ IN BUILDING TYPE AND OUTPUT CONTROLS
C         IF ICOL=1, THERE IS A NO-STORAGE COLLECTOR ATTATCHED TO THE BUILDING.
C         IF IVENT=1, THE STRUCTURE IS COOLED BY VENTILATION WITH AMBIENT AIR.
C         IF ISKP=1, ONLY PRINT OUT BUILDING DESCRIPTION AND LOADS.
C          OTHERWISE, ALSO PRINT OUT TILTED SURFACE RADIATION AND
C          CRITICAL LEVELS.
C
```

```
      READ(-,-) ICOL,IVENT,ISKP
      IF (ICOL .NE. 1) GO TO 5
C
C     IF THERE IS A NO-STORAGE SOLAR COLLECTOR, INPUT COLLECTOR
C     DESCRIPTION
C       ACOL IS THE COLLECTOR AREA [M**2]
C       TAUC IS THE TRANSMITTANCE-ABSORPTANCE PRODUCT
C       ULC IS THE LOSS COEFFICIENT [W/M**2-C]
C       BTAC IS THE COLLECTOR SLOPE [DEGREES]
C       AZMC IS THE COLLECTOR AZIMUTH [DEGREES]
C       TRM IS THE INSIDE TEMPERATURE DURING THE HEATING SEASON [C]
C
      READ(-,-) ACOL,TAUC,ULC,BTAC,AZMC,TRM
5     IF (IVENT .NE. 1) GO TO 6
C
C     IF VENTILATION WITH AMBIENT AIR IS USED FOR COOLING, INPUT
C     DESCRIPTION
C       TRMC IS THE INSIDE TEMPERATURE DURING THE COOLING SEASON [C]
C       XMCP IS THE CAPACITANCE RATE OF THE VENTILATION STREAM [W/C]
C
      READ(-,-) TRMC,XMCP
6     CONTINUE
C
C     READ IN TITLE
C
      READ(-,500) ITITLE
500   FORMAT(4A6)
      DO 20 J=1,NWALLS
C
C     READ IN DESCRIPTIONS FOR ABSORBING SURFACES
C       BTA IS THE SLOPE [DEGREES]
C       AZM IS THE AZIMUTH [DEGREES]
C       UA IS THE CONDUCTANCE [W/C]
C       ALPH IS THE SOLAR ABSORPTANCE
C
20    READ(-,-) BTA(J),AZM(J),UA(J),ALPH(J)
      DO 30 J=1,NWNDWS
      I=J+NWALLS
C
C     READ IN DESCRIPTIONS FOR TRANSMITTING SURFACES
C       BTA IS THE SLOPE [DEGREES]
C       AZM IS THE AZIMUTH [DEGREES]
C       UA IS THE AREA [M**2]
C       ALPH IS THE TRANSMITTANCE-ABSORPTANCE PRODUCT
C
30    READ(-,-) BTA(I),AZM(I),UA(I),ALPH(I)
C
C     READ IN GENERAL BUILDING INFORMATION
C       UAINFL IS THE INFILTRATION CONDUCTANCE [W/C]
C       HO IS THE OUTER SURFACE LOSS COEFFICIENT [W/M**2-C]
C       TBASE IS THE HEATING BASE TEMPERATURE [C]
C       TBASEC IS THE COOLING BASE TEMPERATURE [C]
C       TAU IS THE THERMAL TIME CONSTANT FOR THE BUILDING, EQUAL TO
C         THE RATIO OF THE LUMPED EFFECTIVE THERMAL CAPACITANCE TO
C         THE OVERALL BUILDING CONDUCTANCE [HOURS]
```

```
C       ALAT IS THE LATITUDE OF THE LOCATION [DEGREES]
C
      READ(-,-) UAINFL,HO,TBASE,TBASEC,TAU,ALAT
      DO 4 I=1,12
C
C     READ IN 12 MONTLY-AVERAGE VALUES OF AMBIENT TEMPERATURE AND SOLAR
C     RADIATION
C       TBAR IS THE MONTHLY-AVERAGE DAILY AMBIENT TEMPERATURE [C]
C       HBAR IS THE MONTHLY-AVERAGE DAILY SOLAR RADIATION  [KJ/M**2]
C
4     READ(-,-) TBAR(I),HBAR(I)
C     UNITS CONVERSIONS
      ALAT=ALAT*RC
      NLP=NWALLS+NWNDWS
      DLTSET=TBASEC-TBASE
      IF (ICOL .NE. 1) GO TO 36
      NLP=NLP+1
      BTA(NLP)=BTAC
      AZM(NLP)=AZMC
36    DO 35 I=1,NLP
      BTA(I)=BTA(I)*RC
35    AZM(I)=AZM(I)*RC
C     FIND OVERALL BUILDING CONDUCTANCE
      UATOT=UAINFL
      DO 40 J=1,NWALLS
40    UATOT=UATOT+UA(J)
C     ESTIMATE STANDARD DEVIATION FOR MONTHLY-AVERAGE TEMPERATURE
      DO 31 J=1,12
      TAV=TAV+TBAR(J)/12.
31    SGYR=SGYR+TBAR(J)*TBAR(J)
32    SGYR=SQRT((SGYR-12.*TAV*TAV)/11.)
      DO 33 J=1,12
33    SGMA(J)=(1.45-.029*TBAR(J)+.0664*SGYR)*SQRT(FLOAT(NDY(J)))
C     CALCULATE MONTHLY-AVERAGE CLEARNESS INDEX VALUES
      DO 34 J=1,12
      D=FLOAT(IDX(J))
      DEC=23.45*RC*SIN(2.*PI*(284.+D)/365.)
      SNDC(J)=SIN(DEC)
      CSDC(J)=COS(DEC)
      WS=ACOS(-TAN(ALAT)*TAN(DEC))
      HR=37210.2*(1.+.033*COS(2.*PI*D/365.))*(COS(ALAT)*COS(DEC)*
     *SIN(WS)+WS*SIN(ALAT)*SIN(DEC))
      XKTB(J,25)=HBAR(J)/HR
      XKTB(J,25)=AMIN1(1.,XKTB(J,25))
C     FIND MONTHLY-AVERAGE HOURLY CLEARNESS INDEX VALUES AND MONTHLY-AVERAGE
C     HOURLY EXTRATERRESTRIAL RADIATION
      DO 34 I=1,24
      W1=0.2618*(FLOAT(I-1)-12.)
      W2=W1+0.2618
      WAVE=(W1+W2)/2.
      XKTB(J,I)=XKTB(J,25)*(0.409+0.5016*SIN(WS-1.047)+(0.6609-0.4767*
     *SIN(WS-1.047))*COS(WAVE))
      IF (W1 .GT. WS) GO TO 41
      IF (W2 .LT. -WS) GO TO 41
      IF (W1 .LT. -WS) IHSTRT(J)=I
```

```
      IF (W2 .GT. WS) IHSTP(J)=I
      IF (W1 .LT. -WS) W1=-WS
      IF (W2 .GT. WS) W2=WS
      ETR(J,I)=5168.08*(1.+.033*(COS(2.*PI*D/365.)))*(COS(ALAT)*COS
     *(DEC)*(SIN(W2)-SIN(W1))+(W2-W1)*SIN(ALAT)*SIN(DEC))
      GO TO 34
41    ETR(J,I)=0.
34    CONTINUE
C     ESTIMATE MONTHLY-AVERAGE HOURLY AMBIENT TEMPERATURE AND THE DIFFERENCE
C     BETWEEN THE MONTLY-AVERAGE TEMPERATURES FOR THE DAYTIME AND NIGHTTIME
C     PERIODS
      DO 70 I=1,12
      AMPL=25.8*XKTB(I,25)-5.21
      TDST=2.*PI*FLOAT(IHSTRT(I)-1)/24.
      TDSTP=2.*PI*FLOAT(IHSTP(I)-1)/24.
      AVTSWG(I)=AMPL*12./(PI*(IHSTP(I)-IHSTRT(I)+1))*(0.4632*(SIN(TDSTP
     *-3.805)-SIN(TDST-3.805))+0.0984*(SIN(2.*TDSTP-0.36)-SIN(2.*TDST
     *-0.36)))
      DO 70 J=1,24
      TSTR=2.*PI*FLOAT(J-1)/24.
70    THBAR(I,J)=TBAR(I)+AMPL*(0.4632*COS(TSTR-3.805)+0.0984*COS(2.*TSTR
     *-0.360)+0.0168*COS(3.*TSTR-0.822)+0.0138*COS(4.*TSTR-3.513))
C
C     DEGREE-DAY CALCULATIONS
C
      DO 50 J=1,12
      DO 50 I=1,24
      HSH=(TBASE-THBAR(J,I))/SGMA(J)
      HSH2=(THBAR(J,I)-TBASEC)/SGMA(J)
      HSH3=-HSH
      HSH4=-HSH2
      IF (IVENT.NE.1.OR.I.GT.IHSTP(J).OR.I.LT.IHSTRT(J)) GO TO 52
C     VENTILATION DEGREE-DAYS FOR COOLING SEASON (DAYTIME HOURS ONLY)
      HSH2=(THBAR(J,I)-TRMC)/SGMA(J)
      QTMP(J,I)=(1.+TANH(-THT*HSH2))/2.
      HSTR(J,I)=HSH2
      TBP=UATOT*TBASEC/(UATOT+XMCP)+XMCP*TRMC/(UATOT+XMCP)
      HSTB(J,I)=(THBAR(J,I)-TBP)/SGMA(J)
      QTMP2(J,I)=(1.+TANH(-THT*HSTB(J,I)))/2.
      HSH2=HSTB(J,I)
      TMBP(J,I)=SGMA(J)*(-THT*HSH2*TANH(-THT*HSH2)-ALOG(COSH(-THT*HSH2))
     *-0.693)/(THT*(TANH(-THT*HSH2)+1.))+THBAR(J,I)
      HSH2=HSTR(J,I)
C     HEATING DEGREE-DAYS
52    DDH(J,I)=SGMA(J)*FLOAT(NDY(J))*(HSH/2.+ALOG(COSH(THT*HSH))/3.396
     *+.2041)
C     HEATING DEGREE-DAYS FOR COOLING BASE TEMPERATURE
      DDH2(J,I)=SGMA(J)*FLOAT(NDY(J))*(HSH4/2.+ALOG(COSH(THT*HSH4))/3.39
     *6+.2041)
C     COOLING DEGREE-DAYS FOR HEATING BASE TEMPERATURE
      DDC2(J,I)=SGMA(J)*FLOAT(NDY(J))*(HSH3/2.+ALOG(COSH(THT*HSH3))/3.39
     *6+.2041)
C     COOLING DEGREE-DAYS
50    DDC(J,I)=SGMA(J)*FLOAT(NDY(J))*(HSH2/2.+ALOG(COSH(THT*HSH2))/3.396
     *+.2041)
```

```
      IF (ICOL .NE. 1) GO TO 51
C
C     IF THERE IS A NO-STORAGE COLLECTOR SYSTEM, CHECK TO SEE IF THE
C     COLLECTOR WILL OPERATE FOR THE MONTH AND HOUR OF THE DAY UNDER
C     CONSIDERATION
C
      CALL CKT(NLP,NWALLS,TBASE,TRM,HO,UATOT,ACOL,TAUC,ULC,RDCL)
C
51    NSURF=NLP
C
C     CALCULATE THE MONTHLY-AVERAGE HOURLY INCIDENT SOLAR RADIATION FOR
C     EACH OF THE BUILDING SURFACES.
C
      SNLT=SIN(ALAT)
      CSLT=COS(ALAT)
      DO 81 J=1,12
      D=FLOAT(IDX(J))
      DEC=23.45*RC*SIN(2.*PI*(284.+D)/365.)
      SDC=SIN(DEC)
      CDC=COS(DEC)
      DO 81 I=1,24
C     IF THE HOUR OF THE DAY IS BEFORE SUNRISE OR AFTER SUNSET, SKIP
C     CALCULATION
      IF (I .GT. IHSTP(J) .OR. I .LT. IHSTRT(J)) GO TO 81
      WS=ACOS(-TAN(ALAT)*TAN(DEC))
      DO 80 K=1,NSURF
C     HOUR ANGLES
      W1=0.2618*(FLOAT(I-1)-12.)
      W2=W1+0.2618
C     SURFACE DEPENDENT PARAMETERS
      BTAX=BTA(K)
      AZMX=AZM(K)
      CSBT=COS(BTAX)
      SNBT=SIN(BTAX)
      CSAZ=COS(AZMX)
      SNAZ=SIN(AZMX)
      SKYVF=(1.+CSBT)/2.
      GRNDVF=RHO*(1.-CSBT)/2.
C     MONTHLY-AVERAGE DIFFUSE RADIATION RELATIONSHIP OF ERBS (1980)
      DFR=1.317+((-1.76*XKTB(J,I)+3.372)*XKTB(J,I)-3.023)*XKTB(J,I)
      IF (DFR .GT. 1.) DFR=1.0
      IF (XKTB(J,I) .GT. 0.8) DFR=.156
C     DETERMINE FRACTION OF HOUR THERE IS BEAM RADIATION INCIDENT ON
C     THE SURFACE
      A=CSBT+TAN(ALAT)*CSAZ*SNBT
      B=COS(WS)*CSBT+TAN(DEC)*SNBT*CSAZ
      C=SNBT*SNAZ/CSLT
      IF (ABS(A) .LT. 1.0E-04) A=0.
      IF (ABS(B) .LT. 1.0E-04) B=0.
      ARG1=A*A-B*B+C*C
      IF (ARG1 .LT. 0.) GO TO 12
      WSR=AMIN1(WS,ACOS((A*B+C*SQRT(ARG1))/(A*A+C*C)))
      IF (A .GT. 0. .AND. B .GT. 0. .OR. A .GE. B) WSR=-WSR
      WSS=-AMIN1(WS,ACOS((A*B-C*SQRT(ARG1))/(A*A+C*C)))
      IF (A .GT. 0. .AND. B .GT. 0. .OR. A .GE. B) WSS=-WSS
```

```
      GO TO 11
12    WSR=-WS
      WSS=WS
11    CONTINUE
19    IF (WSS .LT. WSR) GO TO 22
      IF (W1 .LT. WSR) W1=WSR
      IF (W1 .GT. WSS) GO TO 24
      IF (W2 .LT. WSR) GO TO 24
      IF (W2 .GT. WSS) W2=WSS
      IF (ABS(W2-W1) .LT. 1.E-03) GO TO 24
      GO TO 23
22    IF (W1 .LT. -WS) W1=-WS
      IF (W1 .GT. WSS .AND. W2 .LT. WSR) GO TO 24
      IF (W2 .GT. WSS .AND. W1 .LT. WSS) W2=WSS
      IF (W1 .LT. WSR .AND. W2 .GT. WSR) W1=WSR
      IF (W1 .GT. WS) GO TO 24
      IF (W2 .LT. -WS) GO TO 24
      IF (W2 .GT. WS) W2=WS
      IF (ABS(W2-W1) .LT. 1.E-03) GO TO 24
23    CONTINUE
      WFRC=(W2-W1)/.2618
      CWH=((SIN(W2)-SIN(W1))/0.2618)
      SWH=((COS(W1)-COS(W2))/0.2618)
C     COSINE OF THE INCIDENCE ANGLE FOR THE TILTED SURFACE
      CST=WFRC*SDC*SNLT*CSBT-WFRC*SDC*CSLT*SNBT*CSAZ+CDC*CSLT*CSBT*CWH+
     &CDC*SNLT*SNBT*CSAZ*CWH+CDC*SNBT*SNAZ*SWH
C     COSINE OF THE INCIDENCE ANGLE FOR HORIZONTAL (ZENITH ANGLE)
      CSZ=CDC*CSLT*CWH+SDC*SNLT*WFRC
      IF (CST .LT. 1.0E-04) CST=0.0
      IF (CSZ .LT. 1.0E-06) GO TO 24
      RB2=CST/CSZ
      GO TO 21
24    RB2=0.
C     RATIO OF TILTED TO HORIZONTAL SURFACE RADIATION ASSUMING DIFFUSE SKY
C     AND GROUND REFLECTED RADIATION IS ISOTROPIC
21    R1=(1.-DFR)*RB2+DFR*SKYVF+GRNDVF
80    RADTLT(J,I,K)=R1*XKTB(J,I)*ETR(J,I)
81    CONTINUE
C
C     CALCULATE EFFECTIVE SURFACE RADIATION, CRITICAL LEVELS
C
      DO 90 I=1,12
      DO 90 J=1,24
      SUM=0.
      IF (J.GT.IHSTP(I) .OR. J .LT. IHSTRT(I)) GO TO 95
C     CALCULATE Z
      DO 92 K=1,NWALLS
92    SUM=SUM+UA(K)*ALPH(K)
      DO 93 K=1,NWNDWS
      IK=K+NWALLS
93    SUM=SUM+HO*ALPH(IK)*UA(IK)
C     TEST TO SEE IF NO-STORAGE COLLECTOR IS ON
      RTEST=0.
      IF (ICOL .EQ. 1) RTEST=ULC*(TRM-THBAR(I,J))/TAUC
      IF (RTEST .LT. 0.) RTEST=0.
```

```
      IF (ICOL .EQ. 1) COLCRT(I,J)=RTEST
      IF (ICOL .EQ. 1 .AND. RDCL(I,J) .GT. RTEST) SUM=SUM+HO*ACOL*TAUC
C     FIND CRITICAL LEVEL FOR SOL-AIR HEATING DEGREE-DAYS
      RCRIT(1,I,J)=UATOT*HO*(TBASE-THBAR(I,J))/SUM
      RCRIT(1,I,J)=AMAX1(RCRIT(1,I,J),0.)
      IF (ICOL .EQ. 1 .AND. RDCL(I,J) .GT. RTEST) RCRIT(1,I,J)=RCRIT(1
     *,I,J)+HO*ACOL*ULC*(TRM-THBAR(I,J))/(SUM)
      RCRIT(1,I,J)=AMAX1(RCRIT(1,I,J),0.)
C     FIND CRITICAL LEVEL FOR SOL-AIR COOLING DEGREE-DAYS
      RCRIT(2,I,J)=UATOT*HO*(TBASEC-THBAR(I,J))/SUM
      IF (IVENT .EQ. 1) RCRIT(2,I,J)=UATOT*HO*(TBASEC+XMCP*(TRMC-TMBP
     *(I,J))/UATOT-THBAR(I,J))/SUM
      RCRIT(2,I,J)=AMAX1(RCRIT(2,I,J),0.)
      XIMLT(I,J)=SUM/(HO*UATOT)
C     FIND EQUILIBRIUM TEMPERATURE DIFFERENCE FOR NIGHTTIME IN HEATING SEASON
95    HBH=(TBASE-THBAR(I,J))/SGMA(I)
      TALHB=SGMA(I)*(THT*HBH*TANH(THT*HBH)-ALOG(COSH(THT*HBH))-0.6931)
     */(THT*(TANH(THT*HBH)+1.))+THBAR(I,J)
      DTEQN(I,J)=TBASE-TALHB
      IF (J.GT.IHSTP(I) .OR. J .LT. IHSTRT(I)) GO TO 90
C     FIND CRITICAL LEVELS FOR HEATING LOAD CAPACITANCE CORRECTION
      RCRIT(3,I,J)=UATOT*HO*(TBASE-TALHB)/SUM
      RCRIT(3,I,J)=AMAX1(RCRIT(3,I,J),0.)
      DLTDAY=(IHSTP(I)-IHSTRT(I))+1.
      RCRIT(4,I,J)=RCRIT(3,I,J)+UATOT*HO*(DLTSET/(1.-EXP(-DLTDAY/TAU)
     *))/SUM
      RCRIT(4,I,J)=AMAX1(RCRIT(4,I,J),0.)
90    CONTINUE
C     FIND EFFECTIVE SURFACE INCIDENT RADIATION AND PROPERTIES
      DO 130 I=1,12
      DO 130 J=1,24
      SUM1=0.
      SUM2=0.
      IF (J.GT.IHSTP(I) .OR. J .LT. IHSTRT(I)) GO TO 130
      DO 132 K=1,NWALLS
      SUM1=SUM1+UA(K)*ALPH(K)*RADTLT(I,J,K)
132   SUM2=SUM2+UA(K)*ALPH(K)*RADTLT(I,J,K)*COS(BTA(K))
      DO 133 K=1,NWNDWS
      IK=K+NWALLS
      SUM1=SUM1+HO*UA(IK)*ALPH(IK)*RADTLT(I,J,IK)
133   SUM2=SUM2+HO*UA(IK)*ALPH(IK)*RADTLT(I,J,IK)*COS(BTA(IK))
      IF (ICOL .EQ. 1 .AND. RDCL(I,J) .GT. COLCRT(I,J)) SUM1=SUM1
     *+ACOL*TAUC*HO*RADTLT(I,J,NLP)
      IF (ICOL .EQ. 1 .AND. RDCL(I,J) .GT. COLCRT(I,J)) SUM2=SUM2
     *+ACOL*TAUC*HO*RADTLT(I,J,NLP)*COS(BTA(NLP))
      BETA(I,J)=SUM2/SUM1
      ROBAR(I,J)=SUM1/(XIMLT(I,J)*UATOT*HO)
      RTILDA(I,J)=ROBAR(I,J)/(XKTB(I,J)*ETR(I,J))
130   CONTINUE
      DO 140 I=1,12
      HBH=(TBASE-TBAR(I))/SGMA(I)
      QTBH=(1.+TANH(THT*HBH))/2.
      DO 140 J=1,24
      IF (J .GT. IHSTP(I) .OR. J .LT. IHSTRT(I)) GO TO 68
C     EVALUATION OF HOURLY UTILIZABILITY FUNCTION
```

```
      XC=RCRIT(1,I,J)/ROBAR(I,J)
      XC2=RCRIT(2,I,J)/ROBAR(I,J)
      CSBT=BETA(I,J)
      XK2=XKTB(I,J)
      RH2=RTILDA(I,J)
      CDC=CSDC(I)
      XM=1.85+.169*RH2/(XK2*XK2)-.0696*CSBT/(XK2*XK2)-.981*XK2/(CDC*CDC)
      IF (ICOL .NE. 1) GO TO 55
      XC3=COLCRT(I,J)/RADTLT(I,J,NLP)
      RBCL=RADTLT(I,J,NLP)/(XKTB(I,J)*ETR(I,J))
      XM2=1.85+.169*RBCL/(XK2*XK2)-.0696*COS(BTA(NLP))/(XK2*XK2)-.981*
     *XK2/(CDC*CDC)
      PHI3=PHIDC(XC3,XM2)
55    PHI=PHIDC(XC,XM)
C     SOL-AIR HEATING DEGREE-DAYS
53    DSH(I)=DSH(I)+DDH(I,J)-XIMLT(I,J)*FLOAT(NDY(I))*ROBAR(I,J)
     &*(1.-PHI)*QTBH
C     SOL-AIR COOLING DEGREE-DAYS FOR HEATING BASE TEMPERATURE
      DSH3(I)=DSH3(I)+DDC2(I,J)+XIMLT(I,J)*NDY(I)*ROBAR(I,J)*PHI
     **QTBH
C     SOL-AIR HEATING DEGREE-DAYS FOR NO-STORAGE SOLAR SYSTEM
      IF (ICOL .EQ. 1 .AND. RDCL(I,J) .GT. COLCRT(I,J)) DSH(I)=DSH(I)
     *+FLOAT(NDY(I))*ACOL*TAUC*RADTLT(I,J,NLP)*(1.-PHI3)/UATOT
      PHI2=PHIDC(XC2,XM)
      IF (IVENT .NE. 1) GO TO 63
C     VENTILATION SOL-AIR COOLING DEGREE-DAYS
      DSC(I)=DSC(I)+DDC(I,J)+FLOAT(NDY(I))*(SGMA(I)/2.*(XMCP+UATOT)/
     *UATOT*((ALOG(COSH(THT*HSTB(I,J)))-ALOG(COSH(THT*HSTR(I,J))))/
     *THT+(HSTR(I,J)-HSTB(I,J))*TANH(THT*HSTR(I,J)))+XIMLT(I,J)*ROBAR
     *(I,J)*PHI2+(1.-QTMP(I,J))*(TRMC-TBASEC))
      GO TO 140
C     SOL-AIR COOLING DEGREE-DAYS
63    DSC(I)=DSC(I)+DDC(I,J)+XIMLT(I,J)*FLOAT(NDY(I))*ROBAR(I,J)*PHI2
C     SOL-AIR HEATING DEGREE-DAYS FOR COOLING BASE TEMPERATURE
      DSC3(I)=DSC3(I)+DDH2(I,J)-XIMLT(I,J)*NDY(I)*ROBAR(I,J)*(1.-PHI2)
      GO TO 140
C     DEGREE-DAYS FOR NIGHTTIME PERIOD
68    DSH(I)=DSH(I)+DDH(I,J)
      DSC(I)=DSC(I)+DDC(I,J)
      DSH3(I)=DSH3(I)+DDC2(I,J)
      DSC3(I)=DSC3(I)+DDH2(I,J)
140   CONTINUE
C
C     CAPACITANCE CORRECTION PROCEDURE
C
      DO 150 I=1,12
      GAIN=0.
      DTNT=0.
      DO 151 J=1,24
      IF(J .GT. IHSTP(I) .OR. J .LT. IHSTRT(I)) GO TO 152
C     DAYTIME STORAGE OF EXCESS GAINS DURING HEATING SEASON
      XC1=RCRIT(3,I,J)/ROBAR(I,J)
      XC2=RCRIT(4,I,J)/ROBAR(I,J)
      CSBT=BETA(I,J)
      XK2=XKTB(I,J)
```

```
      RH2=RTILDA(I,J)
      CDC=CSDC(I)
      XM=1.85+.169*RH2/(XK2*XK2)-.0696*CSBT/(XK2*XK2)-.981*XK2/(CDC*CDC)
      PHI1=PHIDC(XC1,XM)
      PHI2=PHIDC(XC2,XM)
      GAIN=GAIN+ROBAR(I,J)*(PHI1-PHI2)*XIMLT(I,J)
      GO TO 151
152   DTNT=DTNT+DTEQN(I,J)
151   CONTINUE
      DLTDAY=(IHSTP(I)-IHSTRT(I))+1.
      DLTNIT=24.-DLTDAY
      QGND=UATOT*GAIN*(TAU/DLTDAY)*(1.-EXP(-DLTDAY/TAU))
C     ADDITIONAL NIGHTTIME LOSSES DUE TO DAYTIME STORAGE OF EXCESS GAINS
      DTRDY=QGND/(TAU*UATOT)
      DTRDY=AMAX1(0.,AMIN1(DTRDY,DLTSET))
      DTNT=DTNT/DLTNIT
      IF (ABS(DTNT) .LT. 1.0E-06) DTNT=1.0E-06
      XBR=DTRDY/DTNT
      DTDCHG=TAU*ALOG(1.+XBR)
      IF (DTDCHG .GT. DLTNIT) GO TO 153
      TELNT=DTNT*(TAU/DLTNIT)*(XBR-ALOG(1.+XBR))
      GO TO 154
153   TELNT=DTNT*(TAU/DLTNIT)*((1.+XBR)*(1.-EXP(-DLTNIT/TAU))
     *-(DLTNIT/TAU))
154   QLSN=UATOT*TELNT*DLTNIT
C     CORRECTION OF ZERO CAPACITANCE HEATING LOADS
      HBH=(TBASE-TBAR(I))/SGMA(I)
      QTBH=(1.+TANH(THT*HBH))/2.
      DSH2(I)=UATOT*DSH(I)-QTBH*NDY(I)*(QGND-QLSN)
      DSH2(I)=AMAX1(DSH2(I),0.)
      DSH(I)=UATOT*DSH(I)
C     STORAGE OF NIGHTTIME LOSSES DURING COOLING SEASON
      GSOL=0.
      DO 155 J=1,24
155   GSOL=GSOL+ROBAR(I,J)*XIMLT(I,J)
C     LOWER BOUNDS ON AMBIENT TEMPERATURE FOR COOLING LOADS TO EXIST
C     AND FOR MAXIMUM INTERIOR TEMPERATURE SWING
      TBSC=TBASEC-AVTSWG(I)*(1.+DLTDAY/DLTNIT)-GSOL/DLTDAY
      TBCD=TBASEC-DLTSET/(1.-EXP(-DLTNIT/TAU))
      QGED=0.
      DD1=0.
      DD2=0.
      QTB=0.
      QTB2=0.
C     CALCULATION OF REQUIRED BASE TEMPERATURE VALUES
      TBSC2=TBASEC-GSOL/DLTDAY+AVTSWG(I)
      DO 156 J=1,24
      IF (J .GT. IHSTP(I) .OR. J .LT. IHSTRT(I)) GO TO 157
      HBSC=(TBSC2-THBAR(I,J))/SGMA(I)
      HBC=(TBASEC+AVTSWG(I)*(1.+DLTDAY/DLTNIT)-THBAR(I,J))/SGMA(I)
      TAGCB=SGMA(I)*(THT*HBC*TANH(THT*HBC)+ALOG(COSH(THT*HBSC))-THT*
     *HBSC*TANH(THT*HBSC)-ALOG(COSH(THT*HBC)))/(THT*(TANH(THT*HBC)-
     *TANH(THT*HBSC)))+THBAR(I,J)
C     EXCESS GAINS FOR WARMUP DURING DAYTIME PERIOD FOLLOWING NIGHTTIME
C     COOLDOWN
```

```
      XC=(TBASEC-TAGCB)/(XIMLT(I,J)*ROBAR(I,J))
      XC=AMAX1(XC,0.)
      CSBT=BETA(I,J)
      XK2=XKTB(I,J)
      RH2=RTILDA(I,J)
      CDC=CSDC(I)
      XM=1.85+.169*RH2/(XK2*XK2)-.0696*CSBT/(XK2*XK2)-.981*XK2/(CDC*CDC)
      PHI=PHIDC(XC,XM)
      QGED=QGED+ROBAR(I,J)*PHI*XIMLT(I,J)
      GO TO 156
157   IF(TBSC .GE. TBCD) GO TO 159
C     EXCESS NIGHTTIME LOSSES WHEN INTERIOR TEMPERATURE REACHES HEATING
C     SETPOINT
      H1=(TBASEC-THBAR(I,J))/SGMA(I)
      H2=(TBCD-THBAR(I,J))/SGMA(I)
      H3=(TBSC-THBAR(I,J))/SGMA(I)
      DD1=DD1+SGMA(I)*(H1/2.+ALOG(COSH(THT*H1))/3.396+.2041)
      DD2=DD2+SGMA(I)*(H2/2.+ALOG(COSH(THT*H2))/3.396+.2041)
      QTB=QTB+(1.+TANH(THT*H3))/2.
      QTB2=QTB2+(1.+TANH(THT*H1))/2.
      GO TO 156
C     EXCESS NIGHTTIME LOSSES WHEN INTERIOR TEMPERATURE DOES NOT REACH
C     HEATING SETPOINT
159   H1=(TBASEC-THBAR(I,J))/SGMA(I)
      H2=(TBSC-THBAR(I,J))/SGMA(I)
      DD1=DD1+SGMA(I)*(H1/2.+ALOG(COSH(THT*H1))/3.396+.2041)
      DD2=DD2+SGMA(I)*(H2/2.+ALOG(COSH(THT*H2))/3.396+.2041)
      QTB=QTB+(1.+TANH(THT*H2))/2.
      QTB2=QTB2+(1.+TANH(THT*H1))/2.
156   CONTINUE
C     STORAGE OF NIGHTTIME LOSSES FOR MONTH
      IF(TBSC .GE. TBCD) GO TO 158
      DTRN=(1.-EXP(-DLTNIT/TAU))*(DD1/DLTNIT-DD2/DLTNIT-QTB/DLTNIT*
     *DLTSET/(1.-EXP(-DLTNIT/TAU)))
      GO TO 160
158   DTRN=(1.-EXP(-DLTNIT/TAU))*(DD1/DLTNIT-DD2/DLTNIT-QTB/DLTNIT*
     *(GSOL/DLTDAY+AVTSWG(I)*(1.+DLTDAY/DLTNIT)))
C     ADDITIONAL DAYTIME GAINS FOR AVERAGE DAY OF MONTH
160   TEQD=QGED/DLTDAY
      IF (ABS(TEQD) .LT. 1.0E-06) TEQD=1.0E-06
      XBRC=DTRN/TEQD
      DTCHG=TAU*ALOG(1.+XBRC)
      IF (DTCHG .GT. DLTDAY) GO TO 161
      QGD=TEQD*(TAU/DLTDAY)*(XBRC-ALOG(1.+XBRC))
      GO TO 162
161   QGD=TEQD*(TAU/DLTDAY)*((1.+XBRC)*(1.-EXP(-DLTDAY/TAU))-(DLTDAY
     */TAU))
162   QGD=QGD*UATOT*NDY(I)*(QTB2/DLTNIT-QTB/DLTNIT)*DLTDAY
C     CORRECTION OF ZERO CAPACITANCE COOLING LOADS FOR THE EFFECT OF
C     BUILDING THERMAL CAPACITANCE
      QGLN=UATOT*TAU*DTRN*NDY(I)
      DSC2(I)=UATOT*DSC(I)-QGLN+QGD
      DSC2(I)=AMAX1(DSC2(I),0.)
150   DSC(I)=UATOT*DSC(I)
      CONVERT ANGLES BACK TO DEGREES
```

```
      DO 170 I=1,NLP
      BTA(I)=FLOAT(IFIX(BTA(I)/RC+0.5))
      IF (AZM(I) .GE. 0.) GO TO 171
      AZM(I)=FLOAT(IFIX(AZM(I)/RC-0.5))
      GO TO 170
171   AZM(I)=FLOAT(IFIX(AZM(I)/RC+0.5))
170   CONTINUE
C     CALCULATE LOADS FOR INFINITE THERMAL CAPACITANCE, CONVERT UNITS FOR
C     LOADS TO MJ
      DSC1T=0.
      DSH1T=0.
      DSC2T=0.
      DSH2T=0.
      DSC3T=0.
      DSH3T=0.
      DO 180 I=1,12
      DSC3(I)=UATOT*DSC3(I)
      DSH3(I)=UATOT*DSH3(I)
      DSC3(I)=AMAX1(0.,(DSC(I)-DSC3(I)))
      DSH3(I)=AMAX1(0.,(DSH(I)-DSH3(I)))
      DSH(I)=DSH(I)*3.6E-06
      DSC(I)=DSC(I)*3.6E-06
      DSH2(I)=DSH2(I)*3.6E-06
      DSC2(I)=DSC2(I)*3.6E-06
      DSH3(I)=DSH3(I)*3.6E-06
      DSC3(I)=DSC3(I)*3.6E-06
      DSC1T=DSC1T+DSC(I)
      DSH1T=DSH1T+DSH(I)
      DSC2T=DSC2T+DSC2(I)
      DSH2T=DSH2T+DSH2(I)
      DSC3T=DSC3T+DSC3(I)
180   DSH3T=DSH3T+DSH3(I)
C
C     OUTPUTS
C
C     TITLE
      WRITE(-,501) ITITLE
      WRITE(-,290)
      WRITE(-,300)
C     BUILDING DESCRIPTION
      DO 200 J=1,NWALLS
200   WRITE(-,301) BTA(J),AZM(J),UA(J),ALPH(J)
      WRITE(-,302)
      DO 201 J=1,NWNDWS
      I=J+NWALLS
201   WRITE(-,301) BTA(I),AZM(I),UA(I),ALPH(I)
      WRITE(-,303) UAINFL,HO,TBASE,TBASEC,UATOT
      IF (ISKP .EQ. 1) GO TO 399
C     OUTPUT (IF REQUESTED) MONTHLY-AVERAGE TILTED SURFACE RADIATION,
C     EFFECTIVE SURFACE RADIATION, CRITICAL LEVELS FOR HEATING AND
C     COOLING SOL-AIR DEGREE-DAY CALCULATIONS
      WRITE(-,310)
      WRITE(-,311)
      DO 202 J=1,NSURF
      WRITE(-,312) J
```

```
      DO 202 I=1,24
202   WRITE(-,313)(RADTLT(K,I,J),K=1,12)
      WRITE(-,314)
      DO 203 I=1,24
203   WRITE(-,315)(ROBAR(J,I),J=1,12)
      WRITE(-,316) TBASE
      WRITE(-,322)
      DO 204 I=1,24
204   WRITE(-,317)(RCRIT(1,J,I),J=1,12)
      WRITE(-,318) TBASEC
      DO 205 I=1,24
205   WRITE(-,319)(RCRIT(2,J,I),J=1,12)
399   CONTINUE
C     OUTPUT MONTHLY AND ANNUAL HEATING AND COOLING LOADS FOR ZERO,
C     FINITE AND INFINITE BUILDING THERMAL CAPACITANCE VALUES
      WRITE(-,323)
      WRITE(-,320)
      DO 206 I=1,12
206   WRITE(-,321) DSH(I),DSH2(I),DSH3(I),DSC(I),DSC2(I),DSC3(I)
      WRITE(-,321) DSH1T,DSH2T,DSH3T,DSC1T,DSC2T,DSC3T
501   FORMAT(1X,///,20X,4A6)
290   FORMAT(1X,////,30X,'BUILDING DESCRIPTION')
300   FORMAT(1X,//,3X,'SLOPE',2X,'AZIMUTH',2X,'CONDUCTANCE, W/C',2X,
     *'SOLAR ABSORPTANCE')
301   FORMAT('  ',F5.1,4X,F5.1,6X,F8.2,12X,F5.3)
302   FORMAT(1X,//,3X,'SLOPE',2X,'AZIMUTH',2X,'WINDOW AREA, M**2',2X,
     *'TRANSMITTANCE-ABSORPTANCE')
303   FORMAT('0INFIL.=',1X,F7.2,5X,'HO=',1X,F5.2,5X,'HEATING TB=',1X,
     *F5.1,5X,'COOLING TB=',1X,F5.1,5X,'UATOT=',1X,F8.2)
310   FORMAT(1X,////,30X,'RADIATION STATISTICS')
311   FORMAT(1X,//,9X,'MONTHLY-AVERAGE HOURLY TILTED SURFACE RADIATION')
312   FORMAT(' FOR SURFACE',1X,I2,5X,'JAN',5X,'FEB',5X,'MAR',5X,'APR',5X
     *,'MAY',5X,'JUN',5X,'JUL',5X,'AUG',5X,'SEP',5X,'OCT',5X,'NOV',5X,
     *'DEC')
313   FORMAT(16X,12(2X,F6.1))
314   FORMAT(1X,////,10X,'EFFECTIVE SURFACE AVERAGE RADIATION')
315   FORMAT(16X,12(2X,F6.1))
322   FORMAT(1X,////,10X,'BUILDING CRITICAL RADIATION LEVELS')
316   FORMAT(' HEATING TB=',1X,F5.1,5X,'JAN',5X,'FEB',5X,'MAR',5X,'APR',
     *5X,'MAY',5X,'JUN',5X,'JUL',5X,'AUG',5X,'SEP',5X,'OCT',5X,'NOV',5X,
     *'DEC')
317   FORMAT(18X,12(2X,F6.1))
318   FORMAT(' COOLING TB=',1X,F5.1,5X,'JAN',5X,'FEB',5X,'MAR',5X,'APR',
     *5X,'MAY',5X,'JUN',5X,'JUL',5X,'AUG',5X,'SEP',5X,'OCT',5X,'NOV',5X,
     *'DEC')
319   FORMAT(18X,12(2X,F6.1))
320   FORMAT(1X,////,1X,'ZERO CAP HEATING',2X,'FINITE CAP HEATING',2X
     *,'INFINITE CAP HEATING',2X,'ZERO CAP COOLING',2X,'FINITE CAP COOLI
     *NG',2X,'INFINITE CAP COOLING')
321   FORMAT(6X,F7.2,11X,F7.2,15X,F7.2,12X,F7.2,12X,F7.2,16X,F7.2)
323   FORMAT(1X,////,20X,'BUILDING LOADS, GJ')
      STOP
      END
```

SUBROUTINE CKT

```
C     THIS SUBROUTINE SOLVES FOR THE HOURLY CLEARNESS INDEX VALUE
C     WHERE THE SOLAR GAINS DUE TO ABSORPTION BY OUTER SURFACES, TRANSMISSION BY
C     WINDOWS, AND COLLECTION BY A NO-STORAGE SOLAR SYSTEM JUST EQUAL THE RATE OF
C     HEAT LOSSES TO AMBIENT.  A SECANT METHOD IS USED TO FIND THE SOLUTION.
C     THIS VALUE OF CLEARNESS INDEX IS USED TO DECIDE WHEITHER THE NO-STORAGE
C      SYSTEM WILL BE ABLE TO SUPPLY ANY HEATING ENERGY TO THE BUILDING FOR THE
C     HOUR OF THE DAY AND MONTH UNDER CONSIDERATION.
C
      SUBROUTINE CKT(NSURF,NWALLS,TBASE,TRM,HO,UATOT,ACOL,TAUC,ULC,RDCL)
      DIMENSION RDCL(12,24),XKCT(12,24),SRAD(12,24),TOTQ(12,24)
      COMMON /BLOCK1/ THBAR(12,24),IHSTP(12),IHSTRT(12)
      DATA EPS/0.001/
      DO 10 J=1,12
C     LOOP OVER ALL MONTHS AND HOURS OF THE DAY
      DO 10 I=1,24
      NIT=0
C     IF THE HOUR IS DURING THE NIGHT, SKIP THE CALCULATION PROCEDURE
      IF (I .GT. IHSTP(J) .OR. I .LT. IHSTRT(J)) GO TO 15
C     FIND THE HEAT LOSS RATE TO AMBIENT
      T1DF=TBASE-THBAR(J,I)
      T2DF=TRM-THBAR(J,I)
      T1DF=(ABS(T1DF)+T1DF)/2.
      T2DF=(ABS(T2DF)+T2DF)/2.
      TQT=HO*UATOT*T1DF+HO*ACOL*ULC*T2DF
C     INITIAL GUESSES FOR CLEARNESS INDEX
      XKG1=.1
      XKG2=.2
      RDSM1=SUMRAD(NSURF,NWALLS,HO,ACOL,TAUC,ULC,XKG1,J,I,RDCOL)
C     F1 AND F2 ARE THE INTIAL FUNCTION VALUES.  SOLUTION IS THE GLEARNESS
C     INDEX WHICH RESULTS IN A VALUE OF F2 OF ZERO
      F1=RDSM1-TQT
C     SECANT METHOD
11    RDSM2=SUMRAD(NSURF,NWALLS,HO,ACOL,TAUC,ULC,XKG2,J,I,RDCOL)
      F2=RDSM2-TQT
C     CHECK FOR LOSS OF PRECISION
      IF (ABS(F1-F2) .LT. 1.0E-07) GO TO 13
      XKGN=XKG2-F2*(XKG2-XKG1)/(F2-F1)
C     CHECK FOR CONVERGENCE
      IF (ABS(XKGN-XKG2) .LT. EPS) GO TO 12
      XKG1=XKG2
      F1=F2
      XKG2=XKGN
      NIT=NIT+1
C     CHECK FOR FAILURE TO CONVERGE
      IF (NIT .GT. 100) GO TO 14
      GO TO 11
13    WRITE(-,210) NIT
210   FORMAT(' LOSS OF PRECISION AFTER',2X,I3,2X,'ITERATIONS')
C
C     SET OUTPUTS
      RDCL(J,I)=RDCOL
```

```
      XKCT(J,I)=XKG2
      SRAD(J,I)=RDSM2
      TOTQ(J,I)=TQT
      GO TO 10
14    WRITE(-,220)
220   FORMAT(' FAILURE TO CONVERGE IN 100 ITERATIONS')
      RDCL(J,I)=RDCOL
      XKCT(J,I)=XKG2
      SRAD(J,I)=RDSM2
      TOTQ(J,I)=TQT
      GO TO 10
12    RDCL(J,I)=RDCOL
      XKCT(J,I)=XKG2
      SRAD(J,I)=RDSM2
      TOTQ(J,I)=TQT
      GO TO 10
15    RDCL(J,I)=0.
      XKCT(J,I)=0.
      SRAD(J,I)=0.
      TOTQ(J,I)=0.
10    CONTINUE
      RETURN
      END
```

FUNCTION SUMRAD

```
C     THIS FUNCTION ROUTINE IS USED BY THE SUBROUTINE CKT TO SUM UP THE
C     SOLAR ENERGY GAINS FOR A BUILDING DUE TO ABSORPTION BY OUTER SURFACES,
C     COLLECTION BY A NO-STORAGE SOLAR SYSTEM WHICH HEATS THE BUILDING
C     AND TRANSMISSION BY WINDOWS.  THE INFORMATION DESCRIBING EACH OF THE
C     ABSORBING AND TRANSMITTING SURFACES IS CONTAINED IN THE COMMON BLOCK
C     BLOCK2.  THE GAINS ARE SUMMED FOR A PARTICULAR VALUE OF HOURLY CLEARNESS
C     INDEX, XKG, WHICH IS SUPPLIED BY CKT.
C
      FUNCTION SUMRAD(NS,NW,HO,AC,TAUC,ULC,XKG,J,I,RDCOL)
      DIMENSION RDSURF(20)
      COMMON /BLOCK2/ BTA(20),AZM(20),UA(20),ALPH(20),ETR(12,24),IDX(12)
     *,ALAT,RHO
      DATA PI/3.1415927/,RC/.0174533/
C     SUM IS THE TOTAL SOLAR GAINS FOR THE BUILDING DUE TO ABSORPTION AND
C     TRANSMISSION BY SURFACES.
      SUM=0.
C     GEOMETRICAL PARAMETERS
      SNLT=SIN(ALAT)
      CSLT=COS(ALAT)
      D=FLOAT(IDX(J))
      DEC=23.45*RC*SIN(2.*PI*(284.+D)/365.)
      SDC=SIN(DEC)
      CDC=COS(DEC)
      WS=ACOS(-TAN(ALAT)*TAN(DEC))
      DO 80 K=1,NS
C
C     FIND THE INCIDENT RADIATION FOR EACH SURFACE
C
C     HOUR ANGLES
      W1=0.2618*(FLOAT(I-1)-12.)
      W2=W1+0.2618
C     SURFACE PARAMETERS
      BTAX=BTA(K)
      AZMX=AZM(K)
      CSBT=COS(BTAX)
      SNBT=SIN(BTAX)
      CSAZ=COS(AZMX)
      SNAZ=SIN(AZMX)
      SKYVF=(1.+CSBT)/2.
      GRNDVF=RHO*(1.-CSBT)/2.
C     FIND THE HOURLY DIFFUSE RADIATION USING THE RELATIONSHIP OF ERBS (1980)
      DFR=1.0-0.09*XKG
      IF(XKG .GT. 0.22) DFR=.9511+(((12.336*XKG-16.638)*XKG+4.388)*XKG
     *-.1604)*XKG
      IF (XKG .GT. 0.8) DFR=0.165
C     FIND THE FRACTION OF THE HOUR BEAM RADIATION IS INCIDENT ON THE SURFACE
      A=CSBT+TAN(ALAT)*CSAZ*SNBT
      B=COS(WS)*CSBT+TAN(DEC)*SNBT*CSAZ
      C=SNBT*SNAZ/CSLT
      IF (ABS(A) .LT. 1.0E-04) A=0.
      IF (ABS(B) .LT. 1.0E-04) B=0.
      ARG1=A*A-B*B+C*C
```

```
      IF (ARG1 .LT. 0.) GO TO 12
      WSR=AMIN1(WS,ACOS((A*B+C*SQRT(ARG1))/(A*A+C*C)))
      IF (A .GT. 0. .AND. B .GT. 0. .OR. A .GE. B) WSR=-WSR
      WSS=-AMIN1(WS,ACOS((A*B-C*SQRT(ARG1))/(A*A+C*C)))
      IF (A .GT. 0. .AND. B .GT. 0. .OR. A .GE. B) WSS=-WSS
      GO TO 11
12    WSR=-WS
      WSS=WS
11    CONTINUE
19    IF (WSS .LT. WSR) GO TO 22
      IF (W1 .LT. WSR) W1=WSR
      IF (W1 .GT. WSS) GO TO 24
      IF (W2 .LT. WSR) GO TO 24
      IF (W2 .GT. WSS) W2=WSS
      IF (ABS(W2-W1) .LT. 1.E-03) GO TO 24
      GO TO 23
22    IF (W1 .LT. -WS) W1=-WS
      IF (W1 .GT. WSS .AND. W2 .LT. WSR) GO TO 24
      IF (W2 .GT. WSS .AND. W1 .LT. WSS) W2=WSS
      IF (W1 .LT. WSR .AND. W2 .GT. WSR) W1=WSR
      IF (W1 .GT. WS) GO TO 24
      IF (W2 .LT. -WS) GO TO 24
      IF (W2 .GT. WS) W2=WS
      IF (ABS(W2-W1) .LT. 1.E-03) GO TO 24
23    CONTINUE
      WFRC=(W2-W1)/.2618
      CWH=((SIN(W2)-SIN(W1))/0.2618)
      SWH=((COS(W1)-COS(W2))/0.2618)
C     COSINE OF THE INCIDENCE ANGLE FOR BEAM RADIATION ON THE SURFACE
      CST=WFRC*SDC*SNLT*CSBT-WFRC*SDC*CSLT*SNBT*CSAZ+CDC*CSLT*CSBT*CWH+
     &CDC*SNLT*SNBT*CSAZ*CWH+CDC*SNBT*SNAZ*SWH
C     COSINE OF THE INCIDENCE ANGLE FOR BEAM RADIATION ON THE HORIZONTAL
      CSZ=CDC*CSLT*CWH+SDC*SNLT*WFRC
      IF (CST .LT. 1.0E-04) CST=0.0
      IF (CSZ .LT. 1.0E-06) GO TO 24
      RB2=CST/CSZ
      GO TO 21
24    RB2=0.
C     RATIO OF TILTED SURFACE TO HORIZONTAL SURFACE TOTAL HOURLY RADIATION
C     ASSUMING ISOTROPIC DIFFUSE RADIATION
21    R1=(1.-DFR)*RB2+DFR*SKYVF+GRNDVF
80    RDSURF(K)=R1*XKG*ETR(J,I)
C     RDCOL IS THE INCIDENT RADIATION LEVEL FOR THE COLLECTOR FOR THE HOURLY
C     CLEARNESS INDEX PROVIDED BY CKT
      RDCOL=RDSURF(NS)
C     SUM RADIATION ABSORBED BY OUTER SURFACES
      DO 30 JJ=1,NW
30    SUM=SUM+UA(JJ)*ALPH(JJ)*RDSURF(JJ)
      NWD=NS-NW-1
C     SUM RADIATION TRANSMITTED BY WINDOWS
      DO 31 II=1,NWD
      JJ=II+NW
31    SUM=SUM+HO*ALPH(JJ)*UA(JJ)*RDSURF(JJ)
C     SUM RADIATION COLLECTED BY SOLAR SYSTEM
      SUM=SUM+AC*TAUC*HO*RDSURF(NS)
      SUMRAD=SUM
      RETURN
      END
```

FUNCTION PHIDC

```
C     THIS FUNCTION ROUTINE EVALUATES THE HOURLY UTILIZABILITY FOR SOLAR
C     RADIATION USING THE RELATIONSHIP DEVELOPED BY CLARK ET AL. (1983).
C     THE RELATIONSHIP IS A FUNCTION OF THE DIMENSIONLESS CRITICAL LEVEL,
C     XC, WHICH IS THE RATIO OF THE CRITICAL RADIATION LEVEL TO THE MONTHLY-
C     AVERAGE HOURLY INCIDENT RADIATION FOR THE SURFACE, AND THE MAXIMUM
C     VALUE OF XC, DENOTED BY XM.  THE RELATIONSHIP FOR XM IS GIVEN IN
C     THE MAIN ROUTINE.
      FUNCTION  PHIDC(XC,XM)
      IF (XC .LT. 1.0E-06) GO TO 10
      IF (XC .GE. XM) GO TO 11
      IF (XM .GT. 1.99 .AND. XM .LT. 2.01) GO TO 12
      A=(XM-1.)/(2.-XM)
      PHIDC=ABS(ABS(A)-SQRT(A*A+(1.+2.*A)*(1.-XC/XM)**2))
      GO TO 13
10    PHIDC=1.
      GO TO 13
12    PHIDC=(1.-XC/XM)**2
      GO TO 13
11    PHIDC=0.
13    RETURN
      END
```

PROGRAM SOLBINGEN

```
      REAL NTSA(100,100),MTSA(100,100),LAMDA(53),ETR(12,24),RB(12,24),
     *RHO(12),TB(12,24),KT(12,25),HO(12,24),SGHR(12,24),SNDC(12),
     *CSDC(12),SNWH(24),CSWH(24),TAV(24),SGYR(24),NDY(12),IDX(12),AKT(3)
     *,BKT(3),KTMX,KTX,TBM(12),TX(100),TSX(100),PKT(100,24),TYX(100)
      INTEGER HST,HSTP,MB(2),ME(2),IHS(12),IHSP(12)
      DATA NDY/31.,28.,31.,30.,31.,30.,31.,31.,30.,31.,30.,31./,TAV/24*0
     *./,SGYR/24*0./,RC/.0174533/,PI/3.1415927/,THT/1.698/,IDX/17.,
     *47.,75.,105.,135.,162.,198.,228.,258.,288.,318.,344./,RHO/.2,.2,
     *.2,.2,.2,.2,.2,.2,.2,.2,.2,.2/,KTMX/.864/,LAMDA/1.0E-08,.0481,
     *.2848,.5158,.7419,.9637,1.1819,1.3971,1.6097,1.8204,2.0296,2.2378,
     *2.4454,2.6529,2.8607,3.0693,3.279,3.4905,3.7042,3.9205,4.14
     *,4.3632,4.5909,4.8236,5.0621,5.3071,5.5596,5.8206,6.0911,6.3724
     *,6.666,6.9735,7.2968,7.6382,8.0002,8.386,8.7992,9.2442,9.7262,
     *10.2516,10.8284,11.4661,12.1769,12.976,13.8827,14.9223,16.1276,
     *17.5433,19.2306,21.2764,23.8093,27.0268,31.2497/,NTSA/10000*0./,
     *MTSA/10000*0./,AKT/3*0./,BKT/3*0./,PKT/2400*0./,TBM/12*0./,TBY/0./
     *,IDSH/'-----*'/,YHRS/0./,AYHRS/0./
C
C
C     THIS PROGRAM CALCULATES THE NUMBER OF HOURS OR THE PROBABILITY THAT
C     THE AMBIENT TEMPERATURE WAS IN A PARTICULAR BIN AND THE SOL-AIR TEMPERATURE
C     WAS ALSO IN A CERTAIN BIN FOR A CHOSEN GRID OF BINS.  THE METHOD
C     USED DEPENDS UPON A DISTRIBUTION FUNCTION FOR AMBIENT TEMPERATURE
C     DEVELOPED BY ERBS AND A DISTRIBUTION FUNCTION FOR SOLAR RADIATION
C     DEVELOPED BY HOLLANDS AND HUGET (1983).  IT IS ASSUMED THAT THE
C     DISTRIBUTIONS OF SOLAR RADIATION AND AMBIENT TEMPERATURE ARE INDEPENDENT
C     OF EACH OTHER.  THE MONTHLY-AVERAGE AMBIENT TEMPERATURE AND SOLAR
C     RADIATION (GLOBAL) ARE REQUIRED FOR  THE DAY.  THE
C     FOLLOWING INPUTS ARE ALSO REQUIRED:
C
C     NBX-NUMBER OF AMBIENT TEMPERATURE BINS FOR MONTHLY CALCULATIONS
C     NYBX-NUMBER OF AMBIENT TEMPERATURE BINS FOR ANNUAL CALCULATIONS
C     NBY-NUMBER OF BINS FOR SOL-AIR TEMPERATURE
C     MST-STARTING MONTH (1-12)
C     MSTP-ENDING MONTH (1-12)
C     HST-STARTING HOUR
C     HSTP-ENDING HOUR
C     DELT-BIN SIZE FOR BOTH AMBIENT AND SOL-AIR TEMPERATURES
C     IPRT-PRINTER CONTROL  0=ONLY ANNUAL BIN DATA, 1=MONTHLY AND
C     ANNUAL BIN DATA, 2=ONLY MONTHLY BIN DATA
C     IRO-GROUND REFLECTIVITY CONTROL  0=USE DEFAULT VALUES (.2 FOR ALL
C     MONTHS), -1=READ IN 12 MONTHLY VALUES
C     IHO-OUTSIDE FILM COEFFICIENT CONTROL  1=READ IN SINGLE VALUE, 0=
C     READ IN 12 MONTHLY VALUES, -1=READ IN 24 HOURLY VALUES FOR EACH OF
C     12 MONTHS
C     IBU-BIN UNITS CONTROL  0=UNITS ARE HOURS, -1=UNITS ARE HOURS/HOURS
C     ALAT-SITE LATITUDE, DEGREES
C     SLP-SURFACE SLOPE, DEGREES
C     AZM-SURFACE AZIMUTH, DEGREES
C     ALPHA-SURFACE ABSORPTANCE
C
```

```
      READ(-,-) NBX,NYBX,NBY,MST,MSTP,HST,HSTP,DELT,IPRT
      READ(-,-) IRO,IHO,IBU,ALAT,SLP,AZM,ALPHA,IHPK
C
C     CALCULATE NUMBER OF MONTHS BIN DATA ARE TO BE ESTIMATED FOR
      NMON=MSTP-MST+1
      IF (MST .GT. MSTP) NMON=13-MST+MSTP
      NHRS=HSTP-HST+1
      IF (IRO  .GE. 0) GO TO 2
C     READ 12 MONTHLY VALUES OF GROUND REFLECTIVITY
      READ(-,-) (RHO(J),J=1,12)
2     IF (IHO .LT. 0)  GO TO 6
      IF (IHO .EQ. 0)  GO TO 4
C     READ SINGLE VALUE OF CONVECTION COEFFICIENT
      READ(-,-) SHO
      DO 3 J=1,12
      DO 3 I=1,24
3     HO(J,I)=SHO
      GO TO 10
C     READ 12 MONTHLY VALUES OF CONVECTION COEFFICIENT
4     READ(-,-)(HO(I,1),I=1,12)
      DO 5 J=2,24
      DO 5 I=1,12
5     HO(I,J)=HO(I,1)
      GO TO 10
C     READ HOURLY AND MONTHLY VALUES OF CONVECTION COEFFICIENT
6     DO 7 J=1,24
7     READ(-,-)(HO(I,J),I=1,12)
C     UNITS CONVERSION
10    ALAT=ALAT*RC
      AZM=AZM*RC
      SLP=SLP*RC
C     READ LOGICAL UNIT NUMBERS WHICH MONTHLY-AVERAGE AMBIENT
C     TEMPERATURE AND SOLAR CLEARNESS INDEX (kT) ARE TO BE READ FROM
      READ(-,-) L1,L2,L3
C     READ MONTHLY-AVERAGE DAILY AMBIENT TEMPERATURE
11    READ(L1,101) (TBM(I),I=1,12)
C     CONVERT TEMPERATURES FROM CENTIGRADE TO FAHRENHEIT
      DO 52 I=1,12
52    TBM(I)=1.8*TBM(I)+32.
C     READ MONTHLY-AVERAGE VALUES OF KT
12    READ(L2,102) (KT(I,25),I=1,12)
      CALL CLOSE(L1,1)
      CALL CLOSE(L2,1)
C     CENTER AMBIENT TEMPERATURE AROUND AVERAGE AMBIENT TEMPERATURES
      DO 50 J=1,24
      DO 50 I=1,12
50    TBY=TBY+TBM(I)/12.
C     ESTIMATE MONTHLY-AVERAGE HOURLY VALUES OF AMBIENT TEMPERATURE
      DO 54 I=1,12
      AMPL=1.8*(25.8*KT(I,25)-5.21)
      DO 54 J=1,24
      TSTR=2.*PI*FLOAT(J-1)/24.
54    TB(I,J)=TBM(I)+AMPL*(0.4632*COS(TSTR-3.805)+0.0984*COS(2.*TSTR
     *-0.360)+0.0168*COS(3.*TSTR-0.822)+0.0138*COS(4.*TSTR-3.513))
```

```
C     ROUND MONTHLY-AVERAGE AMBIENT TEMPERATURES
      NHLF=IFIX(FLOAT(NBX)/2.+.5)
      DO 51 I=1,12
      IF (TBM(I) .GE. 0.00001) GO TO 53
      TBM(I)=FLOAT(IFIX(TBM(I)-0.5))-DELT*FLOAT(NHLF)-0.5
      GO TO 51
53    TBM(I)=FLOAT(IFIX(TBM(I)+.5))-DELT*FLOAT(NHLF)-0.5
51    CONTINUE
      NHLF=IFIX(FLOAT(NYBX)/2.+0.5)
      TBY=FLOAT(IFIX(TBY+.5))-DELT*FLOAT(NHLF)-0.5
C     CALCULATE EXTRATERRESTRIAL RADIATION FOR EACH HOUR (MONTHLY-AVERAGE)
      DO 13 J=1,12
      D=IDX(J)
      DEC=23.45*RC*SIN(2.*PI*(284.+D)/365.)
      SNDC(J)=SIN(DEC)
      CSDC(J)=COS(DEC)
      WS=ACOS(-TAN(ALAT)*TAN(DEC))
      DO 13 I=1,24
      W1=0.2618*(FLOAT(I-1)-12.)
      W2=W1+0.2618
      WAVE=(W1+W2)/2.
C     ESTIMATE MONTHLY-AVERAGE VALUES OF CLEARNESS INDEX
      KT(J,I)=KT(J,25)*(0.409+0.5016*SIN(WS-1.047)+(0.6609-0.4767*SIN
     *(WS-1.047))*COS(WAVE))
      IF (W1 .GT. WS) GO TO 14
      IF (W2 .LT. -WS) GO TO 14
      IF (W1 .LT. -WS) IHS(J)=I+1
      IF (W1 .LT. -WS) W1=-WS
      IF (W2 .GT. WS) IHSP(J)=I-1
      IF (W2 .GT. WS) W2=WS
      ETR(J,I)=5168.08*(1.+.033*(COS(2.*PI*D/365.)))*(COS(ALAT)*COS
     *(DEC)*(SIN(W2)-SIN(W1))+(W2-W1)*SIN(ALAT)*SIN(DEC))
      GO TO 13
14    ETR(J,I)=0.
13    CONTINUE
      DO 15 J=1,24
      WH=0.2618*(FLOAT(J-1)-11.5)
      SNWH(J)=SIN(WH)
15    CSWH(J)=COS(WH)
      SNLT=SIN(ALAT)
      CSLT=COS(ALAT)
C     CALCUALTE STANDARD DEVIATION OF MONTHLY-AVERAGE AMBIENT TEMPERATURE
      DO 16 I=1,24
      DO 16 J=1,12
      TAV(I)=TAV(I)+TB(J,I)/12.
16    SGYR(I)=SGYR(I)+TB(J,I)*TB(J,I)
      DO 17 I=1,24
17    SGYR(I)=SQRT((SGYR(I)-12.*TAV(I)*TAV(I))/11.)
      DO 18 I=1,24
      DO 18 J=1,12
18    SGHR(J,I)=(3.538-.029*TB(J,I)+.0664*SGYR(J))*SQRT(NDY(J))
      IF (IBU .GE. 0) GO TO 8
      DO 9 J=1,12
      IF (IHPK .NE. 1) NHRS=IHSP(J)-IHS(J)+1
9     NDY(J)=NDY(J)/(NDY(J)*FLOAT(NHRS))
```

```
8     CSAZ=COS(AZM)
      SNAZ=SIN(AZM)
      CSBT=COS(SLP)
      SNBT=SIN(SLP)
C     FIND THE RATIO OF BEAM RADIATION INTENSITY ON THE TILTED SURFACE TO
C     THAT ON A HORIZONTAL SURFACE FOR EACH DAYLIGHT HOUR
      DO 19 J=1,12
      DO 19 I=1,24
      CDC=CSDC(J)
      SDC=SNDC(J)
      SWH=SNWH(I)
      CWH=CSWH(I)
C     COSINE OF THE INCIDENCE ANGLE FOR BEAM RADIATION FOR THE TILTED SURFACE
      CST=SDC*SNLT*CSBT-SDC*CSLT*SNBT*CSAZ+CDC*CSLT*CSBT*CWH+CDC*SNLT*
     &SNBT*CSAZ*CWH+CDC*SNBT*SNAZ*SWH
C     COSINE OF THE INCIDENCE ANGLE FOR BEAM RADIATION FOR THE HORIZONTAL
      CSZ=CDC*CSLT*CWH+SDC*SNLT
      IF (CSZ .LT. .0523) CSZ=.05
      IF (CST .LT. 1.0E-04) CST=0.0
19    RB(J,I)=CST/CSZ
      SKYVF=(1.+CSBT)/2.
      DO 20 J=1,12
20    RHO(J)=RHO(J)*(1.-CSBT)/2.
C     DETERMINE THE LIMITS FOR THE MONTH LOOPING
      KM=1
      IF (MST .LE. MSTP)  GO TO 21
      KM=2
      MB(1)=MST
      ME(1)=12
      MB(2)=1
      ME(2)=MSTP
      GO TO 22
21    MB(1)=MST
      ME(1)=MSTP
22    DO 43 NK=1,KM
      N1=MB(NK)
      N2=ME(NK)
C     MONTH LOOP
      DO 43 J=N1,N2
      IF (IHPK .EQ. 1) GO TO 99
       HST=IHS(J)
      HSTP=IHSP(J)
99    CONTINUE
C     HOUR LOOP FOR THOSE HOURS WHEN THE SUN IS ABOVE THE HORIZON ON THE
C     AVERAGE DAY OF THE MONTH
      DO 23 I=HST,HSTP
      DT=0.
C     NRTSA IS THE NUMBER OF VALID SOLUTIONS FOR KT FOR THE SMALLER VALUE OF THE
C     SOL-AIR TEMPERATURE DIFFERENCE DEFINING A SOL-AIR TEMPERATURE DIFFERENCE
C     BIN
      NRTSA=1
      AKT(1)=0.
      IF (EIR(J,I) .LT. 1.0E-10) GO TO 37
C     PARAMETERS FOR HOLLANDS AND HUGET KT MODEL
      KTX=KT(J,I)
```

```
      IF (KTX .LT. 0.30001) KTX=0.30001
      IKTM=IFIX((KTX+.005)/.01)-27
      IF (IKTM .LT. 1) IKTM=1
      IF (IKTM .GT. 53) IKTM=53
      RLMB=LAMDA(IKTM)
      C1=EXP(RLMB*KTMX)-1.-RLMB*KTMX
C     FOR EACH INTERVAL OF SOL-AIR TEMPERATURE, FIND INTERVALS OF KT WHICH
C     CORRESPOND.  SOLUTION IS FOUND USING DIFFUSE RELATIONSHIP OF ORGILL
C     AND HOLLANDS
      DO 24 L=1,NBY
C     INCREMENT SOL-AIR TEMPERATURE DIFFERENCE
      DT=DT+DELT
C     NRTSB IS THE NUMBER OF ROOTS FOR THE LARGER SOL-AIR TEMPERATURE DIFFERENCE
      NRTSB=0
      TSX(L)=DT-DELT/2.
      QB=SKYVF+RHO(J)
      QA=0.249*(SKYVF-RB(J,I))
      QC=(HO(J,I)*DT)/(ALPHA*ETR(J,I)*1.8)
C     FIND SOLUTIONS FOR DIFFUSE EQUATION FOR VALUES OF KT LESS THAN 0.35
      IF ((QB*QB-4.*QA*QC) .LT. 1.0E-10) GO TO 26
      RT1=(QB+SQRT(QB*QB-4.*QA*QC))/(2.*QA)
      RT2=(QB-SQRT(QB*QB-4.*QA*QC))/(2.*QA)
C     TEST SOLUTIONS TO DETERMINE WHETHER EITHER IS VALID
      IF (RT1 .GT. 0.35 .OR. RT1 .LT. 1.0E-10) GO TO 25
      NRTSB=NRTSB+1
      BKT(NRTSB)=RT1
25    IF (RT2 .GT. 0.35 .OR. RT2 .LT. 1.0E-10) GO TO 26
      NRTSB=NRTSB+1
      BKT(NRTSB)=RT2
      IF (NRTSB .GT. 1) GO TO 998
C     FIND SOLUTIONS FOR DIFFUSE EQUATION FOR VALUES OF KT BETWEEN 0.35 AND
C      0.75
26    QA=1.84*(SKYVF-RB(J,I))
      QB=1.557*SKYVF+RHO(J)-0.557*RB(J,I)
      IF ((QB*QB-4.*QA*QC) .LT. 1.0E-10) GO TO 28
      RT1=(QB+SQRT(QB*QB-4.*QA*QC))/(2.*QA)
      RT2=(QB-SQRT(QB*QB-4.*QA*QC))/(2.*QA)
C     TEST SOLUTIONS TO DETERMINE IF EITHER OR BOTH ARE VALID
      IF (RT1 .GT. 0.75 .OR. RT1 .LT. 0.35) GO TO 27
      NRTSB=NRTSB+1
      BKT(NRTSB)=RT1
27    IF (RT2 .GT. 0.75 .OR. RT2 .LT. 0.35) GO TO 28
      NRTSB=NRTSB+1
      BKT(NRTSB)=RT2
C     FIND SOLUTION FOR DIFFUSE EQUATION FOR VALUES OF KT GREATER THAN 0.75
28    RT1=QC/(0.823*RB(J,I)+0.177*SKYVF+RHO(J))
C     TEST SOLUTIONS FOR VALIDITY  SET UPPER BOUND TO 0.864
      IF (RT1 .GT. 0.864) RT1=0.864
      IF (RT1 .LT. 0.75) GO TO 29
      NRTSB=NRTSB+1
      BKT(NRTSB)=RT1
C     IF MORE THAN 3 VALID SOLUTIONS (NOT POSSIBLE), SIGNAL ERROR
29    IF (NRTSB .GT. 3) GO TO 999
C     FIND PROBABILITY THAT SOLAIR TEMPERATURE WAS IN CURRENT BIN USING
C     INTERVALS OF KT AND DISTRIBUTION FUNCTION OF HUGET
```

```
      IF (NRTSA .EQ. 2) WRITE(-,-)(AKT(II),II=1,2)
      IF (NRTSB .EQ. 2) WRITE(-,-)(BKT(II),II=1,2)
      IF (NRTSA .EQ. 1 .AND. NRTSB .EQ. 1) GO TO 30
      IF (NRTSA .EQ. 1 .AND. NRTSB .EQ. 3) GO TO 31
      IF (NRTSA .EQ. 3 .AND. NRTSB .EQ. 3) GO TO 32
      IF (NRTSA .EQ. 2 ) GO TO 91
      GO TO 92
91    IF (AKT(1) .LE. AKT(2)) GO TO 92
      AKTX=AKT(1)
      AKT(1)=AKT(2)
      AKT(2)=AKTX
92    IF (NRTSB .EQ. 2) GO TO 94
      GO TO 93
94    IF (BKT(1) .LE. BKT(2)) GO TO 93
      BKTX=BKT(1)
      BKT(1)=BKT(2)
      BKT(2)=BKTX
93    CONTINUE
      IF (NRTSA .EQ. 1 .AND. NRTSB .EQ. 2) GO TO 30
      IF (NRTSA .EQ. 2 .AND. NRTSB .EQ. 3) GO TO 31
      IF (NRTSA .EQ. 2 .AND. NRTSB .EQ. 1) GO TO 30
      IF (NRTSA .EQ. 2 .AND. NRTSB .EQ. 2) GO TO 997
      QF1=((1.+RLMB*KTMX-RLMB*AKT(2))*EXP(RLMB*AKT(2))-
     *(1.+RLMB*KTMX-RLMB*AKT(1))*EXP(RLMB*AKT(1)))/C1
      IF (QF1 .LT. 1.0E-20)QF1 = -QF1
      QF2=((1.+RLMB*KTMX-RLMB*BKT(1))*EXP(RLMB*BKT(1))-
     *(1.+RLMB*KTMX-RLMB*AKT(3))*EXP(RLMB*AKT(3)))/C1
C     SUM PROBABILITIES FOR INTERVALS OF KT WHICH CORRESPOND TO AN INTERVAL
C     OF SOL-AIR TEMPERATURE DIFFERENCE
      PKT(L,I)=PKT(L,I)+QF1+QF2
      GO TO 36
30    QF1=((1.+RLMB*KTMX-RLMB*BKT(1))*EXP(RLMB*BKT(1))-
     *(1.+RLMB*KTMX-RLMB*AKT(1))*EXP(RLMB*AKT(1)))/C1
      PKT(L,I)=PKT(L,I)+QF1
      GO TO 36
31    IF (BKT(1) .LE. BKT(2)) GO TO 33
      BKTX=BKT(1)
      BKT(1)=BKT(2)
      BKT(2)=BKTX
33    QF1=((1.+RLMB*KTMX-RLMB*BKT(1))*EXP(RLMB*BKT(1))-
     *(1.+RLMB*KTMX-RLMB*AKT(1))*EXP(RLMB*AKT(1)))/C1
      QF2=((1.+RLMB*KTMX-RLMB*BKT(3))*EXP(RLMB*BKT(3))-
     *(1.+RLMB*KTMX-RLMB*BKT(2))*EXP(RLMB*BKT(2)))/C1
C     SUM PROBABILTIES
      PKT(L,I)=PKT(L,I)+QF1+QF2
      GO TO 36
C     SWITCH LIMITS TO KEEP PROBABILITIES POSITIVE IN SIGN
32    IF (AKT(1) .LE. AKT(2)) GO TO 34
      AKTX=AKT(1)
      AKT(1)=AKT(2)
      AKT(2)=AKTX
34    IF (BKT(1) .LE. BKT(2)) GO TO 35
      BKTX=BKT(1)
      BKT(1)=BKT(2)
      BKT(2)=BKTX
```

```
35    QF1=((1.+RLMB*KTMX-RLMB*BKT(1))*EXP(RLMB*BKT(1))-
     *(1.+RLMB*KTMX-RLMB*AKT(1))*EXP(RLMB*AKT(1)))/C1
      QF2=((1.+RLMB*KTMX-RLMB*AKT(2))*EXP(RLMB*AKT(2))-
     *(1.+RLMB*KTMX-RLMB*BKT(2))*EXP(RLMB*BKT(2)))/C1
      QF3=((1.+RLMB*KTMX-RLMB*BKT(3))*EXP(RLMB*BKT(3))-
     *(1.+RLMB*KTMX-RLMB*AKT(3))*EXP(RLMB*AKT(3)))/C1
      PKT(L,I)=PKT(L,I)+QF1+QF2+QF3
C     TRANSFER UPPER LIMITS FOR PRESENT SOL-AIR TEMPERATURE BIN TO LOWER LIMITS
C     FOR NEXT SOL-AIR TEMPERATURE BIN
36    DO 39 IK=1,NRTSB
      AKT(IK)=BKT(IK)
39    BKT(IK)=0.
      NRTSA=NRTSB
24    CONTINUE
      GO TO 23
C     FOR HOURS WHEN THERE IS NO SOLAR RADIATION, ALL HOURS ARE IN FIRST SOL-AIR
C     TEMPERATURE DIFFERENCE BIN
37    PKT(1,I)=PKT(1,I)+1.0
23    CONTINUE
C     FIND PROBABILITY OF AMBIENT TEMPERATURE BEING IN EACH BIN, MULTIPLY
C     BY PROBABILITY OF TEMPERATURE BEING IN EACH SOL-AIR BIN
      DO 40 I=HST,HSTP
      TLW=TBM(J)-DELT
      THI=TBM(J)
      SIG=SGHR(J,I)
      TBH=TB(J,I)
      DO 40 L=1,NBX
C     INCREMENT AMBIENT TEMPERATURE BIN
      TLW=TLW+DELT
      THI=THI+DELT
      TX(L)=(THI+TLW)/2.
      H1=(TLW-TBH)/SIG
      H2=(THI-TBH)/SIG
C     PROBABILITY FOR AMBIENT TEMPERATURE BIN
      PTA=(TANH(THT*H2)-TANH(THT*H1))/2.
      DO 40 K=1,NBY
C     PROBABILITY FOR EACH SOL-AIR TEMPERATURE/AMBIENT TEMPERATURE BIN
40    MTSA(L,K)=MTSA(L,K)+PTA*PKT(K,I)*NDY(J)
C
C     REPEAT FOR ANNUAL BIN DATA
      DO 60 I=HST,HSTP
      TLW=TBY-DELT
      THI=TBY
      SIG=SGHR(J,I)
      TBH=TB(J,I)
      DO 60 L=1,NYBX
      TLW=TLW+DELT
      THI=THI+DELT
      TYX(L)=(THI+TLW)/2.
      H1=(TLW-TBH)/SIG
      H2=(THI-TBH)/SIG
      PTA=(TANH(THT*H2)-TANH(THT*H1))/2.
      DO 60 K=1,NBY
C     PROBABILITY FOR ANNUAL SOL-AIR TEMPERATURE/AMBIENT TEMPERATURE BINS
60    NTSA(L,K)=NTSA(L,K)+PTA*PKT(K,I)*NDY(J)
```

```
C     PRINT OUT BIN DATA
      THRS=0.
      DO 70 L1=1,NBX
      DO 70 L2=1,NBY
70    THRS=THRS+MTSA(L1,L2)
      AHRS=NDY(J)*FLOAT(HSTP-HST+1)
      AYHRS=AYHRS+AHRS
      IF (IPRT .LE. 0) GO TO 42
      KR=0
      DO 80 JJ=1,NBX,20
      WRITE(-,200) J
      WRITE(-,205) THRS,AHRS
      KR=KR+20
      IF (KR .GT. NBX) KR=NBX
      NDSH=1*(KR-JJ+2)
      WRITE(-,201)(TX(K),K=JJ,KR)
      DO 88 IJ=1,NBY
      JI=NBY-IJ+1
      IF (IBU .GE. 0) GO TO 82
      WRITE(L3,206)(MTSA(LJ,JI),LJ=JJ,KR)
      GO TO 88
82    WRITE(L3,207)(MTSA(LJ,JI),LJ=JJ,KR)
88    CONTINUE
80    CONTINUE
C     REINITIALIZE BINS FOR MONTHS, CHECK PROBABILITY OF KT
42    DO 44 L1=1,100
      DO 44 L2=1,100
44    MTSA(L1,L2)=0.
      DO 48 L2=HST,HSTP
      PSUM=0.
      DO 47 L1=1,100
      PSUM=PSUM+PKT(L1,L2)
47    PKT(L1,L2)=0.
C     IF PROBABILITY FOR KT OUTSIDE OF BOUNDS, PRINT ERROR MESSAGE
      IF (PSUM .LT. 0.10 .OR. PSUM .GT. 1.05) GO TO 996
48    CONTINUE
43    CONTINUE
      IF (IPRT .GT. 1) GO TO 90
      IF (IBU .GE. 0) GO TO 46
      DO 45 L1=1,100
      DO 45 L2=1,100
45    NTSA(L1,L2)=NTSA(L1,L2)/FLOAT(NMON)
C     OUTPUT ANNUAL BIN DATA
46    KR=0
      DO 71 L1=1,NYBX
      DO 71 L2=1,NBY
71    YHRS=YHRS+NTSA(L1,L2)
      IF (IBU .LT. 0) AYHRS=AYHRS/FLOAT(NMON)
      J=13
      DO 81 JJ=1,NYBX,20
      WRITE(-,200) J
      WRITE(-,205) YHRS,AYHRS
      KR=KR+20
      IF (KR .GT. NYBX) KR=NYBX
      NDSH=1*(KR-JJ+2)
```

```
      WRITE(-,201)(TYX(K),K=JJ,KR)
      DO 87 IJ=1,NBY
      JI=NBY-IJ+1
      IF (IBU .GE. 0) GO TO 83
      WRITE(L3,206)(NTSA(LJ,JI),LJ=JJ,KR)
      GO TO 87
83    WRITE(L3,207)(NTSA(LJ,JI),LJ=JJ,KR)
87    CONTINUE
81    CONTINUE
90    WRITE(-,208)(IHS(J),J=1,12)
      WRITE(-,209)(IHSP(J),J=1,12)
      STOP
208   FORMAT('0STARTING HOURS ARE:',12(2X,I2))
209   FORMAT('0ENDING HOURS ARE:',12(2X,I2))
C     OUTPUT ERROR CONDITIONS
996   WRITE(-,300) L2,PSUM
      GO TO 90
997   WRITE(-,400)
      GO TO 90
998   WRITE(-,500) NRTSB
      GO TO 90
999   WRITE(-,600) NRTSB
      GO TO 90
101   FORMAT(1X,13(F6.2,2X))
102   FORMAT(25F5.3)
200   FORMAT(' ',20X,'FOR THE MONTH',1X,I2,10X,'HORIZONTAL AXIS AMBIENT,
     * VERTICAL AXIS SOLAIR-AMBIENT')
201   FORMAT('0 AMBIENT',20(':',F5.1))
202   FORMAT(' ',3X,22A6)
203   FORMAT(' ',F5.1,':',2X,20('*',F5.1),'*')
204   FORMAT(' ',F5.1,':',2X,20('*',F5.4),'*')
207   FORMAT(1X,20F6.1)
206   FORMAT(1X,20F6.4)
205   FORMAT(' HOURS IN BINS',1X,F9.4,5X,'ACTUAL HOURS IN INTERVAL',1X,
     *F9.4)
300   FORMAT('1FOR HOUR',2X,I2,2X,'CUMULATIVE PROB. OF KT IS',F7.3)
400   FORMAT('1TWO ROOTS FOUND FOR EACH OF TWO RKT')
500   FORMAT('1ONLY ONE ROOT ALLOWED IN FIRST KT INTERVAL, BUT FOUND',1X
     *,I2)
600   FORMAT('1ONLY 3 ROOTS TOTAL POSSIBLE, BUT FOUND',1X,I2)
      END
```

PROGRAM TWBINDAT1

```
C     THIS PROGRAM ESTIMATES TWO-DIMENSIONAL DRY-BULB TEMPERATURE/HUMIDITY
C     RATIO BIN DATA USING DISTRIBUTION FUNCTION MODELS FOR DRY-BULB
C     TEMPERATURE AND RELATIVE HUMIDITY.  THE MONTHLY-AVERAGE HOURLY VALUES
C     OF DRY-BULB TEMPERATURE AND RELATIVE HUMIDITY ARE
C     REQUIRED INPUTS.  BIN DATA ARE ESTIMATED FOR EACH MONTH OF THE YEAR
C     AND FOR THE ENTIRE YEAR.  THE ESTIMATED BIN DATA ARE STORED IN THE
C     ARRAYS WTBDE (FOR EACH MONTH) AND WTBDRE (FOR THE YEAR).  OTHER
C     PROGRAM INPUTS ARE AS FOLLOWS:
C
C       NBX - NUMBER OF BINS FOR DRY-BULB TEMPERATURE FOR MONTHLY BIN DATA
C       NBY - NUMBER OF BINS FOR HUMIDITY RATIO FOR MONTHLY BIN DATA
C       NBXR - NUMBER OF BINS FOR DRY-BULB TEMPERATURE FOR ANNUAL DATA
C       NBYR - NUMBER OF BINS FOR HUMIDITY RATIO FOR ANNUAL DATA
C       L3 - LOGICAL UNIT NUMBER FOR READING IN MONTHLY-AVERAGE AMBIENT
C            TEMPERATURE
C       L4 - LOGICAL UNIT NUMBER FOR READING IN MONTHLY-AVERAGE RELATIVE
C            HUMIDITY
C       XN - 12 MONTHLY AND ANNUAL LOWER BOUNDS FOR DRY-BULB TEMPERATURE BINS
C       XYN - 12 MONTHLY AND ANNUAL UPPER BOUNDS FOR DRY-BULB TEMPERATURE BINS
C       YN - 12 MONTHLY AND ANNUAL LOWER BOUNDS FOR HUMIDITY RATIO BINS
C       YYN - 12 MONTHLY AND ANNUAL UPPER BOUNDS FOR HUMIDITY RATIO BINS
C
      DIMENSION WTBDRE(40,20),WTDBE(12,25,20),RHBAR(12,24)
     *,XN(13),YN(13),XYN(13),YYN(13),TBAR(12,25),
     *WDLT(13),RDY(12),TDLT(13),RYRS(13),SIG(12)
      DATA RDY/31.,28.,31.,30.,31.,30.,31.,31.,30.,31.,30.,31./,
     *WTBDE/6000*0./,WTBDRE/800*0./
      READ(-,-) NBX,NBY,NBXR,NBYR,L3,L4
      READ(-,-)(XN(I),I=1,13)
      READ(-,-)(XYN(I),I=1,13)
      READ(-,-)(YN(I),I=1,13)
      READ(-,-)(YYN(I),I=1,13)
C     CALCULATE MONTHLY DRY-BULB TEMPERATURE AND HUMIDITY RATIO BIN SIZES
      DO 5 J=1,12
      TDLT(J)=(XYN(J)-XN(J))/FLOAT(NBX)
5     WDLT(J)=(YYN(J)-YN(J))/FLOAT(NBY)
C     CALCULATE ANNUAL DRY-BULB TEMPERATURE AND HUMIDITY RATIO BIN SIZES
      TDLT(13)=(XYN(13)-XN(13))/FLOAT(NBXR)
      WDLT(13)=(YYN(13)-YN(13))/FLOAT(NBYR)
C     READ IN MONTHLY-AVERAGE METEOROLOGICAL DATA
      DO 36 J=1,25
36    READ(L3,103)(TBAR(I,J),I=1,12)
      DO 37 J=1,24
37     READ(L4,104)(RHBAR(I,J),I=1,12)
C     ESTIMATE STANDARD DEVIATIONS FOR MONTHLY-AVERAGE DRY-BULB TEMPERATURE
      SGYR=0.
      TYAV=0.
      DO 38 J=1,12
      SGYR=SGYR+TBAR(J,25)*TBAR(J,25)
38     TYAV=TYAV+TBAR(J,25)/12.
      SGYR=SQRT((SGYR-12.*TYAV*TYAV)/11.)
      DO 39 J=1,12
```

```
39      SIG(J)=1.8*(1.45-0.029*TBAR(J,25)+0.0664*SGYR)*SQRT(RDY(J))
C       CONVERT MONTHLY-AVERAGE TEMPERATURES TO FAHRENHEIT
        DO 41 J=1,12
        DO 41 I=1,24
41      TBAR(J,I)=1.8*TBAR(J,I)+32.
C
C       BIN DATA ESTIMATION
C
        DO 42 J=1,12
        DO 42 I=1,24
        A=-0.02691+1.22758*RHBAR(J,I)-0.1488*RHBAR(J,I)**2
        B=0.08165*EXP(5.38015*RHBAR(J,I))+2.27473*EXP(-0.59958*RHBAR(J,I))
        DO 43 K=1,NBX
C       STEP THROUGH DRY-BULB TEMPERATURE BINS
        T1=XN(J)+(K-1)*TDLT(J)
        T2=T1+TDLT(J)
        TB=(T1+T2)/2.
        H1=(T1-TBAR(J,I))/SIG(J)
        H2=(T2-TBAR(J,I))/SIG(J)
C       PROBABILITY FOR DRY-BULB TEMPERATURE BIN
        PTB=(TANH(1.698*H2)-TANH(1.698*H1))/2.
C       SATURATION HUMIDITY RATIO FOR MIDPOINT VALUE OF DRY-BULB TEMPERATURE
        WS=1.4974E07*EXP(-9548./(TB+460.))/(14.696-2.4074E07*EXP(-9548./
     *(TB+460.)))
        IF (TB .LT. 32.) WS=3.0682E08*EXP(-11040./(TB+460.))/(14.696-
     *4.993E08*EXP(-11040./(TB+460.)))
        DO 43 L=1,NBY
C       STEP THROUGH HUMIDITY RATIO BINS
        W1=YN(J)+(L-1)*WDLT(J)
        W2=W1+WDLT(J)
C       FIND RELATIVE HUMIDITY VALUES WHICH CORRESPOND TO THE HUMIDITY RATIO
C       DEFINING A HUMIDITY RATIO BIN AND THE MIDPOINT VALUE OF DRY-BULB TEMP
        RH1=W1*(.62198+WS)/(WS*(.62198+W1))
        RH2=W2*(.62198+WS)/(WS*(.62198+W2))
C       FIND PROBABILITY FOR HUMIDITY RATIO BIN USING RELATIVE HUMIDITY VALUES
C       AND RELATIVE HUMIDITY DISTRIBUTION FUNCTION
        RH1=AMIN1(1.,RH1)
        RH2=AMIN1(1.,RH2)
        PTH=(EXP(-(RH1/A)**B)-EXP(-(RH2/A)**B))/(1.-EXP(-(1./A)**B))
C
C       CALCULATE PROBABILITY FOR DRY-BULB TEMPERATURE/HUMIDITY RATIO BIN
43      WTBDE(J,K,L)=WTBDE(J,K,L)+RDY(J)*PTB*PTH
C
C       REPEAT ABOVE PROCEDURE, BUT FOR ANNUAL BIN DATA
        DO 44 K=1,NBXR
        T1=XN(13)+(K-1)*TDLT(13)
        T2=T1+TDLT(13)
        TB=(T1+T2)/2.
        H1=(T1-TBAR(J,I))/SIG(J)
        H2=(T2-TBAR(J,I))/SIG(J)
        PTB=(TANH(1.698*H2)-TANH(1.698*H1))/2.
        WS=1.4974E07*EXP(-9548./(TB+460.))/(14.696-2.4074E07*EXP(-9548./
     *(TB+460.)))
        IF (TB .LT. 32.) WS=3.0682E08*EXP(-11040./(TB+460.))/(14.696-
     *4.993E08*EXP(-11040./(TB+460.)))
        DO 44 L=1,NBYR
        W1=YN(13)+(L-1)*WDLT(13)
        W2=W1+WDLT(13)
        RH1=W1*(.62198+WS)/(WS*(.62198+W1))
        RH2=W2*(.62198+WS)/(WS*(.62198+W2))
        RH1=AMIN1(1.,RH1)
        RH2=AMIN1(1.,RH2)
        PTH=(EXP(-(RH1/A)**B)-EXP(-(RH2/A)**B))/(1.-EXP(-(1./A)**B))
44      WTBDRE(K,L)=WTBDRE(K,L)+RDY(J)*PTB*PTH
42      CONTINUE
103     FORMAT(1X,12(F6.2,2X))
104     FORMAT(12(1X,F7.5))
        END
```

PROGRAM TWBINDAT2

```
C     THIS PROGRAM ESTIMATES TWO-DIMENSIONAL DRY-BULB TEMPERATURE/HUMIDITY
C     RATIO BIN DATA USING DISTRIBUTION FUNCTION MODELS FOR WET-BULB
C     TEMPERATURE AND RELATIVE HUMIDITY.  THE MONTHLY-AVERAGE HOURLY VALUES
C     OF DRY-BULB TEMPERATURE, CLEARNESS INDEX AND RELATIVE HUMIDITY ARE
C     REQUIRED INPUTS.  BIN DATA ARE ESTIMATED FOR EACH MONTH OF THE YEAR
C     AND FOR THE ENTIRE YEAR.  THE ESTIMATED BIN DATA ARE STORED IN THE
C     ARRAYS WTBDME (FOR EACH MONTH) AND WTBDRE (FOR THE YEAR).  OTHER
C     PROGRAM INPUTS ARE AS FOLLOWS:
C
C       EPS - CONVERGENCE TOLERANCE FOR NUMERICAL CALCULATION OF THE DRY-
C             BULB TEMPERATURE CORRESPONDING TO VALUES OF WET-BULB
C             TEMPERATURE AND RELATIVE HUMIDITY
C       NBX - NUMBER OF BINS FOR WET-BULB TEMPERATURE
C       NBY - NUMBER OF BINS FOR RELATIVE HUMIDITY
C       NBXR - NUMBER OF BINS FOR DRY-BULB TEMPERATURE FOR ANNUAL DATA
C       NBYR - NUMBER OF BINS FOR HUMIDITY RATIO FOR ANNUAL DATA
C       L2 - LOGICAL UNIT NUMBER FOR READING IN MONTHLY-AVERAGE CLEARNESS INDEX
C       L3 - LOGICAL UNIT NUMBER FOR READING IN MONTHLY-AVERAGE AMBIENT
C            TEMPERATURE
C       L4 - LOGICAL UNIT NUMBER FOR READING IN MONTHLY-AVERAGE RELATIVE
C            HUMIDITY
C       NBMX - NUMBER OF DRY-BULB TEMPERATURE BINS FOR MONTHLY DATA
C       NBMY - NUMBER OF HUMIDITY RATIO BINS FOR MONTHLY DATA
C       XWL - 12 MONTHLY LOWER BOUNDS FOR WET-BULB TEMPERATURE BINS
C       XWH - 12 MONTHLY UPPER BOUNDS FOR WET-BULB TEMPERATURE BINS
C       YWL - 12 MONTHLY LOWER BOUNDS FOR RELATIVE HUMIDITY BINS
C       YWH - 12 MONTHLY UPPER BOUNDS FOR RELATIVE HUMIDITY BINS
C       XDL - 12 MONTHLY AND ANNUAL LOWER BOUNDS FOR DRY-BULB TEMPERATURE BINS
C       XDH - 12 MONTHLY AND ANNUAL UPPER BOUNDS FOR DRY-BULB TEMPERATURE BINS
C       YDL - 12 MONTHLY AND ANNUAL LOWER BOUNDS FOR HUMIDITY RATIO BINS
C       YDH - 12 MONTHLY AND ANNUAL UPPER BOUNDS FOR HUMIDITY RATIO BINS
C
      DIMENSION XDL(13),XDH(13),YDH(13),WTBD(100,100),WTBDRE(40,20)
     *,YDL(13),XWL(12),YWL(12),XWH(12),YWH(12),TBAR(12,25),
     *XKTBR(12,25),RHBAR(12,24),WDLT(13),RDY(12),TDLT(13),SIG(12)
     *,TWBAR(12,24),WTBDME(12,25,20)
      DATA RDY/31.,28.,31.,30.,31.,30.,31.,31.,30.,31.,30.,31./,
     *WTBD/10000*0./,WTBDME/6000*0./,WTBDRE/800*0./
      READ(-,-) EPS
      READ(-,-) NBX,NBY,NBXR,NBYR,L2,L3,L4
      READ(-,-) NBMX,NBMY
      READ(-,-)(XWL(I),I=1,12)
      READ(-,-)(XWH(I),I=1,12)
      READ(-,-)(YWL(I),I=1,12)
      READ(-,-)(YWH(I),I=1,12)
      READ(-,-)(XDL(I),I=1,13)
      READ(-,-)(XDH(I),I=1,13)
      READ(-,-)(YDL(I),I=1,13)
      READ(-,-)(YDH(I),I=1,13)
C     CALCULATE BIN SIZES FOR WET-BULB TEMPERATURE AND RELATIVE HUMIDITY
      DO 5 J=1,12
      TDLT(J)=(XWH(J)-XWL(J))/FLOAT(NBX)
```

```
5     WDLT(J)=(YWH(J)-YWL(J))/FLOAT(NBY)
C     CALCULATE DRY-BULB TEMPERATURE AND HUMIDITY RATIO BIN SIZES FOR
C     ANNUAL BIN DATA
      TDLTYR=(XDH(13)-XDL(13))/NBXR
      WDLTYR=(YDH(13)-YDL(13))/NBYR
C     READ IN MONTHLY-AVERAGE WEATHER DATA
      DO 35 I=1,12
35    READ(L2,105)(XKTBR(I,J),J=1,25)
      CALL CLOSE(L2,1)
      DO 36 J=1,25
36    READ(L3,103)(TBAR(I,J),I=1,12)
      DO 37 J=1,24
37     READ(L4,104)(RHBAR(I,J),I=1,12)
      CALL CLOSE(L3,1)
      CALL CLOSE(L4,1)
C     ESTIMATE STANDARD DEVIATIONS FOR WET-BULB TEMPERATURE
      SGYR=0.
      TYAV=0.
      DO 38 J=1,12
      SGYR=SGYR+TBAR(J,25)*TBAR(J,25)
38     TYAV=TYAV+TBAR(J,25)/12.
      SGYR=SQRT((SGYR-12.*TYAV*TYAV)/11.)
      DO 39 J=1,12
39    SIG(J)=1.8*(6.4194-0.06997*TBAR(J,25)-0.3155*SGYR+0.04051*SGYR*
     *SGYR-3.6849*XKTBR(J,25))
C     ESTIMATE MONTHLY-AVERAGE HOURLY WET-BULB TEMPERATURES
      DO 41 J=1,12
      DO 41 I=1,24
      TBAR(J,I)=1.8*TBAR(J,I)+32.
      RHM=RHBAR(J,I)*100.
      TBM=TBAR(J,I)
      CALL PSYCHO(TBM,RHM,TWB,TDP,W,1)
41    TWBAR(J,I)=TWB*1.8+32.
C
C     ESTIMATE WET-BULB TEMPERATURE/RELATIVE HUMIDITY BIN DATA ON A MONTHLY
C     BASIS
      DO 40 J=1,12
      DO 43 I=1,24
      A=-0.02691+1.22758*RHBAR(J,I)-0.1488*RHBAR(J,I)**2
      B=0.08165*EXP(5.38015*RHBAR(J,I))+2.27473*EXP(-0.59958*RHBAR(J,I))
      DO 43 K=1,NBX
C     STEP THROUGH WET-BULB TEMPERATURE BINS
      T1=XWL(J)+(K-1)*TDLT(J)
      T2=T1+TDLT(J)
      TB=(T1+T2)/2.
      H1=(T1-TWBAR(J,I))/SIG(J)
      H2=(T2-TWBAR(J,I))/SIG(J)
C     PROBABILITY FOR WET-BULB TEMPERATURE BIN
      PTB=(TANH(0.84877*H2)-TANH(0.84877*H1))/2.
      DO 43 L=1,NBY
C     STEP THROUGH RELATIVE HUMIDITY BINS
      RH1=YWL(J)+(L-1)*WDLT(J)
      RH2=RH1+WDLT(J)
C     PROBABILITY FOR RELATIVE HUMIDITY BIN
      PTH=(EXP(-(RH1/A)**B)-EXP(-(RH2/A)**B))/(1.-EXP(-(1./A)**B))
```

```
C     PROBABILITY FOR WET-BULB TEMPERATURE/RELATIVE HUMIDITY BIN
43    WTBD(K,L)=WTBD(K,L)+RDY(J)*PTB*PTH
C
C     FIND DRY-BULB TEMPERATURE AND HUMIDITY RATIO VALUES WHICH CORRESPOND
C     TO THE MIDPOINT OF EACH WET-BULB TEMPERATURE/RELATIVE HUMIDITY BIN
C     NUMERICAL SOLUTION REQUIRED  SECANT METHOD USED
      TDLTM=(XDH(J)-XDL(J))/NBMX
      WDLTM=(YDH(J)-YDL(J))/NBMY
      DO 44 K=1,NBX
      DO 44 L=1,NBY
      NIT=0
C     WET-BULB TEMPERATURE AND RELATIVE HUMIDITY FOR BIN MIDPOINT
      TWBX=XWL(J)+(K-1)*TDLT(J)+TDLT(J)/2.
      RHX=YWL(J)+(L-1)*WDLT(J)+WDLT(J)/2.
      RHG=RHX*100.
C     INITIAL GUESS FOR DRY-BULB TEMPERATURE FROM CURVE FIT
      DTDWB=4.34-0.04612*RHG+0.357*TWBX-0.00389*RHG*TWBX+1.1494*TWBX/RHG
      DTDWB=AMAX1(DTDWB,0.)
      TG1=TWBX+DTDWB
      TG2=TG1+1.
      CALL PSYCHO(TG1,RHG,TWBR,TDP,W,1)
C     ITERATE ON WET-BULB TEMPERATURE
      F1=TWBX-TWBR*1.8-32.
49    CALL PSYCHO(TG2,RHG,TWBR,TDP,W,1)
      F2=TWBX-TWBR*1.8-32.
      IF (ABS(F1-F2) .LT. 1.0E-07) GO TO 46
      TGN=TG2-F2*(TG2-TG1)/(F2-F1)
      IF (ABS(TGN-TG2) .LT. EPS) GO TO 47
      TG1=TG2
      F1=F2
      TG2=TGN
      NIT=NIT+1
      IF (NIT .GT. 100) GO TO 48
      GO TO 49
48    TDB=TG2
      WRITE(-,210)
210   FORMAT(' FAILURE TO CONVERGE ON TDB IN 100 ITERATIONS')
      GO TO 45
47    TDB=TGN
      GO TO 45
46    TDB=TG2
      WRITE(-,220) NIT
220   FORMAT(' LOSS OF PRECISION AFTER',2X,I3,2X,'ITERATIONS')
C
C     FIND ANNUAL DRY-BULB TEMPERATURE/HUMIDITY RATIO BIN FOR MIDPOINT
C     OF WET-BULB TEMPERATURE/RELATIVE HUMIDITY BIN
45    IX=IFIX((TDB-XDL(13))/TDLTYR)+1
      IF (IX .LT. 1 .OR. IX .GT. NBXR) GO TO 42
      IY=IFIX((W-YDL(13))/WDLTYR)+1
      IF (IY .LT. 1 .OR. IY .GT. NBYR) GO TO 42
C     SUM HOURS FOR EACH DRY-BULB TEMPERATURE/HUMIDITY RATIO BIN FOR ANNUAL
C     DATA
      WTBDRE(IX,IY)=WTBDRE(IX,IY)+WTBD(K,L)
C     FIND MONTHLY DRY-BULB TEMPERATURE/HUMIDITY RATIO BIN FOR MIDPOINT
C     OF WET-BULB TEMPERATURE/RELATIVE HUMIDITY BIN
42    IX=IFIX((TDB-XDL(J))/TDLTM)+1
      IF (IX .LT. 1 .OR. IX .GT. NBMX) GO TO 44
      IY=IFIX((W-YDL(J))/WDLTM)+1
      IF (IY .LT. 1 .OR. IY .GT. NBMY) GO TO 44
C     SUM HOURS FOR EACH MONTHLY DRY-BULB TEMPERATURE/HUMIDITY RATIO BIN
      WTBDME(J,IX,IY)=WTBDME(J,IX,IY)+WTBD(K,L)
C     ERASE WET-BULB TEMPERATURE/RELATIVE HUMIDITY BIN
44    WTBD(K,L)=0.
40    CONTINUE
105   FORMAT(25F5.3)
103   FORMAT(1X,12(F6.2,2X))
104   FORMAT(12(1X,F7.5))
      END
```

SUBROUTINE PSYCHO

```
      SUBROUTINE PSYCHO(TDF,RHM,TWB,TDP,W,MODE)
C   THIS ROUTINE CALCULATES HUMIDITY RATIO AS A FUNCTION OF
C   DRY BULB AND RELATIVE HUMIDITY (MODE 1),
C  OR DEW POINT AND DRY BULB (MODE 2). DRY-BULB TEMPERATURE
C  MUST BE IN FAHRENHEIT.
      INTEGER RETRN
      DATA EPS/0.001/
C   THE FOLLOWING STATEMENT FUNCTIONS ARE CURVE FITS FOR THE
C  SATURATION PRESSURE OF WATER (IN ATMOSPHERES) AS A FUNCTION
C  OF TEMPERATURE.
      P1(Z)=-7.90298*(Z-1.0)
      P2(Z)=5.02808*ALOG10(Z)
      P3(Z)=-1.3816E-07*(10.**(11.344*(1.-1./Z))-1.)
      P4(Z)=8.1328E-03*(10.**(-3.49149*(Z-1.))-1.)
      P5(Z)=-9.09718*(Z-1.)
      P6(Z)=-3.56654*ALOG10(Z)
      P7(Z)=.876793*(1.-1./Z)
      P8 = -2.2199
C
C   FIND SATURATION PRESSURE OF WATER AT WET BULB, DRY BULB, OR
C  DEW POINT TEMPERATURE.
C
C   CONVERT DRY-BULB TEMPERATURE TO CELSIUS
      TDB=(TDF-32.)/1.8
      T=TDB
      IF (MODE .EQ. 2) T=TDP
      ASSIGN 8 TO RETRN
      GO TO 100
C
C   CALCULATE HUMIDITY RATIO AND WET BULB TEMPERATURE.
8     GO TO (20,30), MODE
C  MODE 1 -- DRY BULB AND RELATIVE HUMIDITY SUPPLIED
20    RH = RHM/100.
      W = .62198 * PSAT*RH/(1.-PSAT*RH)
      GO TO 60
C  MODE 2 -- DRY BULB AND DEW POINT SUPPLIED
30    W = .62198 * PSAT/(1.-PSAT)
C   FIND ENTHALPY AND WET BULB TEMPERATURE.
60    H = 1.005*TDB + W*(2501. + 1.859*TDB)
      IF (H .LT. 9.67) GO TO 70
      Y = ALOG(H+17.68)
      TWB = 26.7453 + Y*(-43.44 + Y*(13.909 - Y*.977))
      GO TO 90
C   USE LINEAR APPROXIMATION WHEN H LT 9.67
70    IF (MODE .EQ. 1) GO TO 72
      T = TDB
      ASSIGN 72 TO RETRN
      GO TO 100
72    WSAT = .62198 * PSAT/(1.-PSAT)
      T = (H - 2501.*WSAT)/(1.005 + 1.859*WSAT)
      ASSIGN 78 TO RETRN
      GO TO 100
```

```
78      WT = .62198*PSAT/(1.-PSAT)
C   FIND POINT ON LINE BETWEEN (T,WT) AND (TDB,WSAT) WITH ENTHALPY H.
        IF (ABS(T-TDB) .GT. 0.01) GO TO 80
        TWB = (T+TDB)*0.5
        GO TO 90
80      SLOPE = (WSAT-WT)/(TDB-T)
        A = 1.859*SLOPE
        B = 1.005 + WSAT*1.859 + SLOPE*(2501.-1.859*TDB)
        C = -H + 2501.*(WSAT - SLOPE*TDB)
        IF (SLOPE .LT. 1.E-7) TWB = -C/B
        IF (SLOPE .GT. .99E-7) TWB = (-B + SQRT(B*B-4.*A*C))/(2.*A)
C   USE SECANT METHOD TO SOLVE FOR WET-BULB TEMPERATURE.  INITIAL GUESS
C   IS FOUND FROM ASHRAE RELATIONSHIP.
90      TG1=TWB
        TG2=TWB+0.5
        NIT=0
        ASSIGN 91 TO RETRN
        T=TG1
        GO TO 100
91      WS1=.62198*PSAT/(1.-PSAT)
C   ITERATE ON HUMIDITY RATIO
        F1=W-((2501.-2.381*TG1)*WS1-(TDB-TG1))/(2501.+1.805*TDB
     *-4.186*TG1)
93      ASSIGN 92 TO RETRN
        T=TG2
        GO TO 100
92      WS2=.62198*PSAT/(1.-PSAT)
        F2=W-((2501.-2.381*TG2)*WS2-(TDB-TG2))/(2501.+1.805*TDB
     *-4.186*TG2)
C   CHECK FOR LOSS OF PRECISION
        IF (ABS(F1-F2) .LT. 1.0E-07) GO TO 98
C   FIND NEW GUESS
        TGN=TG2-F2*(TG2-TG1)/(F2-F1)
C   CHECK FOR CONVERGENCE
        IF (ABS(TGN-TG2) .LT. EPS) GO TO 97
        TG1=TG2
        F1=F2
        TG2=TGN
        NIT=NIT+1
C   CHECK FOR FAILURE TO CONVERGE
        IF (NIT .GT. 100) GO TO 96
        GO TO 93
96      TWB=TG2
        WRITE(-,210)
210     FORMAT(' FAILURE TO CONVERGE IN 100 ITERATIONS')
        RETURN
97      TWB=TGN
        RETURN
98      TWB=TG2
        NIT=NIT+1
        WRITE(-,220) NIT
220     FORMAT(' LOSS OF PRECISION AFTER',2X,I3,2X,'ITERATIONS')
        RETURN
C
C   FIND SATURATION PRESSURE OF WATER AT TEMPERATURE T.

100     IF (T .GT. 0.) GO TO 105
        Z = 273.16/(T+273.16)
        PSAT = 10.**(P5(Z) + P6(Z) + P7(Z) + P8)
        GO TO RETRN, (8,72,78,91,92)
105     Z = 373.16/(T+273.16)
        PSAT = 10.**(P1(Z) + P2(Z) + P3(Z) + P4(Z))
        GO TO RETRN, (8,72,78,91,92)
       END
```

BIBLIOGRAPHY

Aceituno, P., "Statistical Formula to Estimate Heating or Cooling Degree-Days," Agricultural Meteorology, 20, (1979).

Air Force Manual 88-29, Engineering Weather Data, (1978).

Anderson, J.V., Mitchell, J.W. and Beckman, W.A., "Performance Predictions of Air-to-Air Heat Pumps Using Generalized Weather Distributions," ASHRAE Transactions, 88, 2, (1982).

ASHRAE, Handbook of Fundamentals, (1981).

Balcomb, J.D., Jones, R.W., Kosiewicz, C.E., Lazarus, G.S., McFarland, R.D. and Wray, W.O., Passive Solar Design Handbook--Volume III and Supplement, American Solar Energy Society, Inc., New York, (1983).

BLAST, The Building Loads Analysis and System Thermodynamics Program--Users Manual--Volume 1, Report E-153, U.S. Army Construction Engineering Research Laboratory, (1979).

Butson, K.D. and Katch, W.L., "Selective Guide to Climatic Data Sources," Key to Meteorological Records Documentation No. 411, U.S. Department of Commerce, (1979).

Clark, D.R., Klein, S.A. and Beckman, W.A., "Algorithm for Evaluating Hourly Radiation Utilizability Function," ASME Journal of Solar Energy Engineering, 105, 3, (1983).

Collares-Pereira, M. and Rabl, A., "The Average Distribution of Solar Radiation--Correlations Between Diffuse and Hemispherical and Between Daily and Hourly Insolation Values," Solar Energy, 22, 2, (1979).

Dodd, A.V., "Dew Point Distribution in the Contiguous United States," Monthly Weather Review, 93, 2, (1965).

DOE-2 Reference Manual, Version 2.1, Report LBL-8706, Revision 1, Lawrence Berkeley Laboratory, (1980).

Duffie, J.A. and Beckman, W.A., Solar Engineering of Thermal Processes, John Wiley and Sons, New York, (1980).

Erbs, D.G., Klein, S.A. and Duffie, J.A., "Estimation of the Diffuse Radiation Fraction for Hourly, Daily and Monthly-Average Global Radiation," Solar Energy, 28, 4, (1982).

Evans, B.L., "Design Methods for Active-Passive Hybrid Space Heating Systems," Masters Thesis in Mechanical Engineering, University of Wisconsin-Madison, (1983).

Federal Register, Part III, Department of Energy, Office of Conservation and Solar Energy, "Test Procedures for Central Air Conditioners, Including Heat Pumps," (1979).

Fischer, R.D., Flanigan, R.D., Talbert, S.G. and Jaffe, D., "Degree-Days Method for Simplified Energy Analysis," ASHRAE Transactions, 88, 2, (1982).

Harris, W.S., Anderson, G.Y., Fitch, C.H. and Spurling, D.F., "Estimating Energy Requirements for Residential Heating," ASHRAE Journal, 7, 10, (1965).

Hastings, N.A.J. and Peacock, J.B., Statistical Distributions; A Handbook For Students and Practitioners, John Wiley and Sons, New York, (1975).

Hines, W.W. and Montgomery, D.C., Probability and Statistics in Engineering and Management Science, John Wiley and Sons, New York, (1980).

Hitchin, E.R., "Degree-Days in Britain," Building Services Engineering Research and Technology, 2, 2, (1981).

Hollands, K.G.T. and Huget, R.G., "A Probability Density Function for the Clearness Index, with Applications," Solar Energy, 30, 3, (1983).

Horn, J.C., "Investigation of Various Thermal Capacitance Models," Masters Thesis in Mechanical Engineering, University of Wisconsin-Madison (1982).

Klein, S.A., "Calculation of Flat-Plate Collector Utilizability," Solar Energy, 21, 5, (1978).

Klein, S.A. et al., "TRNSYS, A Transient Simulation Program," University of Wisconsin-Madison, Engineering Experiment Station Report 38-11, Version 11.1, (1981).

Knapp, C.L., Stoffel, T.L. and Whitaker, S.D., Insolation Data Manual, Solar Energy Research Institute, Publication SERI/SP-755,789, (1980).

Kusuda, T. and Saitoh, T., "Simplified Heating and Cooling Energy Analysis Calculation for Residential Application," National Bureau of Standards, Report NBSIR 80-1961, (1980).

Liu, B.Y.H. and Jordan, R.C., "The Interrelationship and Characteristic Distribution of Direct, Diffuse, and Total Solar Radiation," Solar Energy, 4, (1960).

Lunde, P.J., "Adjusting Degree Days," Solar Age, 7, 11, (1982).

Mitchell, J.W., "Heat Transfer From Spheres and Other Animal Forms," Biophysical Journal, 16, (1976).

Monsen, W.A., Klein, S.A. and Beckman, W.A., "Prediction of Direct Gain Solar Heating System Performance," Solar Energy, 27, 2, (1981).

Monsen, W.A., Klein, S.A. and Beckman, W.A., "The Un-utilizability Design Method for Collector-Storage Walls," Solar Energy, 29, 5, (1982).

Odell, M.P., "Solar-Assisted Refrigerant-Filled Collector Heat Pumps," Masters Thesis in Mechanical Engineering, University of Wisconsin-Madison, (1982).

Orgill, J.F. and Hollands, K.G.T., "Correlation Equation for Hourly Diffuse Radiation on a Horizontal Surface," Solar Energy, 19, 4, (1977).

Parken, W.H. and Kelley, G.E., "Estimating Residential Seasonal Cooling Requirements," ASHRAE Transactions, 87, Part 1, (1981).

Ryan, T.A., Joiner, B.L. and Ryan, B.F., MINITAB Student Handbook, Duxbury Press, North Scituate, MA, (1976).

Ryshpan, J. and Henkel, J., NONLINEAR REGRESSION ROUTINES--Reference Manual for 1100 Series Computers, Academic Computing Center, University of Wisconsin-Madison, (1972).

Seaton, W.W. and Wright, R.S., "ASHRAE Research 1983-84," ASHRAE Journal, 25, 10, (1983).

SOLMET Typical Meteorological Year, Tape Deck 9734, National Climatic Center, Asheville, North Carolina, (1978).

SOLMET, Volume 2--Final Report, Tape Deck 9724, U.S. Department of Commerce, National Climatic Center, Asheville, North Carolina, (1979).

Sonderreger, R.C. and Garnier, J.Y., "A Simplified Method for Calculating Heating and Cooling Energy in Resi-ential Buildings," Lawrence Berkeley Laboratory Report LBL-13508, (1981).

Steadman, R.G., "The Determination and Metrication of Degree Days," ASHRAE Journal, 20, 12, (1978).

Thom, H.C.S., "Seasonal Degree-Day Statistics for the United States," Monthly Weather Review, 80, 9, (1952).

Thom, H.C.S., "Normal Degree-Days Below Any Base," Monthly Weather Review, 82, 5, (1954).

Thom, H.C.S., "The Rational Relationship Between Heating Degree-Days and Temperature," Monthly Weather Review, 82, 1, (1954).

Thom, H.C.S., "Normal Degree-Days Above Any Base by the Universal Truncation Coefficient," Monthly Weather Review, 94, 7, (1966).

Walsh, P.J. and Miller, A.J., "The Relation Between Degree Days and Base Temperature," Applied Energy, 13, (1983).

Whiting, R.M., "Standard Deviation of Monthly Average Temperature in the U.S.," Technical Report EDS 3, U.S. Department of Commerce, (1978).

Yao, A.Y.M., "A Statistical Model for the Surface Relative Humidity," Journal of Applied Meteorology, 13, 2, (1974).